FINAL REPORT TO ESA

Final Report to the European Space Agency

Global validation of ERS Wind and Wave Products

January 1998

Authors: D. LeMeur, L. Isaksen, B. Hansen, R. Saunders and P. Janssen

ESA contract No. 8488/95/NL/CN

European Centre for Medium-Range Weather Forecasts
Europäisches Zentrum für mittelfristige Wettervorhersage
Centre européen pour les prévisions météorologiques à moyen terme

Final report to ESA

Global validation of ERS Wind and Wave Products

by

D. LeMeur, L. Isaksen, B. Hansen,
R. Saunders and P. Janssen

European Centre for Medium Range Weather Forecasts

January 1997

(ESA contract No. 8488/95/NL/CN)

1. Introduction

The ERS-1 scatterometer winds were first used operationally in the ECMWF analysis when the new 3 dimensional variational assimilation system was introduced at the end of January 1996. Since then ERS-1 and subsequently ERS-2 scatterometer ambiguous winds retrieved using the CMOD-4 retrieval have been assimilated continuously at ECMWF. A global dataset of collocations of surface observations, scatterometer winds and model winds was used to derive an "ocean calibration" to remove any biases in the scatterometer measurements before their assimilation. In November 1997 the operational assimilation system became the 4 dimensional variational analysis (taking into account the time of the observation) which studies have shown will make even better use of the scatterometer winds. The benefits of the ERS scatterometer winds in the analysis system are documented below and in the attached reports. In particular the improved performance of the model in terms of skill in predicting the intensity and position of tropical cyclones out to 5 days is clearly demonstrated. Plans were also made to assimilate the NSCAT winds from ADEOS but the failure of the satellite in mid 1997 prevented this from being implemented.

After the successful calibration and a promising validation of the ERS-1 Radar Altimeter wave and wind data ECMWF introduced mid August 1993 an optimum interpolation (O.I.) scheme to improve the initial conditions for the medium range wave forecasts using quality controlled Radar Altimeter wave observations. With the launch of ERS-2 a second source of Radar Altimeter wave and wind data became available for a period of almost 14 month. During the ERS-2 commissioning phase this allowed for a cross calibration between ERS-1 and ERS-2 using ECMWF atmospheric and wave model results as a reference standard. The validation studies revealed that the ERS-2 Radar Altimeter wave heights were higher than those of ERS-1 by 8-9% and showed a better agreement with the wave model data and buoy data than ERS-1 data. Although there was in general good agreement a detailed analysis showed that the Radar Altimeter wave height retrieval should be sea state dependent. A corrective scheme that uses the first guess wave model spectra has been proposed and tested on simple cases. Also, consequences of the sea state dependence for the Radar Altimeter range measurement have been explored. Furthermore, comparison of ERS-2 Radar Altimeter wind speed with ECMWF surface winds revealed initially serious biases in the Radar Backscatter. After corrective action by ESA a good quality wind product resulted.

The validation studies resulted in the substitution of the ERS-1 Radar Altimeter wave observations by those obtained with ERS-2 in the O.I. scheme from April 1996. The change from ERS-1 to ERS-2 had a considerably positive impact on the wave analysis and wave forecast in the Tropics; wave forecast verification scores against analysis showed a considerable reduction in the bias of the forecast wave height suggesting a better balance between analysis and forecast.

The contract provided partial support for D. Le Meur and L. Isaksen for the scatterometer wind validation and B. Hansen for the Radar Altimeter and SAR wave validation studies for the period from Jan 1996 to Dec 1997.

This final contract report summarises the main work carried out during the contract. The detailed scientific results are attached as annexes. The report is divided into sections on the scatterometer related work and the Radar Altimeter/SAR work. A list of meetings attended and papers written is given at the end.

2. Validation of ERS-2 scatterometer winds

2.1 - ERS-2 scatterometer commissioning phase

The first task of the project was the commissioning of the ERS-2 scatterometer from January to March 1996. The ECMWF contribution was to provide monitoring reports providing systematic comparisons between the scatterometer products and the first guess wind data from the ECMWF Numerical Weather Prediction (NWP) model analyses and short range forecast fields.

The commissioning reports, delivered on a weekly basis during the first 35-day repeat cycle of the commissioning process and thereafter every two weeks, were helpful to identify and solve the underestimation problems in sigma noughts that affected the ERS-2 UWI retrievals since their release in November 1995. The so-called "ocean calibration" procedure described in Annex B. allowed antenna biases to be derived from the first week, and these remained valid until the end of the commissioning phase. Moreover subtracting these biases from the raw backscatter measurements demonstrated, well before the final engineering calibration, that wind products of a similar quality to those of the ERS-1 instrument could be obtained from ERS-2.

The full results from these monitoring activities and the impact studies carried out are described in the geophysical validation part of the commissioning report part of which is attached as Annex A and also in the paper attached as Annex C.

2.2 - Routine Monitoring

Another key task was the production of monitoring reports on the operations of the ERS-1 and ERS-2 scatterometers. These reports were supplied on a monthly basis until September 1997, and since then for every 35-day repeat cycle at the request of the ESRIN Product Control Service. For ERS-2 the routine monitoring phase started after the completion of the commissioning in March 1996, whereas in the case of ERS-1 the monitoring continued until the switch-off of the instrument in June 1996.

Although the ERS-1 scatterometer performance proved to remain remarkably stable in time, the monitoring information was still useful to deal with initial calibration problems regarding the ERS-2 data. In particular, the "ocean calibration" process was once again valuable to confirm and assess the negative sigma nought bias that occurred after the transfer to the redundant on-

board electronics system in August 1996. ESRIN relied on the ECMWF input to define an appropriate correction in the scatterometer look-up tables. ESRIN were also grateful for the feedback that was obtained in near real time from ECMWF after the implementation of this correction, as well as that of other similar changes to their operational data processing.

The ECMWF routine monitoring was also used to highlight any problems arising in the quality of the data or in the format and timeliness of the products provided by ESA to other users. For example the consequences that occasional orbital maintenance manoeuvres can have on the scatterometer wind speeds was demonstrated. This has resulted in ESA now notifying users of such events well in advance. The use of the corrupt data by the NWP model also led to a revised quality control scheme being developed at ECMWF to automatically identify periods of large anomalous sigma nought departures. The issue of the reduced data coverage that often results from the operation of the Active Microwave Instrument in SAR image mode in coastal areas was also recently raised due to the model's inability to identify tropical cyclone *Pauline* off the Mexican coast. This was partly due to the lack of scatterometer coverage in this area. Suggestions have been made to improve the scatterometer coverage especially in critical situations such as tropical cyclones which can on many occasions be forecast up to 5 days in advance.

2.3 - Production of collocation files

In addition to the monitoring activities mentioned above, systematic collocations were made with the conventional surface wind observations from ships and buoys assimilated by the ECMWF model to help the calibration and validation of the scatterometer products. Collocation files were produced every 6 hours according to the format agreed in a previous contract (No. 9097/90/NL/BI), starting from 1995 for the ERS-1 scatterometer and 1996 for the ERS-2 instrument.

These collocation files were mainly used to re-assess the wind calibration of the CMOD4 transfer function in collaboration with Ad Stoffelen (KNMI). This turned out to be a vital tool for the assimilation of the winds, especially in the case of high wind speeds. A triple collocation analysis was performed for that purpose, by considering the model fields interpolated to each dual collocation between conventional observations and scatterometer data. The error estimates deduced from that analysis were then applied to the derivation of a wind speed bias correction by direct regression between all the collocated scatterometer and model data available. A sigma nought bias correction, established by "ocean calibration", was also implemented to refine the fit of the transfer function in the measurement space and compensate for any instrumental calibration problems such as those with ERS-2 in the summer of 1996. The new calibration scheme obtained for CMOD4 was implemented in the ECMWF model in September 1997 and suggested to the members of the ASCAT Science Advisory Group (SAG) as a possible basis for the development of a new transfer function (CMOD5). The new scheme is described in more detail in Annex B.

Collocation files were also produced more recently (from January 1997 onwards) with additional data from the wave model, WAM, run at ECMWF. The main application here has been to investigate the effects of sea-state on the scatterometer measurements. A clear influence of the significant wave height has already been found on the wind retrieval at low incidence angles,

with a substantial impact in terms of wind speed. This result, also reported within the ASCAT SAG, should soon be the subject of a further refinement in the processing of ERS scatterometer data before assimilation in the ECMWF model.

2.4 - Improvements to use of scatterometer data and impact studies

In addition to the calibration studies described above, research was also undertaken to assess the impact of ERS scatterometer data on NWP analyses and forecasts using the ECMWF model. Changes in the data preprocessing and assimilation were always tested in impact experiments to show the benefits for the analyses and forecasts.

An important step in this respect was when the ERS-1 ambiguous winds were introduced in the ECMWF model at the same time as the new 3D-Var analysis scheme in January 1996. The implicit ambiguity removal provided by the 3D-Var method was shown to represent a significant improvement with respect to the statistical filter used in the old preprocessing scheme (PRESCAT). Clear improvements were found in the sea-surface wind analyses with a positive impact on the short range forecasts especially in the Southern Hemisphere.

A new area of investigation concerned the role played by the data coverage of the instrument in these results and the gain that could be expected from using multiple or double-swath scatterometers. The tandem operations of the ERS-1 and ERS-2 scatterometers in the first half of 1996 and the assimilation experiments that had already been performed for validation purposes with the ERS-2 data in that period were taken as an opportunity to study this aspect. Four assimilation experiments were carried out over the first week of April 1996, using either no scatterometer data, ERS-1 or ERS-2 data only or both ERS-1 and ERS-2 data. The comparison of the different first guess wind fields obtained with the scatterometer data before assimilation showed that the respective improvements observed in the sea-surface wind analysis with the ERS-1 and ERS-2 data were basically complementary when both scatterometers were used at the same time. No significant redundancy could be seen on average in spite of the 24-hour orbit phasing between both satellites, and some synergistic effects could appear in the most significant impact cases. A similar complementarity was found when studying the forecast performance. Here the gains associated with each single assimilation case tended to be added in terms of anomaly correlation scores in the tandem case whatever the geographical area, and the impact became clearly positive around forecast day 6 in average over the Northern Hemisphere while it was close to neutral when only one scatterometer was used. The results of this work are described in more detail in the paper attached as Annexes C and E.

Special attention has also been given to the impact of scatterometer data on analysing and forecasting tropical cyclones, given its importance for communities threatened by such events. Dedicated studies were first performed to investigate the impact of using ERS-1 scatterometer data together with the 3D-Var analysis scheme for analysing and forecasting such events with the ECMWF model during the summer 1995 hurricane season over the tropical Atlantic. Assimilation experiments run with the scatterometer data and 3D-Var were compared with the operational outputs obtained without these data using an optimum interpolation analysis scheme in the case of hurricanes Humberto, Karen, Iris and Luis. The study of the cyclone centre position inferred from the maximum of vorticity at 850 hPa showed systematic improvements when the

scatterometer data were assimilated, with averaged reductions in positional error from 173 km to 111 km in the analyses and from 216 km to 161 km in the 24 hour forecasts respectively, taking the observations from the U.S National Hurricane Centre as a reference. Furthermore the cyclone structure appeared to be better described in the presence of the ERS-1 observations, with stronger winds at shorter distances from the centre especially in the case of Luis. The results of this work are described in several papers and reports listed in section 5. A paper on this work is attached as Annex D.

ECMWF has started to use a 4-dimensional variational analysis system (4D-Var) in November 1997 which can make better use of satellite data due to their asynoptic observation times. A number of impact studies have been performed to study the impact of ERS-1 and ERS-2 scatterometer data in 4D-Var. Despite the relatively narrow swath of the scatterometer compared to TOVS for example it has been shown that scatterometer winds have a positive impact on the analyses and forecasts in the autumn/winter periods when weather systems are most intense. This is in spite of the coverage of conventional data. The scatterometer data makes it possible to identify mid-latitude cyclones earlier over the oceans and to give a better measure of the intensity of cyclones already identified. The impact of scatterometer data on extratropical areas is documented in the report in Annex E.

A new set of assimilation experiments to investigate the impact of ERS scatterometer winds on analyses and forecasts of Atlantic hurricanes was recently carried out using 4D-Var. The use of ERS-data near the centre of the four hurricanes during the summer 1995 period was carefully investigated. The position and intensity of the hurricanes were identified in both analyses and medium range forecasts with or without use of ERS scatterometer data. The general conclusions are that hurricane analyses and forecasts are improved in most cases when ERS-data is available in the vicinity of the hurricane. The improvements are biggest when the scatterometer 'hits' the hurricane during the pre-mature phases. Fortunately this is when it is most important because hurricane warnings can be issued earlier to the public. Figure 1 is a dramatic example of the impact of scatterometer data on the 5 day forecast of hurricane Luis. The top panel shows the forecast from the old assimilation system (OI) without scatterometer data, the middle panel using the 4D-Var system but without scatterometer data and the bottom panel with scatterometer data included in the 4D-Var assimilation. Figure 2 shows the verifying analysis for these 5 day forecasts. The improvement in the forecast with the scatterometer data is clear. It is planned to write this work up as a refereed paper in the near future

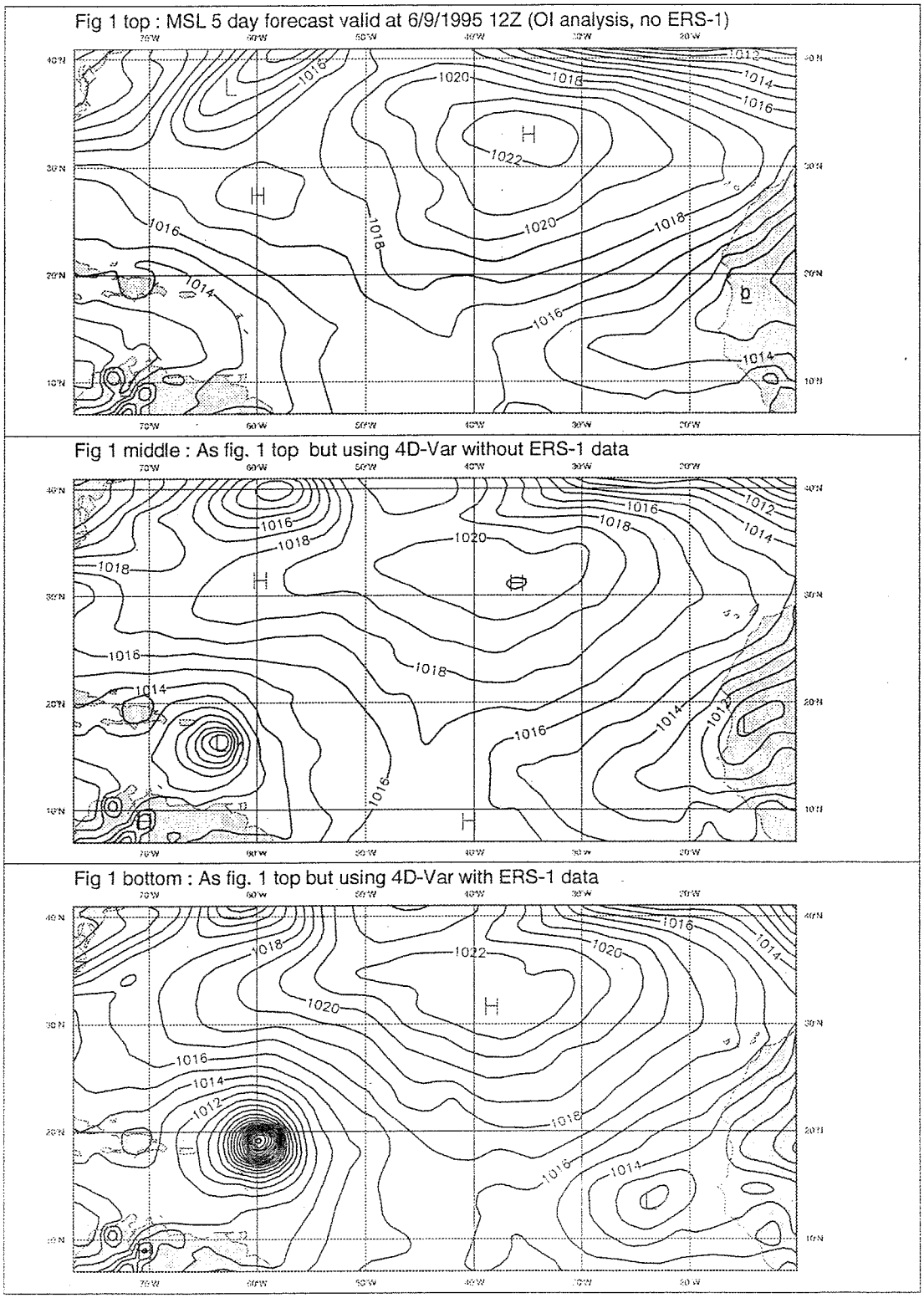

FIGURE 1. ANALYSIS WITH NO ERS-1 DATA (WHICH WAS THE OPERATIONAL, SYSTEM AT THE TIME) IN THE UPPER PANEL, FOR THE 4D-VAR ANALYSIS WITH NO ERS-1 DATA (MIDDLE PANEL) AND THE 4D-VAR ANALYSIS WITH ERS-1 DATA (BOTTOM PANEL)

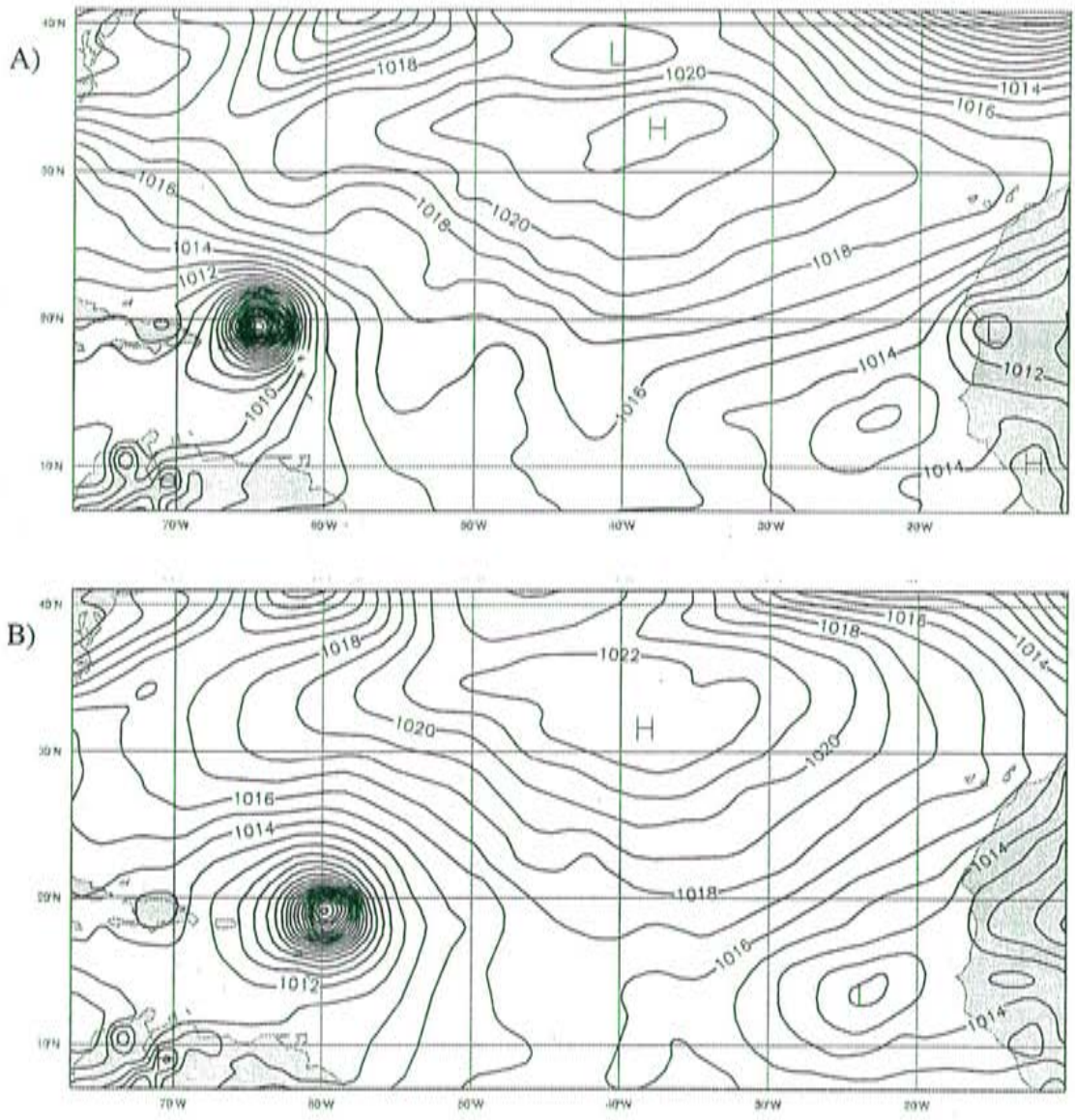

FIGURE 2. A) THE ANALYSED MEAN SEA LEVEL PRESSURE FIELD FOR 6 SEP 1995 CORRESPONDING TO THE 5 DAY FORECASTS SHOWN IN FIGURE 1. B) THE 5 DAY FORECAST FIELD VALID AT THE SAME TIME FOR 4D-VAR WITH ERS-1 DATA.

3. Validation of Radar Altimeter and SAR products

3.1 - Radar Altimeter

3.1.1 Commissioning Phase

For the commissioning phase a group of 48 members of the altimetric community, the ERS-2 Radar Altimeter and Microwave Radiometer Commissioning Working Group (ERS-2 RA &MWR-2 CWG) was established May 1994 in order to jointly perform the calibration and validation.

After the successful launch of ERS-2 by Ariane 4on Friday 21 April 1995 1:44 GMT the Radar Altimeter (RA) was initiated 3 days later on Monday 24 April 1995 12:30 GMT and first test data were transmitted to ECMWF for inspection and for testing the transmission facilities on 29 April 1995. These data were generated during the payload switch-on test performed between 28 and 30 April 1995. The full calibration and validation within the commissioning phase lasted from 29 April 1995 until 27 August 1995 to cover three 35-day repeat cycles. Throughout this period ECMWF generated weekly reports and made them available to the ESR-2 RA & MR CWG.

Initially only the surface winds (U_{10}) and the significant wave heights (H_s) as observed by the RAs onboard ERS-1 and ERS-2 were compared with modelled values. Since the U_{10} observations from ERS-2 were initially of a very poor quality (biased low by almost 5m/s when compared with ECMWF analysed surface winds) histograms of the underlying backscatter signals (σ_0) were also produced to allow a better identification of the problems. Based on the comparison of the σ_0 of the two instruments the antenna gain bias for ERS-2 could be determined and when applied reduced the bias in U_{10} to -0.75m/s when compared with ECMWF analysed surface winds.

The ERS-2 H_s observations were from the first day of remarkable good quality when compared with first-guess modelled wave heights. When compared with ERS-1 H_s data a higher cut off for the low wave heights appeared for ERS-2. At the end of the commissioning phase using the wave model results as transfer standard it was found that ERS-2 H_s were 8 to 9% higher than those from ERS-1.Annex F contains the summary report of ECMWF for the commissioning phase.

3.1.2 Operational Phase

Since 17 August 1995 ERS-2 Radar Altimeter is in routine operations and the fast delivery products are available to the user community. Since then ECMWF monitored the quality of the wind and wave products for both satellites on a daily, weekly and monthly basis until ERS-1 was phased out 17 June 1996. The monitoring continued for ERS-2 only.

Assimilation studies (Annex G) carried out early 1996 for the period of December 1995 demonstrated that the use of ERS-2 Radar Altimeter wave data in the analysis improved the quality of analysed and of forecasted wave heights when compared against boy wave height data as well as the quality of the wave forecast when compared against its own analysis.The operational use of ERS-2 in the wave analysis was subsequently introduced 30 April 1996 and therefore replaced ERS-1. The paper attached as Annex J provides detailed results of the improvements to the wave analysis and to the wave forecast after April 1996 and confirmed the results found in the assimilation studies (Annex G).

During the first year of the operational phase fine tuning of the wind and wave observations continued. One objective was to enhance the wave height correctness in the range 0-1 meter by recalculating the two parameters κ_1 and κ_2 used in the retrieval of H_s in the fast deliver product generation. None of the proposed modifications found a common agreement within the CWG so that the situation remained unchanged throughout the lifetime of ERS-2. See Annex H for more detailed information.

Another objective was to resolve some discontinuities in the σ_0 distribution and to further improve the quality of the U_{10} observations which still were biased low by -0.8m/s. Investigations revealed a shortcoming in the processing of the data which has been improved since. Furthermore another bias correction to the σ_0 observations was applied. The resulting observed winds were then biased low by -0.26m/s when compared with modelled surface winds and were on average 9% higher than those from ERS-1. See Annex I for further information.

Finally it could be shown that the retrieval of H_s in the fast delivery product (FDP) generation is dependent on the sea-state. For steep waves, namely young wind seas between 2 and 5 m high, it was found that the Radar Altimeter underestimates H_s by as much as 0.5m. The details of this study are attached as Annex J.

Starting from these results more attention has been paid to the theory of the retrieval of the significant wave height from Radar Altimeter return echoes (wave forms) as well as the range determination. The current retrieval algorithm used with ERS-2 is based on the assumption that the sea surface elevation has a Gaussian probability distribution. It has been shown that this assumption can only be made for waves of small slopes. For steep waves the probability distribution of the surface elevation becomes asymmetric about its mean with an increase in skewness depending on the nonlinear dynamics of the ocean waves. Based on the work of Srokosz (1986) who provided a comprehensive theory on the form of Radar Altimeter wave forms due to nonlinear waves Guymer & Srokosz(1986) attempted to obtain correction parameters from Radar Altimeter waveform data to determine the sea-state bias and concluded that the estimates are too noisy to be useful. Furthermore the current operational RA FDP do not contain complete wave forms. We therefore decided to investigate how modelled two dimensional wave spectra could be used to determine the correction parameters. For this purpose we performed simulations with a single grid point version of the WAM model. For the first six hours of the simulation the forcing wind was kept constant at 18.45 m/s, followed by a turn in wind direction by 90° and a decrease in wind speed to 5 m/s. We therefore obtained wind sea spectra from different growth stages of the sea from the first six hours and swell spectra of different stages of decay thereafter. These spectra were then used to determine corrections to the wave height retrieval (fig. 3) and

range determination (fig 4). Figure 3shows the time evolution of the relative correction to κ_1 and figure 4 shows the absolute correction to the range. Figure 4 also shows the sea state dependence of the correction factor α. Usually α is kept constant at a value of 0.064, a value appropriate for old wind sea. Especially for young wind seas our results suggest a considerable correction to κ_1 leading to 10-15% higher waves. For the more linear sea states of swell the correction to κ_1 is relatively small. Our results to the range determination show that ranges for wind sea cases may be 5 to 10 cm shorter than those obtained with standard corrections.

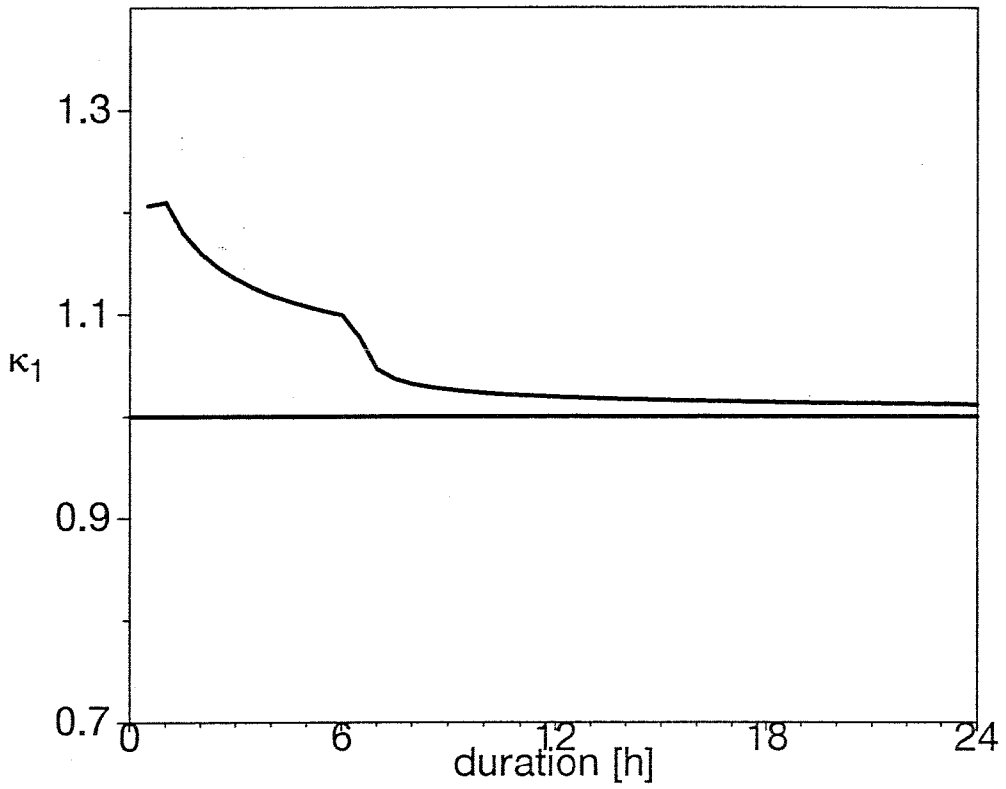

FIGURE 3. TIME EVOLUTION OF THE κ_1 CORRECTION
U_{10} = 18.45 m/s, turns and drops to 5 m/s at t=6 hrs.

During the operational phase we also started to compare ERS-2 Radar Altimeter wave and wind data with wind and wave measurements from moored buoys. Since December 1996 the monthly reports include the corresponding statistics and scatter diagrams. A timeseries of the monthly statistics scatter index and bias can be found as Annex K.

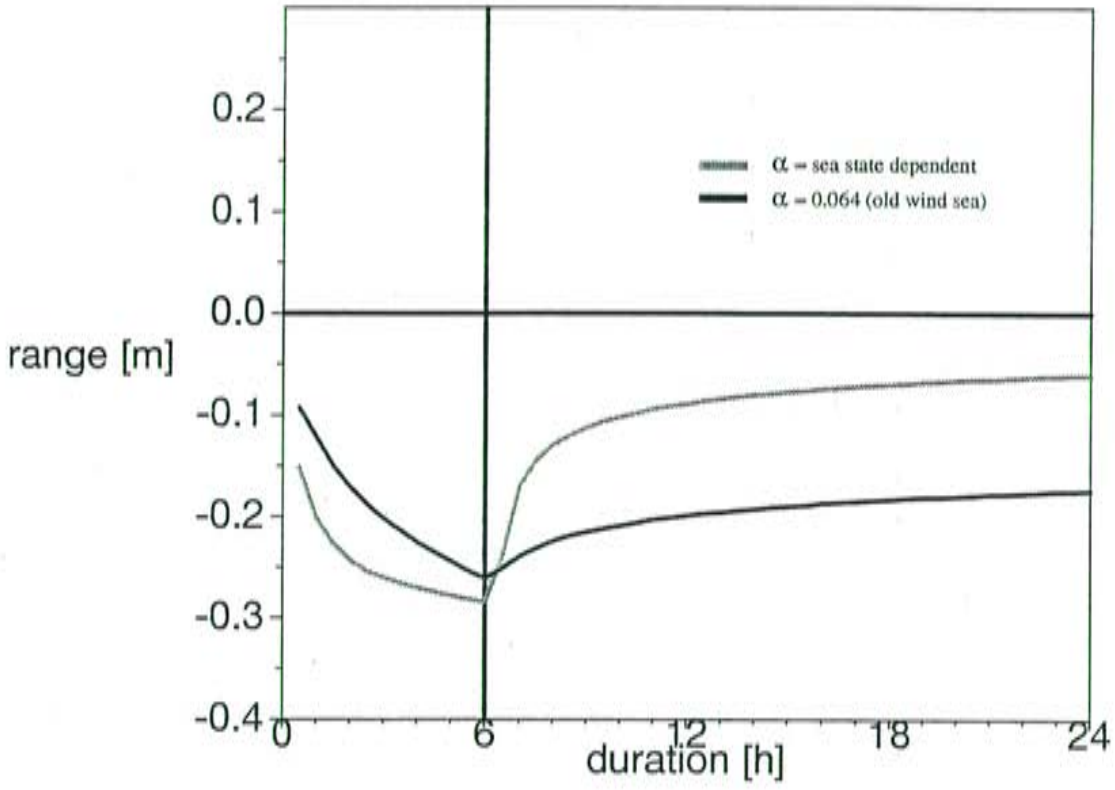

FIGURE 4. TIME EVOLUTION OF RANGE CORRECTION
U_{10} = 18.45 m/s, turns and drops to 5 m/s at t=6hrs

3.1.3 Products and Colocation files

The extensive daily, weekly and monthly monitoring and verification results were made available to the staff at ECMWF for verification. Part of the monthly monitoring results were used for reports sent to ESA. Intermediate data files of relevance as well as final collocation files are permanently archived and can be used for further studies. These are the quality controlled raw data and the collocated averaged data. For the latter in time and space interpolated wind and wave data from the first guess and from the analysed fields of the ECMWF atmospheric and wave models are collocated with along track averages of the wind and wave observations from ERS-2. Since December 1996 quality controlled and averaged wind and wave observations from moored buoys are included. A detailed description of the contents of these files can be found as Annex L.

3.2 - Synthetic Aperture Radar (SAR)

There was no dedicated campaign to calibrate or validate the ERS-2 Synthetic Aperture Radar (SAR) wave mode data as was done for the Radar Altimeter of ERS-2.

First SAR wave mode spectra (254) arrived at ECMWF from three orbits between 25 and 26 April 1995. The delivery of spectra commenced on 24 May 1995 but with only one orbit worth of spectra per day during the entire tandem mission. In the first month of the commissioning (May 1995) about 1000 spectra arrived at ECMWF and have been successfully used in the SAR inversion processing chain. The obtained H_s values have then been compared with modelled first guess data on a daily and on a weekly basis and showed to be biased high by only 0.1m with a symmetric slope of 1.06 and a scatter of 15%, thus agreeing better with the model than those from ERS-1 which have been obtained with an older version of the retrieval package which produced too high waves when compared with wave model data. About 12200 spectra arrived during the period 1 May 1995 and 27 August 1995 when the commissioning of the ERS-2 Radar Altimeter finished and the monitoring showed that the SAR operated stable.

Throughout the current lifetime of ERS-2 the SAR wave mode images have been used to produce observed two-dimensional wave spectra in near real time. The H_s values derived from those wave spectra have then been used to verify the daily operational wave analyses. Consequently the performance of the sensor has been monitored automatically at the same time and showed that the SAR wave mode spectra were of constant and good quality.

As a result of these activities a comprehensive archive of collocated SAR image wave spectra, wave spectra from the wave model WAM and observed wave spectra has been build and is available for further research.

4. Meetings attended

- Participation in the ERS-2 Radar Altimeter and Microwave Radiometer Commissioning Working Group Meetings No. 7, 9 and 10, from July 1995 to April 1996 (Bjorn Hansen and Peter Janssen).

- Participation in the ASCAT Science Advisory Group meetings No. 9 to 12, from February 1996 to October 1997 (Didier Le Meur).

- Participation in the final meeting of the ERS-2 scatterometer commissioning working group held at ESTEC, 26-27 March 1997 (Didier Le Meur).

- NESDIS workshop on the operational use of scatterometer measurements held in Alexandria, 22-23 April 1996 (Didier Le Meur, oral presentation).

- 3rd IFREMER workshop on the ERS applications held in Brest, 18-20 June 1996 (Didier Le Meur, oral presentation + paper).

- 3rd ERS symposium (Florence, 18-21 March 1997): (Didier Le Meur, oral presentation + abstract); Lars Isaksen (oral presentation + paper).

- CEOS Wind and Wave Validation Workshop (Noordwijk, 3-5 June 1997): (Peter A.E.M.Janssen, oral presentation + paper).

5. Papers and Reports

ERS-2 scatterometer commissioning report. Geophysical validation part (Annex A).

Isaksen, L. "Impact of ERS scatterometer data in the ECMWF 4D-Var assimilation system - Preliminary studies" Proc. of the 3rd ERS symposium (Florence, 18-21 March 1997)

Isaksen, L. "Impact of ERS scatterometer winds in ECMWF's Four Dimensional Variational Assimilation System" Paper in WGNE's "Research Activities in Atmospheric and Oceanic Modelling" (1998)

Le Meur, D. Gaffard C. and Saunders R. "Use of ERS scatterometer data at ECMWF" Proc. of 3rd IFREMER workshop on the ERS applications held in Brest, 18-20 June 1996 (Annex C)

Le Meur, D., Isaksen, L. and Stoffelen, A. "Wind speed calibration of ERS scatterometer data for assimilation purposes at ECMWF" Proc. of CEOS wind and wave validation workshop held at ESTEC, 3-5 June 1997 (Annex B)

Tomassini, M., Le Meur, D. and Saunders R. "Near-surface satellite wind observations of hurricanes and their impact on ECMWF model analyses and forecasts". Paper in Monthly Weather Review, special issue on Atlantic hurricanes, February 1998 (Annex D).

Undén, P., Kelly, G., Le Meur, D. and Isaksen L. "Influence of observations on the operational ECMWF system" ECMWF Research Dept. Tech. Memo 244 Dec 97. (Annex E).

Isaksen, L. "Impact of ERS scatterometer winds in ECMWF's Four Dimensional Variational Assimilation System" Paper in WGNE's "Research Activities in Atmospheric and Oceanic Modelling" (1998)

Bidlot, J.-R., Hansen, B., Janssen, P.A.E.M. "Wave modelling and operational forecasting at ECMWF", Paper in Operational Oceanography. The challenge for european co-operation. Proceedings of the First International Conference on EuroGOOS, 1997.

Janssen, P.A.E.M., Hansen, B., Bidlot, J.-R. "Validation of ERS satellite products with the WAM model" Presented at CEOS wind and wave validation workshop ESTEC, 3-5 June 1997

6. Appendices

ANNEX A

- ERS-2 scatterometer commissioning report. Geophysical validation part

ANNEX A

ERS-2 scatterometer commissioning report

Geophysical validation part

ECMWF contribution

Introduction

The ECMWF contribution to the commissioning of the ERS-2 scatterometer was two-fold. On the one hand, the scatterometer data were monitored by comparison with First Guess at Appropriate Time (FGAT) winds from the Centre's Numerical Weather Prediction (NWP) system. On the other hand, they were assimilated in it through dedicated experiments, to assess their impact on NWP. This section reports on the validation results obtained, after a short presentation of the ECMWF forecast system and the pre-processing procedure PRESCAT applied to re-process and quality control the scatterometer data. Results from previous assimilation experiments performed with ERS-1 are also reminded, concerning both the impact of the data on NWP within the ECMWF forecast system and their subsequent utility for numerical wave modelling using the WAM model.

1 - Generalities

1.1 - The ECMWF forecast system

The ECMWF forecast system consists of two components : a general circulation model and a data assimilation system. The general circulation model (see Ritchie et al., 1995 for details) is a spectral, primitive equations model with a truncation of T213 - i.e. an horizontal resolution of about 60 km - and 31 vertical levels, using a semi-Lagrangian time integration with a step of 15 minutes. It includes a comprehensive set of physical parametrizations, representing processes such as convection, clouds, radiation, friction and diffusion.

The data assimilation system combines every 6 hours (synoptic times O, 6, 12 and 18 UTC) the observations available with the model 6 hour forecast (so-called first guess) into an analysis that is used as an initial state for the next forecasts. The process is said to be multivariate : for example, measurements of wind will not only influence the model wind field, but also the associated mass field, through a latitude dependent application of geostrophy. Moreover, the model forecast error is assumed to be spatially correlated, so that the differences between the observations and the first guess (observation increments) will be spread both in the horizontal and the vertical to determine the corrections to apply at each grid point to update the model state (analysis increments). Data from conventional reports (SYNOP, AIREP, DRIBU, TEMP and PILOT) and from satellite reports (cloud motion winds from geostationary imagery SATOB and temperature and humidity soundings from the TOVS sounder) are used for the geopotential height and wind analysis. The analysis of specific humidity relies on TEMP and TOVS observations, and that of temperature is derived from the geopotential height analysis through the hydrostatic equation.

A major change was made in the ECMWF assimilation system on 30 January 1996, when the Optimal Interpolation (OI) analysis scheme (Lorenc, 1981) was replaced by a new three-dimensional variational (3D-Var) method (Courtier et al., 1993). In 3D-Var, the observations are merged with the model first guess through the minimization of a cost function. Compared with OI, one main advantage is that this allows to handle data that are non-linearly related to the analysed quantities. Satellite radiance measurements can thus be assimilated directly. Moreover, the con-

trol of the noise level in the analysis (gravity waves) is done implicitly within the cost function, yielding a more general balance constraint between the mass and wind fields than the seperate initialization step needed in OI.

Another important change that occurred in the ECMWF assimilation system together with the implementation of the 3D-Var analysis scheme is that of the ERS-1 scatterometer data. As detailed below, ERS scatterometer data are assimilated in the 3D-Var context as pairs of ambiguous wind vectors, leaving the minimization process select the most appropriate direction, and their introduction in the case of ERS-1 had a positive impact on the analysed and first guess surface winds, resulting in a significant improvement of the short-range forecasts in the Southern Hemisphere.

The ECMWF winds considered hereafter for the processing and monitoring of ERS scatterometer data are 10 metre winds from the model's First Guess at Appropriate Time (FGAT), which is an interpolation of the current 3 hour, 6 hour and 9 hour range forecasts at the scatterometer measurement time. First guess winds have turned out to compare better with the scatterometer observations than analysed winds because of mass-wind imbalances left by the analysis process in the surface fields : these imbalances, present both with the 3D-Var and OI methods, are solved by the model physics after a few hours, leading to a better accuracy of the surface winds from short range forecasts. Furthermore, the use of data defined at the right time, allthough not necessary in the case of slow-moving, large-scale wind structures, has been found essential for that of rapidly moving systems, causing large phase errors in the first guess at synoptic times.

In practice, the changes made in the assimilation system at the end of January 1996 had little effect on average on the monitoring activities carried out from FGAT winds : from the results of the pre-operational impact studies, only a reduction in the order of 3 % in a vector Root Mean Square (RMS) sense could be expected in the difference between model and scatterometer wind due to the introduction of the ERS-1 data.

1.2 - The PRESCAT pre-processing

ERS scatterometer data have been re-processed and quality controlled in real time at ECMWF since July 1994, within a procedure called PRESCAT and meant as a pre-processing step to their operational assimilation. This procedure was developed from ESA's wind retrieval and ambiguity removal scheme, called CREO (Cavanié and Lecomte, 1987), but several changes were made to improve it, leading to a quite different processing (see Stoffelen and Anderson, 1995 for details).

The inversion method was first reconsidered. The Maximum Likelihood Estimator (MLE) used in CREO to minimize the distance between the scatterometer measurements and the CMOD4 transfer function was found to introduce a distortion of the backscatter space, previleging certain directions in the retrieval process. As a result a new MLE was implemented, computing the distance in the transformed space defined by $z = (\sigma^0)^{0.625}$, where the cone described by CMOD4 is nearly circular and gives a uniform distribution of retrieved directions. Moreover only two solutions were kept, basically that with the smallest MLE residual and the first one in the opposite direction.

The ambiguity removal scheme was also revised. Because of operational constraints, CREO uses only 18 hour to 36 hour range forecasts from ECMWF as a background information and therefore relies strongly on the ranking of the retrieved solutions as a function of their MLE va-

lues to select the right direction (autonomous ambiguity removal). Unfortunately, the upwind/downwind sensitivity is less than expected, and the process turns out to fail to provide a solution in about 30% of the cases. Also PRESCAT takes advantage of the real-time availability of the ECMWF short-range forecasts to give more weight to model data. It uses FGAT winds as a background, that already remove 95% of the ambiguities by direct comparison. Most of the remaining ones are then sorted out by means of a vector statistical filter propagating the information from the areas where the confidence in the selected solution is high to areas with a lower confidence.

The quality control was finally extended. The check of the quality information provided by ESA (including Kp noise values and missing packet counters) was just made a preliminary step. The application of a refined land-sea mask and a sea-ice screening deduced from the ECMWF Sea-Surface Temperature (SST) analysis - with a threshold of 0° C - allows to reject typically 15 % more data. Moreover, two additional checks are performed on the retrieval residual (MLE of the rank 1 solution), so-called «normalized distance to the cone». On the one hand, this quantity is kept smaller than 3 (3-standard deviation test), to avoid cases of geophysical effects not explained by the transfer function such as rain, generally located at fronts or close to low pressure centres. On the other hand, it is also forced to remain limited on average over 6 hours for each node; instrumental problems can thus be detected, that relate to the measurement geometry and affect larger areas.

In addition to performing wind retrieval and ambiguity removal, PRESCAT allows monitoring statistics to be produced from the collocations performed between scatterometer and FGAT data. Different procedures have thus been implemented for the ERS-1 scatterometer, and shown their utility both to follow the performance of the instrument in time and to calibrate and validate its measurements immediately after launch. These procedures were naturally applied to the commissioning of the ERS-2 scatterometer.

2 - Monitoring results

2.1 - Antenna biases

A first monitoring procedure developed from the PRESCAT outputs consists of a comparison per beam and node between the backscatter values measured by the scatterometer and those simulated applying the transfer function to the FGAT winds. Special care is taken to remove any directional dependency in the process, in order to reflect as much as possible changes in the mean intensity given by the instrument, independently of the geophysical variability or of the possible errors due to CMOD4. For that, the data are filtered so as to ensure an uniform model wind direction distribution over the full range of wind speeds, and statistics are computed in the transformed space defined by $z = (\sigma^0)^{0.625}$. An «ocean calibration» can then be established, providing an estimate of the antenna sigma nought biases as a function of incidence angle, similarly to the engineering calibration performed in terms of gamma nought from measurements over the rain forest.

This calibration method was applied every week with the data retained by the PRESCAT quality control from the switch-on of the ERS-2 scatterometer at the end of November 1995, separating the satellite´s ascending and descending tracks to better check the stability of the results. The positive biases expected in the backscatter measurements were thus confirmed quickly, and their variation as a function of incidence angle characterized for each beam, with values ranging between 1.5 dB and 3 dB with respect to the model simulated data and being larger at low inci-

dences (Figure 1). The problem was moreover shown to be stable during the two first cycles of the commissioning process, by repeating the test in every monitoring report after correcting the measurements from the biases derived with the first week of data (Figure 2). Finally, after the implementation of new Look-Up Tables (LUT) by ESA for the third cycle on 19 March, the antenna biases were found quite similar to those obtained with the ERS-1 scatterometer, with overall close and flat profiles within + or - 0.2 dB and a slight decrease for the fore and aft beams at incidence angles below 35 degrees, but a little more undesirable oscillations for the mid beam (Figures 3 and 4). The distinction between ascending and descending tracks indicated no significant difference in those results, except a tendency for the fore and aft beams to be biased a little higher (by 0.1 to 0.2 dB) on descending tracks, which could also be observed for the ERS-1 instrument.

2.2 - Distance to the cone and quality control scores

Another procedure set up from the PRESCAT outputs for the ERS-2 scatterometer commissioning and previously used in the case of ERS-1 is the monitoring of the normalized distance to the cone, averaged over 6 hours for each node and scaled by its expected mean value (determined with ERS-1 data). This procedure was implemented both to survey the quality of the backscatter measurements in time and get a better idea of the ability of CMOD4 to describe them. To make the diagnosis more accurate, the mean normalized distance to the cone was plotted along with an indication of the total amount of incoming data presented to PRESCAT and of the number of quality controlled data taken into account for its computation (proportion of data rejected by the ESA flag, the sea-ice screening from the SST analysis or the refined land-sea mask).

The results obtained before the engineering re-calibration from 19 March (Figure 5) exhibited abnormally large distances to the cone due to the positive biases in the sigma nought measurements. The mean normalized values were in the order of 1.5 to 2 instead of 1 at low incidences, causing all the data to be rejected in most cases, because of the maximum threshold of 1.7 employed to detect instrumental problems. But at the same time, the plots produced after applying the «ocean calibration» deduced from the first week of data showed that a retrieval residual quite close to the ERS-1 case could be obtained (Figure 6), and with comparable quality control scores.

Significantly higher mean normalized distances (1.2 to 1.3) were still present at low incidence angles and to a smaller extent at high incidence angles, but turned out to be largely due to the use of a different version of CMOD4 when the ERS-1 data were implemented together with the 3D-Var analysis scheme in the ECMWF NWP system at the end of January : the transfer function applied to the ERS-1 data within PRESCAT was then updated with the same version as the ERS-2 data, and similarly higher distances became visible in the ERS-1 plots produced for comparison. It appeared that the new version of CMOD4, corresponding to the official one used by ESA (Cmod_Zad), had been derived from the old version (Cmod_Sad) by transforming a beam-dependent sigma nought correction into an incidence only dependent correction, and that this had slightly decreased its ability to fit the backscatter measurements.The application of this new version of the transfer function in the operational data processing was nevertheless not questioned because of its negligible impact on the retrieved winds.

The similarity between the retrieval residual and quality control performances attainable with the ERS-1 and ERS-2 scatterometers was confirmed after the antenna calibration correction performed by ESA in March (Figures 7 and 8). Moreover, the efficiency of the mean normalized distance to detect technical anomalies in both cases could be checked from the first days, when

analoguous transmission problems gave rise to similar responses for the two instruments in a one-day interval (from 21 to 22 March).

2.3 - Wind speed and direction statistics

The ERS-2 data were finally monitored with the help of PRESCAT in terms of wind speed and direction. Scatterometer minus FGAT statistics were computed every 6 hours for these parameters at each node, and scatterplots were also used to summarize the comparison results obtained every week and exhibit possible wind speed dependencies. To be more significant, the outputs were produced only for the data retained by PRESCAT's quality control (excluding however the global test on mean normalized distance to the cone), and limited to the wind speeds exceeding 4 m/s in the case of the direction statistics. Moreover, both the raw and re-processed data (UWI and PRESCAT) were considered, taking into account in the second case the sigma nought bias correction established from the first week of data.

Before the LUT change from 19 March, the wind speed statistics showed a positive bias in the UWI case, ranging from 2 m/s at high incidences to 3 m/s or more at low incidences and with a standard deviation of the same order (Figure 9), in agreement with the overestimation in the backscatter measurements. The direction statistics were on the contrary rather normal, with no significant bias and a standard deviation varying between 40 and 60 degrees as for ERS-1. Also the PRESCAT corrected data, displaying speed biases and standard deviations around -0.5 or -1 m/s and 2 m/s respectively (Figure 10), already indicated that wind products of a similar quality to ERS-1 could be achieved solving the antenna bias problem.

As expected, this was fully confirmed during the third cycle of the commissioning, when the UWI speed statistics came down to almost the same figures as obtained previously with PRESCAT (biases between -0.5 and -1 m/s and standard deviations smaller than 2 m/s, see Figure 11), whereas the direction statistics remained unchanged in both the UWI and PRESCAT cases, and comparable to what they used to be with ERS-1 (no significant bias and standard deviations varying between 40 and 60 degrees or 20 and 30 degrees respectively, due to the better de-aliasing provided by the use of FGAT data within PRESCAT).

The sigma nought bias correction performed previously was then abandoned, and identical processings were applied to the ERS-1 and ERS-2 data, that clearly seemed to have reached the same performance level. In particular a speed bias correction implemented to avoid the underestimation of high winds produced by CMOD 4 with ERS-1 (see below) was kept unchanged for ERS-2, and turned out to yield equivalent benefits (reduction of the mean underestimation to less than 0.5 m/s and better symmetry of the scatterplots with respect to the model data for wind speeds exceeding 15 m/s).

3 - Impact studies

3.1 - Previous studies with ERS-1

a) OI assimilation experiments

The impact of scatterometer data on NWP has already been investigated within the ECMWF forecast system in the case of the ERS-1 scatterometer. After a little conclusive preliminary study with ESA raw data (Hoffman, 1993), assimilation experiments were first performed in the OI context from PRESCAT de-aliased winds (Stoffelen and Anderson, 1995).

Analysis/forecast cycles were run successively with and without scatterometer data over a 11-day period (18 to 28 March 1993) at the spectral truncation T213. The PRESCAT winds were sampled every 100 km to match the model resolution without introducing horizontal correlation, and the results showed a clear improvement of the first guess surface wind field when they were assimilated. The vector RMS departures between scatterometer and FGAT data were typically reduced by 5 %, with more visible effects in the Southern Hemisphere where conventional observations are sparser. Since the orbit geometry is such that the satellite flies roughly over the same geopraphical area after 12 hours, the improvement was related to the information kept from the scatterometer data within that time. However the impact on the medium-range forecasts, measured classically in terms of anomaly correlation of geopotential height (with an average over 11 cases), was found to be neutral.

As previous studies suggested that the difficulty to improve the ECMWF forecasts with scatterometer data was due to their already high performance, new experiments were made in a degraded assimilation system (from 26 April to 1 May 1993), removing the SATEM satellite temperature observations from the TOVS sounder and the SATOB satellite cloud motion winds. A positive impact was then found in the Southern Hemisphere, where both SATEM and SATOB contribute significantly to the forecasts scores. Also the lack of impact on medium-range forecasts, in spite of the improvement observed in terms of RMS error in short ranges, was explained by a redundancy with these observations at large scales. Moreover the fixed error structure assumed in the OI analysis scheme, especially in the vertical, was identified as a critical point to take advantage of the information brought at smaller scales in the surface.

b) 3D-Var assimilation experiments

As mentioned earlier, the 3D-Var analysis scheme has provided a more general framework to process scatterometer data into the ECMWF forecast system and given rise to new assimilation experiments with the ERS-1 data before being implemented together with them in January 1996.

The principle consists in minimizing a cost function $J = J_B + J_O + J_C$, where J_B and J_O are quadratic terms measuring the distance from the model state to its background estimate (first guess) and the observations respectively, and J_C is a penalty term expressing additional physical constraints (especially the absence of fast growing gravity waves). For scatterometer data, it has been shown more successful to specify J_O in terms of wind vector rather than backscatter measurements (Stoffelen and Anderson, 1995). Indeed, the observation errors are practically gaussian in wind components, whereas the high non-linearity of the transfer function complicates their description in the backscatter space. Therefore ERS scatterometer data are assimilated in the 3D-VAR system as pairs of ambiguous wind vectors, through a two-minima cost function of the following form :

$$J_O^{scat} = (J_1 \, . \, J_2)/(J_1^p + J_2^p)^{1/p}$$

with :

$$J_i = (u_i - u)^2/\delta u^2 + (v_i - v)^2/\delta v^2, \; i = 1, 2$$

where u and v are the model 10 metre wind components, u_i and v_i ($i = 1, 2$) the scatterometer observations, δu and δv the associated errors and p an empirical exponent set to 4. The ambiguity removal is thus performed implicitly during the minimization process, taking into account

all the information from the background field and the surrounding observations carried by the cost function, as well as the corresponding physical constraints. The two solutions provided by PRESCAT are used as input, thinned to a 100-km resolution as in the OI context. Furthermore, a speed bias correction is applied to remove the underestimation of high winds produced by CMOD4. This bias correction, derived from collocations with buoy data, was crucial to make good use of scatterometer data in 3D-VAR : before it was introduced, assimilation experiments showed a systematic tendency to «fill» mid-latitude lows because of too low wind speeds inferred from the scatterometer measurements.

Prior to the operational implementation from January 1996, dedicated assimilation experiments were performed to assess the impact of the ERS-1 scatterometer data within the 3D-Var system, at the reduced spectral truncation T106 (horizontal resolution 125 km) and over a 2-week period in December 1994 (Gaffard and Roquet, 1996).

The benefits of the 3D-VAR ambiguity removal were thus confirmed. The de-aliased wind vectors obtained turned out to differ from those given by the PRESCAT statistical filter in about 1.7 % of the cases. The differences corresponded most of the time to situations with low wind speeds or phase errors in the first guess, and on visual inspection the 3D-VAR results generally showed wind structures of a much better consistency (Figure 12). Moreover, a clear improvement was found in the analysed and first guess surface fields, associated to a decrease of the RMS departures between the first guess and the different types of observations used in the analysis. That decrease was in the order of 3 % for scatterometer data and 2 % for buoy pressure measurements, and seemed to be more perceptible in the Southern Hemisphere as in the case of OI. But this time a significant improvement was also observed for the 12 hour range forecasts in this region in terms of geopotential height error : compared with the analyses including scatterometer data, the difference between the RMS errors of the geopotential heights forecast at 1000 hPa with and without scatterometer data was overall negative, and locally smaller than -5 m over large areas around latitude 60 degrees South (Figure 13).

The impact on medium-range forecasts in terms of anomaly correlation was eventually found neutral or slightly positive everywhere, with a maximum over Northern America, due to the particular conditions that prevailed during the study period (storms developing in the eastern part of the North Pacific). It is likely that the 3D-VAR scheme, in spite of its advantages for ambiguity removal, does not yet allow an optimum use of surface wind observations because of the fixed error correlation structure it still assumes. However it opens the way to 4D-VAR assimilation schemes which will follow the same implementation framework and bring a variation of the structure functions dynamically consistent with the meteorological conditions.

c) Case of tropical cyclones

In addition to the pre-operational experiments reported above, case studies have been carried out to better assess the impact of ERS-1 scatterometer data together with the 3D-Var assimilation system on analysing and forecasting Atlantic tropical cyclones, called hurricanes. These case studies were undertaken within a more general investigation concerning also the potential for such applications of new high resolution satellite cloud motion winds produced by ESA from the METEOSAT visible imagery (Tomassini et al., 1996).

The 1995 hurricane season was chosen as a study period, and the impact of the scatterometer data was investigated from the outputs of a preliminary 3D-Var assimilation experiment performed with them from 24 August to 5 October (SCAT/3D-Var). These outputs were compared

with those from the OI assimilation process run operationally without scatterometer data for the same period (OPS), and the results were consequently not free from influence from the new analysis scheme. This was as well not the case for the pre-operational impact study detailed previously, where the experiments with and without scatterometer data had been performed in exactly the same 3D-Var context. However, the main differences between the two assimilation configurations clearly seemed to be related to the inclusion or not of scatterometer data, and did correspond to an improvement in their presence.

The position of the cyclone centre deduced from the maximum of vorticity at 850 Hpa in the model analyses was systematically compared with that reported by the U.S. National Hurricane Centre in the case of four tropical cyclone events : Humberto, Iris, Karen and Luis. The mean positional error appeared to be reduced from 173 km to 111 km between the OPS and SCAT/3D-Var experiments, and the difference was found significant at the 95 % confidence level given the number of centres identified by the vorticity maximum method (31 and 32 respectively). On the contrary, no significant change with respect to the operational analyses was observed doing the same evaluation for assimilation experiments including or excluding cloud motion wind data because of their lower spatial resolution.

The impact of the scatterometer data was further investigated through a direct study of the analysed and 48 hour forecast surface wind and pressure fields from the OPS and SCAT/3D-Var experiments in the most significant phases of the Iris and Luis events, where swaths crossing or passing close to the cyclone centre almost every day gave the most substantial benefits (analysis periods from 28 to 31 August and 29 August to 3 September respectively). The improvements obtained in the analysed centre positions thus turned out to be well integrated in the model forecasts, and to yield a better agreement with the subsequent analyses in the case of Iris (Figure 14). Moreover with Luis, an underestimation of the cyclone intensity while it was strenghtening over the Caribbean Sea was largely corrected, with constantly lower pressure minima and higher wind speeds close to the centre both in the SCAT/3D-Var analyses and forecasts (Figure 15).

d) Impact on wave modelling

The impact of the ERS-1 data within the ECMWF forecast system has finally been studied through its consequences on numerical wave forecasting with the WAM model, run operationally with the wind analyses and forecasts from the NWP model. The same SCAT/3D-Var assimilation experiment as for tropical cyclones was considered, extended by a second experiment taking into account slightly modified physics from 6 to 28 October 1995, and used to drive the wave model in parallel to its OPS operation in the OI context and without scatterometer data (Janssen and Hansen, 1996).

If comparisons with buoy data, rather sparse, exhibited little difference between the OPS and SCAT/3D-Var analysed wave heights, an evaluation against the measurements from the ERS-1 altimeter showed a considerable improvement of the first guess wave height and analysed wind speed in the presence of scatterometer data in the Southern Hemisphere. The standard deviation errors of the model fields were reduced by about 10 % in both cases, out of mean values in the order of 50 cm and 2 m/s respectively. First guess wave height and analysed wind speed were also improved in the Northern Hemisphere, allthough to a smaller extent. A detrimential effect was however observed in the Tropics, where the mean wind speed increased by 30 cm/s, but with no consequence on the wave field.

Moreover the verification of the wave forecasts against the subsequent analyses valid at the same time indicated an overall positive impact of the scatterometer data used together with the 3D-Var analysis scheme, as well in terms of anomaly correlation as standard deviation error. For the first period of the experiment (Figure 16), the standard deviation error in the wave height was reduced by 10 % at day 5 in the Southern Hemisphere, while the usefulness of the forecast was extended by half a day, and similar benefits were obtained for the second period in the Northern Hemisphere (Figure 17).

3.2 - New studies with ERS-2

New impact studies within the 3D-Var context have been performed from the ERS-2 scatterometer since the completion of its commissioning. Exactly the same processing has been kept as with ERS-1, since the performances of both instruments turned out to be virtually identical.

Preliminary experiments confirmed the improvements observed with ERS-1 for the analysed and first guess surface fields from a 2-day analysis period (1-2 April 1996). The assimilation of the scatterometer data affected mainly the model fields in the Southern Hemisphere, and simultaneously the RMS departures between first guess and observations were reduced consistently with the results from the 2-week experiments from December 1994 (by 2 % in the case of surface wind compared with the scatterometer data themselves and by 1.5 % in that of surface pressure compared with buoy measurements). Moreover, the vector RMS departure between the analysed surface wind and the ERS-1 scatterometer data was also significantly decreased (by 1 %), in spite of the small amount of data taken into account and the generally lower quality of the analysis for surface wind. These improvements allowed as well to expect the same benefits as had been observed with ERS-1 in terms of short range forecasts. Also, the ERS-2 data were substituted for their ERS-1 counterparts in the operational assimilation system on 1 June 1996, before the switch-off of ERS-1's instruments on 3 June.

Those 2-day experiments were then taken as an opportunity to study the impact of the two instruments together, in order to get a first idea of what can be expected from future double-swath scatterometers such as NSCAT or ASCAT. For that purpose, the analysis period was extended to 5 days in a first approach (1-5 April 1996), and four assimilation configurations were tested : no scatterometer data, ERS-1 or ERS-2 data only, and both ERS-1 and ERS-2 data.

A substantial gain has thus been found on average in the fit between first guess and observations in the tandem configuration : the vector RMS difference between scatterometer and FGAT wind decreases by 13 cm/s (out of 3.40 m/s) when both instruments are effectively used, instead of 9 cm/s and 7 cm/s respectively when only the ERS-1 or ERS-2 data are assimilated. Further, a study of the most significant cases, imposing an arbitrary minimum value, so-called «impact threshold», on the vector differences induced by the data in the first guess field, indicates that the main improvements brought by the ERS-1 scatterometer are little reduced when the ERS-2 data are already assimilated (Figure 18).

Nevertheless, the reverse is far from being true (Figure 19), as if the orbit phasing between the two satellites, leading ERS-2 to fly over the same areas as ERS-1 24 hours later, made its data redundant with the information kept from ERS-1 after one day. This tends to be confirmed when the impact of the ERS-2 data is evaluated against the ERS-1 or ERS-2 data only (Figure 20), instead of those from both scatterometers : the improvements already brought by ERS-1 seem to be harder to increase along the ERS-2 swaths, and so to remain effectively to a large extent in the places where they have been generated.

Those early results suggest that it might be necessary to have well separated data coverages, both in time and space, to make the best use of measurements from double-swath or multiple scatterometers in NWP. However, the possible loss in case of redundancy, with a reduction from 6 cm/s to 4 cm/s on average for the RMS gain brought by the redundant scatterometer in the ERS tandem case, appears to be limited. The assimilation experiments will be classically extended to 2 weeks anyway, and 10 day forecasts will be made from the analyses obtained to allow more definite conclusions to be drawn.

References

Cavanié, A and P Lecomte, 1987 : Study of a method to dealias winds from ERS–1 data. Finalreport of ESA contract No 6874/87/CP–I, vol. 1, ESA publication division.

Courtier, P et al., 1993 : Variational assimilation at ECMWF. ECMWF Research Department Tech. Memo. 194, available from ECMWF.

Gaffard, C and H Roquet, 1996 : Impact of the ERS-1 scatterometer wind data on the ECMWF3D-VAR assimilation system. Submitted to Q.J.R. Meteorol. Soc.

Hoffman, R N, 1993 : A preliminary study of the impact of C-band scatterometer wind data on global scale numerical weather prediction. J. Geophys. Res., 98, 10233-10244.

Janssen, P and B Hansen, 1996 : Analysis of results from 3D-Var E-suites using the WAM model. ECMWF Research Department Memorandum, available from ECMWF.

Lorenc, A, 1981 : A global three-dimensional multivariate statistical interpolation scheme. Mon. Wea. Rev., 109, 701-721.

Ritchie, H, C Temperton, A Simmons, M Hortal, T Davies, D Dent and M Hamrud, 1995 : Implementation of the semi-lagrangian method in a high resolution version of the ECMWF forecast model. Mon. Wea. Rev., 123, 489-514.

Stoffelen, A and D Anderson, 1995 : The ECMWF contribution to the characterization,interpretation, calibration and validation of ERS–1 scatterometer backscatter measurements and winds, and their use in Numerical Weather Prediction Models. Final report of ESA contract No 9097/90/NL/BI, ESA publication division.

Tomassini, M, D Le Meur and R Saunders, 1996 : Satellite observations of hurricanes and theirimpact on NWP model analyses and forecasts. Submitted to Mon. Wea. Rev.

Figure Legends

Figure 1. Antenna biases obtained by «ocean calibration» with the first week of data.

Figure 2. Antenna biases obtained by «ocean calibration» for the fifth week of the commissioning after removing the biases estimated from the first week of data.

Figure 3. Antenna biases obtained by «ocean calibration» after the LUT change from 19 March 1996.

Figure 4. Same as Figure 3, but for ERS-1.

Figure 5. Mean normalized distance to the cone and quality control scores obtained for the fifth week of the commissioning.

Figure 6. Same as Figure 5, but after removing the antenna biases estimated from the first week of data.

Figure 7. Mean normalized distance to the cone and quality control scores obtained after the LUT change from 19 March 1996.

Figure 8. Same as Figure 7, but for ERS-1.

Figure 9. Wind speed statistics obtained for the fifth week of the commissioning (UWI data).

Figure 10. Same as figure 9, but after removing the antenna biases estimated from the first week of data (PRESCAT data).

Figure 11. Wind speed statistics obtained after the LUT change from 19 March 1996.

Figure 12. De-aliased wind vectors given respectively by PRESCAT (black flags) and the 3D-Var analysis (grey flags) for ERS-1 on 17 December 1994 at O UTC.

Figure 13. Difference between the RMS errors of the geopotential heights forecast at 1000 hPa with and without scaterrometer data, taking the analyses including scatterometer data as a reference. Contouring is done only for values greater than 5 m or lower than -5 m, with a 5-m interval, and negative areas are shaded.

Figure 14. OPS and SCAT/3D-Var 48 hour forecasts (a) and b)) and associated analyses (c) and d)) for Hurricane Iris on 1 September 1995 at 12 UTC. The arrows represent the surface wind field and the isolines the surface pressure in mb. The reported cyclone centre is marked by the black square.

Figure 15. OPS and SCAT/3D-Var analyses for Hurricane Luis on 3 September 1995 at 12 UTC (a) and b)) and corresponding 48 hour forecasts valid on 5 September 1995 at 12 UTC (c) and d)). The arrows represent the surface wind field and the isolines the surface pressure in mb. The reported cyclone centre is marked by the black square.

Figure 16. Forecast scores for wave height obtained with the SCAT/3D-Var (solid line) and OPS (dotted line) experiments in the Southern Hemisphere from 24 August to 5 October 1995 (average over 43 cases). a) represents standard deviation errors and b) anomaly correlations.

Figure 17. Same as Figure 16, but for the Northern Hemisphere and the period from 4 to 16 October 1995 (average over 13 cases).

Figure 18. Vector RMS differences between scatterometer and FGAT winds when no scatterometer data or only ERS-1 data are assimilated (left), and when only ERS-2 or both ERS-1 and ERS-2 data are assimilated (right). The FGAT winds are referred to as NOSCAT, ERS1, ERS2 and ERS1+2 respectively, and the results are represented as a function of the impact thresholds associated to the (ERS1 - NOSCAT) and (ERS1+2 - ERS2) differences. The dotted lines indi-

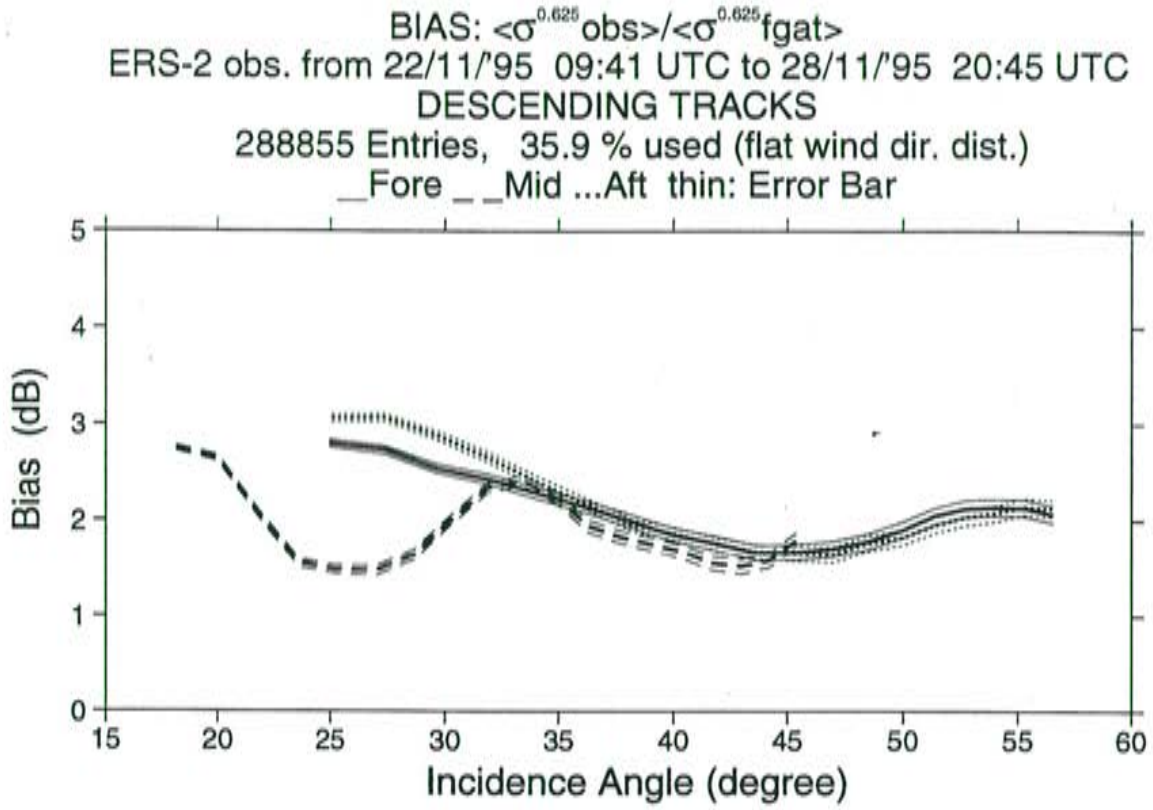
BIAS: <σ^0.625obs>/<σ^0.625fgat>
ERS-2 obs. from 22/11/'95 09:41 UTC to 28/11/'95 20:45 UTC
DESCENDING TRACKS
288855 Entries, 35.9 % used (flat wind dir. dist.)
_Fore _ _Mid ...Aft thin: Error Bar
Bias (dB)
Incidence Angle (degree)

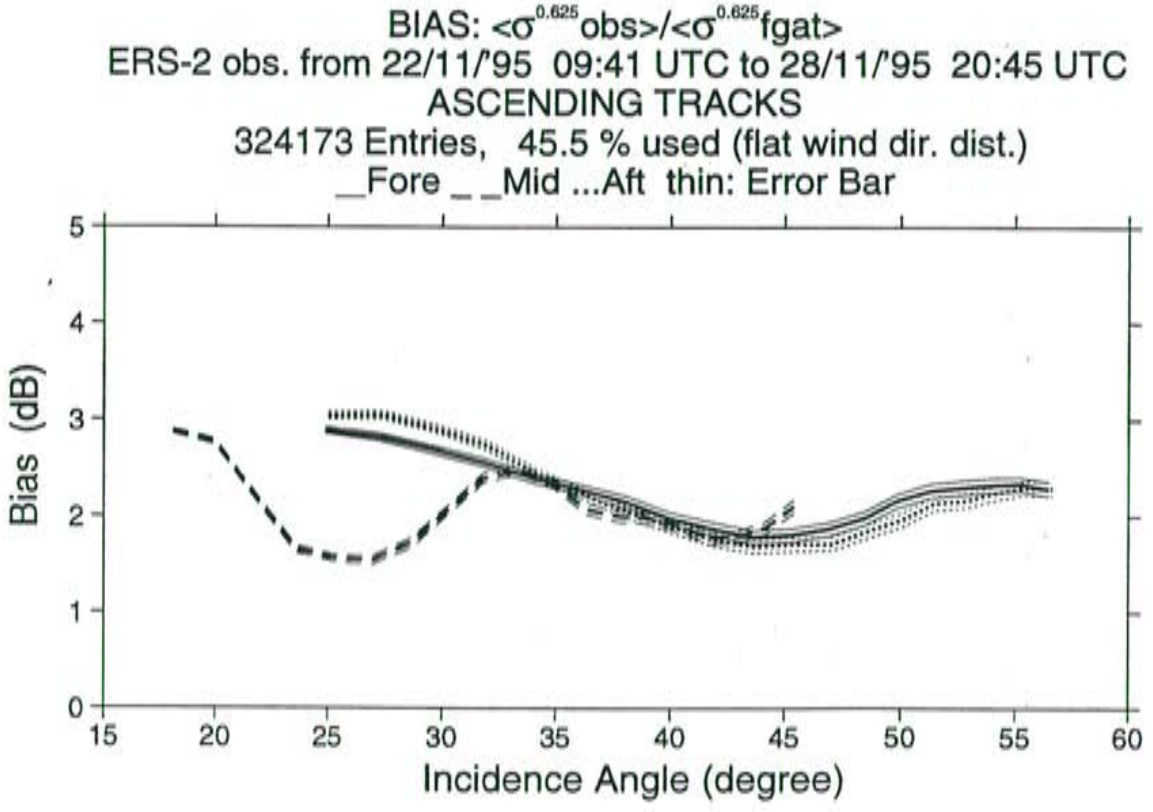
BIAS: <σ^0.625obs>/<σ^0.625fgat>
ERS-2 obs. from 22/11/'95 09:41 UTC to 28/11/'95 20:45 UTC
ASCENDING TRACKS
324173 Entries, 45.5 % used (flat wind dir. dist.)
_Fore _ _Mid ...Aft thin: Error Bar
Bias (dB)
Incidence Angle (degree)

cate the proportion of data exceeding a given threshold in logarithmic scale. Both the ERS-1 and ERS-2 data are taken into account to compute the RMS differences.

Figure 19. Same as Figure 18, but for the cases where no scatterometer data or only ERS-2 data are assimilated (left), and when only ERS-1 or both ERS-1 and ERS-2 data are assimilated (right). The results are now represented as a function of the impact thresholds associated to the (ERS2 - NOSCAT) and (ERS1+2 - ERS1) differences.

Figure 20. Vector RMS differences between scatterometer and FGAT winds when only ERS-1 or both ERS-1 and ERS-2 data are assimilated, taking into account either the ERS-1 data (left) or the ERS-2 data (right) to compute the RMS differences. The FGAT winds obtained with ERS-1 and both ERS-1 and ERS-2 are referred to as ERS1 and ERS1+2 respectively, and the results are represented as a function of the impact thresholds associated to the (ERS1+2 - ERS1) differences. The dotted lines indicate the proportion of data exceeding a given threshold in logarithmic scale.

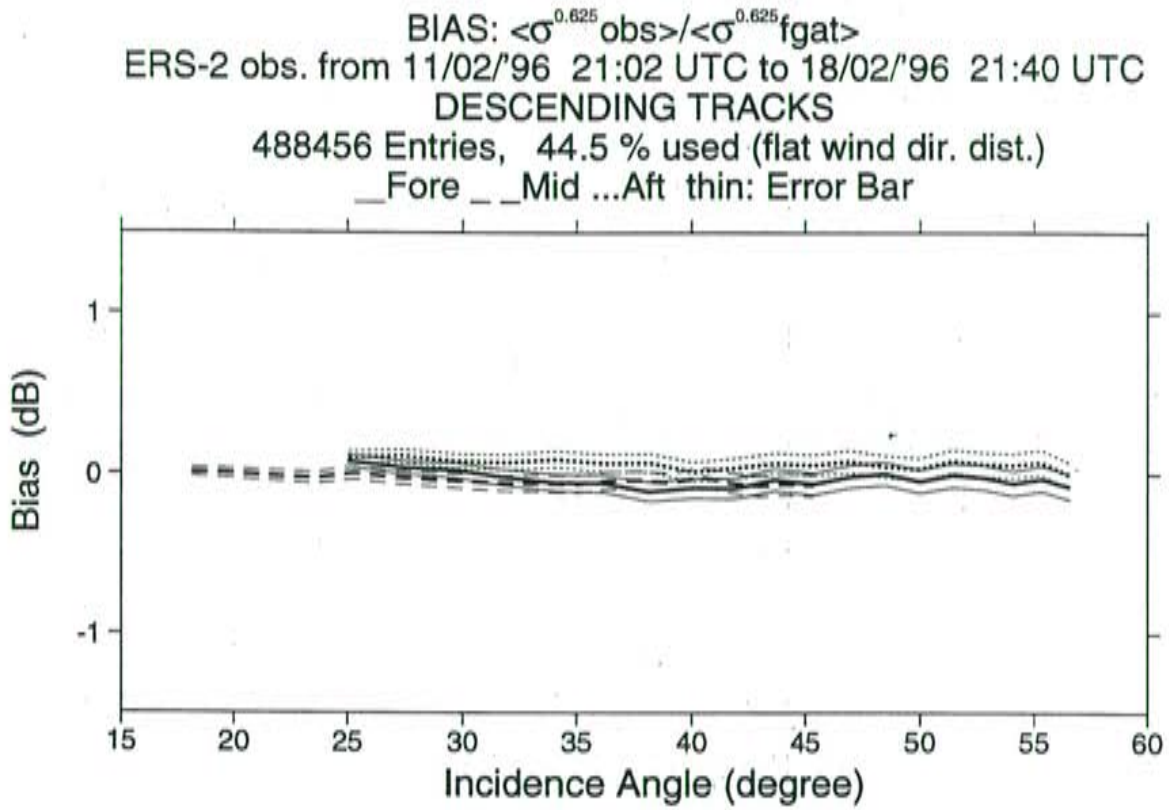
BIAS: <σ^0.625 obs>/<σ^0.625 fgat>
ERS-2 obs. from 11/02/'96 21:02 UTC to 18/02/'96 21:40 UTC
DESCENDING TRACKS
488456 Entries, 44.5 % used (flat wind dir. dist.)
_Fore _ _Mid ...Aft thin: Error Bar
Bias (dB)
1
0
-1
15
20
25
30
35
40
45
50
55
60
Incidence Angle (degree)

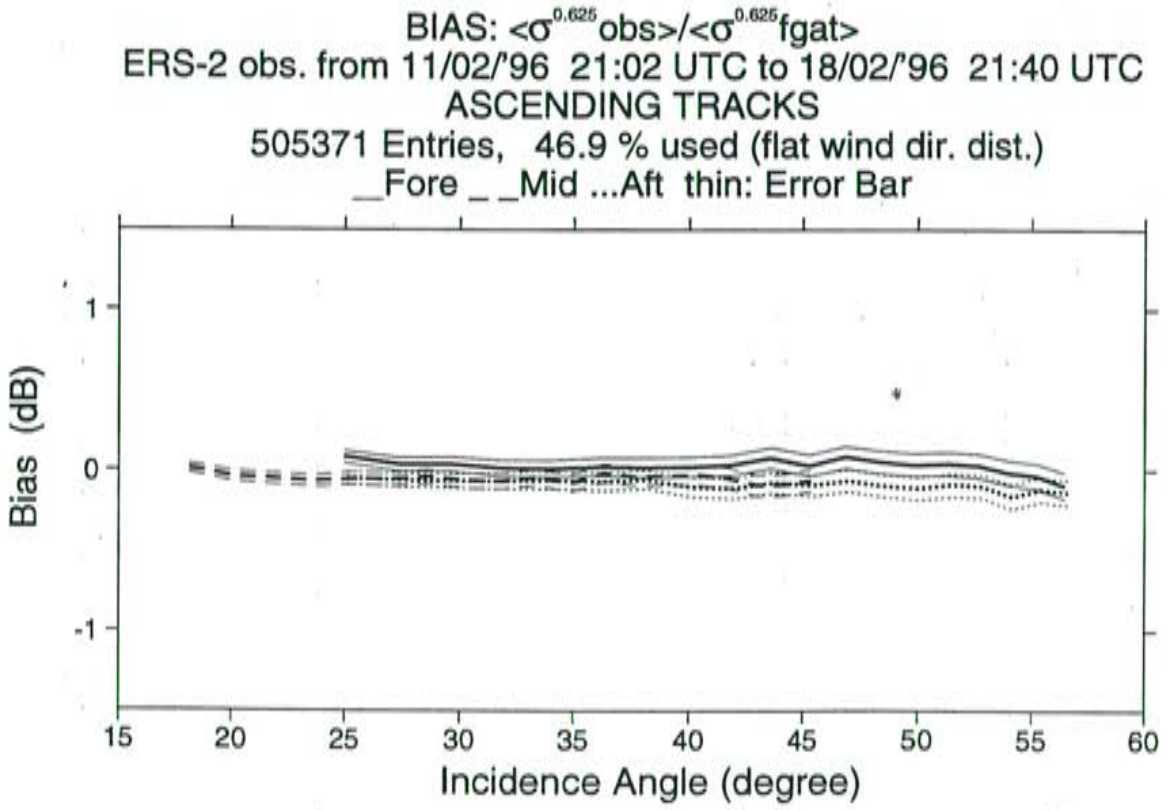
BIAS: <σ^0.625 obs>/<σ^0.625 fgat>
ERS-2 obs. from 11/02/'96 21:02 UTC to 18/02/'96 21:40 UTC
ASCENDING TRACKS
505371 Entries, 46.9 % used (flat wind dir. dist.)
_Fore _ _Mid ...Aft thin: Error Bar
Bias (dB)
1
0
-1
15
20
25
30
35
40
45
50
55
60
Incidence Angle (degree)

BIAS: $<\sigma^{0.625}obs>/<\sigma^{0.625}fgat>$
ERS-2 obs. from 18/03/'96 21:17 UTC to 01/04/'96 03:00 UTC
DESCENDING TRACKS
944949 Entries, 43.0 % used (flat wind dir. dist.)
_Fore _ _Mid ...Aft thin: Error Bar

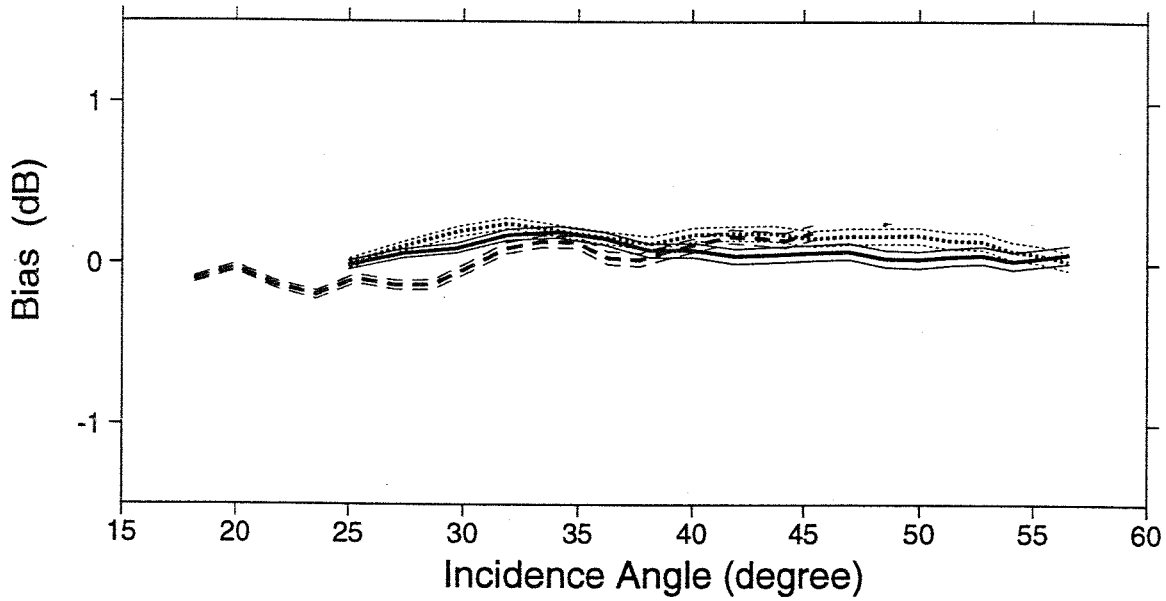

BIAS: $<\sigma^{0.625}obs>/<\sigma^{0.625}fgat>$
ERS-2 obs. from 18/03/'96 21:17 UTC to 01/04/'96 03:00 UTC
ASCENDING TRACKS
993667 Entries, 40.7 % used (flat wind dir. dist.)
_Fore _ _Mid ...Aft thin: Error Bar

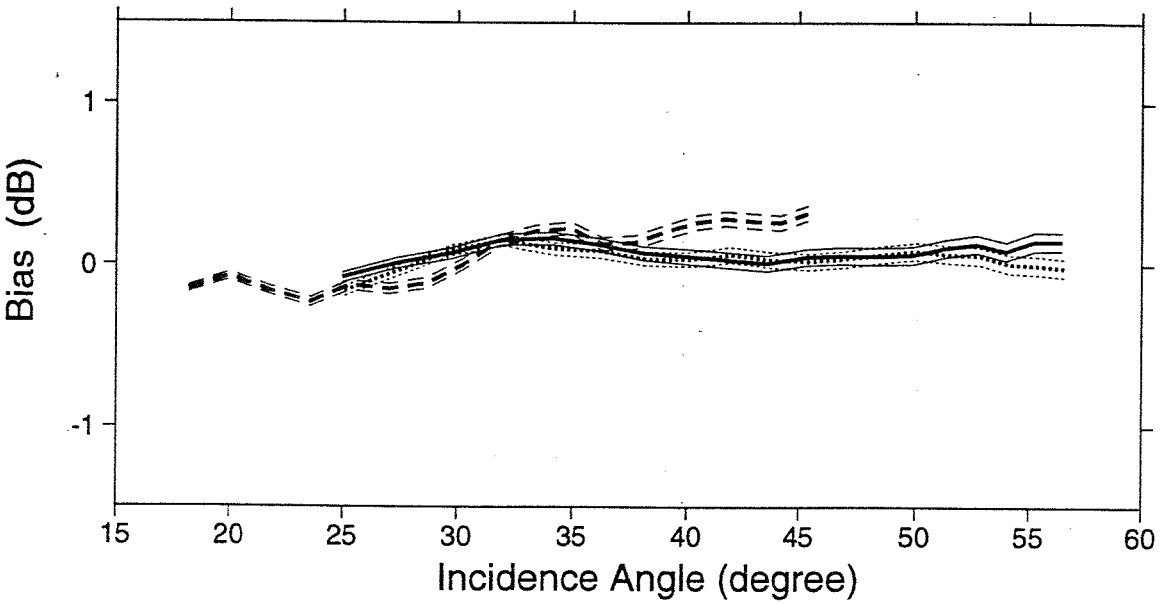

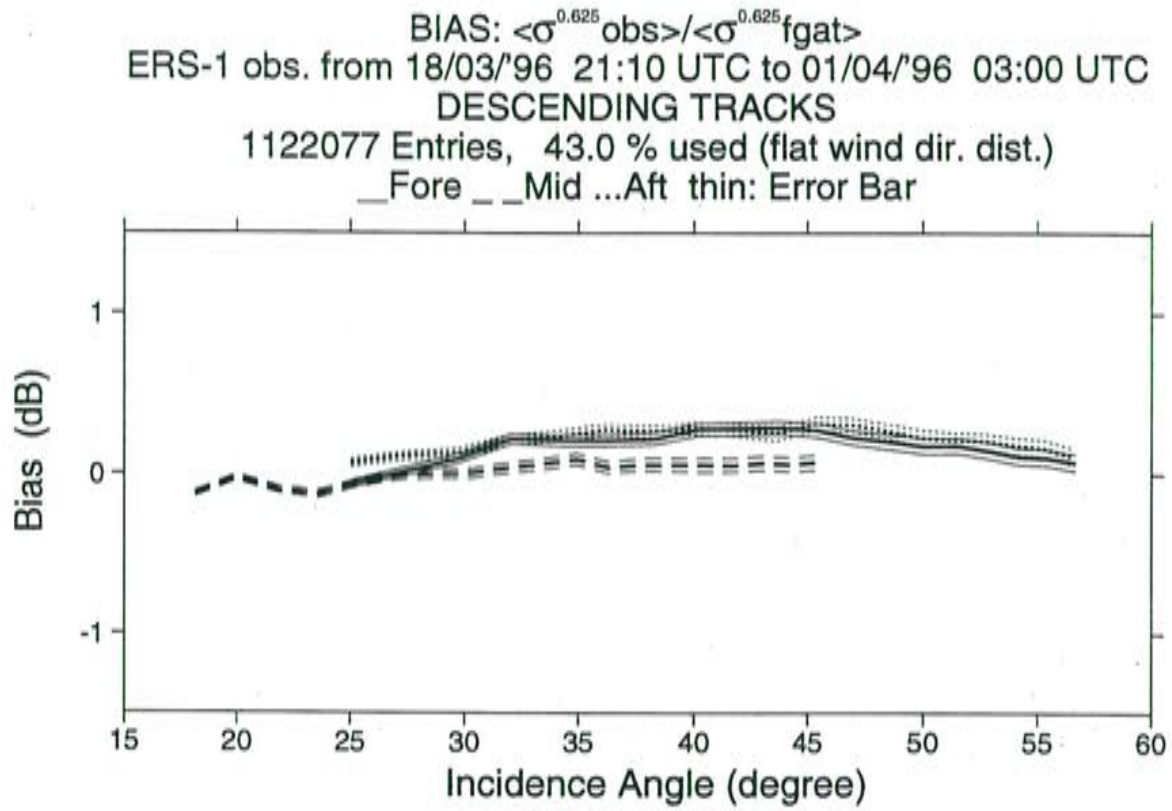
BIAS: <σ^0.625obs>/<σ^0.625fgat>
ERS-1 obs. from 18/03/'96 21:10 UTC to 01/04/'96 03:00 UTC
DESCENDING TRACKS
1122077 Entries, 43.0 % used (flat wind dir. dist.)
_Fore _ _Mid ...Aft thin: Error Bar
Bias (dB)
1
0
-1
15
20
25
30
35
40
45
50
55
60
Incidence Angle (degree)

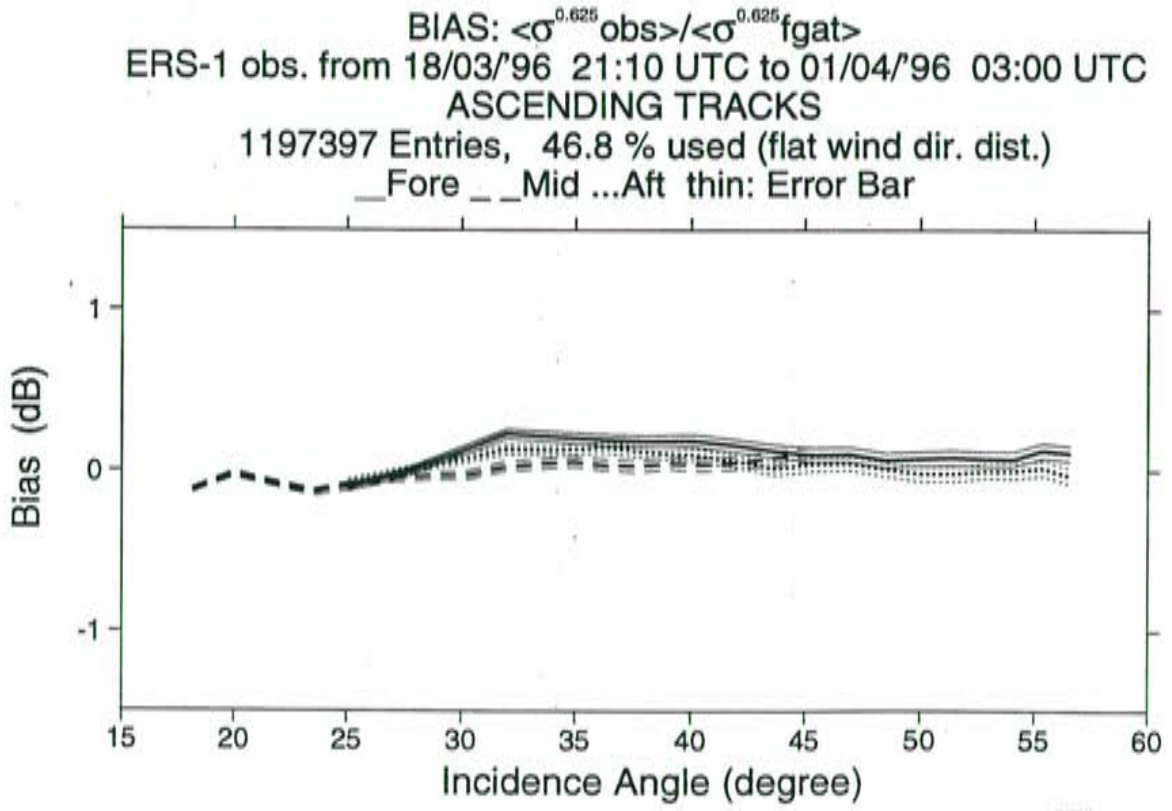
BIAS: <σ^0.625obs>/<σ^0.625fgat>
ERS-1 obs. from 18/03/'96 21:10 UTC to 01/04/'96 03:00 UTC
ASCENDING TRACKS
1197397 Entries, 46.8 % used (flat wind dir. dist.)
_Fore _ _Mid ...Aft thin: Error Bar
Bias (dB)
1
0
-1
15
20
25
30
35
40
45
50
55
60
Incidence Angle (degree)

Monitoring of Sigma0 triplets versus CMOD4 for ERS2

from 960212 to 960219

(solid) mean normalised distance to the cone over 6 h

(dashed) nb of data rejected by ESA flag, SST or land-sea mask / total number

(dotted) total number of data in log. scale (1 for 60000)

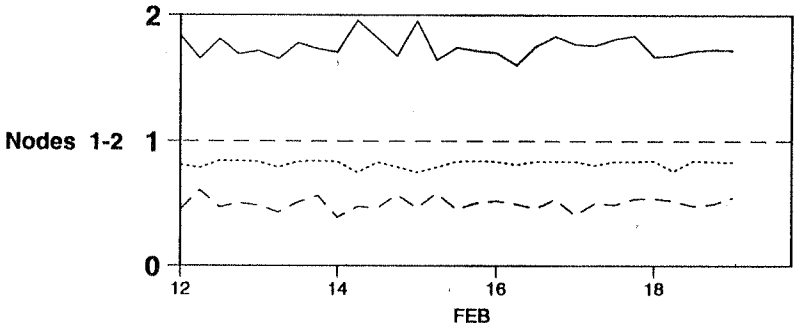

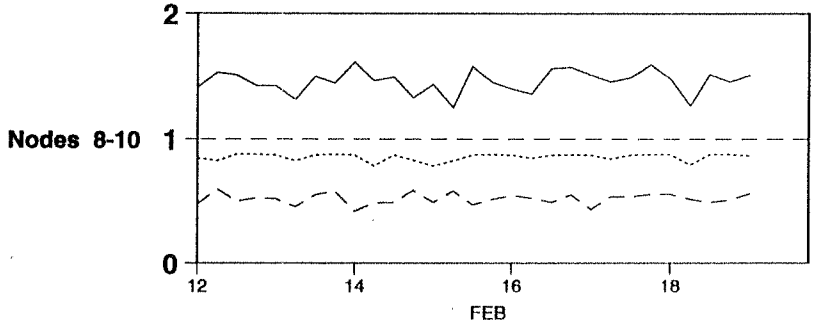

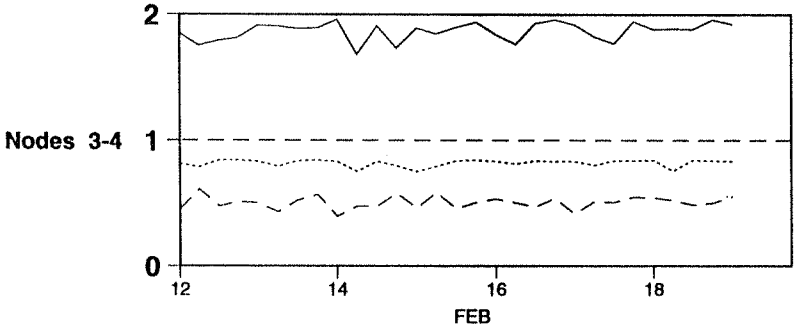

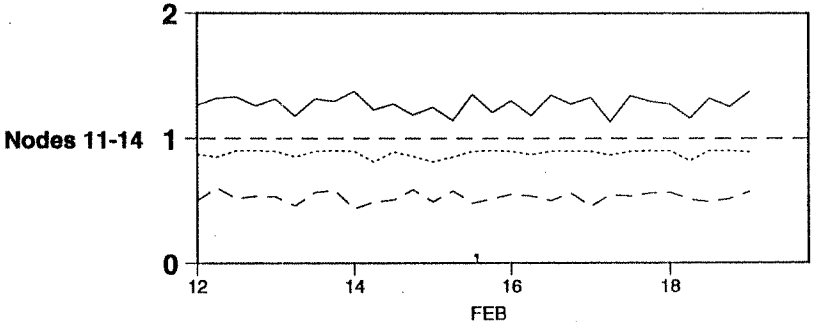

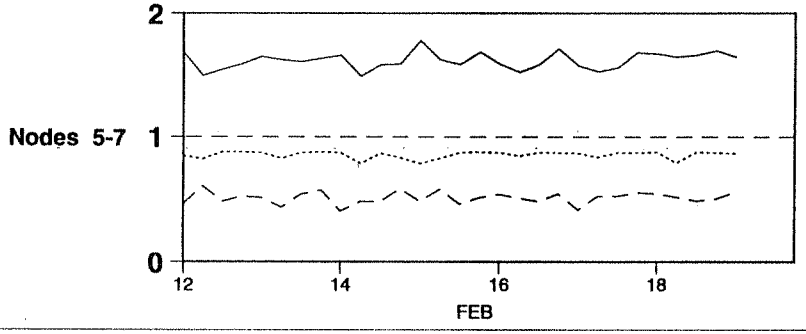

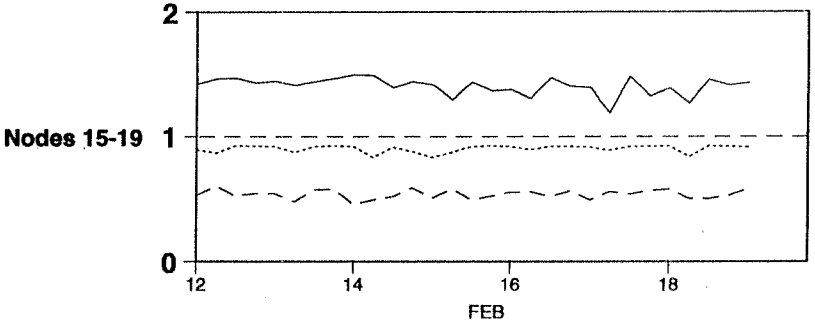

Monitoring of Sigma0 triplets versus CMOD4 for ERS2

from 960212 to 960219

(solid) mean normalised distance to the cone over 6 h

(dashed) nb of data rejected by ESA flag, SST or land-sea mask / total number

(dotted) total number of data in log. scale (1 for 60000)

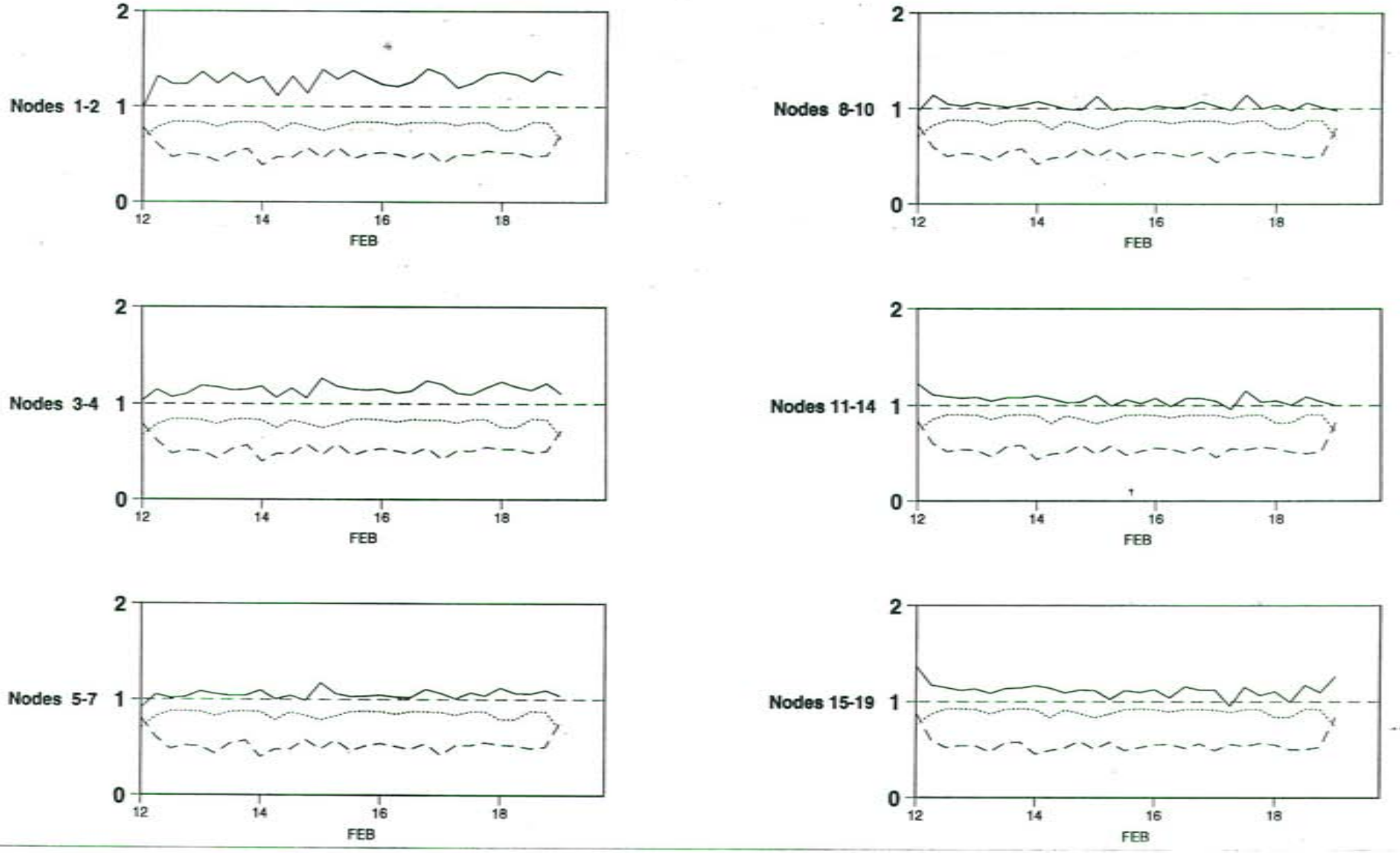

Monitoring of Sigma0 triplets versus CMOD4 for ERS2

from 960318 to 960401

- (solid) mean normalised distance to the cone over 6 h

(dashed) nb of data rejected by ESA flag, SST or land-sea mask / total number

(dotted) total number of data in log. scale (1 for 60000)

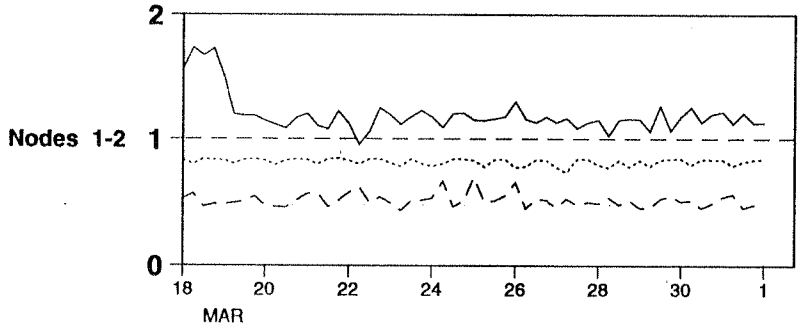

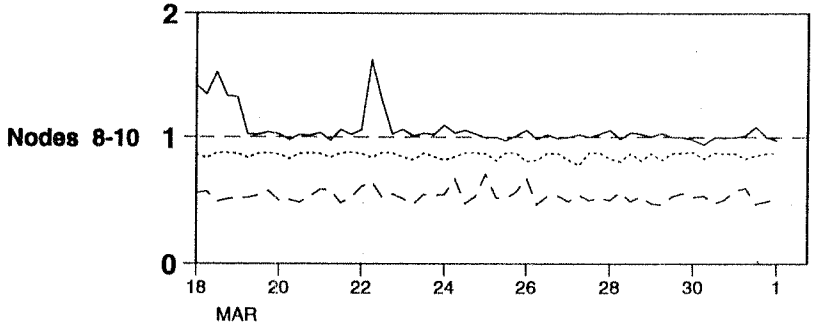

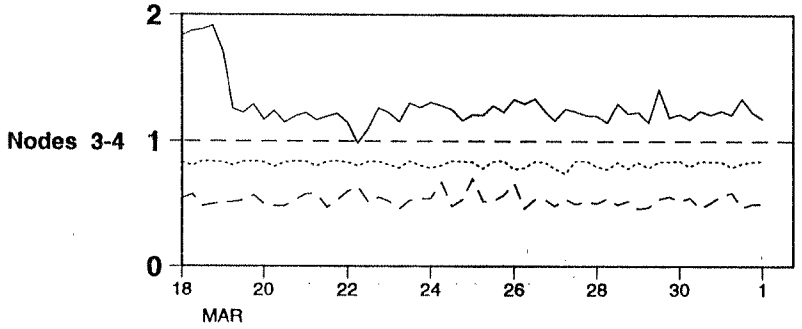

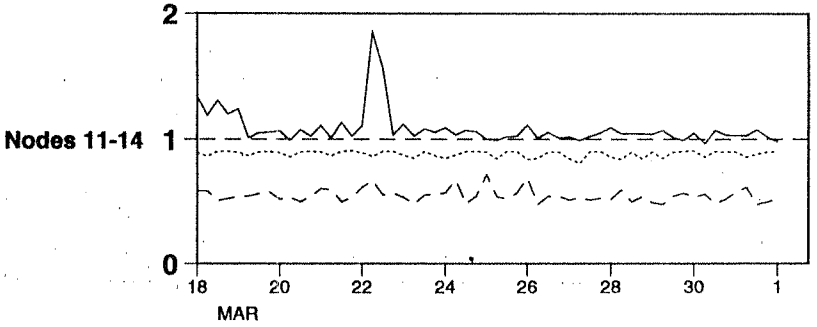

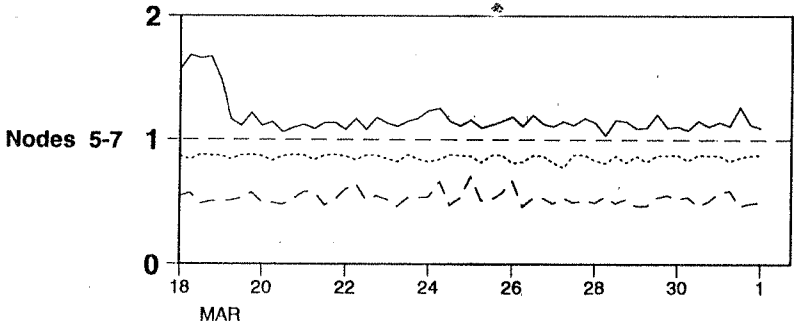

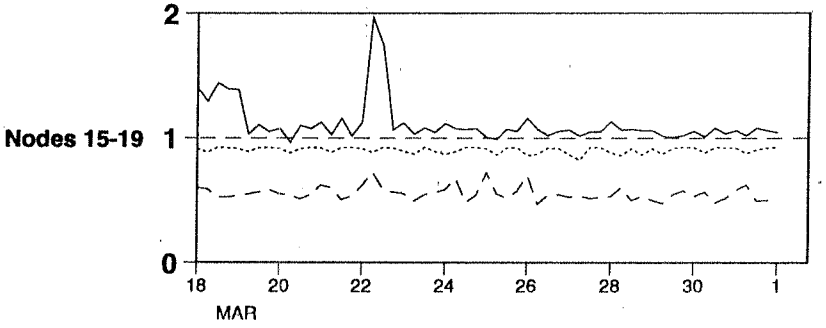

Monitoring of Sigma0 triplets versus CMOD4 for ERS1

from 960318 to 960401

(solid) mean normalised distance to the cone over 6 h

(dashed) nb of data rejected by PRESCAT quality control / total number

(dotted) total number of data in log. scale (1 for 60000)

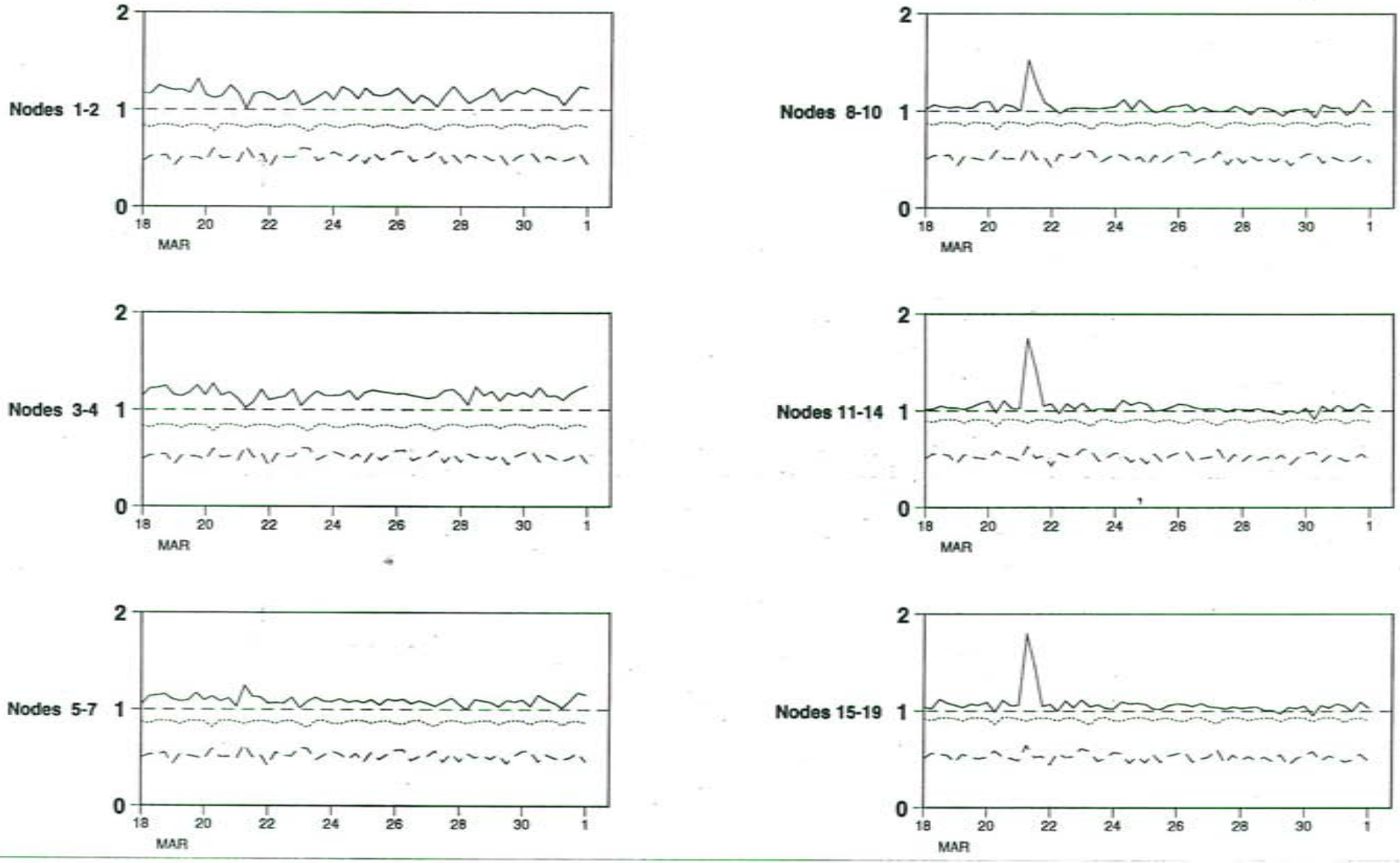

Monitoring of UWI winds versus FGAT for ERS2

from 960212 to 960219

(solid) wind speed UWI - FGAT mean over 6h (m/s)

(dashed) wind speed UWI - FGAT standard deviation over 6h (m/s)

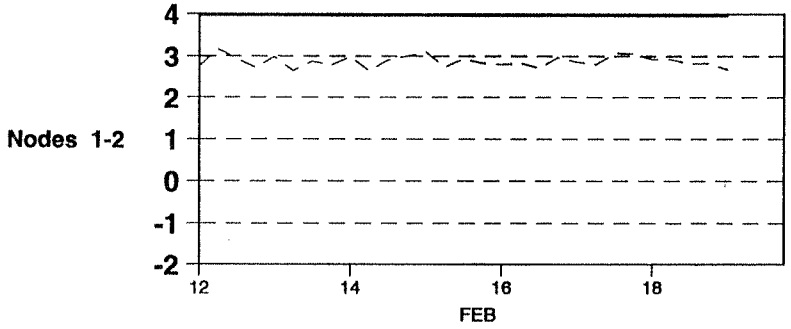

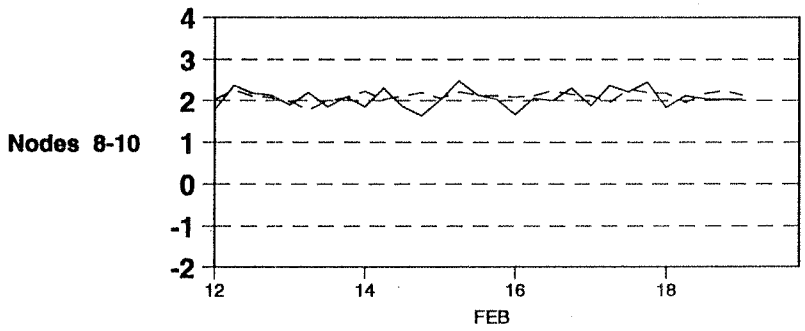

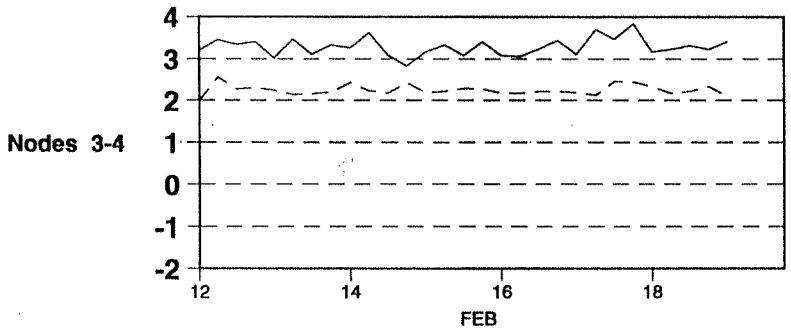

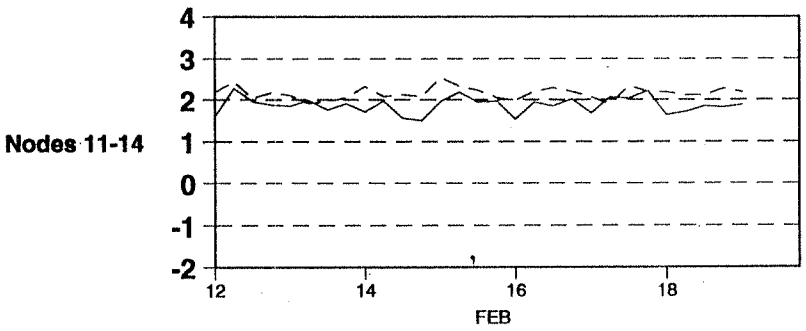

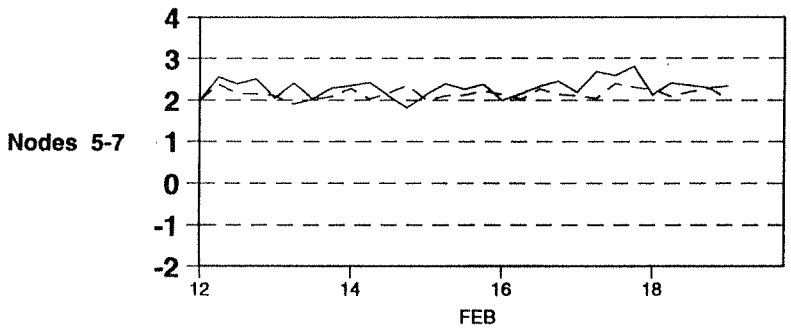

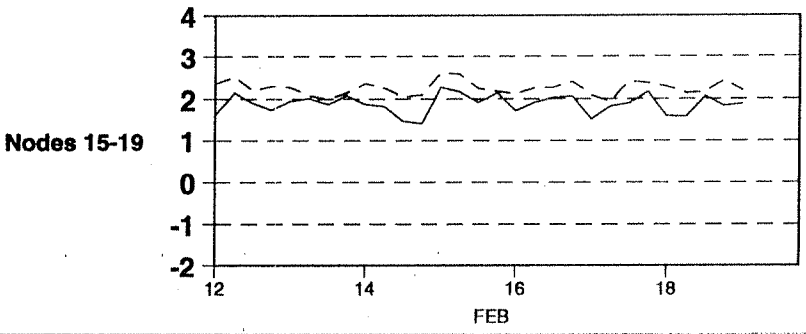

Monitoring of PRESCAT winds versus FGAT for ERS2

from 960212 to 960219

(solid) wind speed PRESCAT - FGAT mean over 6h (m/s)

(dashed) wind speed PRESCAT - FGAT standard deviation over 6h (m/s)

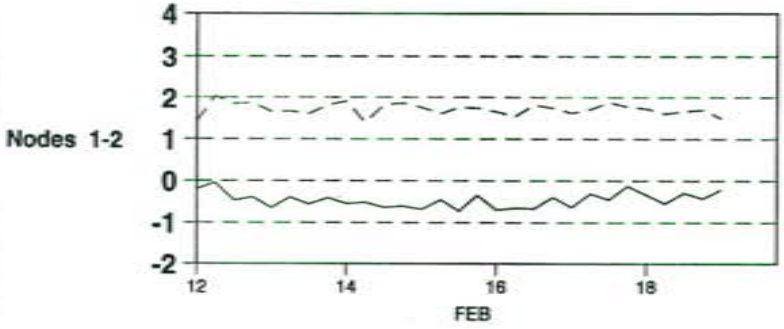

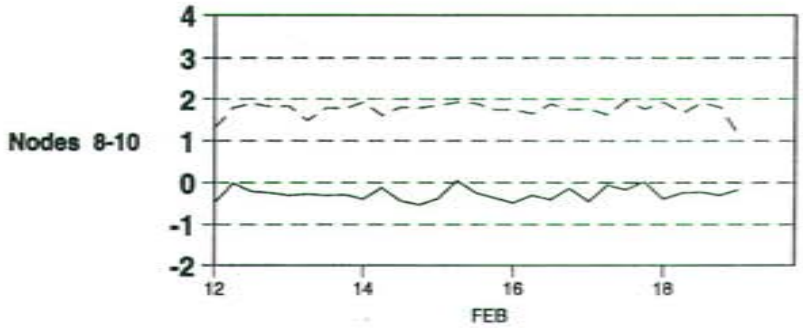

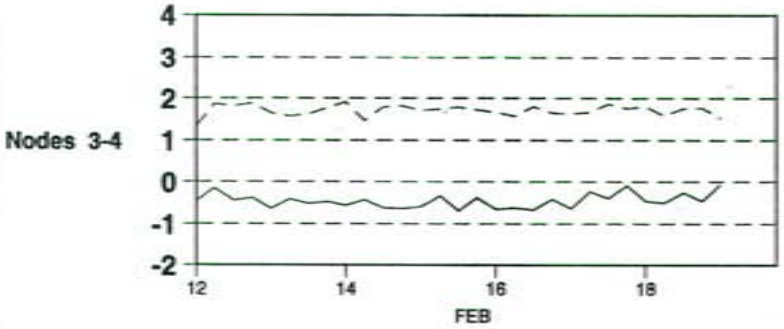

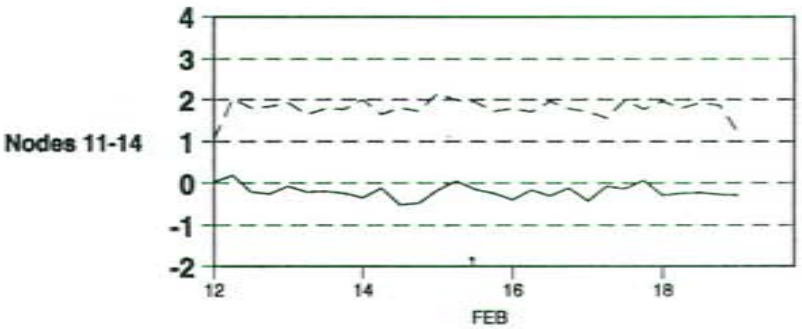

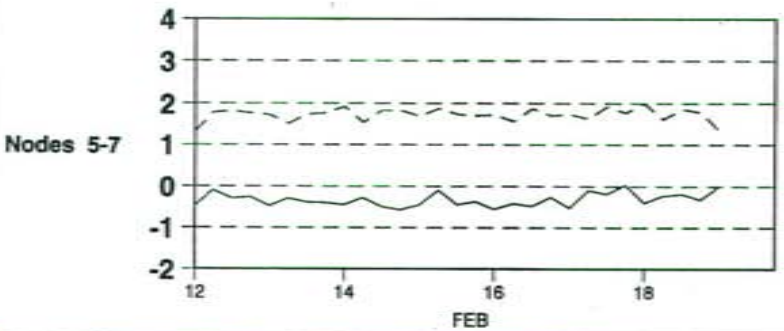

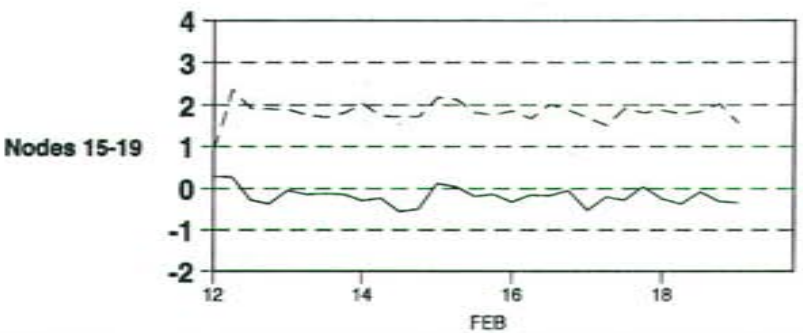

Monitoring of UWI winds versus FGAT for ERS2

from 960318 to 960401

(solid) wind speed UWI - FGAT mean over 6h (m/s)

(dashed) wind speed UWI - FGAT standard deviation over 6h (m/s)

Nodes 1-2

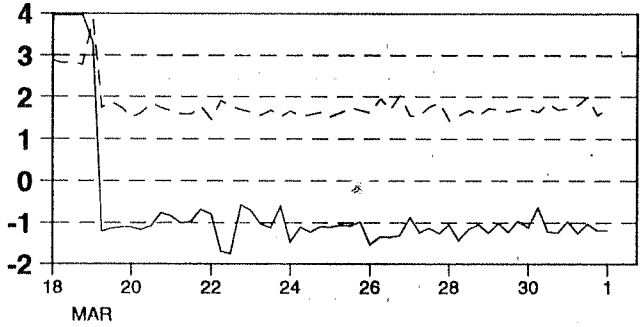

Nodes 8-10

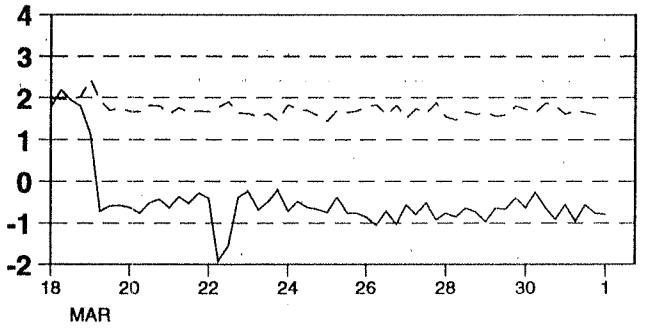

Nodes 3-4

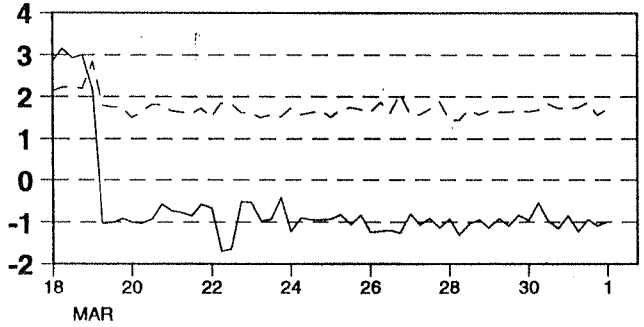

Nodes 11-14

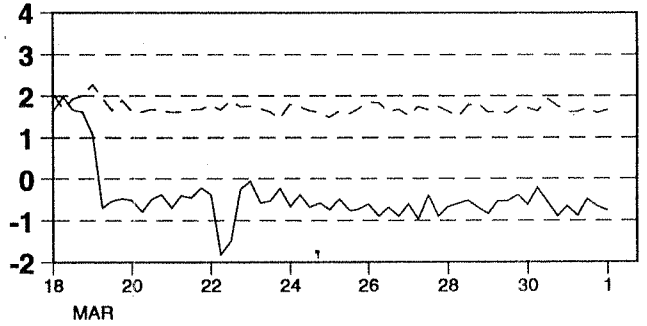

Nodes 5-7

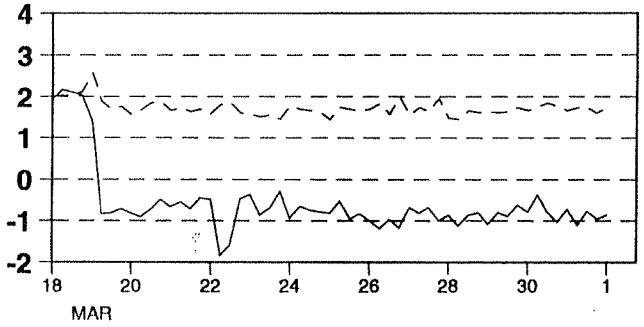

Nodes 15-19

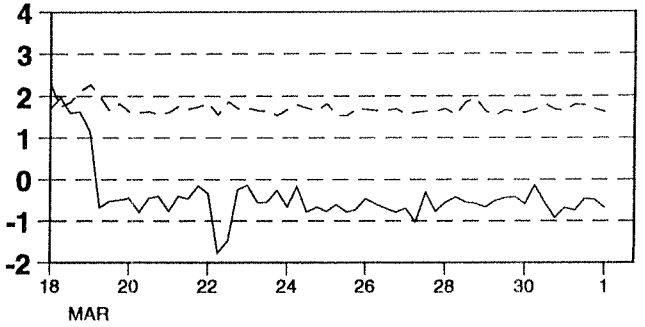

date : 941217 time 0
Prescat 3dvar h2dana

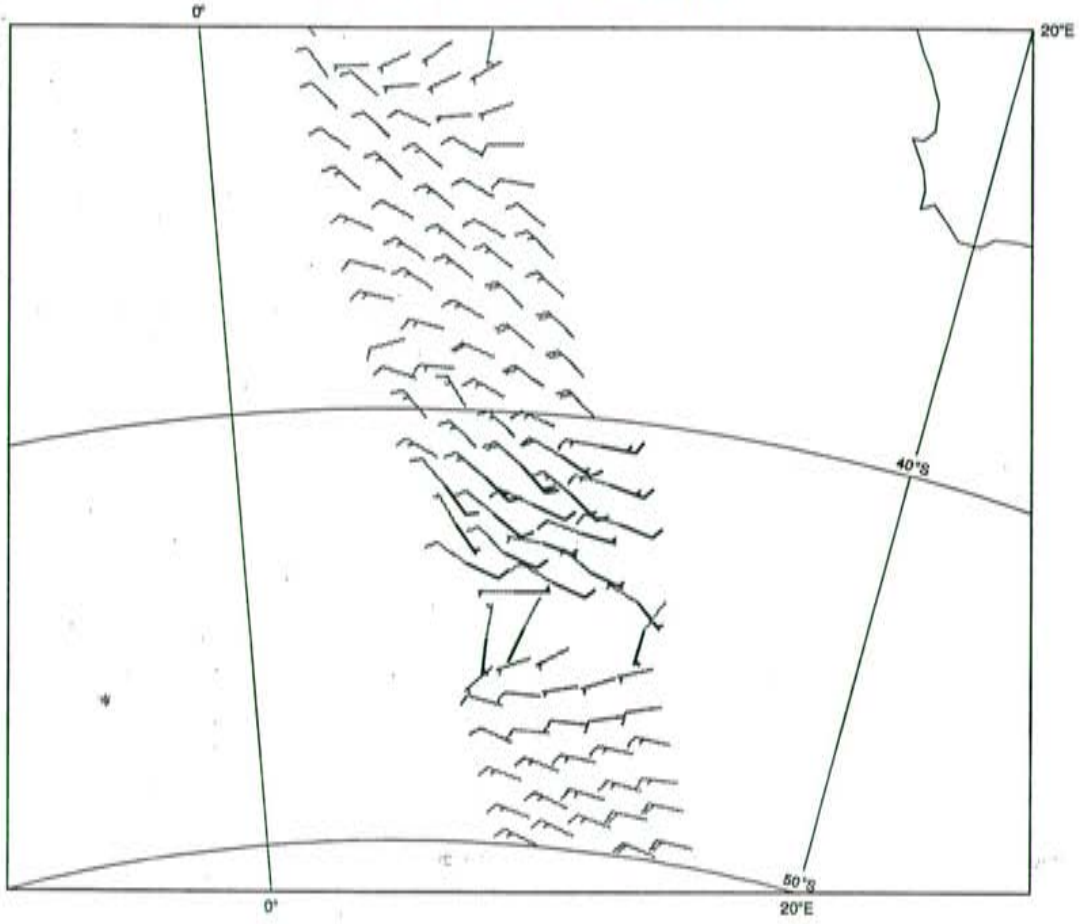

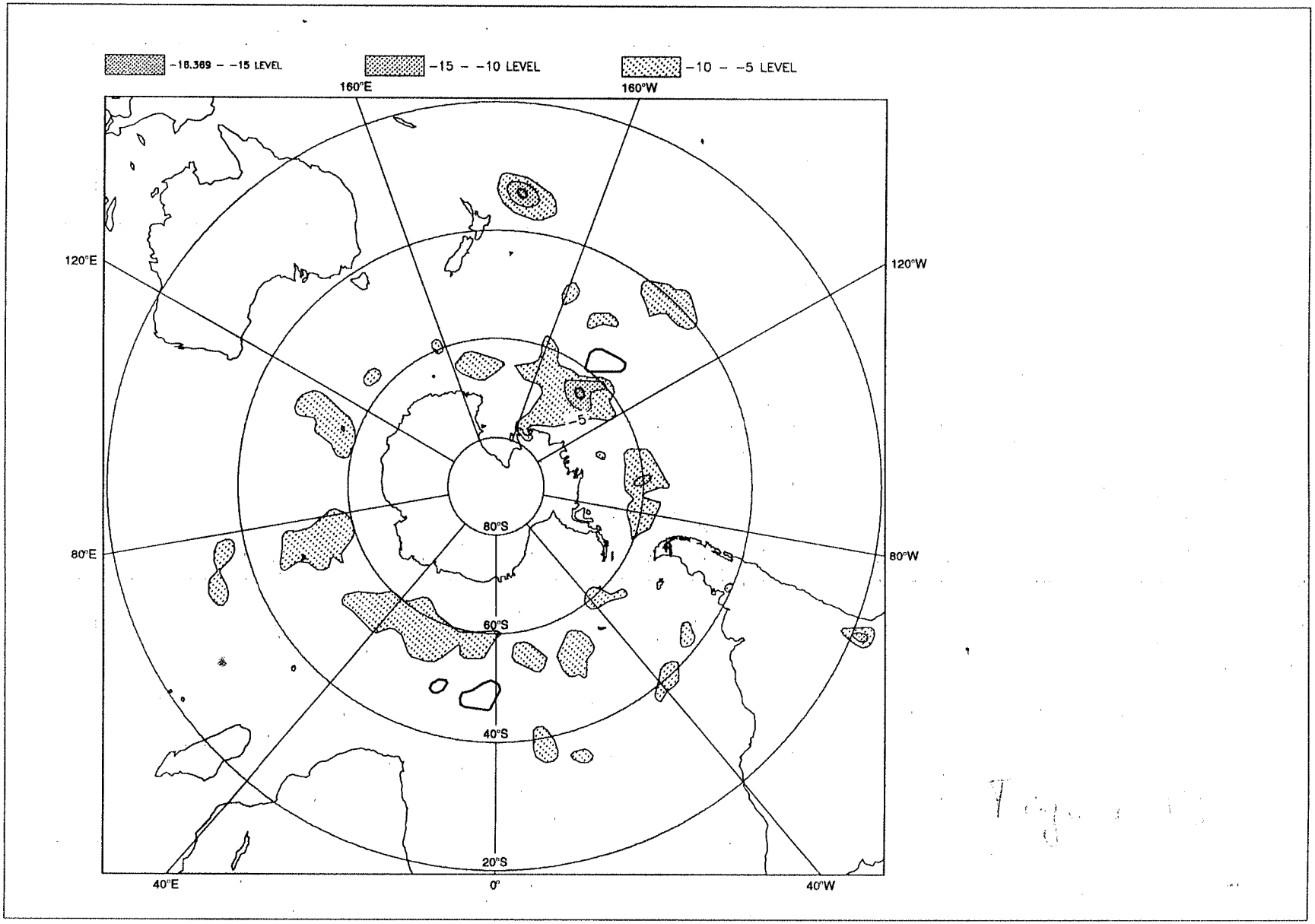
-16.369 - -15 LEVEL
-15 - -10 LEVEL
-10 - -5 LEVEL
160°E
160°W
120°E
120°W
80°E
80°W
40°E
0°
40°W
80°S
60°S
40°S
20°S
-5

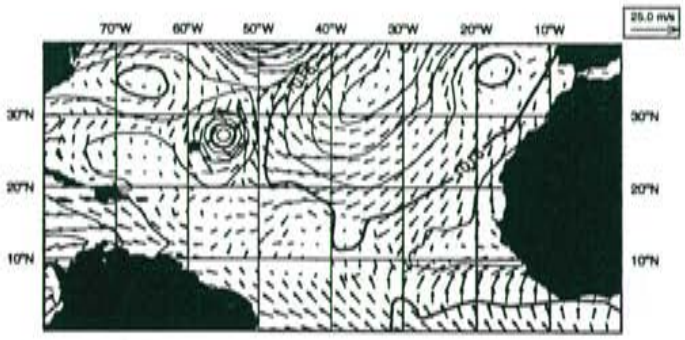
25.0 m/s
70°W
60°W
50°W
40°W
30°W
20°W
10°W
30°N
20°N
10°N
1012
1016

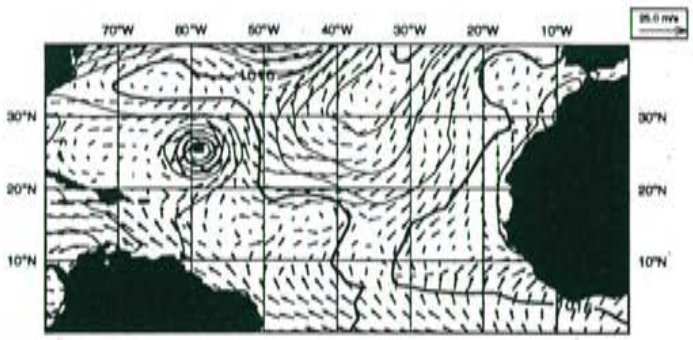
25.0 m/s
70°W
60°W
50°W
40°W
30°W
20°W
10°W
30°N
20°N
10°N
1016

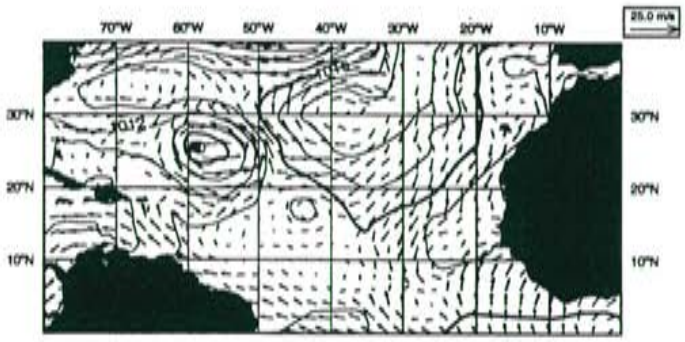
25.0 m/s
70°W
60°W
50°W
40°W
30°W
20°W
10°W
30°N
20°N
10°N
1012

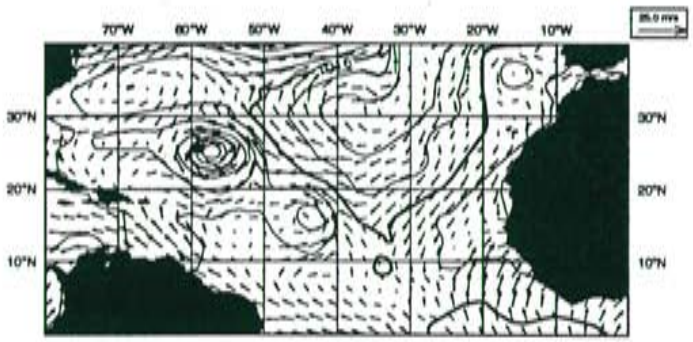
25.0 m/s
70°W
60°W
50°W
40°W
30°W
20°W
10°W
30°N
20°N
10°N

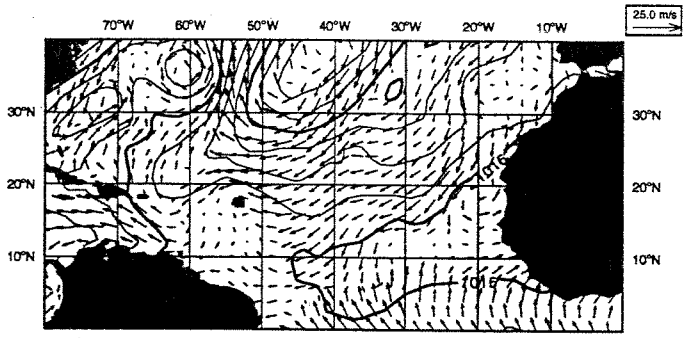
25.0 m/s
70°W
60°W
50°W
40°W
30°W
20°W
10°W
30°N
20°N
10°N
1016

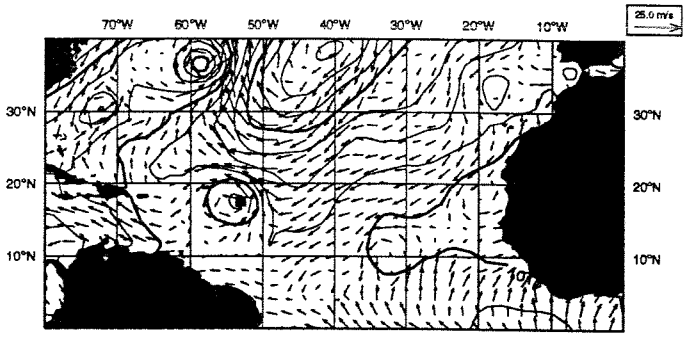
25.0 m/s
70°W
60°W
50°W
40°W
30°W
20°W
10°W
30°N
20°N
10°N

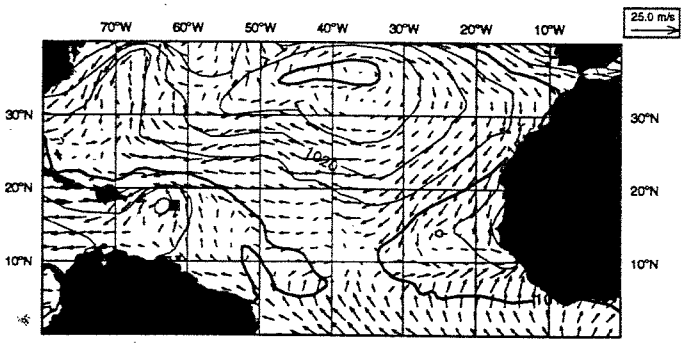
25.0 m/s
70°W
60°W
50°W
40°W
30°W
20°W
10°W
30°N
20°N
10°N
1020

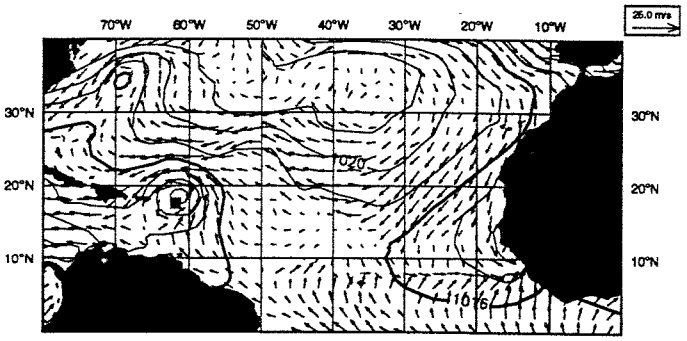
25.0 m/s
70°W
60°W
50°W
40°W
30°W
20°W
10°W
30°N
20°N
10°N
1020
1016

a)

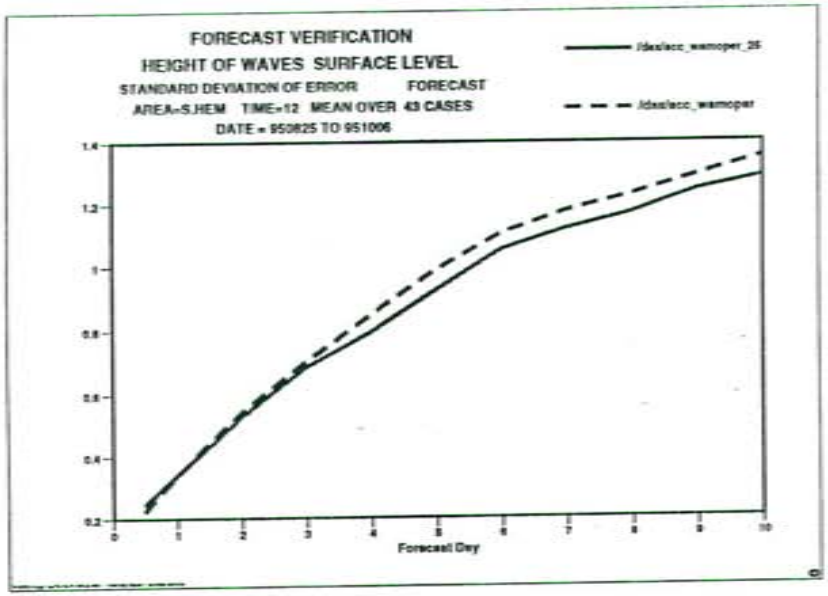
FORECAST VERIFICATION
HEIGHT OF WAVES SURFACE LEVEL
STANDARD DEVIATION OF ERROR FORECAST
AREA=S.HEM TIME=12 MEAN OVER 43 CASES
DATE = 950825 TO 951006
/dea/ecc_wamoper_25
/dea/ecc_wamoper
Forecast Day

b)

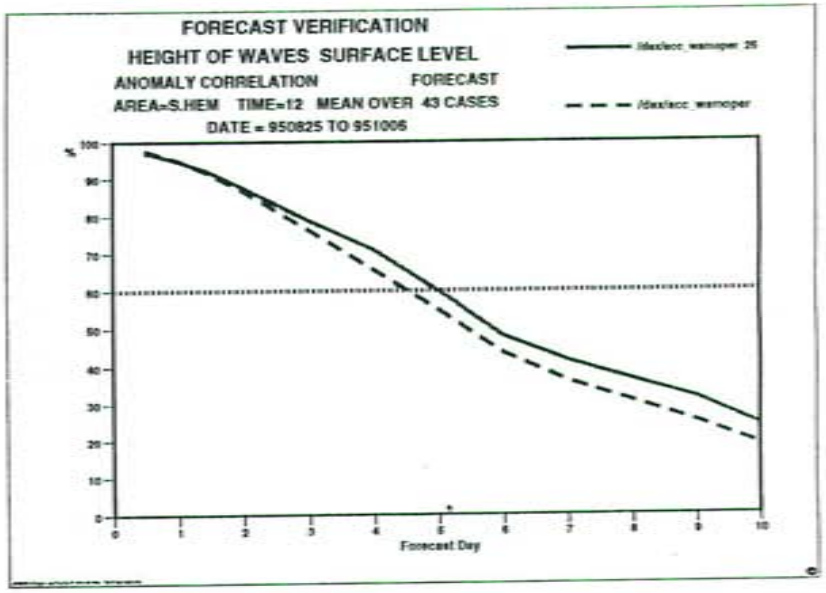
FORECAST VERIFICATION
HEIGHT OF WAVES SURFACE LEVEL
ANOMALY CORRELATION FORECAST
AREA=S.HEM TIME=12 MEAN OVER 43 CASES
DATE = 950825 TO 951006
/dea/ecc_wamoper_25
/dea/ecc_wamoper
Forecast Day

Figure 16

a)

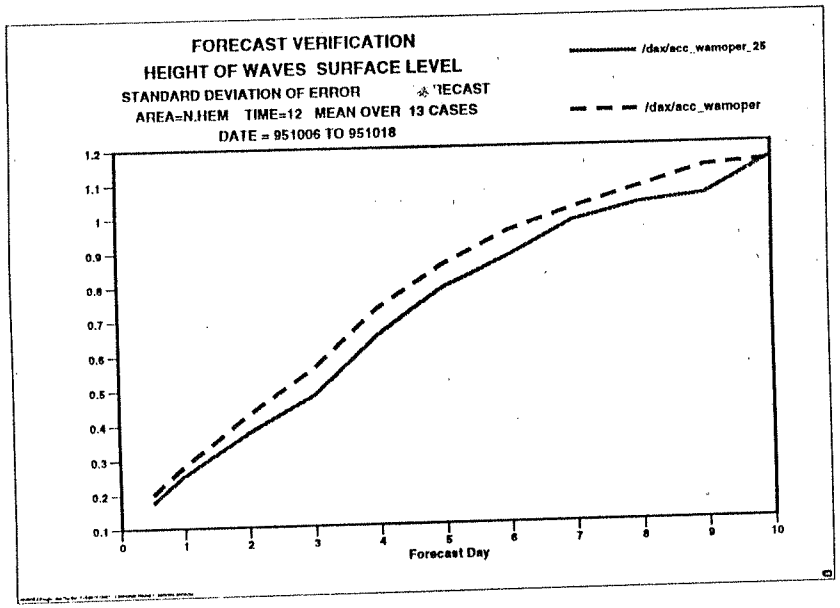
FORECAST VERIFICATION
HEIGHT OF WAVES SURFACE LEVEL
STANDARD DEVIATION OF ERROR
AREA=N.HEM TIME=12 MEAN OVER 13 CASES
DATE = 951006 TO 951018
/dax/acc_wamoper_25
/dax/acc_wamoper
Forecast Day

b)

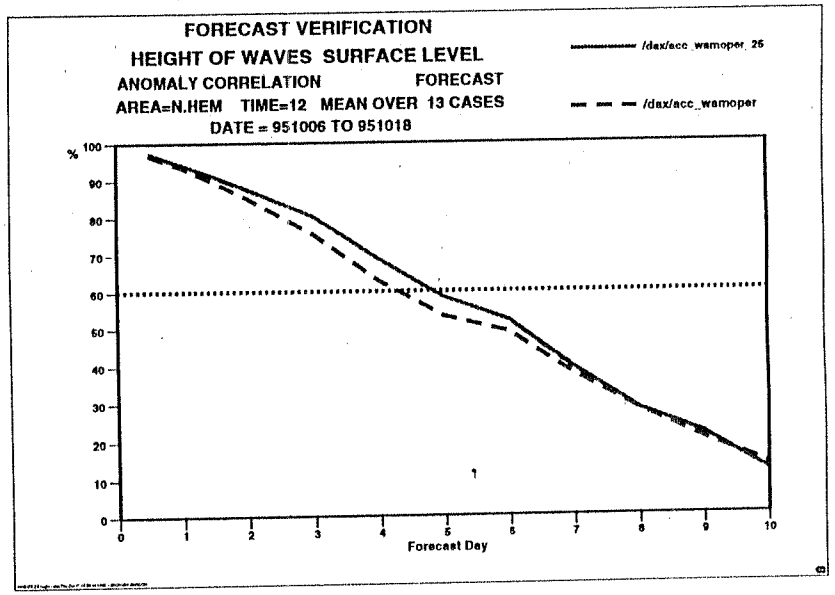
FORECAST VERIFICATION
HEIGHT OF WAVES SURFACE LEVEL
ANOMALY CORRELATION FORECAST
AREA=N.HEM TIME=12 MEAN OVER 13 CASES
DATE = 951006 TO 951018
/dax/acc_wamoper_25
/dax/acc_wamoper
%
Forecast Day

Figure 17

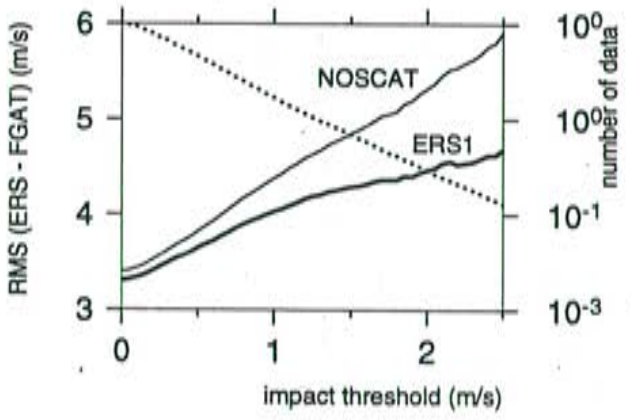
RMS (ERS - FGAT) (m/s)
6
5
4
3
0
1
2
impact threshold (m/s)
NOSCAT
ERS1
10^0
10^0
10^{-1}
10^{-3}
number of data

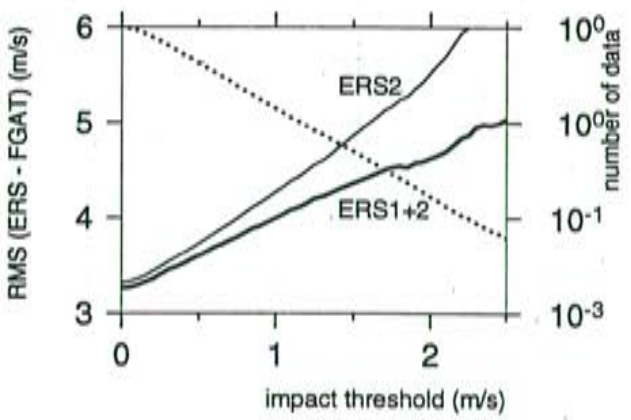
RMS (ERS - FGAT) (m/s)
6
5
4
3
0
1
2
impact threshold (m/s)
ERS2
ERS1+2
10^0
10^0
10^{-1}
10^{-3}
number of data

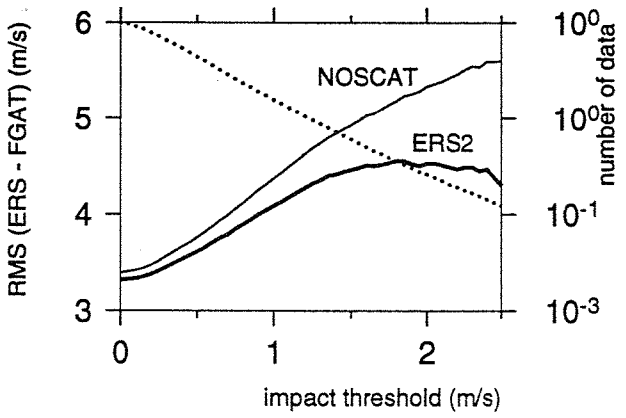
RMS (ERS - FGAT) (m/s)
6
5
4
3
0
1
2
impact threshold (m/s)
NOSCAT
ERS2
10^0
10^0
10^{-1}
10^{-3}
number of data

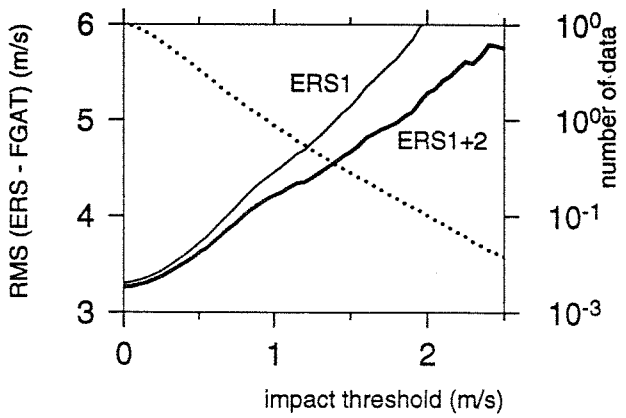
RMS (ERS - FGAT) (m/s)
6
5
4
3
0
1
2
impact threshold (m/s)
ERS1
ERS1+2
10^0
10^0
10^{-1}
10^{-3}
number of data

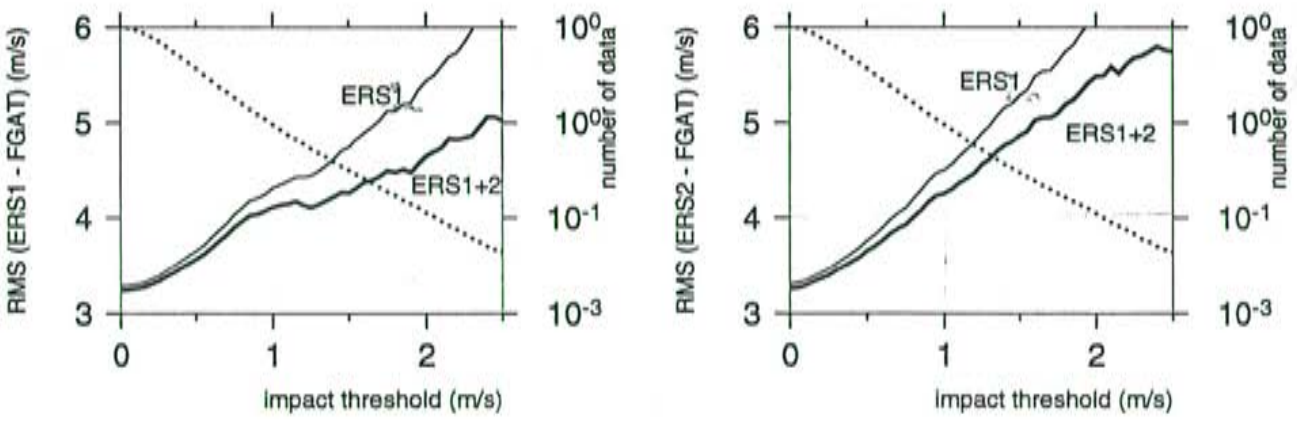
RMS (ERS1 - FGAT) (m/s)
6
5
4
3
0
1
2
impact threshold (m/s)
ERS1
ERS1+2
10^0
10^0
10^{-1}
10^{-3}
number of data
RMS (ERS2 - FGAT) (m/s)
6
5
4
3
0
1
2
impact threshold (m/s)
ERS1
ERS1+2
10^0
10^0
10^{-1}
10^{-3}
number of data

ANNEX B

- Wind speed calibration of ERS scatterometer data for assimilation purposes at ECMWF

WIND SPEED CALIBRATION OF ERS SCATTEROMETER DATA FOR ASSIMILATION PURPOSES AT ECMWF

Didier Le Meur, Lars Isaksen

ECMWF, Shinfield Park, Reading RG2 9AX, England

Ad Stoffelen

KNMI, Postbus 201, 3730 AE de Bilt, The Netherlands

ABSTRACT

Some modifications have recently been studied to improve the wind calibration of ERS scatterometer data within their pre-processing before assimilation in the ECMWF Numerical Weather Prediction model. A first point concerned the introduction of a sigma nought bias correction to remove the underestimation noted in the ERS-2 scatterometer measurements since the instrumental calibration change they underwent in summer 1996, and at the same time refine their description by the transfer function CMOD4 in terms of backscatter. Another issue was then the derivation of a new wind speed bias correction to compensate for the overestimation induced by this sigma nought bias correction in the wind domain and allow to use the scatterometer products up to higher winds speeds. These modifications were implemented together with a sea-ice screening from a decreased Sea Surface Temperature (SST) threshold, so as to further extend the use of the data at high latitudes. Pre-operational assimilation experiments have demonstrated their interest and allowed to expect again more benefits from scatterometer data in the ECMWF model in terms of surface wind analysis and short range forecasts.

1. INTRODUCTION

ERS scatterometer data have been assimilated operationally in the ECMWF Numerical Weather Prediction model since January 1996. The method followed relies on the use of a three-dimensional variational analysis scheme (3D-Var), in which the model state is updated by minimizing a cost function measuring both its distance from its background estimate, so-called «first guess» (6-h range forecast), and from the observations available (Ref. 1). The scatterometer data are thus processed as pairs of ambiguous wind vectors, and implicitly de-aliased through the application of a 2-minima observation cost term. This 3D-Var processing, providing an optimal treatment of the scatterometer wind information, has allowed to improve significantly the ECMWF surface wind analysis and also had a positive impact on the short-range forecasts, especially in the Southern Hemisphere (Ref. 2). However, a crucial point for its success was the implementation of a wind speed dependent bias correction in the Prescat wind retrieval and ambiguity removal scheme (Ref. 3) used in a pre-processing step. This bias correction, aimed at matching the scatterometer wind speeds retrieved through the transfer function CMOD4 with those from the ECMWF model first guess, recently had to be reconsidered. Following the underestimation problems that affected the ERS-2 scatterometer data after the instrumental calibration change they underwent in summer 1996, an additional sigma nought bias correction was introduced in Prescat, but turned out to have an impact on the wind speed dependent bias. This paper presents the new wind calibration scheme that has thus been developed within the 3D-Var pre-processing of scatterometer data, based on a preliminary sigma nought bias correction of CMOD4 and a subsequent tuning in the wind domain as a function of wind speed. A special importance is given to the triple collocation methodology followed to deal with the latter point with as much accuracy as possible. The practical implementation is then described, and pre-operational assimilation results are shown.

2. SIGMA NOUGHT BIAS CORRECTION

On the 6th of August 1996, following repeated failures in July, a redundant calibration system was activated on board of the ERS-2 scatterometer instead of the nominal one. Contrary to the expectations, this change turned out to have an impact on the measured sigma nought level, which decreased by about 0.2 dB, involving a wind speed decrease of the order of 0.2 m/s. An engineering re-calibration was considered by ESA, but the problem first had to be well understood and nothing had still been done at the end of the autumn. Although the wind speed underestimation that followed was not critical for the operational assimilation of the data in the ECMWF 3D-Var system, the possibility to implement a sigma nought bias correction in their pre-processing was investigated.

The solution adopted was to apply the results from the so-called «ocean» calibration procedure used to monitor every month the scatterometer data from the ECMWF model winds. This method (Ref. 4) consists of comparing the sigma noughts measured by the scatterometer with those deduced from the ECMWF first guess 10 metre winds through CMOD4 over a filtered dataset with a uniform direction distribution for each class of wind speed. Working in the transformed space defined by $z^0 = (\sigma^0)^{0.625}$ where the directional dependency is harmonic, antenna biases can then be estimated for each node across the swath, by taking the differences between the measurements and the model simulations.

The antenna biases from the «ocean» calibration had already been successfully subtracted from the raw ERS-2 data before the engineering calibration of March 1996, allowing a correction of wind speed biases up to 3 m/s. Using this process again rather than applying a uniform correction of + 0.2 dB was an opportunity to improve significantly the fit of CMOD4 to the scatterometer backscatter measurements. However such a refined calibration had to take into account the bias due to the increase of the ECMWF

model winds since the initial tuning of CMOD4 with the same method over March 1992. Ad Stoffelen (Ref. 4) estimated this increase to be of 7 % from the negative bias it yielded for ERS-1 over March 1996. Following his recommendations, the antenna biases of ERS-2 were finally computed with respect to first guess winds decreased by the same ratio (Fig. 1).

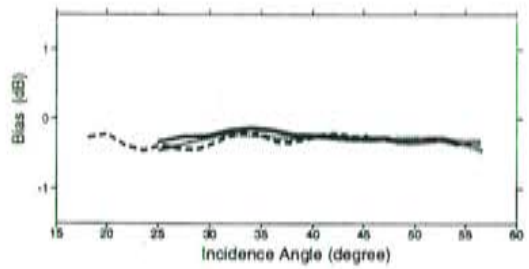

Figure 1. *Antenna biases obtained by «ocean» calibration over October 1996. Solid, dashed and dotted lines stand for the fore, mid and aft antennae respectively.*

The subtraction of these biases was then implemented in Prescat aside the operational 3D-Var processing, applying every month the correction derived with the data from the month before, and starting with the period October-November 1996 during which the measured sigma nought level turned out to stay stable. The results showed a clear improvement in the wind speed bias with respect to the first guess winds, with a reduced underestimation and more uniformity across the swath (Fig. 2). Moreover the wind retrieval also seemed to be improved, with a smaller backscatter residual or «distance to the cone» especially at low incidence angles, resulting in an average reduction by 1 degree (out of about 25) of the direction standard deviation with respect to the model winds. Nevertheless, a positive trend appeared in the wind speed dependent bias, which needed a reassessment of the wind speed bias correction used in Prescat.

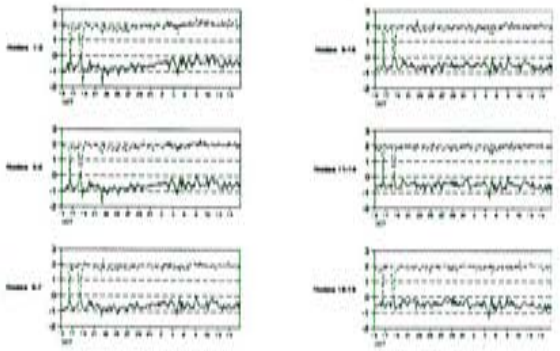

Figure 2. *Wind speed biases (solid lines) and standard deviations (dashed lines) between Prescat and FGAT winds obtained for the different nodes of the swath after substraction of the October 1996 antenna biases. The correction is applied only over November and the results from October are shown for comparison.*

3. SPEED BIAS CORRECTION

a) methodology

The Prescat wind speed bias correction was initially derived from collocations between ERS-1 and buoy data. It was quite efficient at removing the discrepancies between the CMOD4 retrieved and ECMWF first guess wind speeds, and particularly the relative low bias of CMOD4 at high winds. Its implementation in the 3D-Var system allowed thus to avoid systematically filling-in deep lows with underestimated wind observations. Moreover the results turned out to be as good with ERS-2 as with ERS-1. Nevertheless, the small number of buoy data available above 20 m/s did not enable the application beyond that threshold, and this was a serious limitation for the most extreme cases. A major goal in reconsidering this bias correction was therefore to be able to use the scatterometer data up to higher wind speeds.

For that, an accurate calibration method was first necessary. Ad Stoffelen (Ref. 5) recently pointed out that the calibration of wind observations requires a good knowledge of their error characteristics. The observation random errors are of the same order of magnitude as the truth observed, and consequently artificial biases may occur if both their statistics and those of the true distribution are not taken into account. He further showed that the problem has generally too many degrees of freedom to be solved from collocations between only two observation systems, but that adding a third system can allow a solution with less assumptions. The triple collocation methodology he thus developed relying on scatterometer, model and conventional data, as well as the corresponding error modelling, were closely followed to derive a new wind speed bias correction for CMOD4.

Another important issue was to have a good collocated dataset with as much data as possible at high winds. This requirement was partly met by considering all the CONVentional OBServations (CONVOBS hereafter) from ships, buoys and islands processed and quality controlled by the ECMWF operational analysis as a third source of data for triple collocations. The main idea was however to strictly apply a triple collocation analysis only to a preliminary estimation of the model wind errors, and then to derive the final calibration from separate analyses using all the dual collocations available between scatterometer and model, and model and conventional data respectively.

It is worth noting that in this approach each collocated dataset had to be representative of the same spatial and temporal domain, so that the model error estimates derived from the triple collocation analysis stay valid for each subsequent dual collocation analysis. The global coverage provided by the CONVOBS data was essential in this respect, since it enabled to perform the whole study at a global scale. The limited ac-

curacy as compared to higher quality datasets such as the NOAA buoy network was a minor disadvantage in the sense that this aspect is of secondary importance for the estimation of the model errors.

b) collocated data

A 4-month period was considered to perform this calibration exercise, from October 1996 to January 1997. This length was a minimum to get enough data from triple collocations. Moreover the ERS-2 measurements remained stable until January, whereas a slight increase of the sigma nought level occurred in February.

The Prescat winds produced off-line with the sigma nought bias correction had the existing speed bias correction removed, and were collocated with the conventional observations kept by the ECMWF analysis quality control within 100 km and 2 hours, with a minimum separation distance of 50 km to avoid spatial correlations. Triple collocations were obtained by adding the 10-metre First Guess at Appropriate Time (FGAT) winds computed by Prescat at the scatterometer measurement times and locations from the current 3-hour and 6-hour range forecasts. As in their operational processing, the CONVOBS winds were not height corrected (no information is available for that in most cases) and also assumed to be at 10 metres. The dual collocations between scatterometer and model were directly provided by the Prescat outputs, whereas those between model and conventional observations were deduced from the (observation - first guess) increments stored in the analysis feedback files, only for those observations used by the analysis. Since the analysis uses the observations closest to the synoptic time, the latter restriction still ensured first guess winds at the right time and avoided temporal correlations in the case of hourly measurements.

In addition to the quality controls performed by the ECMWF analysis as well as Prescat, a further data selection was applied by excluding all the data located within the Tropics (30°N - 30°S), where the underestimation of CMOD4 with respect to the FGAT winds seemed to exhibit a local increase. This feature, especially noticeable for the zonal wind component, suggests an overestimation of the tradewinds by the ECMWF model as is often reported by ocean modellers. The point was clearly confirmed by recovering similar symptoms when comparing the conventional observations with the model winds. In the case of the triple collocations, the data associated to the 2 first nodes of the swath, for which the CMOD4 winds were visibly affected by larger errors, were also discarded to improve the homogeneity of the dataset. Moreover some more rejections were made by increasing the minimum separation distance to 200 km in the across and along track directions in order to allow for an averaging of both the model and scatterometer data at a 250 km resolution as explained below.

About 2500 triple collocations were finally retained with averaging at 250 km resolution and 3300 without, against 500000 dual collocations between scatterometer and model per node of the swath, and 130000 dual collocations between model and conventional observations. Among the conventional data, those declared as buoy reports according to the WMO conventions appeared to be of a substantial lower quality and were therefore not taken into account. Conversely, those supposed to come from automatic stations on board of ships, and corresponding in fact to moored buoys in most cases, were found to be more accurate and chosen as a reference for refined tunings between model and CONVOBS winds. An additional dataset of about 18000 high quality dual collocations was thus considered.

c) error modelling and calibration principle

Following the previous work by Ad Stoffelen, the random errors of each system were characterized by Gaussian and uncorrelated laws in wind components. They were supposed to be independent of each other and also of the true wind components. The true wind components were equally described by Gaussian laws as a first approximation. Furthermore, the observation errors were defined in terms of calibrated quantities, i.e. such that they measure the departures between the observations and the truth after calibration. Taking the model data as a reference, the wind components of each system were thus primarily described as follows :

$$x = t + x'$$

$$y = f(t + y')$$

$$z = g(t + z')$$

where x, y and z refer to the model, scatterometer and CONVOBS data respectively, t represents the truth, x', y' and z' the observation errors, and the functions f and g describe the respective biases of the scatterometer and the CONVOBS wind components with respect to the model wind components.

This scheme was used mainly for the triple collocation analysis. In the dual collocation cases, a joint formulation in wind components, with a bias term actually related to wind speed, was preferred for more accuracy. Indeed the calibration is believed to be rather speed dependent than component dependent. Moreover the coupling introduced between wind components was a way to virtually double the number of data available. Also the above equations were re-written in the following form :

$$(U_x, V_x) = (U_t + U'_x, V_t + V'_x)$$

$$(U^*_y, V^*_y) = (U_t + U'_y, V_t + V'_y)$$

$$W_y = f(W^*_y)$$

where U_t and V_t are the true wind components, U_x and V_x those of the model, U_y and V_y the scatterometer or CONVOBS wind components, U^*_y and V^*_y their calibrated counterparts, W_y and W^*_y the corresponding raw and calibrated wind speeds, and f is the speed dependent bias function.

Both error models were applied in across and along track components for the cases involving scatterometer data, considering that the errors in the scatterometer winds may be related to the instrument geometry. The model and CONVOBS errors, assumed to be essentially isotropic, were on the contrary equally specified in across and along track or zonal and meridional components. So only the study of the dual collocations between model and conventional data was entirely performed in terms of the usual U and V components.

The calibration problem was then treated in terms of Maximum Likelihood Estimation (MLE), so as to provide a solution in the most general framework. In the simplest case of a separate bidimensional calibration in wind components, the conditional probability of a given pair of collocated observations knowing the truth was thus expressed by :

$$p((x,y)|t) = \frac{\frac{d}{dy}f^{-1}(y)}{e_x e_y} \cdot \exp\left(-\frac{1}{2}\cdot\left(\left(\frac{x-t}{e_x}\right)^2 + \left(\frac{f^{-1}(y)-t}{e_y}\right)^2\right)\right)$$

where e_x and e_y are the error standard deviations associated to x and y.

The corresponding likelihood was deduced by integrating with respect to the probability distribution of the truth, according to Bayès' theorem :

$$L(x,y) = \int p((x,y)|t) \cdot p(t)\, dt$$

with $p(t) = \exp\left(-\frac{1}{2}\cdot\left(\frac{t}{\sigma}\right)^2\right)$, σ being the standard deviation of the truth.

The individual likelihoods $L(x_i, y_i)$ defined over the whole dataset were then multiplied assuming that the collocations were independent, and the resulting global likelihood function $F(f, e_x, e_y, \sigma) = L(x_1, y_1)\ldots L(x_n, y_n)$ was maximized with respect to the different unknown parameters to get their best estimates.

The same principle was applied for the other cases of calibration. However in the triple collocation analysis an error correlation term had to be introduced between the scatterometer and CONVOBS wind components to account for their representativeness errors with respect to the model wind components. Indeed the truth taken into account in each comparison is only that truncated to the scales represented by the model, which has the lowest resolution. The smaller scales resolved by the scatterometer and the CONVOBS are treated as an additional error with respect to this, and that representativity term, identical over their common range of resolution, is a cause of correlation in the three dimensional case.

This correlation between scatterometer and CONVOBS errors involves in practice an extra degree of freedom, which was removed by considering the averaged dataset defined at the 250 km resolution. Since from the previous work by Ad Stoffelen the scatterometer and model winds can be considered to represent the same true variance at this resolution, the calibration problem was thus first solved with a zero correlation. The solution obtained was then used to force successively those of the equivalent problems where either the scatterometer or model data are substituted for their raw counterparts. This allowed to assess successively the effective errors of the scatterometer and model winds at the 250 km resolution and, by difference, to deduce the difference between the corresponding errors at the model resolution. The correlation term was finally determined by imposing this difference on the solution of the problem with both the raw scatterometer and model data.

In the bidimensional cases, the calibration problem also has an extra unknown, but cannot be closed with so little restriction. The solution was then mainly forced through the values of the model errors derived from the triple collocations. Moreover with the wind speed calibration scheme another correlation term had to be taken into account between the true wind components because of the coupling introduced, but this difficulty was avoided by working over a filtered dataset with a uniform direction distribution for each class of wind speed as in the sigma nought calibration. A major cause of correlation between wind components was thus removed, preventing the occurrence of preferred directions. In return, the number of data was typically reduced by 50 %.

d) results

The triple collocation analysis was carried out in the linear framework already used by Ad Stoffelen. The bias functions f and g were then reduced to simple scaling factors. Tables 1 and 2 show the results obtained for the across and along track wind components respectively, such as they arose from the preliminary study of the 250 km-averaged dataset. The model errors turn out to be isotropic, with standard deviations close to 1.6 m/s in both components. The scatterometer winds seem on the contrary to have a larger error along track and be more underestimated by 4 % across track. The CONVOBS winds exhibit similar behaviour in both directions, but are overestimated by 10 % with respect to the model.

These results were not significantly changed when applying the values found for the error covariances to the primary dataset without averaging. Moreover tests with minimum separation distances of 100 and 200 km instead of 50 km, leading to randomly different samplings, confirmed their stability and little sensitivity to the possible spatial correlations induced by the model errors.

	model	scatt.	CONVOBS
scaling factor	1.	0.91	1.10
error (m/s)	1.62	1.63	3.31
error covariance scatt./CONVOBS (m^2/s^2)	0.45		

Table 1. *Triple collocation analysis results for the across track wind component.*

	model	scatt.	CONVOBS
scaling factor	1.	0.95	1.10
error (m/s)	1.64	1.90	3.42
error covariance scatt./CONVOBS (m^2/s^2)	0.25		

Table 2. *Triple collocation analysis results for the along track wind component.*

The study of the dual collocations between model and conventional data was performed in the same linear framework as that of the triple collocations, which turned out to be quite sufficient. With all the conventional data used by the ECMWF analysis, the wind component calibration scheme further confirmed the figures above for the model errors and the CONVOBS scaling factors. The scaling factors were still equal to 1.1 when imposing model errors of 1.6 m/s, both in U and V components.

However, with the subset associated to automatic stations, a similar anisotropy appeared to that observed previously for the scatterometer across and along track components, with a scaling factor roughly lower by 4 % in U than V. A symmetric result could be found introducing an anisotropy factor between the model wind components in the wind speed calibration scheme : over the whole collocated dataset, U had to be decreased by 2.5 % and V increased by the same amount to maximize the likelihood of the solution, which moreover still indicated an overestimation of the CONVOBS winds by 10 % when considering model errors of 1.6 m/s. Furthermore, exactly the same corrections were necessary on the model wind components when repeating the test with the dual collocations between scatterometer and model.

It was therefore concluded that the model errors can be characterized by standard deviations of 1.6 m/s in U and V components, and an overestimation of U by 5 % with respect to V. The scatterometer bias was on the contrary regarded as essentially isotropic and hence better described in terms of wind speed than wind components as expected. As the automatic stations, having the closest measurement heights to 10 metres, did not show any significant bias of the model winds after correction for their anisotropy, the final calibration between scatterometer and model was thus performed from FGAT wind components basically decreased by 2.5 % in U and increased by 2.5 % in V, as well as associated error standard deviations of 1.6 m/s. Moreover, the wind speed calibration scheme was used, and the previous scaling factors replaced by a cubic spline function to take into account the non-linearity of the CMOD4 bias. This spline function was defined with respect to uncalibrated wind speed intervals of 1 m/s.

Figures 3a and 3b illustrate the scatter plots of the scatterometer against the model wind speeds obtained before and after calibration in the case of node 10 (middle of the swath). The dotted lines indicate the average wind speed of each system per bin of that of the other. The non linearity of the CMOD4 bias is evident before correction, but appears to be well described by the spline function, yielding quite symmetric results after correction (Gaussian noises have been added to the wind components with the larger accuracy to match the errors from both systems and make the comparison more symmetric). Furthermore, the fit remains good up to 25 m/s where the highest model winds are available, even if a saturation effect seems to occur above 20 m/s. Such an effect could be insufficiently corrected due to the fact that the spline coefficients have been more constrained at high winds in the MLE minimization procedure to ensure stability in these cases where a reduced number of data is available. A solution would then be to use a different minimization scheme leading to more uniform constraints, but this has not been tested yet.

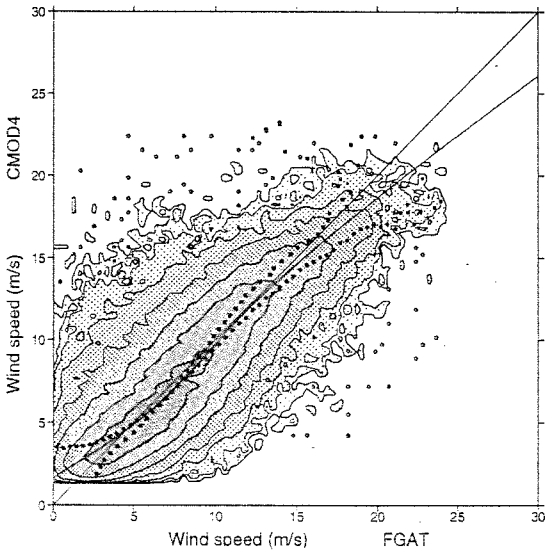

Figure 3a. *Scatter plot of the scatterometer against the model winds speeds before calibration in the case of node 10.*

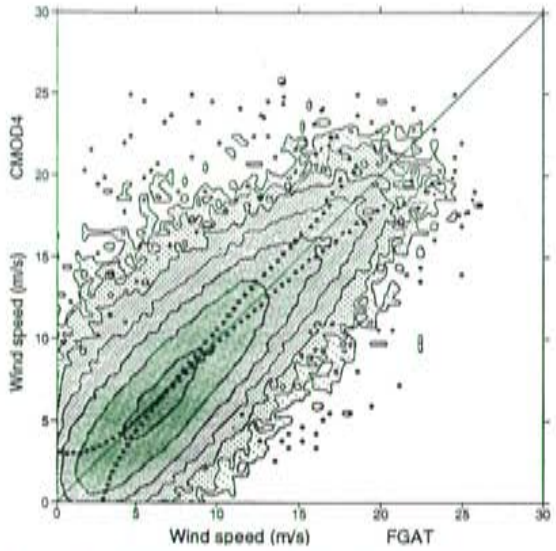

Figure 3b. *Same as Figure 3a, but after calibration.*

Figure 4 shows the calibration curves obtained for the different nodes of the swath, together with that associated to the old bias correction. The old bias correction is clearly exaggerated at the highest winds. Moreover an important gradient appears in the new wind speed bias, which was not taken into account before. The inner nodes turn out to be more underestimated than the outer ones by up to 2 or 3 m/s from wind speeds of about 10 m/s.

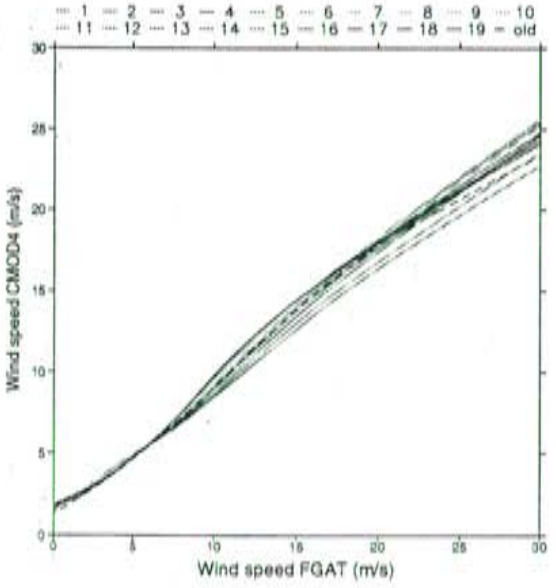

Figure 4. *Wind speed calibration curves obtained for the different nodes of the swath (solid lines), compared with that associated to the old Prescat bias correction (dashed line).*

Also the overall agreement between scatterometer and model is quite improved when comparing the Prescat winds obtained with the new wind speed and sigma nought calibration with those deduced from the old speed bias correction, even when removing the anisotropy correction between the FGAT U and V components as well as the direction filtering and extending the study to the Tropics. In that case, the direction and vector standard deviations are reduced respectively by 1 degree and 4 cm/s (out of about 3.4 m/s). The wind speed bias can also be checked to decrease over most of the wind speed range and especially at high winds (Fig. 5), although an underestimation is still visible due to the overestimation of the model U component and the larger sampling in the corresponding directions. Moreover, the independent comparison provided by the triple collocated CONVOBS confirms the improvement in the direction accuracy, with a standard deviation reduction of roughly the same amount.

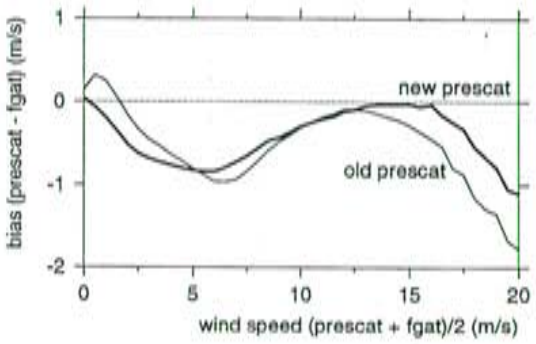

Figure 5. *Wind speed biases between scatterometer and FGAT winds over the original collocated dataset before (thin line) and after (thick line) calibration.*

It should be well noted that the larger underestimation at high winds observed here with the old Prescat products is not contradictory with the exaggeration reported previously, which holds only when applying the old wind speed bias correction after the preliminary sigma nought bias correction.

4. IMPLEMENTATION

The new sigma nought and wind speed bias corrections described above were implemented within the 3D-Var system with an upper wind speed limit increased from 20 m/s to 25 m/s. A new sea-ice screening, using a minimum SST threshold of 0°C instead of 2°C, was introduced at the same time. The existing threshold appeared to be too conservative, especially in the Antarctic region where it led to reject large amounts of data which obviously could still bring useful information. Decreasing it to 0° C while the actual freezing point of the sea is close to -1.7 °C seemed a possibility to increase significantly the scatterometer data coverage at little risk.

One sigma nought bias correction file was supplied for every month, normally produced with the data from the month before, so as to take into account the variations in the scatterometer instrumental calibra-

tion as in real time conditions. This was done from November 1995 when the first ERS-2 scatterometer data were available at ECMWF. The wind speed bias correction, supposed to stay constant, was defined by a single file. Both sigma nought and wind speed bias correction files were designed with two parts, applying respectively to ERS-1 and ERS-2. However for ERS-1 the sigma nought bias correction was not updated, assuming that the instrumental calibration has always remained stable. The antenna biases computed over March 1996 were taken into account. The associated wind speed bias correction was derived over the period October 1995 - January 1996. It is worth noting that the wind speed bias curves obtained for both satellites are very similar, but that the saturation tendency observed with ERS-2 is much less obvious for ERS-1.

5. ASSIMILATION RESULTS

Assimilation experiments were performed to test the modifications introduced in the scatterometer data pre-processing before operational application. The 3D-Var system was run taking them into account over a 2-week period (1-13 February 1997) and the results compared with those of a control experiment using the old pre-processing.

Monitoring statistics with respect to the FGAT winds deduced from the operational 3-h and 6-h range forecasts confirm the improvements noticed previously in the quality of the scatterometer winds retrieved off-line by Prescat with the new bias correction scheme. Compared with the old Prescat outputs, similar benefits can be found with the new 3D-Var processing in terms of wind speed bias and distance to the cone. The direction and vector standard deviations are accordingly reduced to a comparable extent (by 1 degree and 3 cm/s respectively), and the wind speed dependent bias still exhibits the same overall decrease, with limited values at high winds justifying the use of the data up to 25 m/s (Fig. 6). Moreover the study of the agreement between scatterometer and model winds as a function of SST further validates the use between 0°C and 2°C, where the vector RMS difference is not especially increased, while the quality control check on distance to the cone, involving more data rejection, seems sufficient to avoid possible sea-ice contaminations (not shown).

The comparison of the departures between first guess and scatterometer observations obtained respectively in the test and the control experiments shows a positive impact of the previous improvements on the surface wind analysis. Taking into account the new 3D-Var retrieved winds in both cases, the vector RMS difference is reduced by 3 cm/s on average with the modifications implemented in the scatterometer data pre-processing. Furthermore, introducing a minimum «impact threshold» in the comparison to limit it to the data for which the difference between the first guess winds from both experiments is the largest, no detrimental effect appears in the extreme cases, where the vector RMS reduction becomes even systematically more significant (Fig. 7). No sign of deterioration can either be seen as a function of wind speed at high winds, not more with respect to the CONVOBS data than the scatterometer observations. A further validation is moreover provided by the ERS-2 altimeter measurements, indicating an overall reduction by 2.5 cm/s in the standard deviation between analysed and observed wind speeds. In comparison, the gain obtained when the ERS-1 scatterometer data were introduced in the 3D-Var assimilation was at the most equal to 10 cm/s

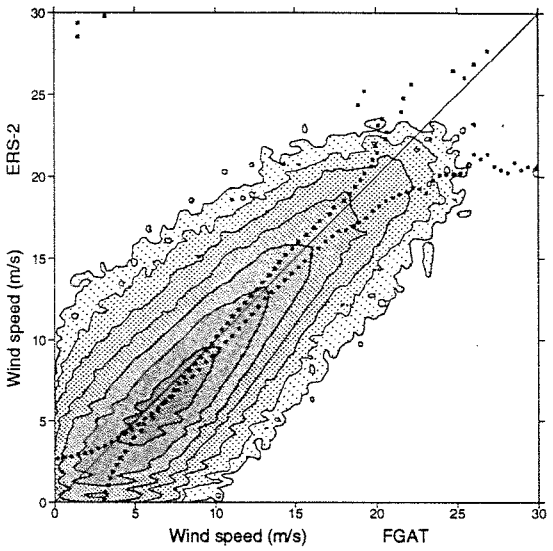

Figure 6. *Scatter plot of the wind speeds associated to the new 3D-Var processed scatterometer products against those from the operational FGAT over the 2 weeks of assimilation.*

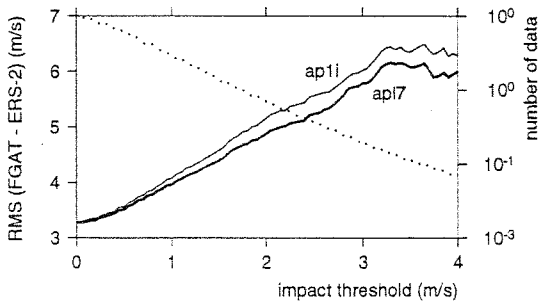

Figure 7. *Vector RMS differences between first guess and scatterometer winds in the test (apl7) and control (ap1i) experiments as a function of the «impact threshold» associated to the modifications introduced in the scatterometer data pre-processing. The dotted line indicates the proportion of data exceeding a given impact threshold in logarithmic scale.*

These different improvements in the accuracy of the first guess and analysed surface winds, although quite evenly distributed, turn out to be more important at high latitudes where the coverage of the scatterometer data is increased over large areas between 0°C and 2°C, and especially in the Antarctic region. Also the impact on the analysed geopotential is essentially concentrated in these areas as can be seen when plotting the mean difference obtained between both experiments at 1000 hPa (not shown). The study of the corresponding RMS forecast error difference shows a substantial benefit for the 12-hour and 24-hour range forecasts, mostly in the Southern Hemisphere where the impact on the analysis is larger (Fig. 8). However for the medium-range, the results are essentially neutral in terms of anomaly correlations, apart from a slightly positive tendency from day 5 over the North Atlantic (Fig. 9).

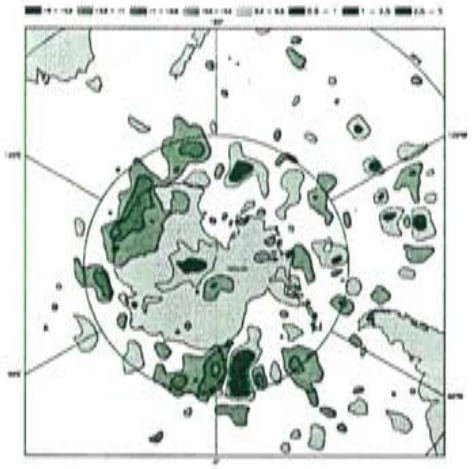

Figure 8. *Mean difference between the 12-h RMS forecast errors for the 1000 hPa geopotential associated to the test and control experiments in metres. The areas where the difference is negative (green and blue) indicate an improvement with the new scatterometer data pre-processing.*

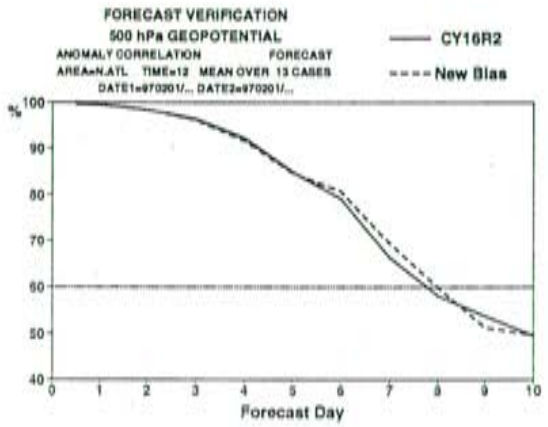

Figure 9. *Anomaly correlation forecast scores for the 500 hPa geopotential associated to the test (dashed line) and control (solid line) experiments over the North Atlantic.*

6. CONCLUSION

A new wind calibration scheme has been implemented within the pre-processing of ERS scatterometer data for assimilation in the ECMWF model, relying on a sigma nought bias correction and a revised wind speed bias correction of the transfer function CMOD4, both derived consistently from comparisons with the model data themselves. The sigma nought bias correction has allowed to systematically solve the bias problems related to changes in the instrumental calibration and at the same time improve the wind retrieval at low incidence angles by refining the description of the scatterometer measurements in the backscatter space. The revised wind speed bias correction has provided a better agreement with the model winds than before and over a wider wind speed range, due to the larger number of collocated data involved in its derivation. The use of a triple collocation analysis also ensured more accuracy by taking into account the errors in the model winds, while the application of a Maximum Likelihood Estimation method was crucial to solve the calibration problem in a suitable way, i.e. in a non-linear framework and in terms of wind speed while the errors were better defined in wind components.

The pre-operational test of this new wind calibration scheme together with a less conservative sea-ice screening has confirmed its potential to enhance the quality of the scatterometer winds processed by the ECMWF 3D-Var assimilation system and shown that it contributes to extend significantly their range of use. Moreover the results obtained enable to expect again more benefits from scatterometer data in the ECMWF model in terms of surface wind analysis and short range forecasts. Minor improvements may however still be useful, especially concerning the minimization scheme or fitting functions to considerer in the MLE algorithm so as to ensure stability at high winds without compromising the quality of the results. The methodology developed with the ERS scatterometers should then be applied successfully to the calibration of the NSCAT instrument.

ACKNOWLEDGEMENTS

This work was supported by ESA under contract number 11699/95/NL/CN.

REFERENCES

1. Courtier, P & al 1993, Variational assimilation at ECMWF, *Research Department Tech. Memo. 194*, ECMWF

2. Gaffard, C and H Roquet 1995, Impact of the ERS-1 scatterometer wind data on the ECMWF 3D-VAR assimilation system, *Research Department Tech. Memo. 217*, ECMWF

3. Stoffelen, A and D Anderson 1997, Ambiguity removal and assimilation of scatterometer data, *Quart. J. Royal Meteorol. Soc.*, 123, 491-518

4. Stoffelen, A 1997, A simple method for calibration of a scatterometer over the ocean, submitted to *J. of Atm. and Oceanic Tech.*

5. Stoffelen, A 1997, Towards the true near surface wind speed: error modelling and calibration using triple collocation, to appear in *J. Geoph. Res.*, special issue on ERS-1

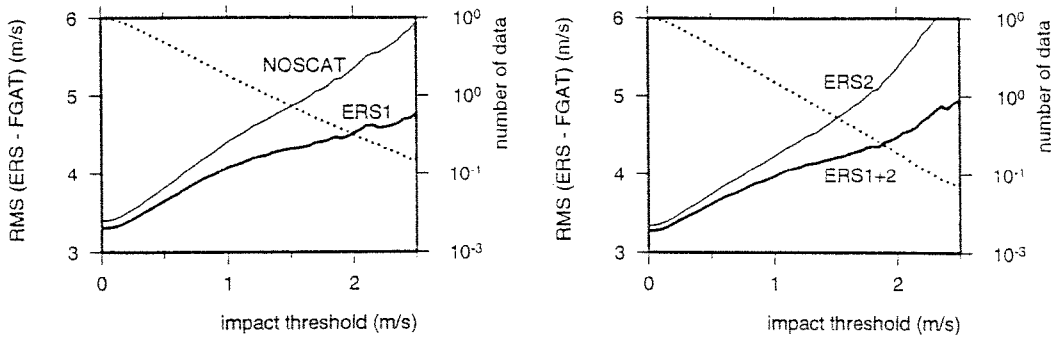

FIGURE 4. *Vector RMS differences between scatterometer and FGAT winds when no scatterometer data or only ERS-1 data are assimilated (left), and when only ERS-2 or both ERS-1 and ERS-2 data are assimilated (right). The FGAT winds are referred to as NOSCAT, ERS1, ERS2 and ERS1+2 respectively, and the results are represented as a function of the impact thresholds associated to the (ERS1 - NOSCAT) and (ERS1+2 - ERS2) differences. The dotted lines indicate the proportion of data exceeding a given threshold in logarithmic scale.*

6 - CONCLUSION

The use of scatterometer winds at ECMWF has reached a mature status. The PRESCAT procedure, in addition to re-processing the ESA data in real time, has allowed to implement efficient monitoring and calibration tools to help maintain the instrumental performance in the long term or improve it in commissioning phases. It has also been the starting point for a wider use of the data available in operational meteorological centres for collocation purposes. Moreover the 3D-VAR assimilation system enabled a successful effective implementation of the data in numerical weather prediction, with the most appropriate solution to the directional ambiguity problem, and provides a basis for further progress with 4D-VAR assimilation schemes. The processing scheme developed with ERS-1 scatterometer data was successfully applied to ERS-2 data, and should be valuable again to deal with NSCAT data in a few months. An important goal for the near future will be the evaluation of the impact of scatterometer data in the 4D-VAR system.

Acknowledgements

This work was supported by ESA under contract number 11699/95/NL/CN.

REFERENCES

Cavanié, A. and P. Lecomte. «Study of a method to dealias winds from ERS-1 data». Final report of ESA contract No 6874/87/CP-I, vol. 1. ESA publication division, 1987.

Courtier, P. et al. «Variational assimilation at ECMWF». Research Department Tech. Memo. 194, ECMWF, 1993.

Gaffard, C., and H. Roquet. «Impact of the ERS-1 scatterometer wind data on the ECMWF 3D-VAR assimilation system». Research Department Tech. Memo. 217, ECMWF, 1995.

Stoffelen, A. and D. Anderson. «ERS-1 scatterometer data characteristics and wind field retrieval skill», in First ERS-1 Symposium, Cannes, France. Digest, 1992, pp. 41-44.

Stoffelen, A. «Surface wind observations from the ERS scatterometers». ECMWF Newsletter 66, ECMWF, 1994.

Stoffelen, A. and D. Anderson. «The ECMWF contribution to the characterization, interpretation, calibration and validation of ERS-1 scatterometer backscatter measurements and winds». Final report of ESA contract No 9097/90/NL/BI. ESA publication division, 1995.

ANNEX C

- Use of ERS scatterometer data at ECMWF

ANNEX C

USE OF ERS SCATTEROMETER DATA AT ECMWF

Didier LE MEUR, Catherine GAFFARD, Roger SAUNDERS

ECMWF, Shinfield Park, Reading RG2 9AX, England

Abstract

ERS scatterometer data have been re-processed in real time at ECMWF since July 1994. The procedure applied, called PRESCAT, benefits from an improved quality control with respect to the ESA products and a better ambiguity removal, using short range forecasts as a background. Moreover it produces monitoring statistics from the comparison with these forecasts, that are particularly useful for calibration and validation purposes. In January 1996, the PRESCAT outputs from ERS-1 scatterometer were introduced operationally into the ECMWF numerical weather prediction model, through the implementation of its 3D-VAR analysis scheme. Pre-operational experiments have shown a positive impact on the analysed and first guess surface fields, resulting in a significant improvement of the short range forecasts in the Southern Hemisphere. Similar results have been obtained with the ERS-2 scatterometer since the completion of its commissioning, so that its data were implemented in 3D-VAR before the switch-off of ERS-1's instruments on 3 June 1996.

1 - INTRODUCTION

ERS scatterometer data have been processed at ECMWF since the launch of ERS-1. The wealth of information provided by the ECMWF numerical weather prediction model enabled an important contribution to the calibration and validation of the ERS-1 scatterometer, and led to the design and the adoption by ESA of a new transfer function (CMOD4), more appropriate than the pre-launch one (Stoffelen and Anderson, 1992). The subsequent progress made in the interpretation of the scatterometer measurements further showed that a wind product of high quality could be achieved taking advantage of the real-time availability of the model information. It also became clear that the utility of such a product for numerical weather prediction would depend on the ability of assimilation methods to make good use of surface wind observations (see e.g. Stoffelen, 1994). A first step towards an effective use of ERS scatterometer data at ECMWF was therefore the implementation of the PRESCAT wind retrieval and ambiguity removal scheme in July 1994 to reprocess the ESA data in real time. The next step was provided by the introduction of a 3D-VAR analysis scheme in the operational assimilation system in January 1996. This paper gives an overview of the operational stage that has been reached in the use of scatterometer data. Sections 2 and 3 present respectively the pre-processing performed within PRESCAT and the subsequent monitoring activities. Section 4 describes the assimilation of the data in the 3D-VAR system, and section 5 focuses on the impact obtained both with ERS-1 and ERS-2.

2 - THE PRESCAT PRE-PROCESSING

PRESCAT (PRE-processing of SCATterometer data) was developed from ESA's wind retrieval and ambiguity removal software, called CREO (Cavanié and Lecomte, 1987). Several changes were made to improve the original scheme, leading to a quite different processing (see Stoffelen and Anderson, 1995 for details).

The inversion method was first reconsidered. The maximum likelihood estimator (MLE) used in CREO to minimize the distance between the scatterometer measurements and the transfer function was found to introduce a distortion of the backscatter space, prefering certain directions in the retrieval process. As a result a new MLE was implemented, computing the distance in the transformed space defined by $z = (\sigma^0)^{0.625}$, where the cone described by the transfer function is nearly circular and gives a uniform distribution of retrieved directions. Moreover only two solutions were kept, basically that with the smallest MLE residual and the first one in the opposite direction.

The ambiguity removal scheme was also revised. Because of operational constraints, CREO uses only 18 hour to 36 hour range forecasts as a background information and therefore relies strongly on the ranking of the retrieved solutions as a function of their MLE values to select the right direction (autonomous ambiguity removal). Unfortunately the upwind/downwind sensitivity is less than expected, and the process turns out to fail to provide a solution in about 30% of the cases. Also PRESCAT takes advantage of the real-time availability of the ECMWF short range forecasts to make a greater use of model data. The current 3 hour, 6 hour and 9 hour range forecasts are interpolated at the scatterometer measurement time, yielding a First Guess at Appropriate Time (FGAT) that already removes 95% of the ambiguities by direct comparison. Most of the remaining ones are then sorted out by means of a vector statistical filter propagating the information from the areas where the confidence in the selected solution is high to areas with a lower confidence.

Finally the quality control was extended. In PRESCAT, the check of the quality information provided by ESA (including Kp values and missing packet counters) is just a preliminary step. The application of a refined land-sea mask and a sea-ice screening deduced from the ECMWF sea-surface temperature analysis allow a typical 15 % further data rejection. Moreover two additional checks are done on the retrieval residual (MLE of the rank 1 solution), so-called «normalized distance to the cone». On the one hand, this quantity must always stay smaller than 3 (3-σ test), to avoid cases of geophysical effects not explained by the transfer function such as rain, generally located at fronts or close to low pressure centres. On the other hand, it has also to remain limited on average over 6 hours for each node; instrumental problems can thus be detected, that relate to the measurement geometry and affect larger areas.

3 - MONITORING ACTIVITIES

In addition to performing wind retrieval and ambiguity removal, PRESCAT allows monitoring statistics to be produced from the comparison between scatterometer data and FGAT winds. These statistics can be useful both to follow the performance of the instrument in time and to calibrate and validate its measurements immediately after launch. So procedures have been implemented for ERS-1 and then applied to ERS-2.

Among those procedures, the monitoring of the mean normalized distance to the cone (averaged over 6 hours) is of a great practical interest. Another particularly relevant diagnosis consists of a comparison per beam and node between the backscatter values measured by the scatterometer and those simulated applying the transfer function to the FGAT winds. Special care is taken to remove any directional dependency in the process. For that, the data are filtered so as to ensure a uniform direction distribution for each class of wind speed; the transformed space defined by $z = (\sigma^0)^{0.625}$ is also considered. An «ocean calibration» can then be established, which already served the derivation of CMOD4 with ERS-1, and was very helpful to identify and solve the beam bias problems met with ERS-2. In this case, the biases computed with the first week of

data (Fig. 1) turned out to remain valid all over the commissioning phase, and their simple subtraction from the raw data demonstrated from the beginning that wind products of a similar quality to ERS-1 could be achieved.

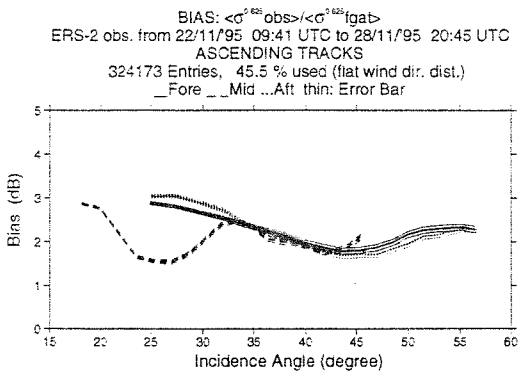

FIGURE 1. *Antenna biases produced by the «ocean calibration» for the ERS-2 scatterometer over its first week of data (ascending tracks only).*

In order to benefit more from the data available at ECMWF, the collocations provided by PRESCAT between scatterometer and FGAT winds have been completed by systematic collocations with conventional observations from ships, buoys and islands. These collocations take advantage of the quality control performed by the operational analysis, as well as its automatic blacklisting procedure. A further monitoring is thus made possible. Moreover the triple collocated data set obtained between scatterometer, model and conventional observations should enable a refined calibration of both ERS-1 and ERS-2 data in the wind domain. In parallel, routine collocations are also being implemented with wave data from the WAM model. Another way to better control and interpret the measurements can consequently be expected, through an investigation of their dependencies on sea-state.

4 - ASSIMILATION IN 3D-VAR

ECMWF's 3D-VAR analysis scheme (Courtier et al., 1993) relies on the minimization of a cost function $J = J_B + J_O + J_C$, where J_B and J_O are quadratic terms measuring the distance from the model state to its background estimate (first guess) and the observations respectively, and J_C is a penalty term expressing additional physical constraints. For scatterometer data, it has been shown more appropriate to specify J_O in terms of wind rather than backscatter (Stoffelen and Anderson, 1995). Indeed, the observation errors are practically gaussian in wind components, whereas the high non-linearity of the transfer function makes their description difficult in the backscatter space. Therefore ERS scatterometer data are assimilated in the 3D-VAR system as pairs of ambiguous winds, through a two-minima cost function of the following form :

$$J_O^{scat} = (J_1 \, . \, J_2)/(J_1^p + J_2^p)^{1/p}$$

with :

$$J_i = (u_i - u)^2/\delta u^2 + (v_i - v)^2/\delta v^2, \; i = 1, 2$$

where u and v are the model 10 metre wind components, u_i and v_i ($i = 1, 2$) the scatterometer observations, δu and δv the associated errors and p an empirical exponent. The ambiguity removal is thus performed implicitly during the minimization process, taking into account all the information from the background field and the surrounding observations carried by the structure functions, as well as the physical constraints of the cost function.

In practice, the observation errors δu and δv are assigned a value of 2 m/s, and p is set to 4. The two solutions provided by PRESCAT are used as input, sampled every 100 km to match the model resolution without introducing horizontal correlation. Moreover a wind speed bias correction is applied in the pre-processing, so as to avoid the systematic underestimation of high winds produced by CMOD4. That bias correction, derived from collocations between ERS-1 and buoy data from Météo-France, turned out to be crucial to make a good use of scatterometer data in 3D-VAR : early assimilation experiments revealed a systematic tendency to fill up deep lows because of too small pressure analysis increments associated to too small wind observation increments, so that the impact was negative in the most interesting cases.

The 3D-VAR ambiguity removal turns out to give different results from the PRESCAT statistical filter in about 1.7 % of the cases. The differences correspond most of the time to situations with low wind speeds or phase errors in the first guess. On visual inspection, the 3D-VAR results generally show wind structures of a much better consistency (Fig. 2).

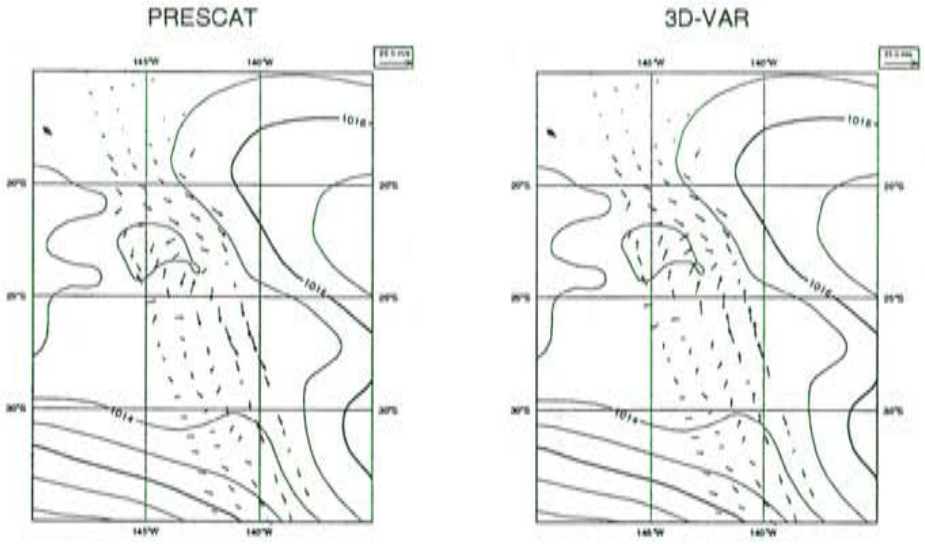

FIGURE 2. *Wind solutions given respectively by PRESCAT and the 3D-VAR analysis for the ERS-2 scatterometer on 10/06/96 at 6 UTC*

5- IMPACT RESULTS

ERS-1 scatterometer data have been used operationally in the ECMWF 3D-VAR assimilation system since its implementation in January 1996. Pre-operational experiments were carried out to assess their impact, performing parallel runs with or without them at a spectral truncation T106 (horizontal resolution 125 km) and over a 2 week period in December 1994 (Gaffard and Roquet, 1995). A clear improvement was found in the analysed and first guess surface fields, associated to a decrease of the departures between the first guess and the different types of observations used in the assimilation system. That decrease was in the order of 4 % for scatterometer data and 2 % for buoy pressure measurements in a RMS sense, and generally seemed more significant in the Southern Hemisphere. An improvement was also observed for the 12 hour-range forecasts in the Southern Hemisphere. Moreover the impact on medium-range forecasts, measured in terms of anomaly correlation, was found neutral or slightly positive everywhere, with a maximum over Northern America (Fig. 3), due to the particular conditions that prevailed during the study period (storms developing in the eastern part of the North Pacific).

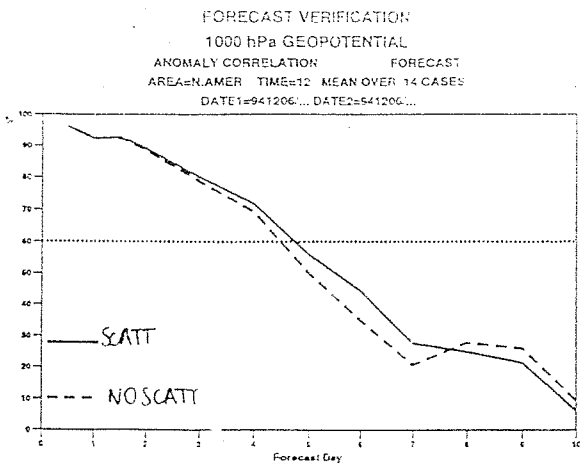

FIGURE 3. *Forecast scores obtained with (solid line) and without (dashed line) ERS-1 scatterometer data over Northern America, averaged over 14 cases.*

These results are in agreement with those obtained in previous studies using OI assimilation schemes, which generally indicated substantial benefits for surface fields in the short term, mainly in the Southern Hemisphere where the observations are sparse, but a limited impact in the long term because of a redundancy of scatterometer data with other types of observations (e.g. satellite temperature soundings) at large scales. It is likely that the 3D-VAR scheme, in spite of its advantages for ambiguity removal, does not yet enable an optimum use of surface wind observations because of the fixed error correlation structure it still assumes, especially in the vertical direction. However it opens the way to 4D-VAR assimilation schemes which will follow the same implementation framework and bring a variation of the structure functions dynamically consistent with the meteorological conditions.

New assimilation experiments have been performed from the ERS-2 scatterometer since the completion of its commissioning at the end of March 1996. As its performance was demonstrated to be virtually identical to ERS-1, exactly the same data pre-processing was kept. Similar improvements were confirmed for the analysed and first guess surface fields. Consequently the ERS-2 data were substituted to their ERS-1 counterparts in the operational system on 1 June 1996, before the switch-off of ERS-1's instruments on 3 June.

These experiments were taken as an opportunity to study the impact of the two instruments together, in order to get a first idea of what can be expected from future two-swath scatterometers such as NSCAT or ASCAT. For that purpose, four assimilation configurations were tested over a 4 day period (1-4 April 1996) : no scatterometer data, ERS-1 or ERS-2 data only, and both ERS-1 and ERS-2 data. Preliminary results show an appreciable gain on average in the fit between first guess and observations in the tandem configuration : the vector RMS difference between the scatterometer and FGAT winds decreases by 13 cm/s (out of 3.40 m/s) when both instruments are effectively used, instead of 9 cm/s and 7 cm/s respectively when only ERS-1 or ERS-2 data are assimilated. Moreover, a study of the most significant cases, imposing an arbitrary minimum value, so-called «impact threshold», on the vector differences induced by the data in the first guess field, indicates that the main improvements brought by ERS-1 are little reduced when the ERS-2 data are already assimilated (Fig. 4). Nevertheless, the reverse is far from being true. It seems that the orbit phasing between the two satellites, leading ERS-2 to fly over the same areas as ERS-1 24 hours later, makes the ERS-2 data redundant with the information kept from ERS-1 after one day.

ANNEX D

- Near-surface satellite wind observations of hurricanes and their impact on ECMWF model analyses and forecasts

Near-surface satellite wind observations of hurricanes and their impact on ECMWF model analyses and forecasts

by

M. Tomassini, D. LeMeur and R. W. Saunders

European Centre for Medium-Range Weather Forecasts

Shinfield Park, Reading RG2 9AX,

United Kingdom

Abstract

During August/September 1995 new near surface wind datasets over the tropical Atlantic from both the ERS-1 scatterometer and METEOSAT satellites were available at ECMWF. At this time there was an unusually high number of hurricanes present in the tropical Atlantic and so the impact of these data on analysing and forecasting the main cyclones was investigated. Assimilation experiments using a new variational scheme, with the ERS-1 winds, showed clear improvements both in the analyses and short range forecasts, compared with the Optimal Interpolation scheme without these data. For example the forecast positions for hurricane Iris were reduced by almost 50% when the scatterometer data was included. For hurricane Luis the improvement was for a higher percentage of cases when the model identified the cyclone in the 24 and 48 hour forecasts. For the 72 hour forecasts 80% of the reported cyclones were detected compared with only 33% for the analyses without ERS-1 data.

The impact of the METEOSAT lower-tropospheric cloud motion winds was found to be small due to lack of coverage in the vicinity of the centre of the hurricanes at this time. The impact of one profile from a ship in the vicinity of hurricane Luis just before its approach to the Caribbean Islands was clearly demonstrated by large improvements to both analyses with and without the scatterometer winds.

1. Introduction

Accurate forecasts of tropical cyclone (TC) positions and intensities are vital for countries affected by their associated severe weather. Several operational global forecast centres (e.g. U.K. Meteorological Office, U.S. National Weather Service) routinely disseminate TC forecasts to national meteorological services. The forecasting of TCs by global numerical weather prediction (NWP) models has improved recently through a better representation of the physical processes in the models and higher model resolutions allowing the TCs to be better represented (Shun 1992). The current operational forecast model at the European Centre for Medium-range Weather Forecasts (ECMWF) resolves half wavelengths to about 90 km (referred to as T213) but there are plans to improve this within the next few years allowing more of the structure of a TC to be resolved. Another factor leading to improvements is a better definition of the initial state of the atmosphere through improved data assimilation systems. ECMWF has recently implemented a 3 dimensional variational assimilation (3D-Var) system (Courtier et. al. 1993) and a subjective study comparing the forecast skill of the previous optimal interpolation scheme and 3D-Var for over 60 TC cases showed an overall improvement in short range (<96 hour) forecasts (A. Lanziger, ECMWF, pers. comm.). However to date the lack of conventional data and satellite observations (Reed et al. 1988) over the tropical oceans hampers significant improvements in the model analyses in the vicinity of TCs. This has led to "bogusing" techniques being developed by some centres (Serrano and Unden, 1994; Heming et. al., 1995) which derive synthetic observations for assimilation into the analysis to improve the position of the TC.

The current resolution of the ECMWF T213 model does not allow the possibility of resolving the fine-scale structure and physical processes of the TC centre. However the model can analyse the large-scale flow in which the TC exists, giving indications of its intensity and position. Since no bogusing is performed, good data coverage is essential for accurate analysis. In recent years several new sources of satellite data have become available in near real time on the Global Telecommunication System that potentially could improve the analysis of TCs. Firstly a satellite dataset which has been assimilated operationally at ECMWF from 30 January 1996 is the microwave scatterometer surface winds from the European Space Agency polar orbiting satellites ERS-1 and ERS-2. These data are unaffected significantly by cloud and precipitation allowing the sea surface winds in the vicinity of a TC to be inferred. Their only drawback is the relatively narrow swath width (450 km) and hence limited coverage of the ERS instru-

ments although this will be improved for future instruments. In spite of this there have been positive impacts in the short range forecast demonstrated over the southern hemisphere oceans and northern Pacific Ocean due to the inclusion of scatterometer data in the analysis (Gaffard and Roquet, 1995). Secondly low level geostationary cloud motion winds (CMW) can have a better coverage if the higher resolution visible channel images are tracked during daylight. From June 1994 until November 1995 the European Space Operations Centre (ESOC) produced such a product from the METEOSAT visible channel imagery in an attempt to improve the CMW coverage over the Atlantic and SW Indian Oceans (Ottenbacher et al. 1996).

The 1995 hurricane (i.e. Atlantic TCs) season was characterised by an unusually high level of activity. At least 19 tropical cyclone events were identified between June and the end of October, generally developing off the west African coast and crossing the tropical region of the North Atlantic. Among these, eleven were classified as hurricanes. This paper gives some examples during this period of the impact of the scatterometer near-surface winds combined with the new variational assimilation for improving the analysis of hurricanes in the ECMWF forecast system and also their impact on the short range forecasts. The impact of the METEOSAT low level CMWs was also investigated.

2. Characteristics of the ECMWF forecast system

a) The model

The ECMWF forecast system consists of two components: a general circulation model and a data assimilation system. The general circulation model (see Ritchie et al., 1995 for details) is a spectral, primitive equations model with a horizontal truncation of T213 and 31 vertical levels, using a semi-Lagrangian time integration with a time step of 15 minutes. The spectral model truncation of T213 corresponds to a smallest resolved half-wavelength of a little over 90km and the computational grid has a resolution of about 60km. The model includes a comprehensive set of physical parametrizations, representing processes such as convection, clouds, radiation, friction and diffusion. The cloud parametrization scheme allows the main cloud related processes to be treated in a consistent manner by forecasting both cloud fraction and cloud water/ice content with prognostic equations. The model can generate intense cyclonic systems, but its ability to represent the structure of hurricanes is limited by resolution.

The momentum transport in the convection scheme (Tiedtke, 1989) prevents the surface pressure values from reaching unrealistically low values for this model resolution.

b) Data assimilation

A major change in the ECMWF data assimilation system was made at the end of January 1996, when the Optimal Interpolation (OI) method was replaced by a new three-dimensional variational analysis (3D-Var) scheme. In 3D-Var the observations are combined with the model first guess (6 hour forecast) through the minimization of a cost function (Courtier et al., 1993). Compared with OI, one major advantage of 3D-Var is that it can handle observations which are non-linearly related to the analysed quantities, for example it can directly assimilate radiance measurements from satellites. 3D-Var includes coupling between mass and wind fields through the correlation in background errors of mass and wind. At the time of these experiments however this multivariate formulation was used only in the extra-tropics, so both the 3D-Var and OI schemes were univariate in the tropics.

The data used for the geopotential height and wind field analyses come from in situ observations from surface stations, aircraft, radiosondes and drifting buoys and from remotely sensed data such as Cloud Motion Winds (CMW) from various geostationary satellites and radiances from the TOVS (TIROS Operational Vertical Sounder). The temperature analysis increments are derived from the geopotential height increments assuming hydrostatic equilibrium. The analysis of specific humidity relies on radiosondes and TOVS radiances. Low level CMW and TOVS data are used only over oceanic areas. The OI and 3D-Var systems include the same observations, with two exceptions: TOVS data are assimilated in OI as retrieved profiles (Eyre et al., 1993) and in 3D-Var as radiances (Andersson et al., 1994); secondly the ERS scatterometer data are not assimilated in OI. The scatterometer data are assimilated in 3D-Var directly using the retrieved ambiguous wind vectors with the most appropriate wind vector being selected during the minimization process itself (see below).

3. Satellite surface wind observations

Conventional observations on the West African coast help identify the easterly waves which may evolve into tropical storms over the Atlantic Ocean. Data coverage is usually rather poor as the disturbance moves across the Atlantic, where only sparse wind soundings from occasional ships are available. The consistent coverage offered by sat-

ellites over the ocean can be essential for improving TC monitoring. An example of this is given in Figure 1a, where a METEOSAT visible image on 31 August 1995 at 12Z reveals four tropical storms present at this time. The yellow vectors are scatterometer surface winds derived from two swaths of the ERS-1 satellite, at 12:45Z and 14:45Z respectively; the green and red vectors are respectively visible and infrared METEOSAT Cloud Motion Winds (CMW) below 700 hPa. Note the CMW data from the GOES EAST satellite were not available at this time but the TOVS radiances were always used if a NOAA-12 or NOAA-14 overpass occurred during the analysis period. The conventional wind reports, shown separately in Figure 1b were rather sparse, and almost absent from the large area relevant for the formation of TCs. Thus the potential benefit of the new satellite datasets, particularly the scatterometer winds as shown in Figure 1a, is clear.

The scatterometers on board the ERS-1 and ERS-2 satellites use 3 antennae, pointing in azimuths of 45, 90 and 135 degrees with respect to the satellite ground track. These antennae measure the microwave backscatter from the sea surface in the C band (5.3 GHz), at a 50 km resolution, within a 450 km wide swath related to a grid with a mesh of 25 km in the across and along track directions. Wind vectors are retrieved from the measured microwave backscatter triplets obtained in that grid by inverting an empirical model (Stoffelen and Anderson, 1997) expressing the backscatter coefficient as a function of the surface wind speed and its direction with respect to the viewing azimuth. Since the wind-driven waves responsible for backscattering show little asymmetry when viewed in the upwind or downwind directions, the inversion results in a directional ambiguity, with two possible wind vectors of similar amplitudes and roughly opposite directions. This ambiguity needs a priori information to be removed.

The 3D-Var analysis scheme relies on the minimization of a cost function J,

$$J = J_B + J_O + J_C \qquad (1)$$

where J_B and J_O are quadratic terms measuring the distance from the model state to its background estimate (first guess) and the observations respectively, and J_C is a penalty term imposing physical constraints (especially the absence of fast growing gravity waves). For scatterometer data, it has been shown to be more successful to specify J_O in terms of wind vector rather than backscatter measurements (Stoffelen and Anderson, 1997). The observation errors are close to gaussian in wind components, whereas the

high non-linearity of the transfer function complicates the specification of the observation errors in the backscatter domain.

ERS scatterometer data are assimilated in the 3D-Var system as pairs of ambiguous winds, through a two-minima cost function of the following form:

$$J_O^{scatt} = (J_1 \cdot J_2)/(J_1^p + J_2^p)^{1/p} \qquad (2)$$

with:

$$J_i = (u_i - u)^2/du^2 + (v_i - v)^2/dv^2 \qquad (3)$$

where u and v are the analysed 10 m wind components, u_i and v_i (i = 1, 2) the scatterometer observations, du and dv the associated measurement errors, assumed to be 2 $m.s^{-1}$, and p an empirical exponent set to 4. The ambiguity is thus removed implicitly during the minimization process, taking into account all the information from the background field and the surrounding observations carried by the cost function, together with the corresponding physical constraints. The scatterometer winds are propagated in the model fields through the error structure functions of the J_B term, both in vertical and horizontal directions, and in terms of mass as well as wind - with the restriction that the 3D-Var scheme was actually univariate in the Tropics at the time of the assimilation experiments considered in this study.

Before being passed to 3D-Var, the ERS data are processed and quality controlled within a pre-processing procedure called PRESCAT (Stoffelen and Anderson, 1997). They are also sampled every 100 km to match the model resolution without introducing horizontal correlation. In addition a speed bias correction is applied, to remove the underestimation of high winds produced by the transfer function, CMOD4 (Gaffard and Roquet, 1995). This bias correction, derived from collocations with buoy data, was crucial to make good use of scatterometer data in the 3D-Var system. Before it was applied, assimilation experiments showed a systematic tendency to "fill" deep mid-latitudes lows because of too low wind speeds inferred from the scatterometer measurements.

ERS scatterometer data have been used operationally in the ECMWF 3D-Var system since its implementation in January 1996, starting with ERS-1 and switching to ERS-2 after the decommissioning of ERS-1 in June 1996. The orbit of the satellite is such that the swaths (see Figure 1a) are separated by about 100 minutes in time and 2500 km in distance at the equator, and roughly cover the same geographic area around local noon and midnight. It should be noted that this data coverage is sometimes reduced, especially in coastal areas where only two antennae are often available, or in places where the Synthetic Aperture Radar (SAR) is operated in image mode, which requires the scatterometer to be switched off. However none of these cases occurred in the region and period studied, and the data availability was remarkably stable.

4. Results of assimilation experiments

a) The study period

The study period was from the 24 August to 8 September 1995. Four major tropical disturbances occurred over the tropical Atlantic in this period: Humberto, Iris, Karen and Luis. Humberto and Iris had already reached the stage of mature hurricanes at the beginning of the assimilation period. Karen only developed to tropical storm intensity, while Luis was one of the most devastating hurricanes of the year causing much damage on the Leeward Islands. Karen and Luis could be followed from their initial development in the Eastern Atlantic, just to the west of Africa. Reports on the position and intensity of the cyclones from the U.S. National Weather Service (National Hurricane Centre, Miami) provided the best estimate of the hurricane positions for the evaluation of the performance of the analyses and forecasts of the ECMWF model.

b) Description of the assimilation experiments

The impact of the scatterometer and METEOSAT winds on the analyses and forecasts was studied in a series of data assimilation experiments. Initial experiments using the new 3D-Var analysis scheme at T106 resolution (half wavelength of 180km) and scatterometer data showed clearly that this configuration of the assimilation system was performing better than the OI analysis (also at T106 resolution) without scatterometer data. Experiments at T106 resolution using low level CMW from METEOSAT derived from both infrared and visible channel data indicated little impact from these data because of their limited coverage for the period and area of interest.

Given the positive impact of 3D-Var with scatterometer data at T106 resolution, it was decided to assess the impact of a SCAT/3D experiment at the operational (i.e. T213) resolution. This experiment was started on 24 August 1995 and ran for 16 days. The results were compared to those of the operational assimilation run which used the OI assimilation scheme with no scatterometer winds. This control run, denoted hereafter as CON, had the same model physical parametrizations as the SCAT/3D experiment. Finally to investigate the relative contributions of the scatterometer data and the 3D-Var analysis to the improved performance, two 3D-Var experiments were rerun with and without the scatterometer data.

In the SCAT/3D case, given the orbit pattern of the ERS-1 satellite and the range of longitudes under consideration, only four swaths were available on most days, with two swaths in the analysis period centred on 12 Z (descending tracks) and two centred on 0Z (ascending tracks). With their 450 km width and nearly 2500 km separation distance at the equator, these swaths when present led to a data coverage ratio of the order of 20%. However their influence was increased to almost 40% of the area of interest if one takes into account the 250 km correlation distances of the error structure functions used in the analysis scheme.

c) Impact on the analysis

During the study period the National Hurricane Centre reported the position of the four tropical cyclones at 12 Z for a total of 32 cases. The location of the cyclone in the analysis was estimated from the latitude and longitude of the maximum in the relative vorticity field at 850 hPa as proposed by Reed et al (1988). Recent work on the ability of the ECMWF re-analysis fields to describe TCs showed that TC tracking is more accurate when performed following vorticity maxima rather than pressure minima (E. Serrano, ECMWF, pers. comm.). A threshold of 5×10^{-5} s^{-1} was required for the relative vorticity maxima values to be considered representative of a strong circulation and below this value the TC was considered as missed by the analysis. Only the cases when the TC was located equatorward of 30°N were considered. The results are influenced by the resolution of the model itself which is approximately 90 km. Table 1 shows for each identified TC the mean difference between the analysed position and the reported position, the number of cases successfully detected as a TC for each experiment and the number of cases improved by the SCAT/3D assimilation.

In the SCAT/3D analysis all the reported TC positions were detected, while one, for Karen on 30 August 1995, was missed by CON. Out of the 32 cases considered, 22 had a better position in SCAT/3D. More significantly the mean position error was reduced, from 173 km to 111 km. The difference in the means was found to be significant at the 95% confidence level. As the uncertainty in the TC position is limited by the model resolution of 90 km, the mean value achieved by SCAT/3D is close to the maximum precision achievable with this model resolution.

To study the day to day model performance it is useful to refer to the time evolution of the wind and relative vorticity fields at 850 hPa at 12Z for SCAT/3D and CON over the tropical Atlantic as shown in Figure 2. The contour of the vorticity field starts at $5x10^{-5}$ s^{-1}, to make the interpretation of the maps easier and to be consistent with the threshold method used for the location of the hurricanes.

The initial development of the cyclones is generally well described in both analyses. The formation of Karen and Luis can be clearly recognized in the high relative vorticity values around 10°N - 20°W on the 24 and 27 August respectively. The capability of the model to form these type of disturbances, using synoptic observations and CMW, has already been demonstrated (Reed et al, 1988). The main problem is the conservation of the system over the sea. After leaving the African coast, easterly waves frequently weaken when they encounter colder water in mid-Atlantic. In the CON analysis the signature of the TC is systematically weaker than in the SCAT/3D analysis. This is particularly evident in the case of Hurricane Luis between the 31 August and 3 September. Only a weak circulation is present in CON whereas SCAT/3D exhibits a more realistic system with more sustained winds (see Fig. 2) and better positioning of the storm centre (the mean position error for these four days is 64km for SCAT/3D compared with 212km for CON). The case of Karen on 30 August is another example, with the storm being missed by the CON analysis while SCAT/3D has its intensity correct and a position error of 83km.

The later stages of the hurricane development (i.e. intensification whilst approaching the Caribbean Islands) were well described in both the CON and SCAT/3D analyses. For example the high relative vorticity values of Iris at the beginning of the study period and of Luis from the 4 September onwards were well represented as shown in Figure 2. The main difference between the two experiments is in the location of the storms, with SCAT/3D being more accurate. For example the mean position error for

Hurricane Iris from the 28 to the 31 August is 49km in SCAT/3D, an improvement of 200km with respect to CON.

In summary SCAT/3D improved the analysis of the three storms: Iris, Karen and Luis, while it was neutral for Hurricane Humberto (which had already reached a mature stage of development at the beginning of the assimilation period). The higher performance of SCAT/3D with respect to CON is a combined effect of the change from the OI to the 3D-Var assimilation scheme and of the use of scatterometer winds (see below). Figure 3 is an example, showing the scatterometer swath covering the storm Karen on the 31 August at 0 Z (a) and the SCAT/3D First Guess (FG) (b) and analysed (c) wind field at 850 hPa valid at the same time. The analysis minus FG increments arise from the lowest model level in correspondence with the scatterometer swaths and are then transferred to the wind field at 850 hPa through the analysis vertical structure functions. The same increments were not present in the CON analysis (not shown) which missed the storm at that time.

A case showing positive impact of the conventional data is that of Hurricane Luis on 4 September at 12Z. The circulation at 850 hPa was intensified to the east of the Caribbean Islands in both SCAT/3D and CON and the reason for this is the modification of the analyses by a critical SHIP/TEMP observation at 19.4°N - 57.9°W reporting a wind speed of 32 $m.s^{-1}$ and 37 $m.s^{-1}$ at 850 hPa and 820 hPa respectively, compared with the CON and SCAT/3D first guesses of 13 and 20 $m.s^{-1}$ respectively. This profile was from a vessel participating in the Automated Shipborne Aerological Programme (ASAP). The assimilation of this single observation was especially beneficial for CON, giving considerable increments to its analysis. Subsequently the better data coverage from the Caribbean Island stations and aircraft in this region resulted in a more accurate description of the hurricane in CON and hence small analysis differences between the two experiments from this point on. Note that at the end of the period the model gave values of 977hPa for the minimum surface pressure compared with 942hPa reported due to the limited resolution.

d) Impact on the forecast

The impact of the scatterometer data with 3D-Var was investigated in terms of forecasts by repeating the maximum vorticity study with the 24, 48 and 72 hour forecasts with the same method employed for the analysis. The results are shown in Tables 2, 3

and 4 and are limited to the cases of Humberto, Iris and Luis which were the only ones to actually become hurricanes. Note that the forecasts for the first days were not available (as SCAT/3D analyses were not computed before the experiment period) resulting in a lower number of cases than for the analyses. Cases are considered missed by the forecast when the maximum vorticity is lower than the threshold of $5x10^{-5}$ s^{-1} (as for the analysis) and also when the location of the reported and forecast maxima are more than 400 km apart. These "missed" cases must be taken into account when evaluating the forecast performance. The mean 24 hour forecast error is reduced from the 216 km of CON to 161 km of SCAT/3D, with just one more case missed by SCAT/3D. A similar improvement is found also in the 48 hour forecast, from 197km to 182km, with more positions detected in the SCAT/3D forecast. Finally a most striking improvement is found in the 72 hour forecast. At this range the SCAT/3D experiment is able to forecast 17 TC positions (80% of the total reports) with an error of 266 km compared with only 7 cases detected in CON (the large difference in number of cases means the position errors in Table 4 cannot be compared except for Iris). For all forecast ranges examined SCAT/3D improves the position error of half of the total cases reported.

The forecast impact is almost neutral for Humberto (same as the analysis impact), whilst it is very positive for Iris and Luis. For Iris, as the number of cases detected by the two experiments only differ by a maximum of one, the forecast errors can be compared. SCAT/3D misses one case, the forecast from the first day of the assimilation period, but its reduction in the one day forecast error is almost 50%. For Luis the improvement is for a higher percentage of cases where SCAT/3D is able to forecast all the reported positions in the 24 and 48 hour ranges and misses only one in the 72 hour forecast (corresponding to seven for CON).

For forecasts beyond 72 hours the impact of the improved analyses was lost as forecast model errors became more important in the prediction of the position and strength of the hurricanes.

As the SCAT/3D experiment improved the analysis of Hurricanes Iris and Luis, case studies were used to illustrate the impact on the corresponding forecasts. The analyses and 48 hour forecasts from the SCAT/3D and CON experiments were examined individually and compared for the most significant phases of both events. The study focused on the surface wind and pressure fields.

For Hurricane Iris, the CON analyses exhibit an erroneous eastward shift of 180-360 km in the position of the low pressure centre from 28 to 31 August, which does not occur in the SCAT/3D analyses using scatterometer data. A study of the forecasts shows that the improvement is retained by the model. A swath covering the storm centre in the 12Z analysis period from 28 August, followed by new swaths crossing the centre of the system every day from 30 August, either around 0Z or 12Z, contributes to reduce the SCAT/3D position error to about 90 km or less. A similar shift to that found in the analyses appears in the CON 48hr forecasts valid for 30 August to 1 September - i.e. 48 hours later -, and is greatly reduced in the SCAT/3D case as illustrated in Figure 4 with the forecast from 30 August. The analyses of SCAT/3D and CON shown for verification indicate a better agreement between the forecast and analysed fields for the former.

With Hurricane Luis, the impact of SCAT/3D is seen more in terms of intensity than position. Indeed, the cyclone centre is fairly well located in the CON analyses throughout the period, but the low pressure and the associated wind speeds are significantly underestimated as the system strengthens between 1 and 5 September before reaching the Caribbean Islands. As before, scatterometer swaths crossed or passed very close to the centre every day from 29 August to 3 September, alternately around 0 Z and 12 Z, and improved the analyses having a positive impact on the forecasts. The benefits of SCAT/3D are greatest for the analysis period from 1 to 3 September (see Fig. 2) when the lack of conventional data is the most severe and virtually causes CON to miss the development of Luis. The analysed minimum surface pressure remains lower by 2 to 3 hPa with SCAT/3D than CON every day, and the 48 hour forecast pressure also remains lower. The results are more obvious for wind speed, as shown in Figure 5: the SCAT/3D forecasts display systematically much stronger winds close to the centre, although the vortex is roughly located at the same place in both cases. Even when the operational analysis has captured the cyclone correctly on 4 September and produces more realistic wind speeds, the SCAT/3D winds remain stronger at shorter distances from the centre.

e) Relative impact of the 3D-Var analysis and the scatterometer winds

Two additional assimilation experiments were performed at a later stage of the study to check the respective roles of the scatterometer observations and the 3D-Var analysis scheme in the above results. As it was not possible to recreate identical conditions to

the 1995 pre-operational tests, the 3D-Var assimilation system was re-run over the first part of the study period with the latest version of the ECMWF model and 3D-Var at T213 resolution, successively with and without scatterometer data.

Although the use of a slightly different version of 3D-Var made the comparison with the previous SCAT/3D results difficult, the study of the analysed cyclone centre positions from the maximum of vorticity at 850 hPa clearly confirmed the positive impact of the scatterometer data on the analysis, and hence on the forecast. The mean position error was again significantly reduced in the experiment including scatterometer data, and the cyclone centre was analysed systematically whereas it was virtually missed for Luis in the 3D-Var experiment with no scatterometer data (for the few days included in the rerun i.e 1-2 September). In the latter case the improvements could be related to the analysis increments observed along the ERS-1 tracks as in the example showed with Karen previously in Fig. 3. However a positive contribution from the 3D-Var analysis scheme was also evident, especially in the case of Iris where the mean position error in the absence of scatterometer data was reduced to 157 km from 181 km obtained for the OI scheme in CON. These new results confirm the benefits seen in the SCAT/3D experiment over CON were a combination of both the scatterometer winds and the 3D-Var assimilation.

5. Conclusions

New datasets of satellite near surface wind observations of tropical cyclones have been used during the August/September 1995 period over the tropical Atlantic to investigate their impact on improving the analysis of the hurricanes occurring at that time. Several experiments were carried out, with the new data sources being assimilated into the ECMWF forecast model fields along with all the conventional and other satellite observations available on the Global Telecommunication System.

The scatterometer surface winds used in the operational 3D-Var assimilation system clearly showed instances where the position of the hurricanes had been improved by the inclusion of these data in the analysis. In addition the short-range forecast positions were also improved. The ERS scatterometer has a relatively narrow swath so a pass over a tropical cyclone is not always obtained in one day. However the next generation of scatterometers (e.g. NSCAT on ADEOS, ASCAT on METOP) will provide better

coverage and increase the likelihood of providing surface wind vectors regularly over tropical cyclones. The use of the 3D-Var assimilation system clearly provides a consistent way of selecting the correct wind vector from the 2 ambiguous vectors. It is important to emphasize that in addition to the use of the scatterometer winds some of the benefits come because the 3D-Var assimilation system made better use of all available observations to improve the analysis in the tropics. The optimal use of the new scatterometer data with improved coverage could eliminate the need for bogusing techniques to be applied to NWP analyses.

The impact of the lower tropospheric cloud motion winds from METEOSAT (both the operational infrared low level winds and the high resolution visible winds) was for this period not significant on the analysis. This was due to the relatively poor coverage of the METEOSAT cloud motion winds as in most cases they were only available around the periphery of the hurricanes, making it difficult for the assimilation system to improve the hurricane position and magnitude of the winds. Recently high resolution datasets from the new generation GOES satellites, not available operationally at this time, have demonstrated significant impacts in the NWP models (Velden et al 1997). Satellite operators are encouraged to develop techniques to produce more low level CMW in the vicinity of tropical cyclones.

Finally the importance of radiosonde observations is also clearly shown in this study by the rapid modification of the analyses of Hurricane Luis on 4 September by one key ASAP wind profile observation from a ship to the east of the Caribbean Islands.

6. Acknowledgements

This work was carried out as part of the EUMETSAT fellowship program and an ESA contract (number 11699/95/NL/CN) for monitoring ERS scatterometer winds. The authors are grateful for the useful comments from A. Hollingsworth at ECMWF and two anonymous reviewers.

7. References

Assimilation Quart. J. Roy. Meteorol. Soc 120 p27-p53.

Courtier, P et al., 1993: Variational assimilation at ECMWF. ECMWF Research Department Tech. Memo. 194, available from ECMWF librarian.

Gaffard, C and H Roquet, 1995: "Impact of the ERS-1 scatterometer wind data on the ECMWF 3D-VAR assimilation system" ECMWF Research Department Tech. Memo. 217, available from ECMWF librarian.

Eyre, J R, G Kelly, A P McNally, E Andersson and A Persson. 1993: Assimilation of TOVS radiances through one-dimensional variational analysis. Q J R Meteorol Soc, 119, 1427-1463.

Heming, J.T., J.C.L. Chan and A.M. Radford, 1995 A new scheme for the initialisation of tropical cyclones in the UK Meteorological Office global model. Meteorol. Appl. 2 171-184.

Ottenbacher, A., M. Tomassini, K. Holmlund and J. Schmetz 1996 Low level cloud motion winds from Meteosat high resolution imagery. Weather and Forecasting 12, 175 - 184.

Reed, R.A., A. Hollingsworth, W.A. Heckley and F. Delsol, 1988. An evaluation of the ECMWF operational system analyzing and forecasting tropical easterly wave disturbances over Africa and the tropical Atlantic. Mon. Wea. Rev. 116 824-865.

Ritchie, H., C. Temperton, A. Simmons, M. Hortal, T. Davies, D. Dent and M. Hamrud 1995 Implementation of the semi-lagrangian method in a high resolution version of the ECMWF forecast model. Mon. Wea. Rev. 123, 489-514.

Serrano E. and P. Unden 1994 Evaluation of a tropical cyclone bogusing method in data assimilation and forecasting. Mon. Wea. Rev. 122 1523-1547.

Shun C.M. 1992 Performance of the ECMWF model in tropical cyclone track forecasting over the western North Pacific during 1990-1991. ECMWF Research Department Tech. Memo. 184, available from ECMWF librarian.

Stoffelen, A and D Anderson, 1997 Ambiguity removal and assimilation of scatterometer data. Quart. J. Royal Meteorol. Soc 123 491-518.

Tiedtke, M 1989 A comprehensive mass flux scheme for cumulus parametrization in large scale models. Mon Wea Rev 117 1779-1800.

Velden, C. Olander, T. and S. Wanzon. 1997 The impact of Multispectral GOES-8 Wind Information on Atlantic Tropical Cyclone Track Forecasts in 1995. Part I: Dataset Methodology, Description and Case Analysis. Submitted to Mon. Wea. Rev. (same issue)

Figure Legends

Fig. 1 a) Data coverage for 31 August 1995 at 12Z, of satellite wind observations. ERS-1 scatterometer surface winds (yellow vectors), METEOSAT VIS (green) and IR (red) CMW below 700 hPa are overlaid on a Meteosat visible image. b) The coverage from the conventional observations over the same area between 700 hPa and the surface.

Fig.2 Time sequence of analysed wind and relative vorticity field at 850 hPa from 24 August to 8 September 1995 at 12Z, for OI (CON) versus SCAT/3D. The relative vorticity contour interval is $5x10^{-5}$ s^{-1}. The first letter of the assigned name of each event is also plotted to aid identification (when in brackets the position was not available from the NHC). H=Humberto, K=Karen, I=Iris and L=Luis.

Fig.3 Surface winds measured by the scatterometer (a) for storm Karen on the 31 August at 0 Z. First Guess (b) and analysed (c) wind field and relative vorticity at 850hPa of SCAT/3D valid at the same time. The relative vorticity contour interval is $2.5x10^{-5}$ s^{-1}.

Fig.4 CON (a) and SCAT/3D (b) 48hr forecasts of Hurricane Iris and their respective verifying analyses (c) and (d) for surface winds (arrows) and pressure (isobars) on 1 September 1995 at 12Z . The reported cyclone centre is marked by the black square.

Fig.5 CON (a) and SCAT/3D (b) analyses on 3 September 1995 of Hurricane Luis and their corresponding 48hr forecasts (c) and (d) for surface winds (arrows) and pressure (isobars) on 5 September 1995 at 12Z. The reported cyclone centre is marked by the black square.

TABLE 1. Comparison of SCAT/3D and CON analysis position errors during the period 24 August to 8 September 1995. The number of cases recognized in each experiment is also compared with the number of reported positions. In the last column is given the number of improved SCAT/3D analyses in terms of position error.

	Position Error (km)		No. of cases			
	SCAT/3D	CON	SCAT/3D	CON	Reported	No. impr. SCAT/3D
HUMBERTO	223	218	6	6	6	3
IRIS	71	181	10	10	10	7
KAREN	102	131	5	4	5	3
LUIS	90	156	11	11	11	9
ALL	111	173	32	31	32	22

TABLE 2. Same as Table 1 but for the 24 hour forecast

	Position Error (km)		No. of cases			
	SCAT/3D	CON	SCAT/3D	CON	Reported	No. impr. SCAT/3D
HUMBERTO	267	288	3	4	5	2
IRIS	157	252	8	9	9	5
LUIS	135	156	11	10	11	5
ALL	161	216	22	23	25	12

TABLE 3. Same as Table 1 but for the 48 hour forecast

	Position Error (km)		No. of cases			
	SCAT/3D	CON	SCAT/3D	CON	Reported	No. impr. SCAT/3D
HUMBERTO	190	347	1	2	4	1
IRIS	157	216	5	4	8	3
LUIS	192	150	11	8	11	-
ALL	182	197	17	14	23	11

TABLE 4. Same as Table 1 but for the 72 hour forecast

	Position Error (km)		No. of cases			
	SCAT/3D	CON	SCAT/3D	CON	Reported	No. impr. SCAT/3D
HUMBERTO	385	-	3	0	3	3
IRIS	182	257	4	3	7	2
LUIS	264	190	10	4	11	6
ALL	**266**	**219**	**17**	**7**	**21**	**11**

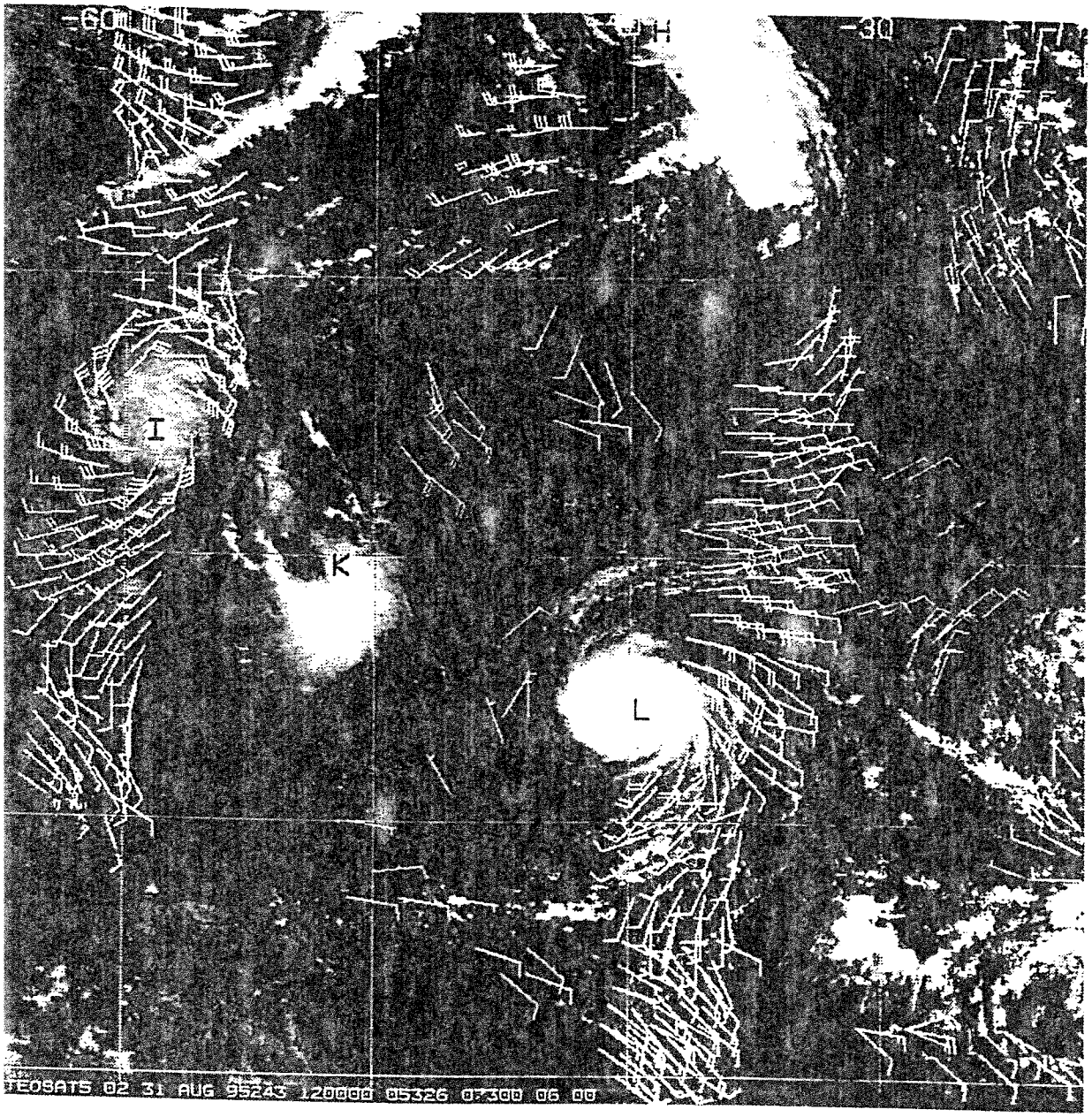

Fig. 1a

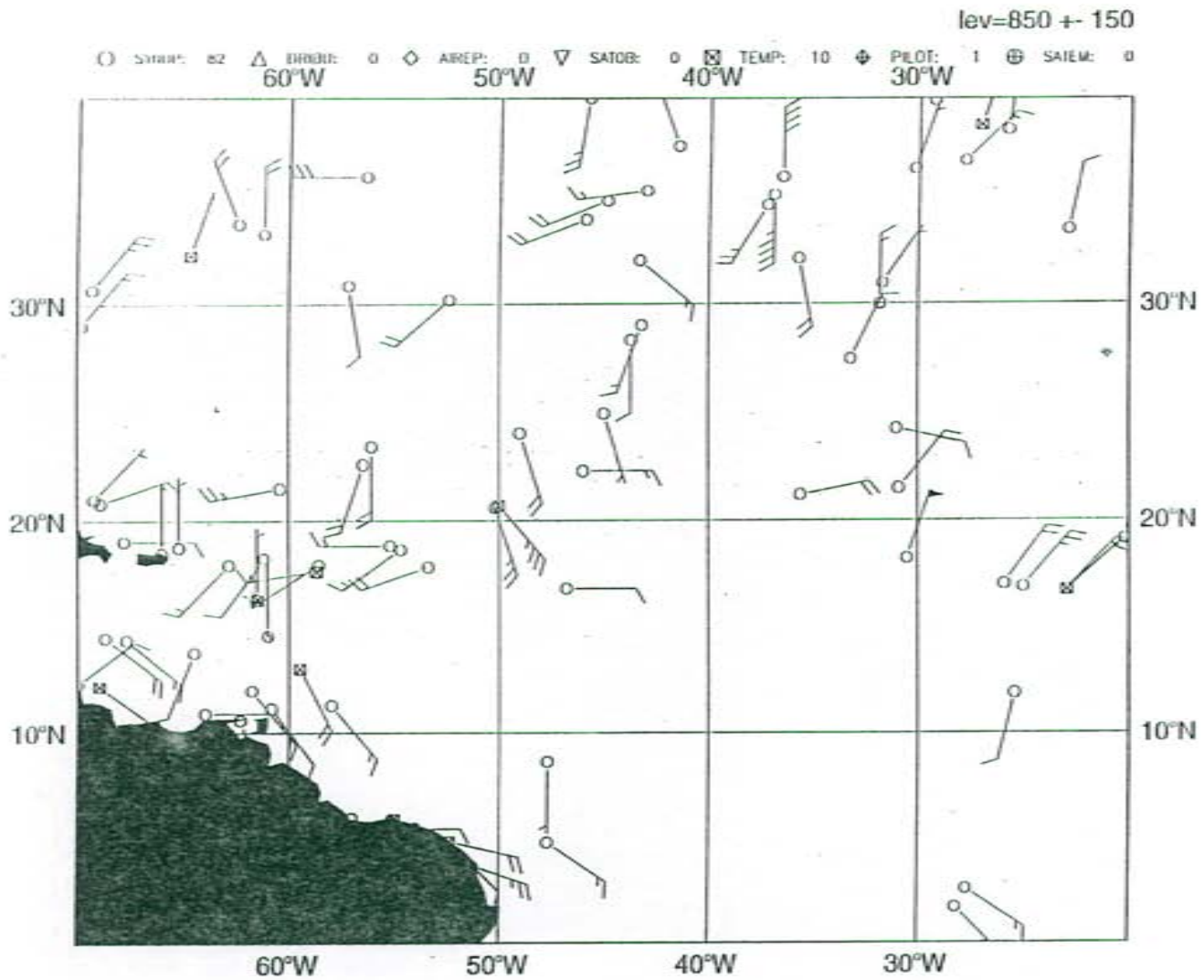
lev=850 +- 150
SYNOP: 82
DRIBU: 0
AIREP: 0
SATOB: 0
TEMP: 10
PILOT: 1
SATEM: 0
60°W
50°W
40°W
30°W
30°N
20°N
10°N

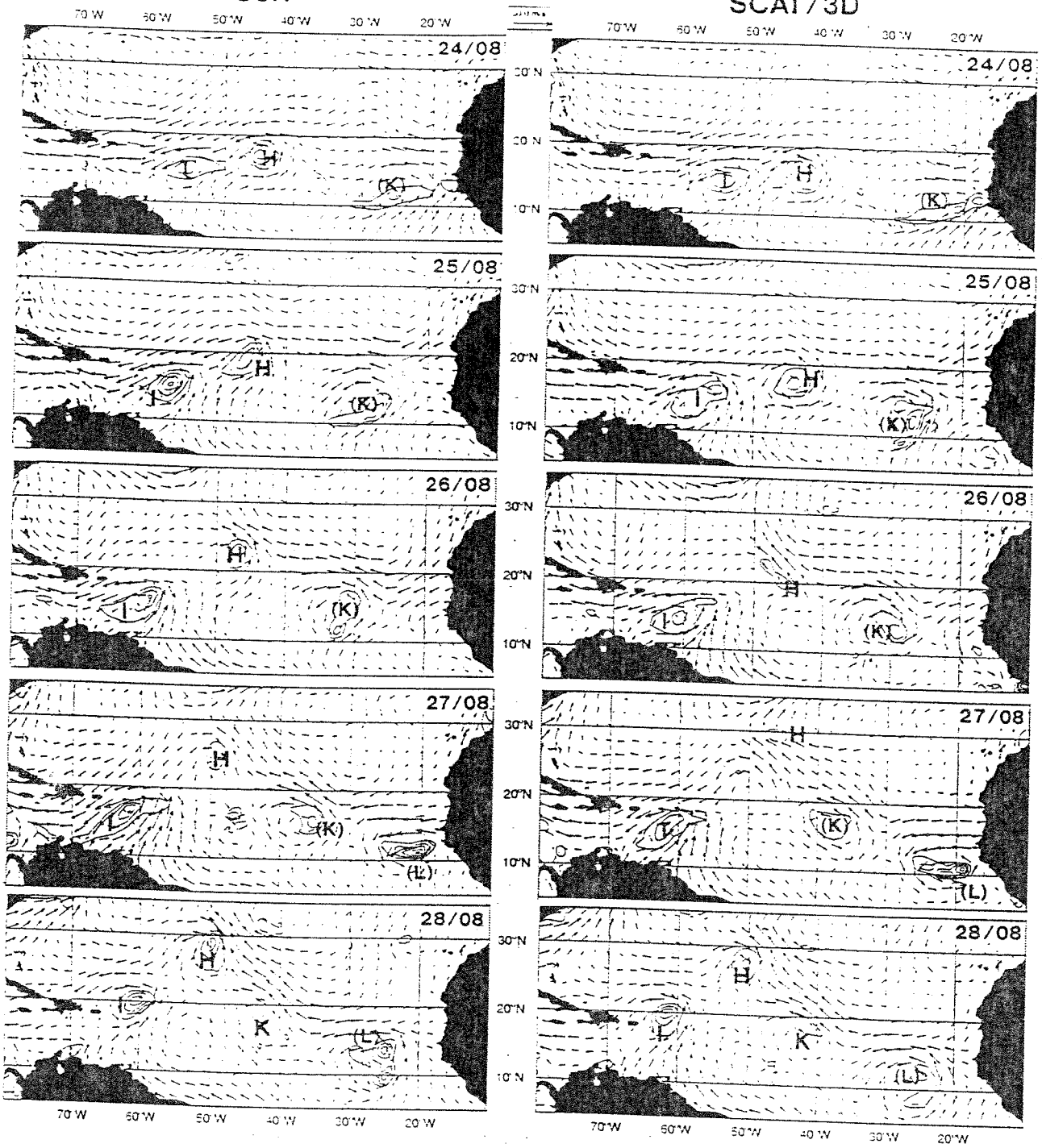
CON
SCAT/3D
70°W
60°W
50°W
40°W
30°W
20°W
30°N
20°N
10°N
24/08
25/08
26/08
27/08
28/08
H
L
K
(K)
(L)

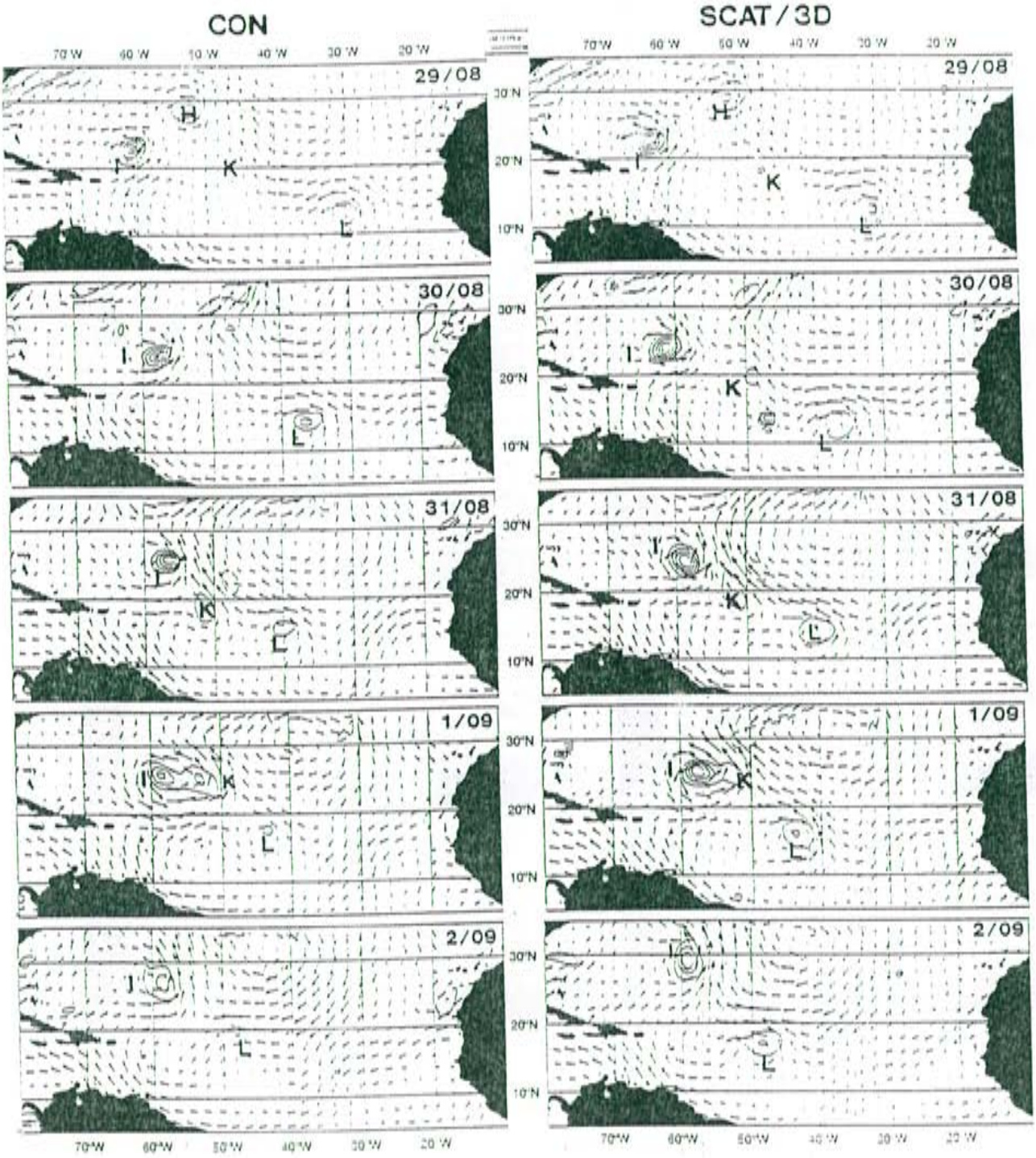
CON
SCAT/3D
70°W
60°W
50°W
40°W
30°W
20°W
30°N
20°N
10°N
29/08
30/08
31/08
1/09
2/09
H
I
K
L

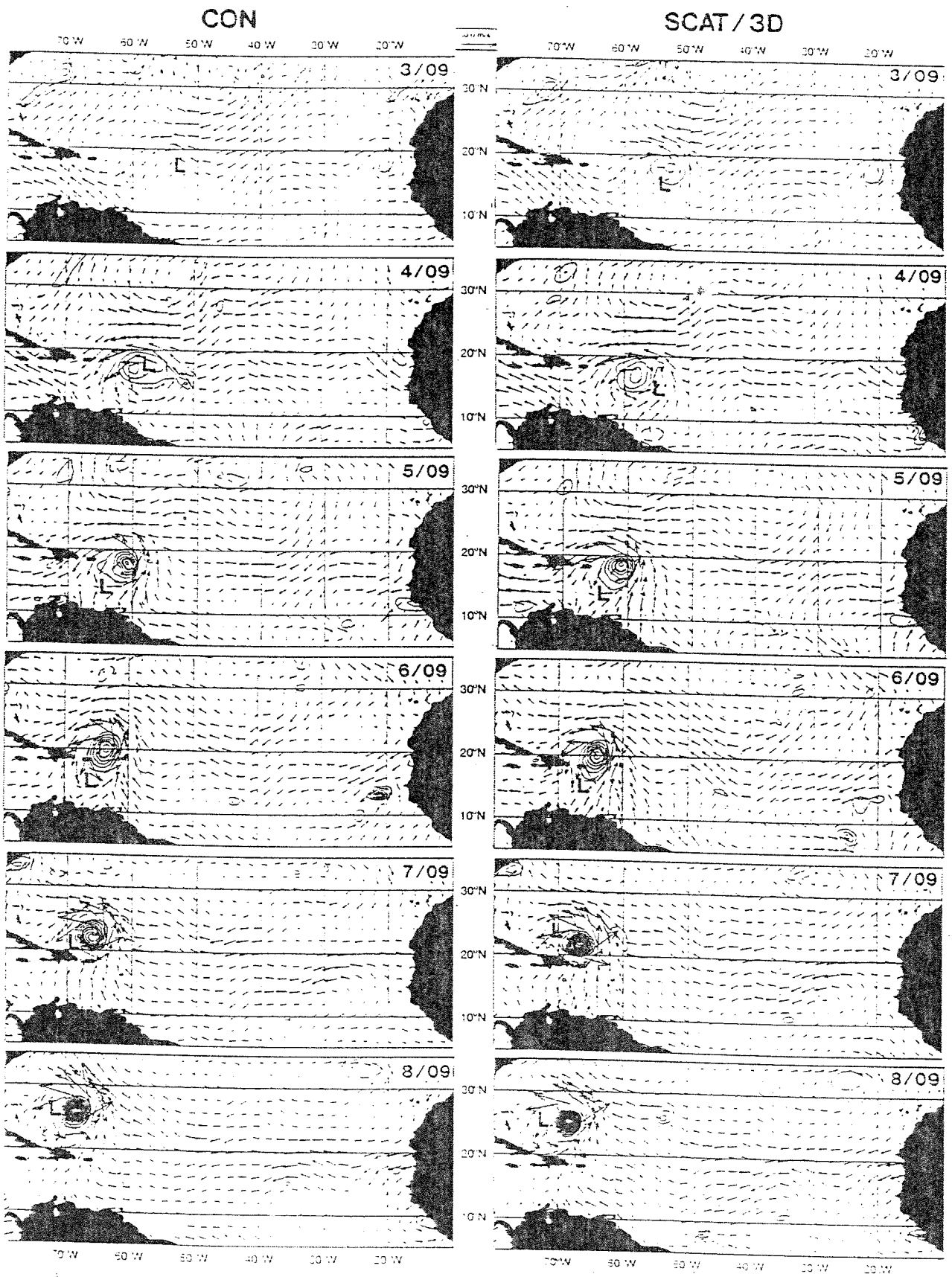
CON
SCAT / 3D
70°W
60°W
50°W
40°W
30°W
20°W
30°N
20°N
10°N
3/09
4/09
5/09
6/09
7/09
8/09
L

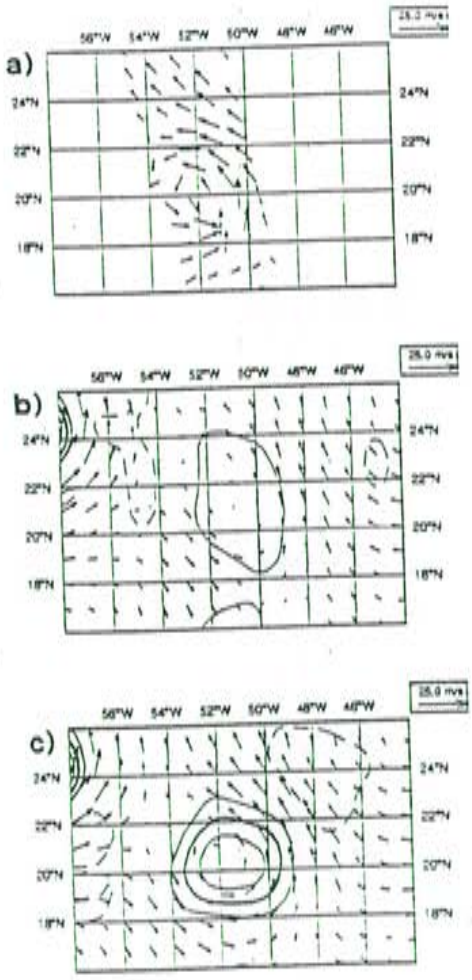
a)
b)
c)
56°W
54°W
52°W
50°W
48°W
46°W
24°N
22°N
20°N
18°N

a)

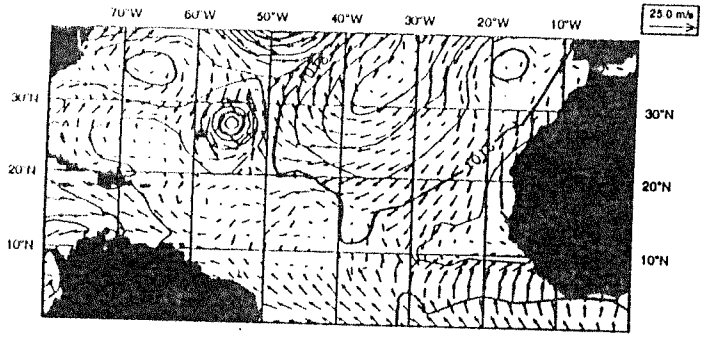

b)

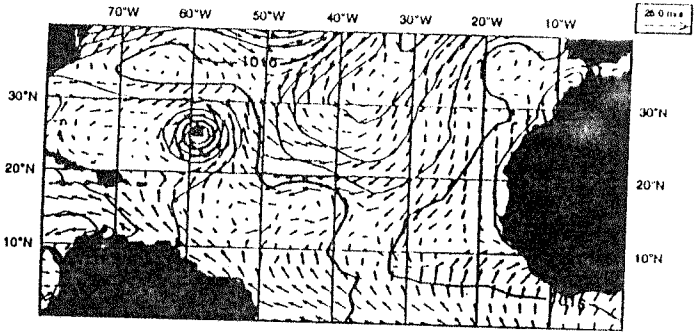

48 hour forecast

c)

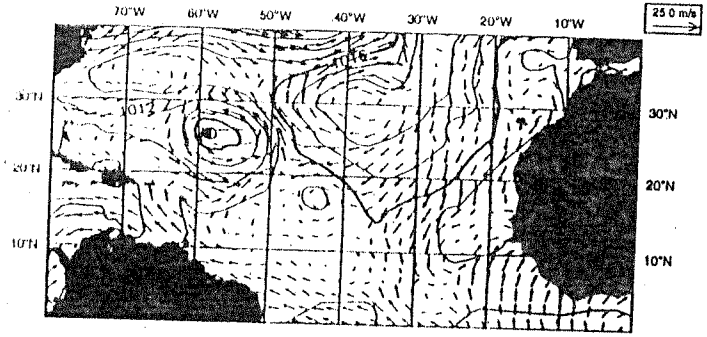

d)

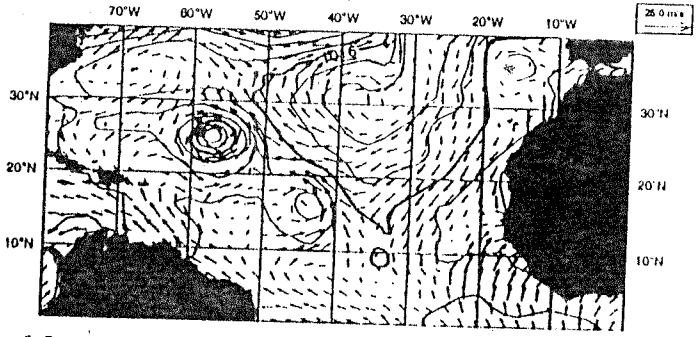

Verification

a)

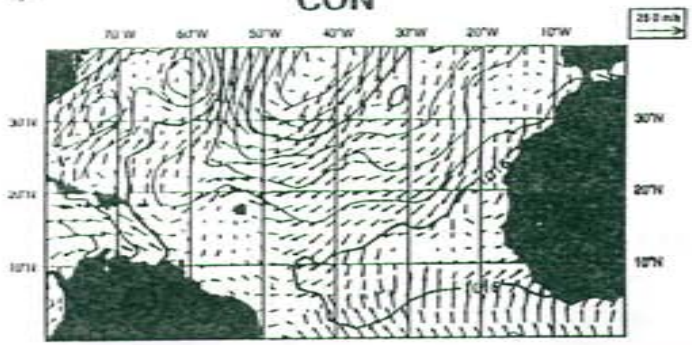

b)

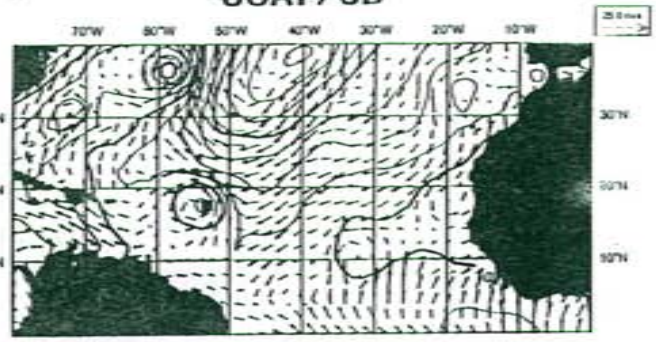

Analysis

c)

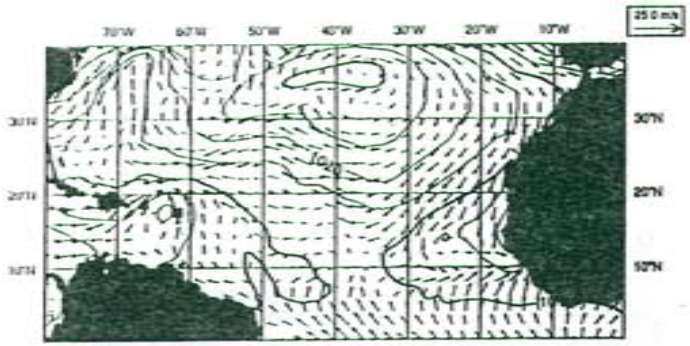

d)

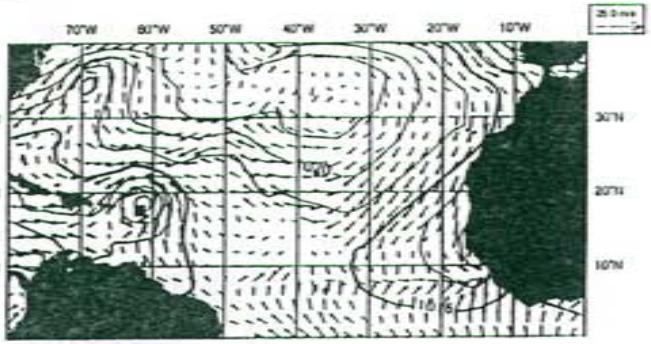

48 hour forecast

ANNEX E

- Influence of observations on the operational ECMWF system

Technical Memorandum

Research Department

Technical Memorandum No. 244

Observing system experiments with the 3D-Var assimilation system

by

Per Undén, Graeme Kelly, Didier Le Meur and Lars Isaksen

December, 1997

European Centre for Medium-Range Weather Forecasts
Europäisches Zentrum für mittelfristige Wettervorhersage
Centre européen pour les prévisions météorologiques à moyen terme

Observing System Experiments with the 3D-Var Assimilation System

Per Undén, Graeme Kelly, Didier Le Meur and Lars Isaksen

1. Introduction

The cost of making observations is by far the largest single cost in the whole process of making a forecast. The cost–efficiency of the composite observing system is uppermost in the minds of those concerned with funding and operating the World Weather Watch. The requirements of a composite observing system vary with the forecast range, forecast area, and forecast weather element. The requirements also vary with the required accuracy for each forecast element. For example, precipitation forecasts are less accurate than pressure forecasts, because of modelling problems and a lack of data on moisture and clouds. Equally, requirements for wind forecast accuracy are more stringent for ocean wave– forecasting than for general marine forecasting, because a wave model is very sensitive to wind forcing. Here we assess through observing system experiments (OSEs) the contribution made by the main ground–based and satellite based operational systems to medium range forecasting. OSEs are data assimilation experiments where one can assess the impact of an operational observing system by deleting its observations from the operational network and then running extended data assimilation and regular forecasts with the reduced system to assess the contribution of the deleted system to the total operational system. Equally OSEs can be used to assess the value of a new or experimental observing system by running extended data assimilation and regular forecasts with and without the new system, to assess its overall impact on forecast and analysis skill.

Given the vast cost of observations it behoves NWP centres to make effective use of observations. Kelly et al. (1993) performed a series of observing system experiments in 1991 with the then-operational ECMWF system based on optimal interpolation (OI, Lorenc, 1981). They used a baseline observational system consisting of in–situ data only and comprising radiosondes, aireps, synops, ships and buoys. They used OSEs to assess the impact of adding SATEMs only, SATOBs only, and SATEMs plus SATOBs to the baseline system. The satellite observing systems were not additive in terms of their forecast impact. Northern Hemisphere forecast scores were best with SATOBs without using SATEMs. Also SATEMs without using SATOBs was slightly better than using both SATEMs and SATOBs in the assimilation. These unsatisfactory results triggered a critical appraisal of the use of data in the OI system. The experiments revealed problems with the use of NESDIS TOVS satellite thicknesses in the Northern Hemisphere (Andersson et al. 1991, Kelly et al. 1991) and as a consequence TOVS data were removed from the Northern Hemisphere and tropical troposphere until the introduction of 1D–VAR in 1992 (Eyre et al.,1993).

Furthermore, it helped to motivate the development a 3D-Var system which could make a direct analysis of TOVS sounding radiances together with all other data. The purpose of the present paper is to repeat and extend the earlier experiments, but this time using the 3D–Var assimilation system, which became operational in early 1996. The present results are much more satisfactory than the earlier results, and demonstrate that the main observing systems are contributing in important ways to medium range forecasts in the Northern Hemisphere, in the tropics, and in the Southern Hemisphere. Equally the results are a validation of the performance of the 3D-Var system, and show that in broad terms it is working as intended in all three areas.

OSEs are normally performed globally at ECMWF in order to study global impacts of observing systems as well as of the data assimilation system itself. With a global medium range forecasting system it becomes natural to study the effects on the global scales since impact spreads over large parts of the hemispheres during medium range forecasts. Such observing

system experiments have been carried out recently for the satellite observing systems and for some of the conventional systems. Impact of scatterometer data has been studied separately in both 3D- and 4D-Var.

Another set of experiments has been performed to study impacts of the extra FASTEX data. The enhancement of the North Atlantic radiosonde network during the period was considerable and probably to the highest level of data coverage ever for that area. In addition the impact of the dropsondes has been studied separately from that of the land- and ship-based radiosondes. First, a long period was assimilated with the dropsondes and the impact gauged. Then, five particularly interesting cases were analysed with targeted dropsondes assimilated over only one or two analysis cycles. This was in order to enable the local direct impact of targeted dropsondes to be determined.

The interpretation of OSEs is not always straight–forward. The value of an observing system is most easily shown when energetic events occur during the test period, and when only one observing system sees the event (Uppala et al. 1985). Thus an observing system's value is easier to demonstrate by adding it to a minimal base–line system, than by deleting it from a maximal base–line system. The stand–alone value of new system may be masked if there are overlaps in the observations. This can happen directly if two systems observe the same variables in the same area. It can also happen indirectly if a multi–variate data assimilation system uses multi–variate relations from observations of other variables in the same area, or if a 4D–Var data assimilation uses the time– history of other observations in the same area or upstream of the area of interest. Equally it is possible that observations critical for one purpose or area may be redundant for another purpose or area. For these reasons we have assessed synoptic aspects of the results as well as assessing forecast scores.

2. Global observing system experiments

Two series of Observing System Experiments (OSEs) were run for periods in December 1996 and February 1997. OSEs are designed to study the forecast impact of different observation types and detect any problems with their combination. The first set used the ECMWF data assimilation and forecasting system with the operational version as of December 1996 (Andersson et al., 1994, 1996). The period chosen was 19961205 00 UTC until 19961219 12UTC and ten-day forecasts were run from 12 UTC every day. Thus there were 15 forecasts in this set. Soon after this time a number of revisions of the 3D-Var analysis were made. A completely new background constraint (J_b) formulation was introduced operationally on 15 May 1997 (Bouttier et al.,1997). A second set of experiments, with the same configurations of observing systems, was run using the data assimilation system as it became operational in May 1997. This second period was from 19970201 00 UTC until 19970214 12 UTC with ten-day forecasts from 12 UTC every day. Combining these 14 new forecasts with the first set of 15 showed very similar average forecast impact of the different observing compared with the first period on its own. Therefore both periods have been combined into one 29-case sample of ten-day forecasts in order to enhance the significance of score averages and distributions.

2.1 Satellite based systems

The first configurations of the OSEs to be described here involve the satellite based systems.

2.1.1 TOVS and SATOB data

The control assimilation used both SATEM retrieved thicknesses in the stratosphere, TOVS radiances in the troposphere and SATOB cloud and water vapour winds in addition to conventional in-situ observations and scatterometer data from ERS-2. Three experiments were then run where a) both TOVS and SATOBs were removed b) TOVS removed and c) SATOBs removed. This allows us to see the impact of TOVS on their own, TOVS without SATOBs, SATOBs on their own, SATOBs without TOVS and TOVS and SATOBs together. Fig. 1 shows geopotential anomaly correlations at 500 hPa for the two hemispheres in the extratropics. The scores are averaged over all the 29 cases. In the Northern

Hemisphere there is a clear (but small) degradation without any of the TOVS or SATOBs data. This is an important finding, as there is often the suggestion that it is not possible to show the impact of the satellite data in the Northern Hemisphere. The SATOBs have a positive impact in the Northern Hemisphere. This impact must come mostly from the tropics, where there are plenty of SATOBs in addition to conventional data and scatterometer data from ERS-2. Withdrawing the TOVS additionally gives a slight further deterioration. Just running without the TOVS shows almost neutral impact in the Northern Hemisphere. The fact that withdrawing TOVS when SATOBs are not used shows a degradation indicates that TOVS only has a positive impact in the Northern Hemisphere in the absence of SATOBs.

The impact of the TOVS is striking in the Southern Hemisphere; its main impact being up to 1 1/2 days in the medium range. With TOVS used there is little impact of the SATOBs and without them the SATOBs do have a small but noticeable effect in terms of forecast score improvement.

The effect on the scores of withholding both satellite systems is significant in both hemispheres, as shown in Fig. 2 for 500 hPa heights. In the Northern Hemisphere the differences in forecast scores are small, but the distribution is well clustered on the lower score side for the NOSAT configuration. Two forecasts are better from the NOSAT assimilation; all the rest are either better or very close to neutral. In the Southern Hemisphere there are no better forecasts without satellites.

The tropics have been verified in terms of RMS errors of wind vectors at 850 and 200 hPa. The satellite systems show a very large impact on the tropical scores (Fig. 3). (In the beginning of the forecasts the discrepancies are however exaggerated by the fact that the operational analysis, which used all the data, was used for verification). Nevertheless, in the medium range, withholding of TOVS shows a considerable degradation compared with the control. Additionally removing the SATOBs shows an ever larger degradation. When TOVS are used the withdrawal of SATOBs has a small negative impact in the medium range. In the shorter range SATOBs have a similar impact to TOVS. Without SATOBs, the removal of TOVS shows a large degradation, especially at 200 hPa.

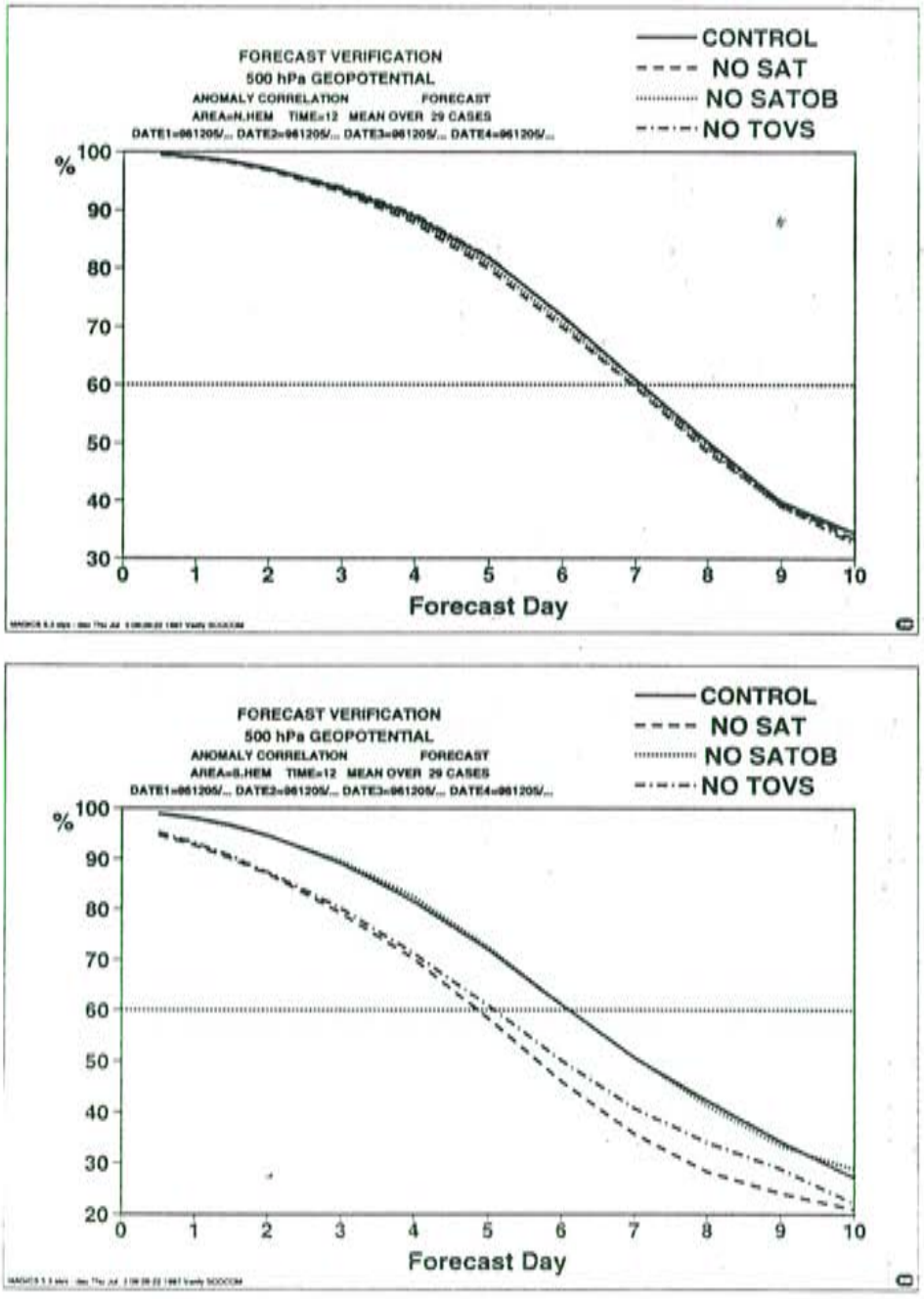

Figure 1. Mean 500 hPa geopotential forecast anomaly correlations in the Northern and Southern Hemisphere extratropics

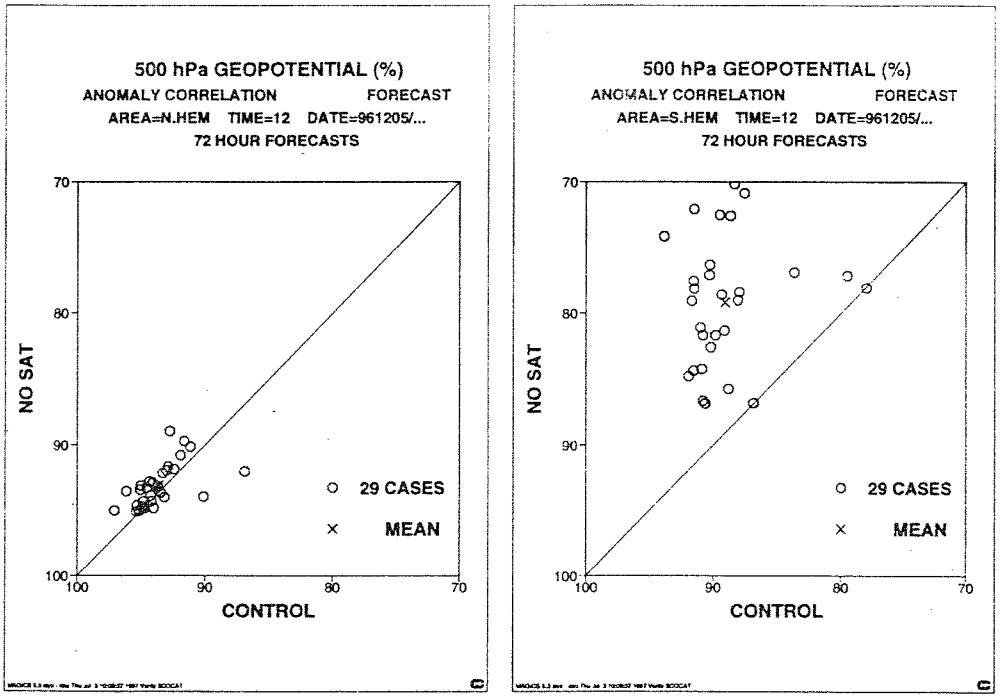

Figure 2. Scatter diagrams of anomaly correlations between forecasts without satellite data (TOVS and SATOBs) and control at 500 hPa and 72 hours forecast range for the Northern and Southern Hemispheres.

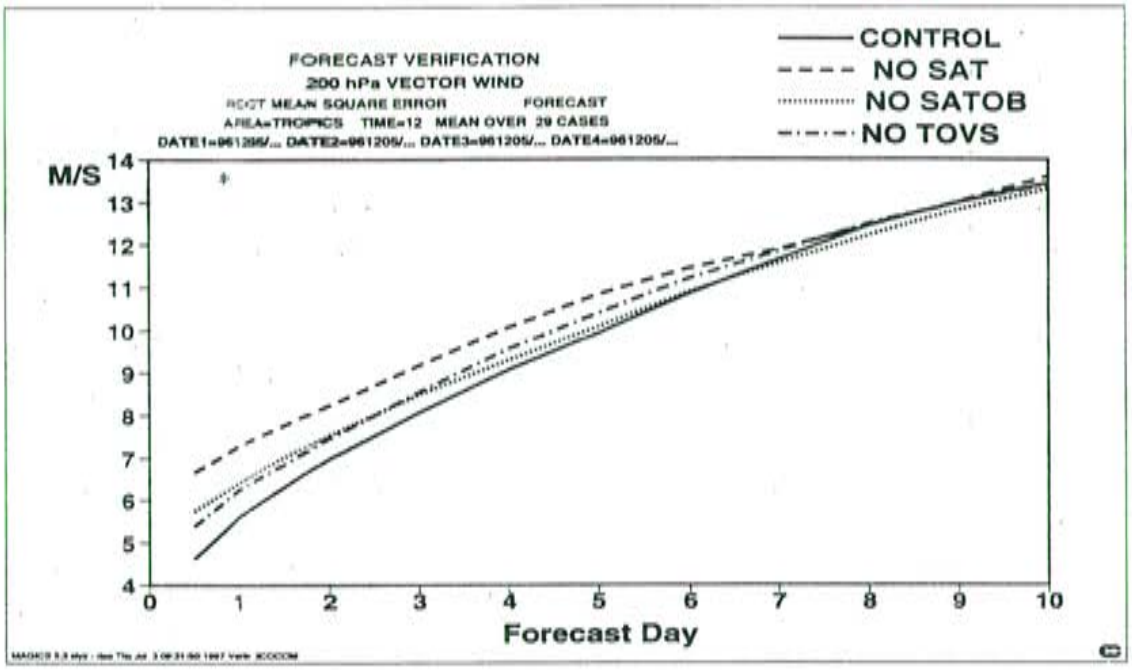

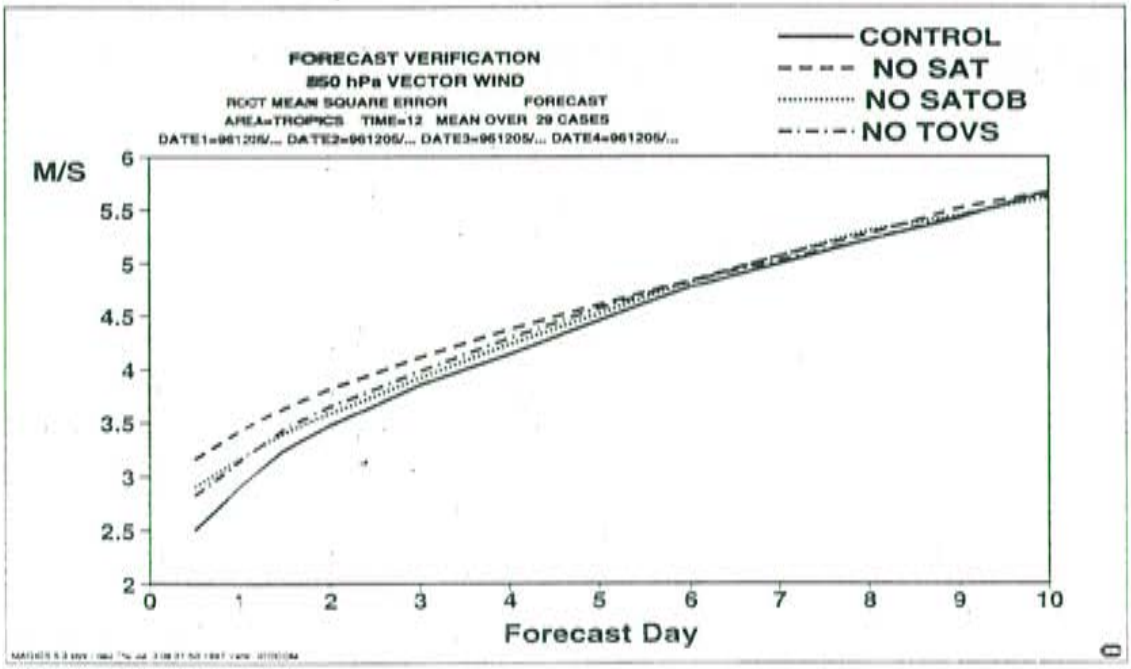

Figure 3. Mean 200 and 850 hPa wind forecast RMS errors in the tropical belt 20° N to 20° S.

2.1.2 Scatterometer data

In order to study the impact of ERS-1 scatterometer data in 3D-Var and 4D-Var a set of assimilations was performed for the last two weeks of January 1996. Reference runs were done with IFS CY15R7 ("old J_b") using four updates for the 4D-Var assimilation. The comparison assimilations were performed using similar configurations except for using scatterometer data.

The results shows that scatterometer data improve the scores for the Northern Hemisphere in both 3D-Var and 4D-Var but that it is most pronounced in 4D-Var. The improvements are largest near the surface but extend throughout the troposphere in 4D-Var. The positive impact in 4D-Var comes from better assimilation of some low pressure systems in the North Pacific. The analysis improvements are maintained by the forecast model leading to better medium-range forecasts for the test period investigated.

For the Southern Hemisphere the use of scatterometer data has a neutral impact on the scores both in 3D-Var and 4D-Var. We believe this is due to less intense weather systems during the Southern Hemisphere summer period.

In addition to the previous studies, the tandem operations of the ERS-1 and ERS-2 scatterometers in April-May 1996 were taken as an opportunity to investigate the impact of the increased data coverage provided by using them together. For that, four parallel assimilation experiments were performed in 3D-Var over the first week of April, using either no scatterometer data (NOSCAT), ERS-1 or ERS-2 data only (ERS1, ERS2), and both ERS-1 and ERS-2 data (ERS1+2). The same version of the ECMWF model as above was used in all cases (CY15R7).

The study was first focused on the impact on the surface wind analysis, comparing the departures between first guess and observations for each experiment. Table 1 shows the average results obtained taking the observations from both scatterometers as a common reference. The vector RMS difference between first guess and observations is reduced respectively by 10 cm/s and 8 cm/s using the ERS-1 and ERS-2 instruments separately, and by 15 cm/s using them together.

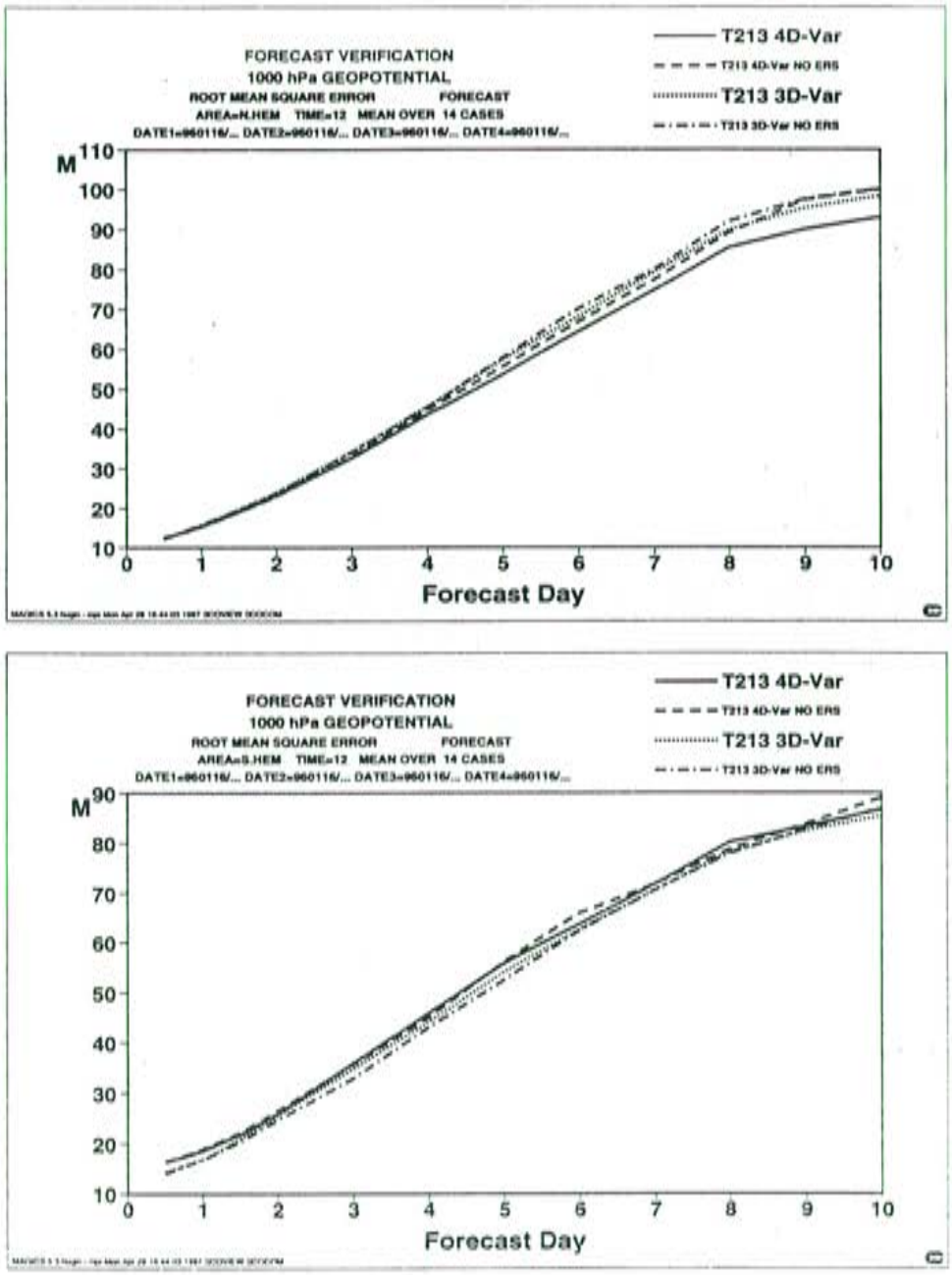

Figure 4. 1000 hPa height forecast RMS errors for Northern and Southern from 4D-Var and 3D-Var assimilations with and without scatterometer data.

Experiment	vector RMS (m/s)	difference wrt NOSCAT
NOSCAT	3.40	/
ERS1	3.30	-0.10
ERS2	3.32	-0.08
ERS1+2	3.25	-0.15

Table 1. RMS departures between first guess and scatterometer observations obtained using no scatterometer data (NOSCAT), ERS-1 or ERS-2 data only (ERS1, ERS2) and both ERS-1 and ERS-2 data.

These average results were then studied further by limiting the comparisons with the NOSCAT experiment to the cases with most significant impact, through the application of a minimum "impact threshold" on the vector difference between the ERS1, ERS2 or ERS1+2 first guess and the NOSCAT first guess at each scatterometer observation. Figure 5 shows the vector RMS first guess minus observation differences thus obtained for the ERS1 and NOSCAT experiments as a function of the "impact thereshold" in the assimilation using ERS-1 data. Very similar RMS reductions were observed for comparable impact thresholds when evaluating the ERS2 and ERS1+2 cases in the same way. The only significant difference was in the number of data exceeding a given impact threshold, which in the tandem assimilation case was roughly the sum of its values in both single assimilation cases. A good complementarity was thus demonstrated between both scatterometers, their separate benefits being juxtaposed without particular overlap when using them together. This was not obvious, since a redundancy could on the contrary be expected due to the fact that the ground tracks of ERS-1 and ERS-2 were following each other with a 24-h delay during their tandem operations.

A similar complementarity was found again when extending the study to the ten-day forecasts. Here the separate improvements obtained in each single assimilation case tended to be systematically added in terms of anomaly correlation scores in the tandem configuration in most of the verification areas. The results were however more clearly positive in the Northern Hemisphere, where a kind of synergy could even be noticed on average, the ERS1+2 experiment exhibiting a gain of 6 hours in the reliability of the forecast around day 7, whereas both ERS1 and ERS2 on their own have a nearly neutral overall impact (Fig. 6).

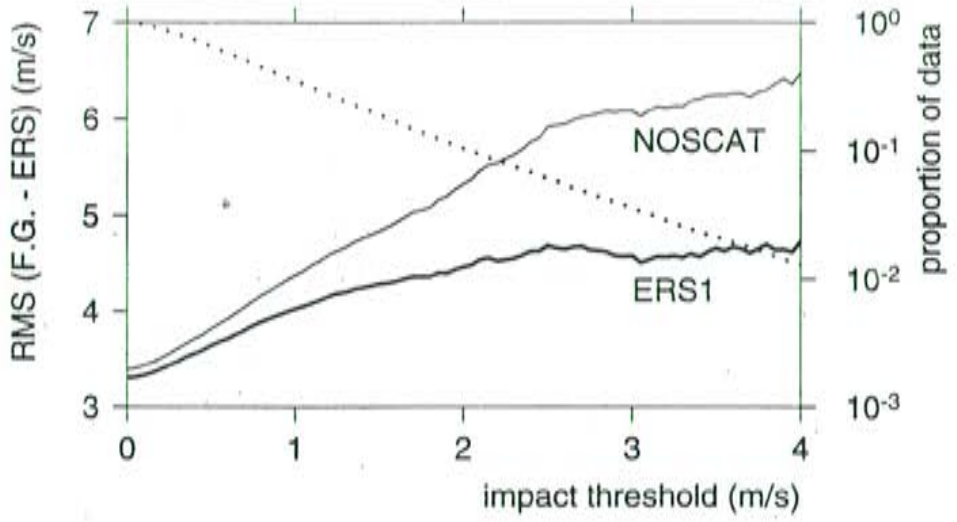

Figure 5. RMS differences between first guess and scatterometer observations using no scatterometer data (NOSCAT) and ERS-1 data only (ERS1) as a function of the "impact threshold" in the assimilation using ERS-1 data. The dotted line indicates the proportion of data exceeding a given threshold in logarithmic scale.

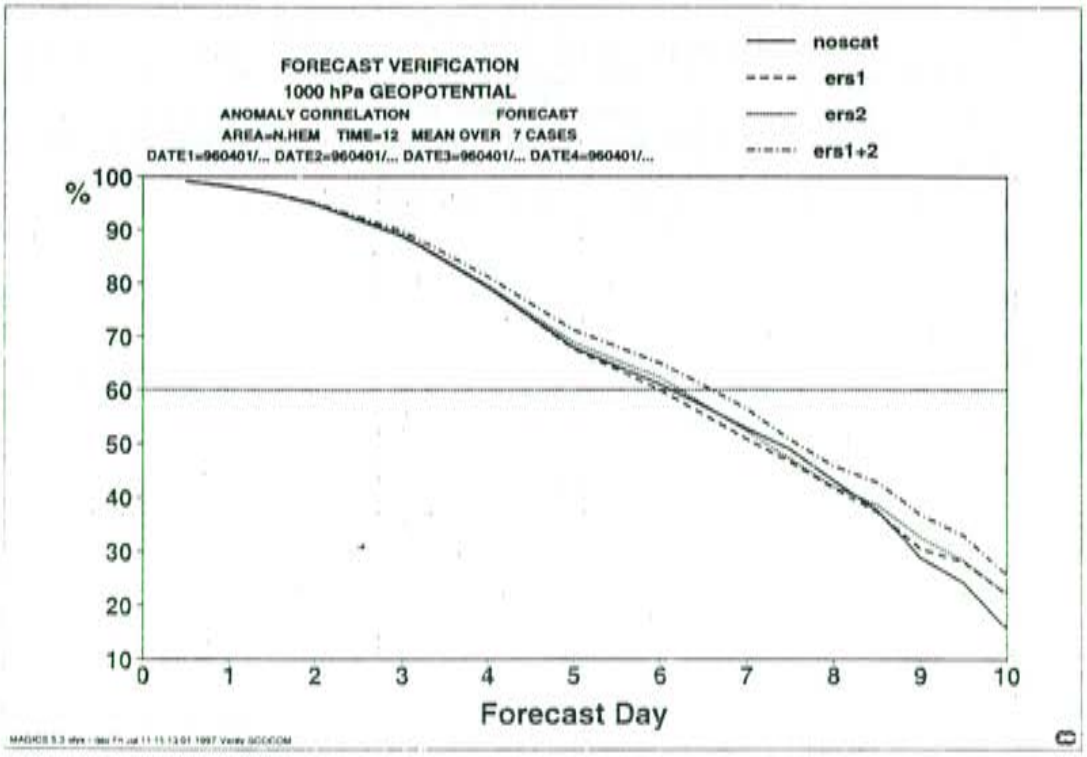

Figure 6. Mean 1000 hPa geopotential forecast anomaly correlations obtained over the Northern Hemisphere using no scatterometer data (NOSCAT), ERS-1 or ERS-2 data only (ERS1, ERS2) and both ERS-1 and ERS-2 data (ERS1+2).

2.2 In-situ observing systems

The second group of experiments involve the impacts of some of the in-situ observing systems. One pair of assimilations was done without TEMP/PILOTs to show the impact of the upper air network globally. The other assimilations were done without AIREP data (all kinds of aircraft observations) and can be compared with the same control as above, which used all the observations.

The impact of the radiosondes and PILOTs is very large in the Northern Hemisphere (Fig. 7a). In the Southern Hemisphere the scarcity of these data compared with the satellite data shows very small impact of the radiosondes in the medium range (Fig. 7b). The radiosondes do however show a slight positive impact in the day 1 -3 range of the Southern Hemisphere forecasts. After day 6 there is even some degradation when radiosondes have been used, but it is at a range when the Southern Hemisphere forecasts are of low quality anyway and when a large sample of forecasts may be needed for reliable results. It may however indicate that some large scale information is not used correctly from the sparse network of radiosondes in the Southern Hemisphere and there may be a problem in the data assimilation system itself as well as with the quality of the observations.

Aircraft observations show a clear positive impact on the Northern Hemisphere forecasts. Their positive impact is somewhat larger at 200 hPa, but still much less then the radiosonde impact. For the different areas, the North Pacific shows the largest sensitivity to radiosondes (Fig. 8a). All the other areas in the Northern Hemisphere also show a significant and large positive impact of radiosondes in the medium range. The aircraft data show particularly large positive impact over North America (Fig. 8b), but still less than the radiosondes do. Over the North Atlantic and Europe (Fig. 9a and b) their impact is also positive but is, especially over Europe, small compared with the radiosonde impact.

Tropical wind scores are mainly affected by the radiosondes, where they have a large positive impact. Aircraft data show a much smaller positive impact in this area (Fig. 10), probably due to a the relatively low number of data in the tropics.

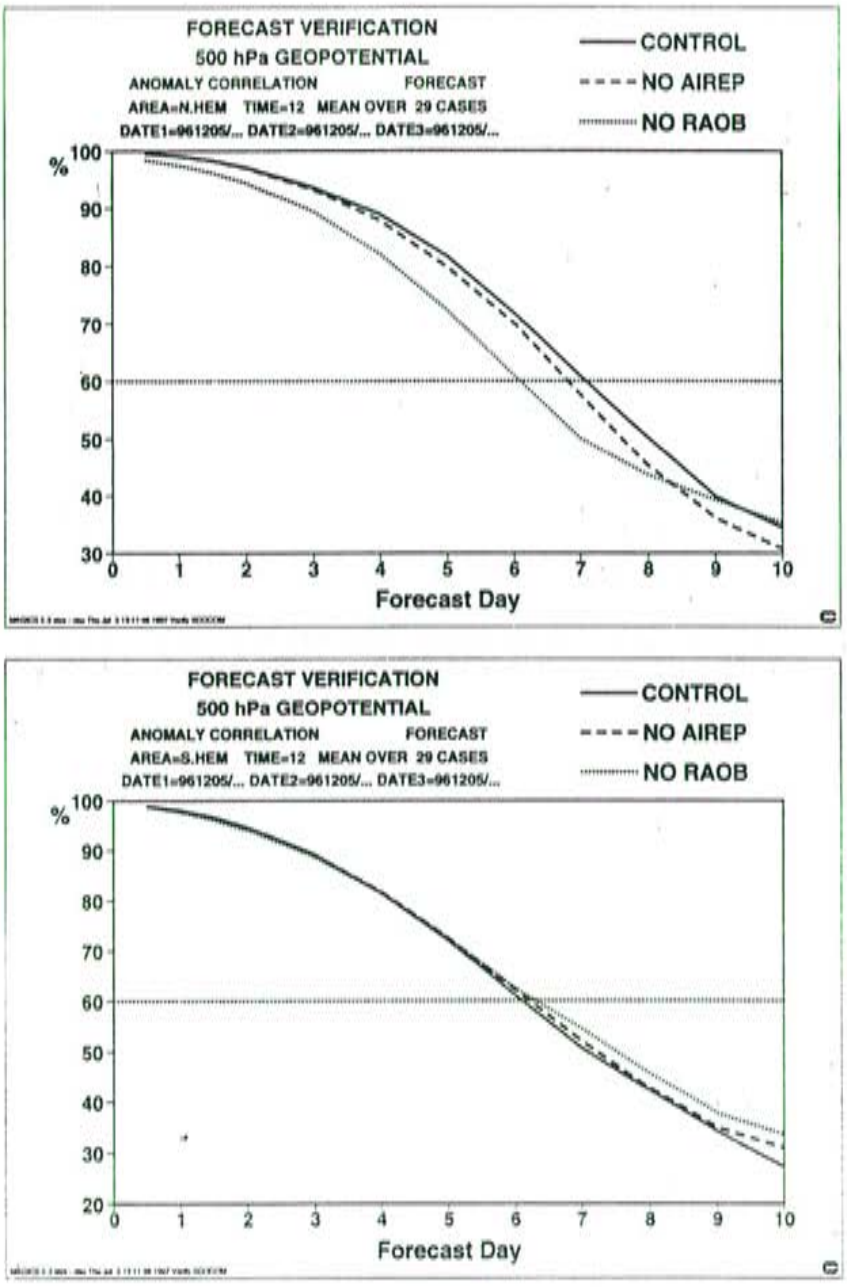

Figure 7. Mean 500 hPa geopotential forecast anomaly correlations for the Northern Hemisphere (top) and Southern Hemisphere (bottom).

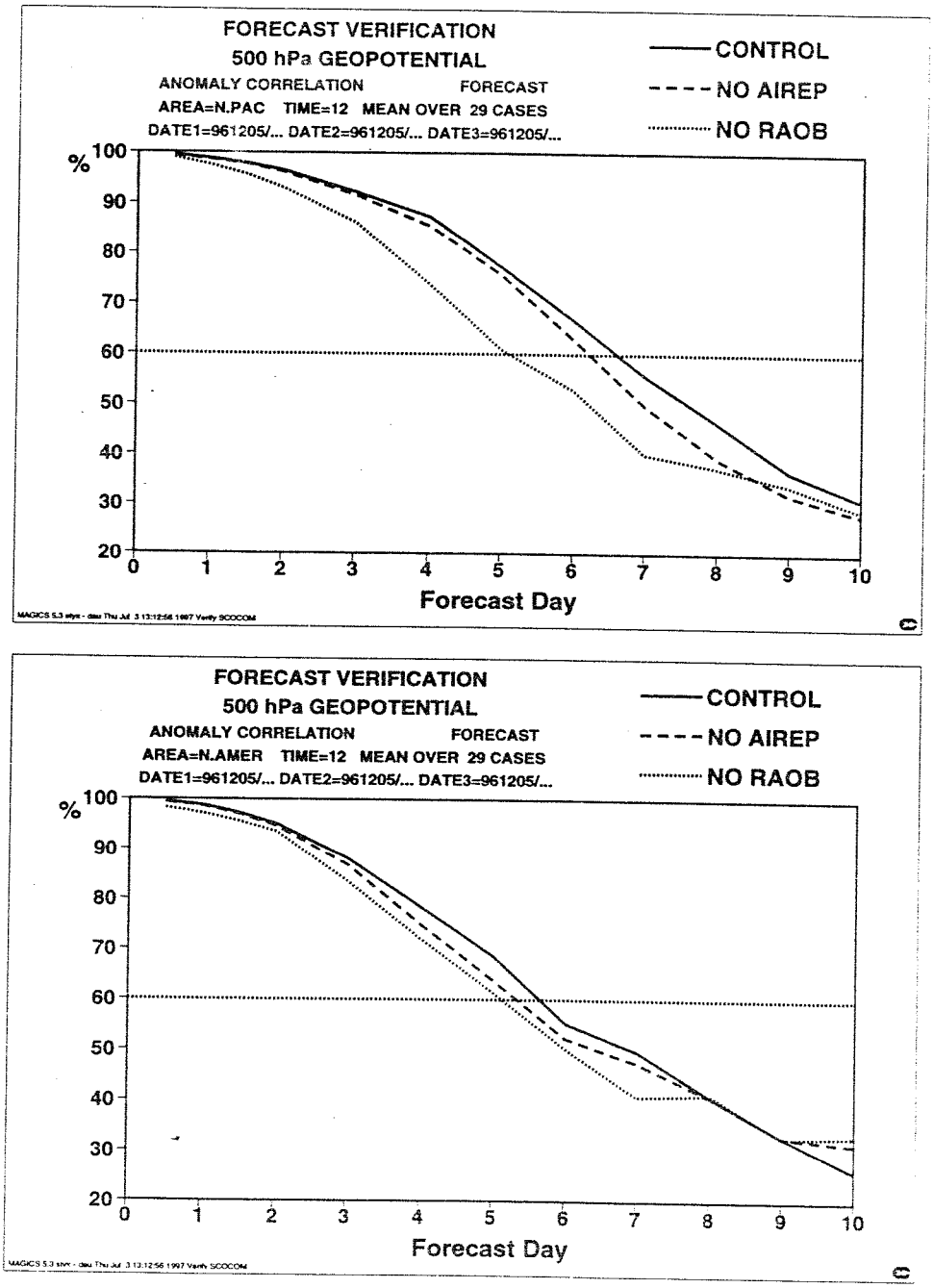

Figure 8. Mean 500 hPa geopotential forecast anomaly correlations for North Pacific (top) and North America (bottom).

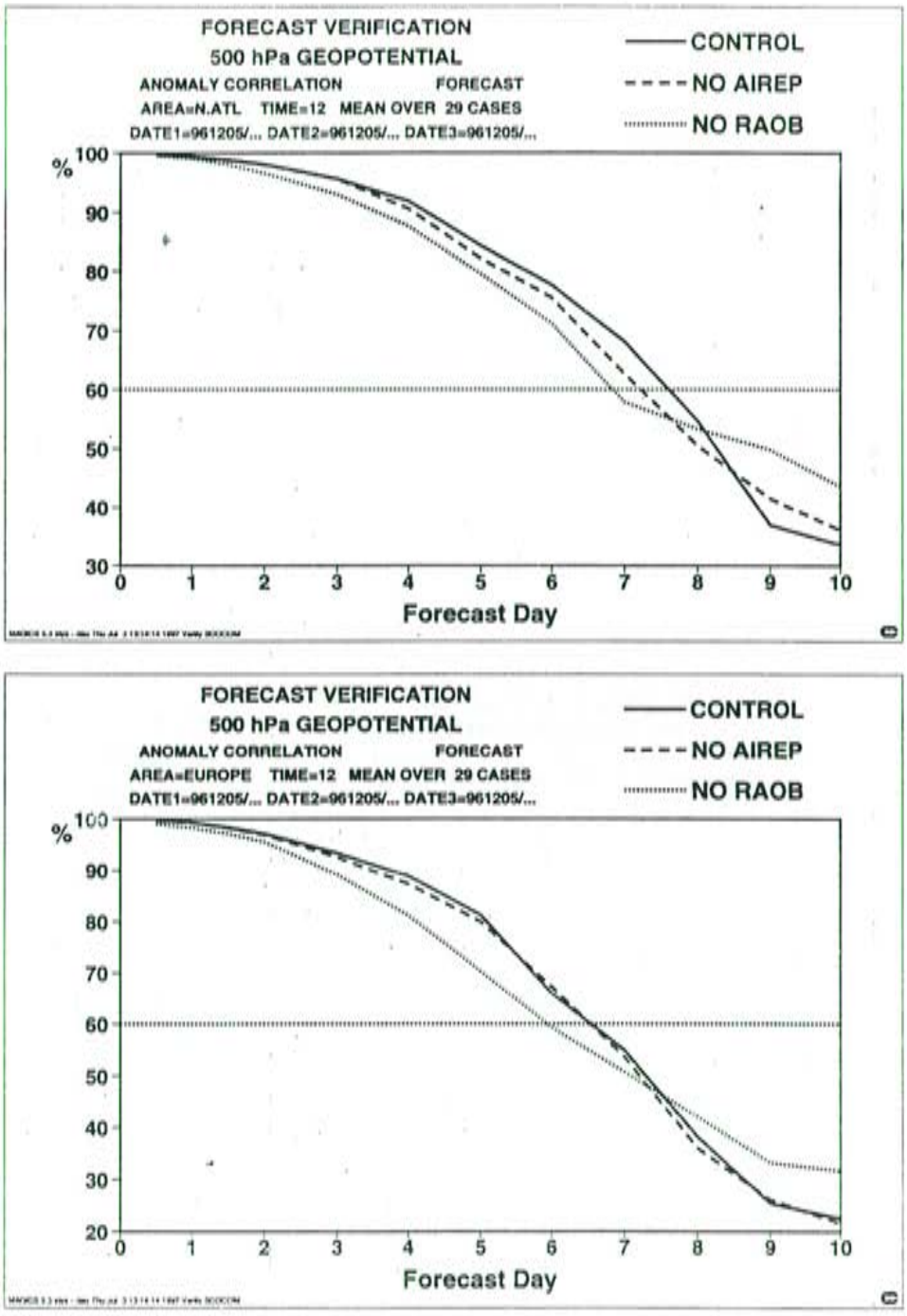

Figure 9. Mean 500 hPa geopotential forecast anomaly correlations for North Atlantic (top) and Europe (bottom).

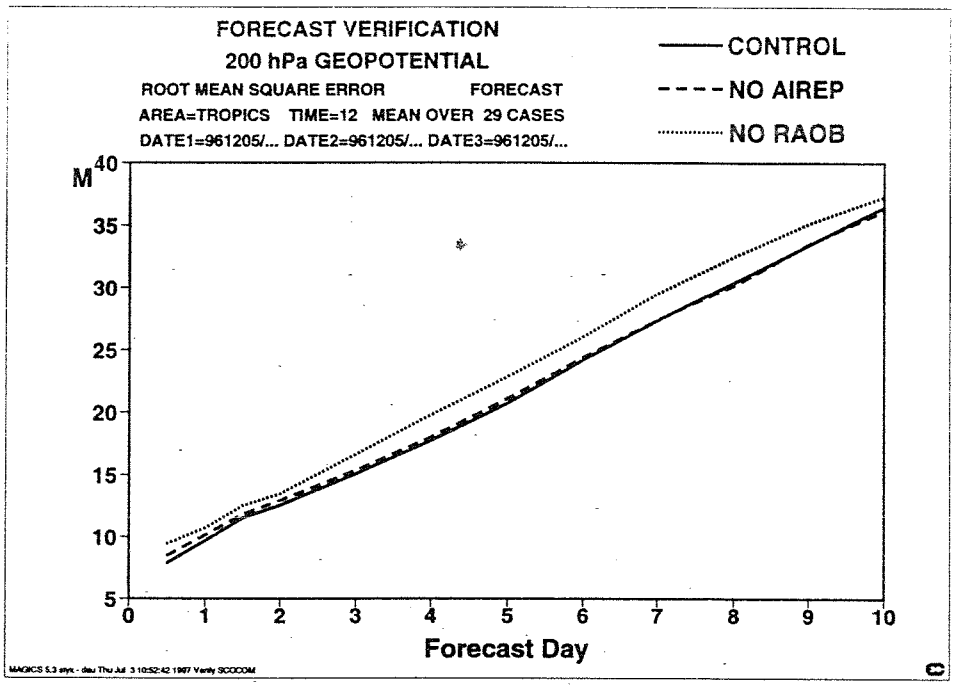

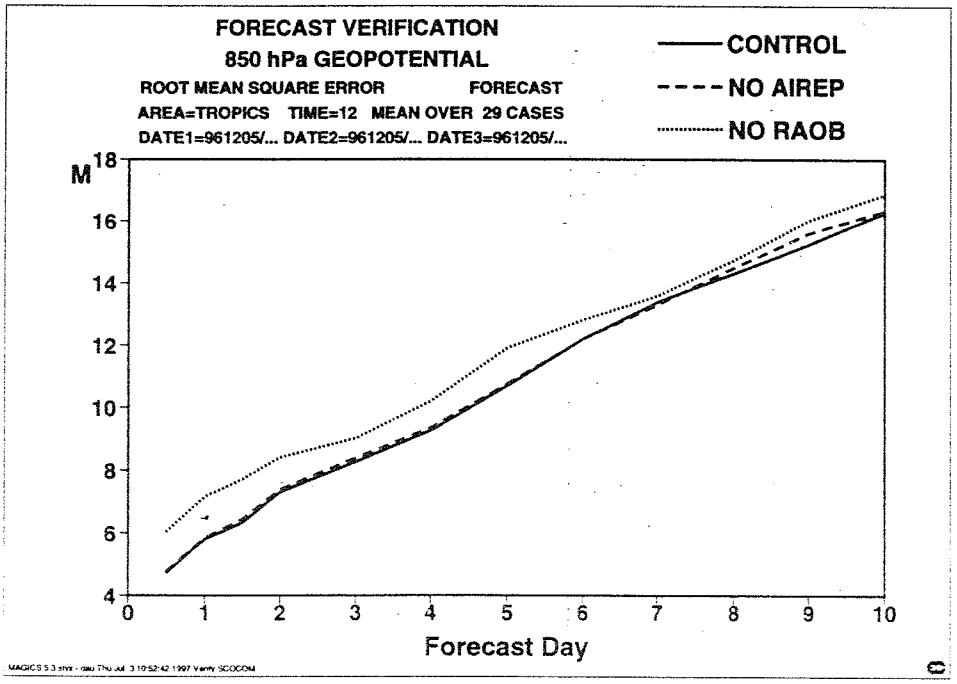

Figure 10. Mean 200 and 850 hPa wind RMS forecast errors in the tropics.

2.3 Synoptic impacts

Impacts from not using radiosondes are very large in the Northern Hemisphere, as seen from the forecast scores. The largest impacts are over the Pacific and large degradations from not using the radiosondes are very evident in almost all synoptic cases. There are very large position errors of major cyclones, troughs and ridges with large phase errors (sometimes completely out of phase) and minor lows which are completely missing or spurious.

Over the North Atlantic and Europe the results of withholding radiosondes are less dramatic but still clearly visible in most synoptic cases. It is more a question of different strengths of the cyclones and errors in their structure and phase errors in troughs and ridges rather than complete misrepresentations. Impacts of not using satellite data are smaller but still important. Such a case is shown in Fig. 11 for four-day forecasts from 19970210 12 UTC. The verifying mean sea level pressure analysis can be compared with the forecast not using radiosondes in the assimilation (NORAOB, b), the control forecast from assimilation with all data (c) and the forecast from the no satellite assimilation (NOSAT, d). Large errors in the position and depth of the cyclone east of Newfoundland can be seen in both the NORAOB and NOSAT forecasts. The NOSAT forecast develops the cyclone much too weakly and has a large south-westerly position error. Also the NORAOB forecast has a westerly position error whereas the control managed to capture both the depth and position of this system better.

Another region in which the NORAOB experiment is further degraded compared with the others is in the complex low pressure system extending from the mid-Atlantic through Scotland to east of the Baltic. The structure of this system is very different from the control or NOSAT experiments. It has a much deeper central part over southern Norway with a strong pressure gradient east of Iceland. The Icelandic part of the low is almost lost. The flow over Scandinavia is very much in error.

The low south of Ireland has only a small position error in the control. The NORAOB forecast has a large south-westerly position error whereas the NOSAT experiment has failed to develop the system, just showing a trough in the area.

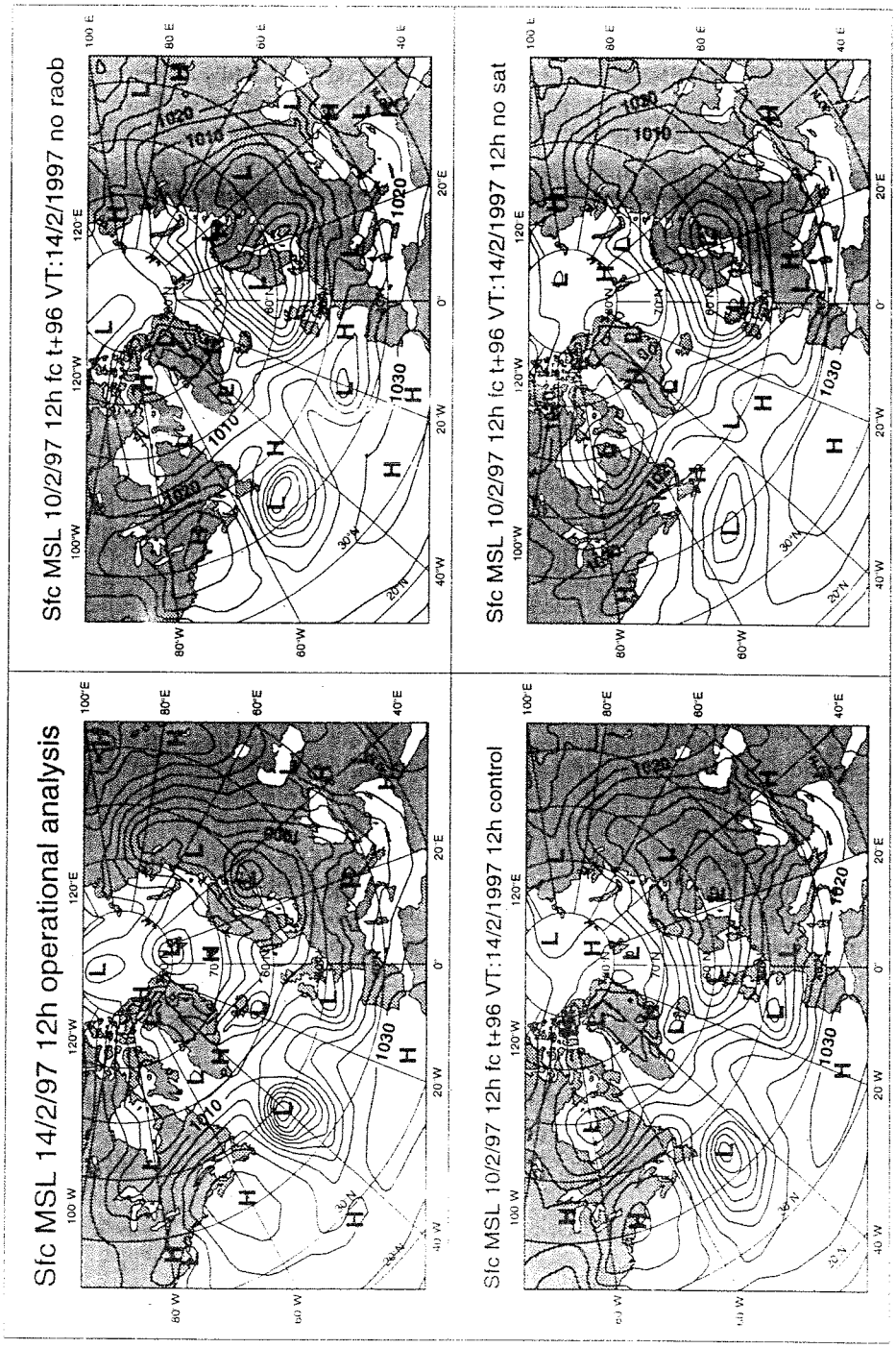

Figure 11. Verifying operational analysis 19970214 12 UTC (a) and 4 day forecast from 19970210 12 UTC from assimilations without radiosondes (b), control (c) and without satellite data (TOVS and SATOBs) (d). Shows mean sea level pressure with isolines for every 5 hPa.

3. Fastex experiments

During the FASTEX experiment the upper air network was considerably enhanced around and over the North Atlantic. 29 normal land stations plus 3 ASAPs in the area increased their launch frequency from twice a day to four times per day. Additionally there were 4 extra FASTEX ASAPs launched four times per day. Thus there was a very good coverage at 06 and 18 UTC during FASTEX in the North Atlantic area. In addition, on a large number of occasions dropsondes were launched from special flights mainly in targeted areas. Hence the combined observation coverage in the area was greatly enriched.

This period gives us a unique opportunity to test the impact of such an enhanced observing system. In fact two experiments have been done. The first measured the impact of the enhanced radiosonde network (but without dropsondes) compared with a reduced, normal network. The second experiment tested the impact of the dropsondes by using them in addition to the enhanced radiosonde network. Furthermore, five individual cases have also been reanalysed using targeted dropsondes for only one or two analysis cycles each.

3.1 Enhanced radiosonde network

The radiosonde network enhancement experiment was run from 1997-01-27 00 UTC until 1997-02-22 12 UTC. In practice the **operational** data assimilation used the enhanced network (without dropsondes) and the experimental assimilation blacklisted (withheld) all the extra radiosonde stations and ASAP ships at the relevant times of the day, when they were supplemental to the normal network. A complete list of the stations that were withheld can be found in Appendix 1. For stations that reported more frequently than every 6 hours, only the closest one to the analysis time was used.

The assimilations have been monitored in terms of observation minus background departures, numbers of used observations, analysis differences and forecast differences. The operational assimilation used more TEMP data than the reduced (= normal) network assimilation did. The observation fits were however almost identical in the two assimilations. Analysis differences between the two assimilations were of course introduced at 06 and 18 UTC near the positions of the extra observations. These differences were then propagated in the short range forecasts, but 6 hours later, at 00 or 12 UTC, when the two assimilations used the same network except for the extra 4 ASAPs, the analysis differences were normally small due to the similarity of the networks. There were however a few occasions when analysis differences could propagate beyond this point and could be traced a bit further in time.

Ten-day forecasts were run from 12 UTC for each day of the experiment. Forecast verification scores were computed and compared with the ECMWF operational ones. Fig. 12a shows that the impact on the Northern Hemisphere average scores is very slight but there is a small improvement over Europe in the scores until forecast day 5 (Fig. 12b). Figure 13 contains scatter plots of the individual scores and shows that at the five-day range there is small positive impact of the enhanced network. There is a fair deal of scatter, so the significance of the improvent is probably small. Similar average positive improvements in forecast scores are however seen for all verification regions in the Northern Hemisphere.

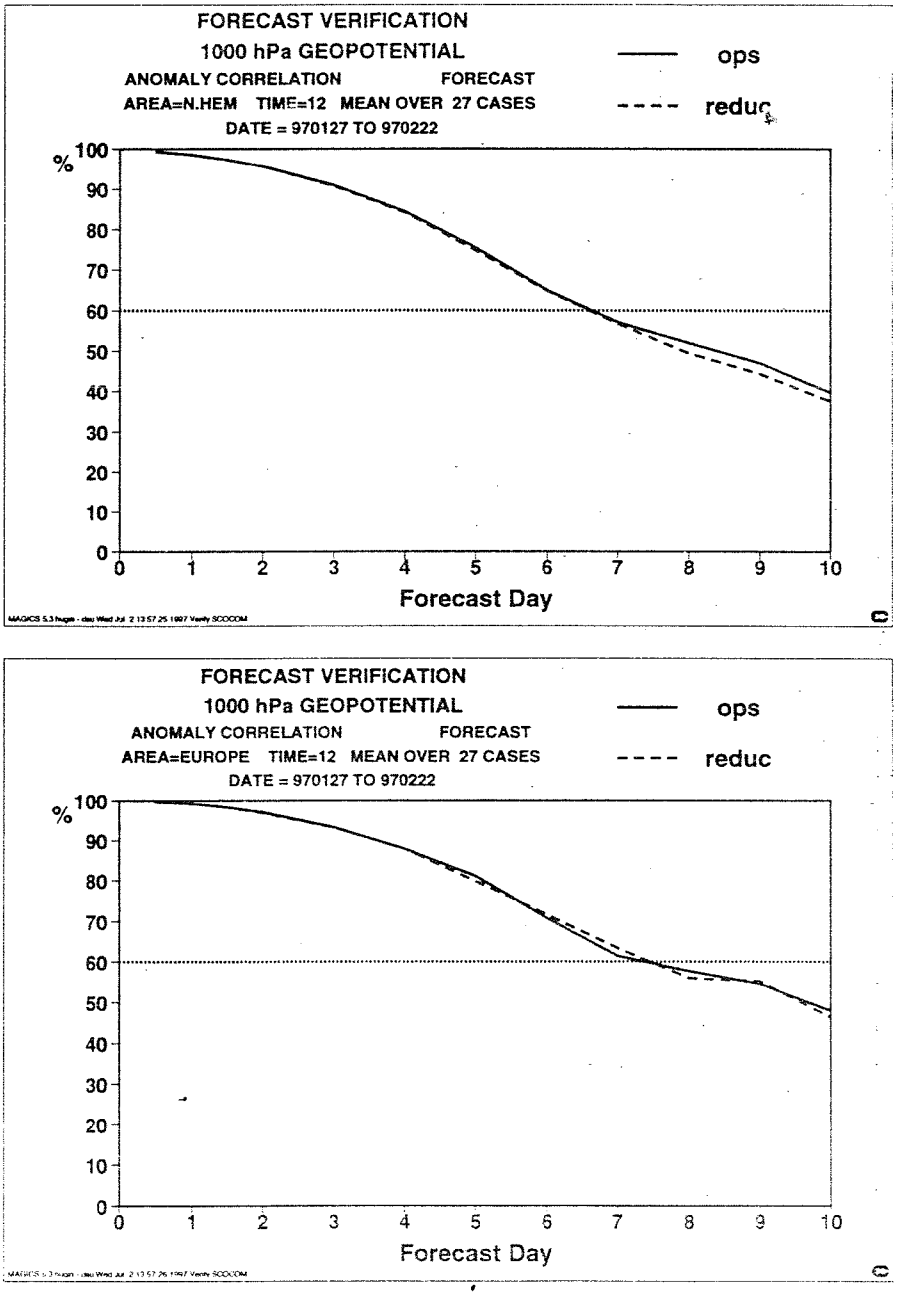

Figure 12. Mean of 1000 hPa geopotential forecast anomaly correlations in the Northern Hemisphere and Europe.

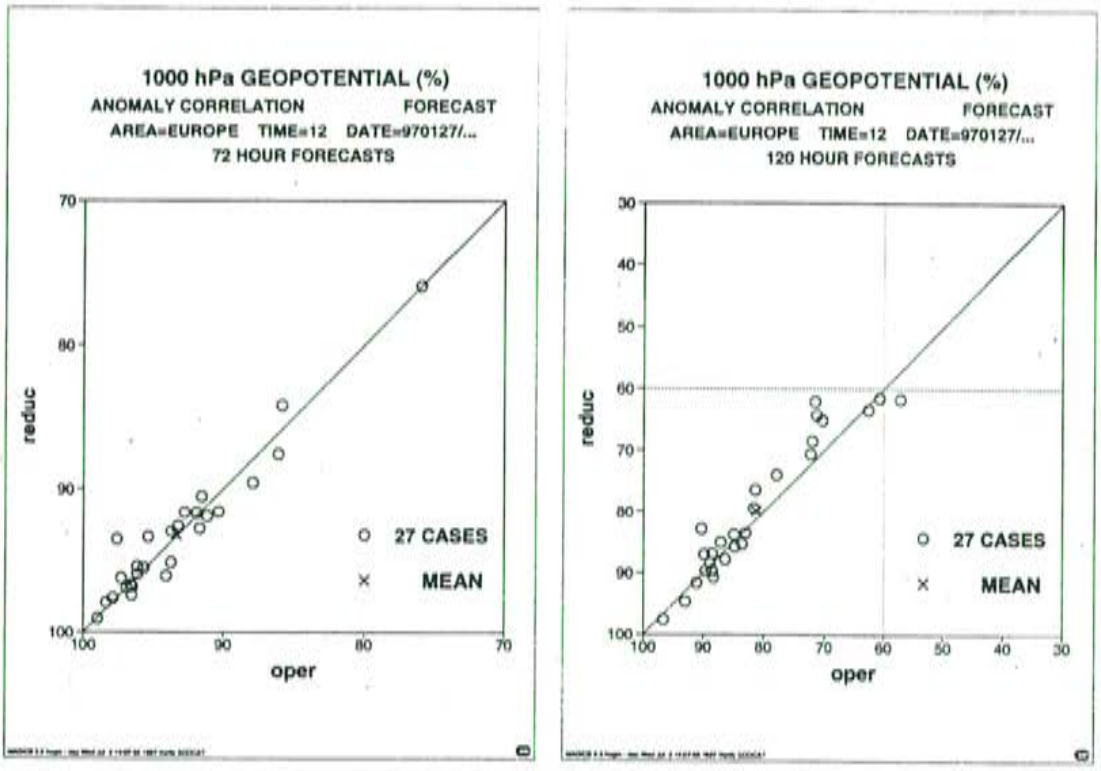

Figure 13. Scatter plots of day 3 and 5 1000 hPa forecast anomaly correlations over Europe.

The differences in forecast scores are fairly small and this is at levels where both forecast sets are very good. Individual forecasts have been scanned for interesting synoptic impacts. Most of the time the synoptic improvements are small in terms of the flow pattern, but a few of the cases show significant improvements. One particular case can be seen in Fig. 14.

The day 4 forecast using the enhanced network from 19970204 (upper left) shows a much better developed 500 hPa low east of Iceland compared with the reduced network (upper right) and this verifies rather well (lower right). The difference of absolute error between the enhanced and reduced network forecasts is shown in the bottom left figure. These forecast error differences can be traced back towards west Greenland in the 24 hour forecast from 1997-02-03 and in the analysis somewhere over southern Greenland on 1997-02-03 06 UTC.

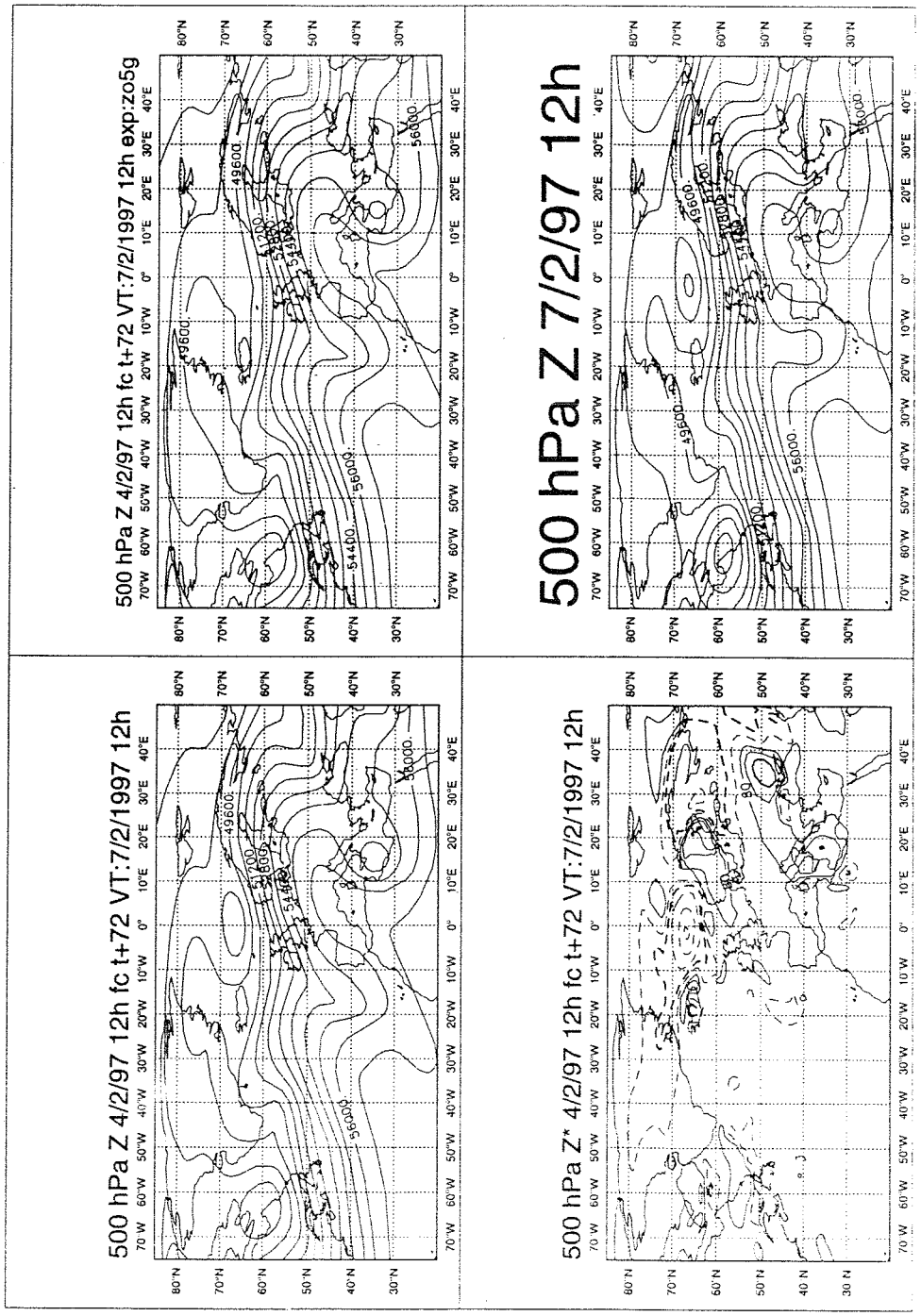

Figure 14. Day 3 500 hPa geopotential forecast with enhanced network from 1997-02-04 12 UTC (lower left), reduced network (upper left), verifying analysis (upper right) and difference of absolute forecast errors (enhanced - reduced, lower right). In geopotential units (J/kg).

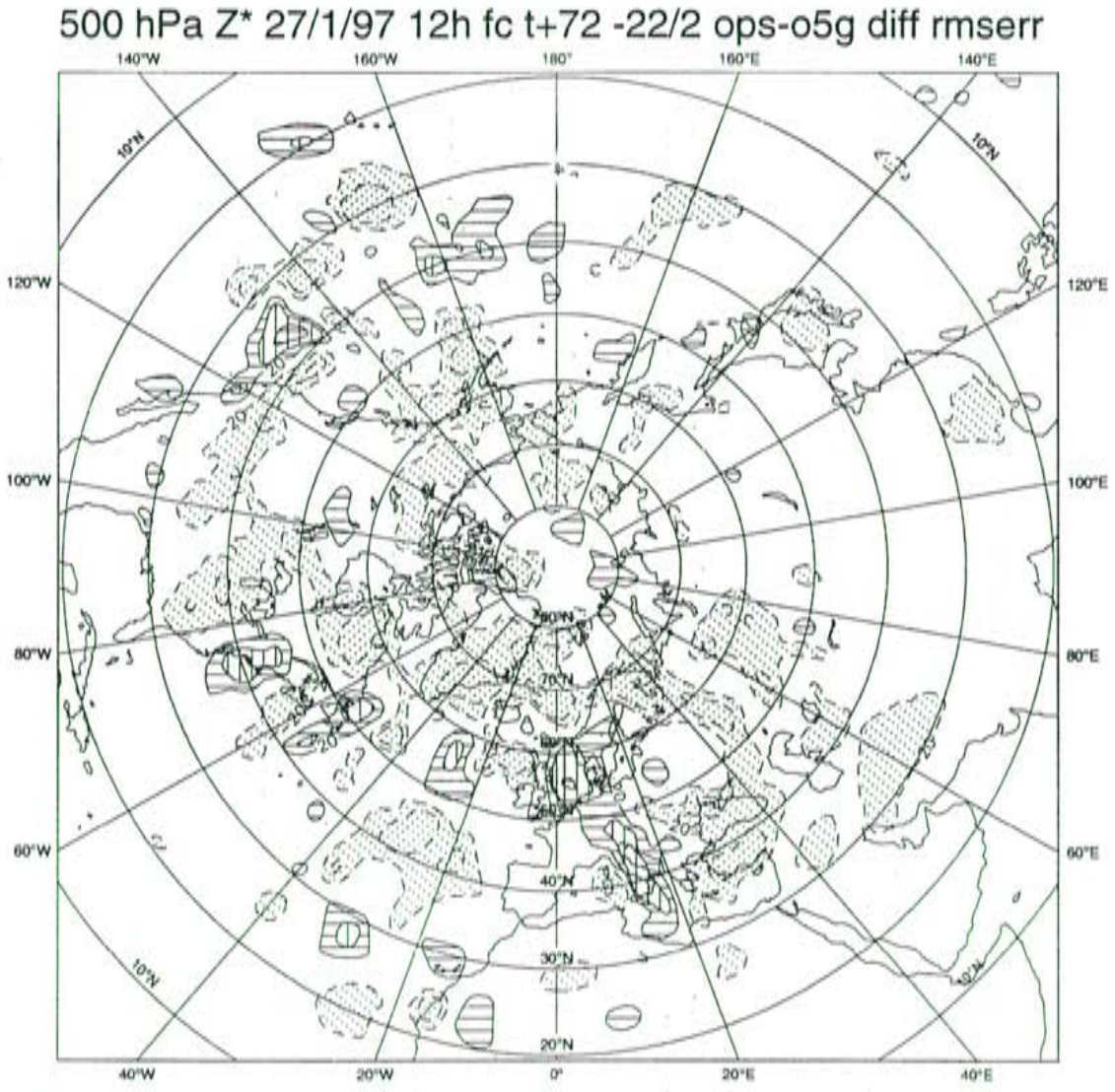

Figure 15. Difference of RMS errors in forecasts with enhanced network compared with reduced. Negative areas dotted with dashed isolines +- 20, 40, 100, 200, 400, 800, 1200, 1600, 2000, 2400, 3200 and 4800 J/kg (geopotential units).

The differences in RMS errors of the two forecast sets has been computed for 500 hPa geopotential and are shown in Fig. 15 for day 3 forecasts. It shows that the reduced errors with the enhanced network are mainly over the northern part of the North Atlantic, Greenland, northern Scandinavia and Russia. Presumably the fact that the flow pattern and dominating activity was at these higher latitudes in the beginning of the period had an influence on these results. Further south in the Atlantic and over central Pacific there are also areas with worse scores. This must be due to random sampling effects in the system.

3.2 Dropsonde impact

A second experiment was then run in order to test the impact of the dropsondes in addition to the already enhanced FASTEX network. This was done by running an assimilation with dropsondes activated and comparing it with ECMWF operations. The dropsondes which were used in these experiments were the ones received in real time at ECMWF from the GTS. We are aware of some more observations that were taken but not inserted onto the GTS and consequently not used in this study.

The dropsondes monitored at ECMWF seemed to have unreliable geopotential data. Most of them displayed large biases against ECMWF background fields. Presumably the reference/sea level pressure is not well known in the case of dropsondes. Because of the unsatisfacory results of the monitoring they were not used operationally at ECMWF. So far only the geopotential has been used operationally at ECMWF as the mass information from radiosondes. In order to extract useful mass information from the dropsondes, in this experiment the observed **temperature** data instead of geopotential data were used from the dropsondes only (geopotentials were still used from all other radiosondes). The use of the temperatures works well in the analysis in terms of drawing to the data and producing mass and wind increments around the dropsondes. This configuration has however not been tested before, so the tuning of observation errors, quality control and horizontal thinning of observations may not be optimal. Another feature of the ECMWF 3D-Var analysis system is that the background departures for observations not on the exact analysis time are still computed using the background forecast valid at the analysis time.

The assimilation of these data, in addition to the other FASTEX data used in operations, was run for the same period as the reduced network experiment discussed earlier (19970127 until 19970222). Analysis impacts of these data are in general not as large as in the previous network experiment since the number of times with extra data is lower. The observations were taken at what are supposedly more optimal positions and might have larger impacts on the ensuing forecasts.

The forecast scores from the dropsonde experiment show very little average impact over the Northern Hemisphere as a whole. Over Europe and North Atlantic there is a slight positive impact (Figs. 16 and 17). The scatter plots of the scores (Fig. 17) show that almost all the three-day forecasts were neutral or slightly improved over Europe and the North Atlantic. Over other areas the scores show less systematic impact and average out to be neutral.

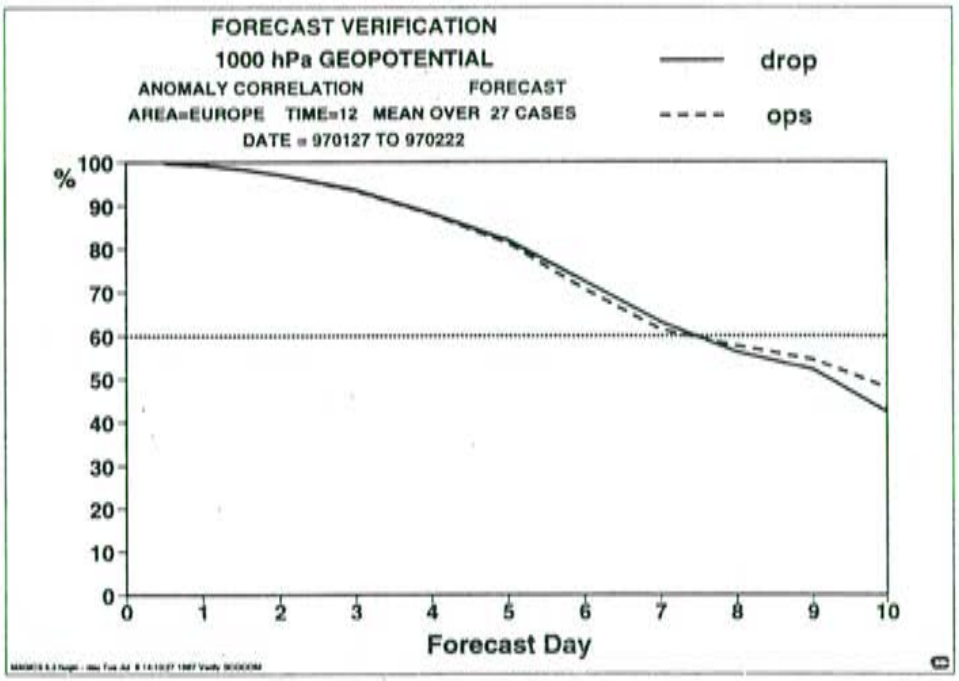

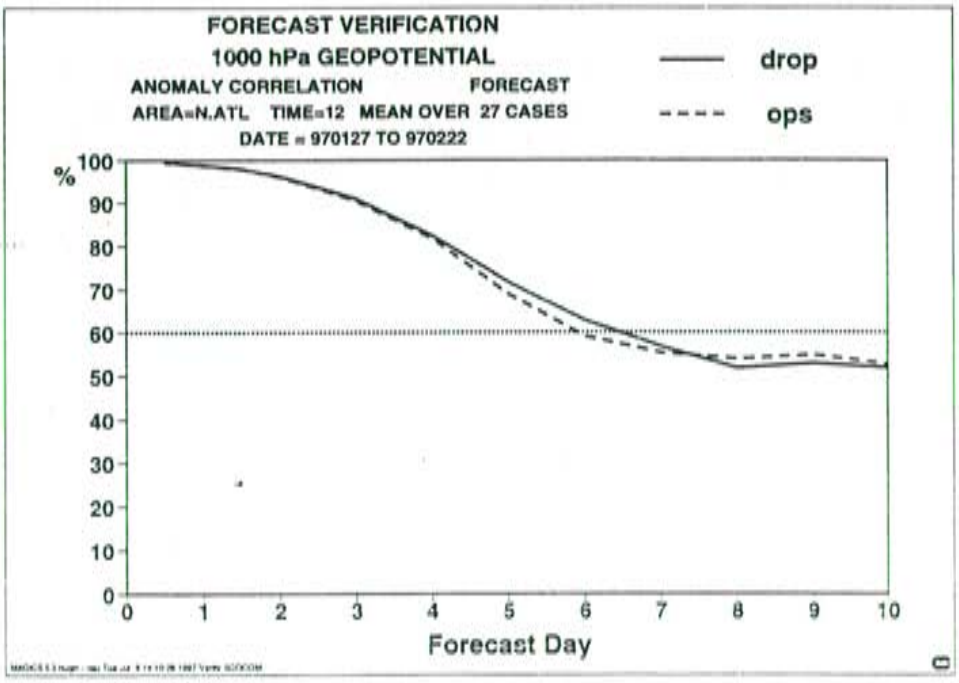

Figure 16. Mean of 1000 hPa geopotential forecast anomaly correlations for Europe and North Atlantic.

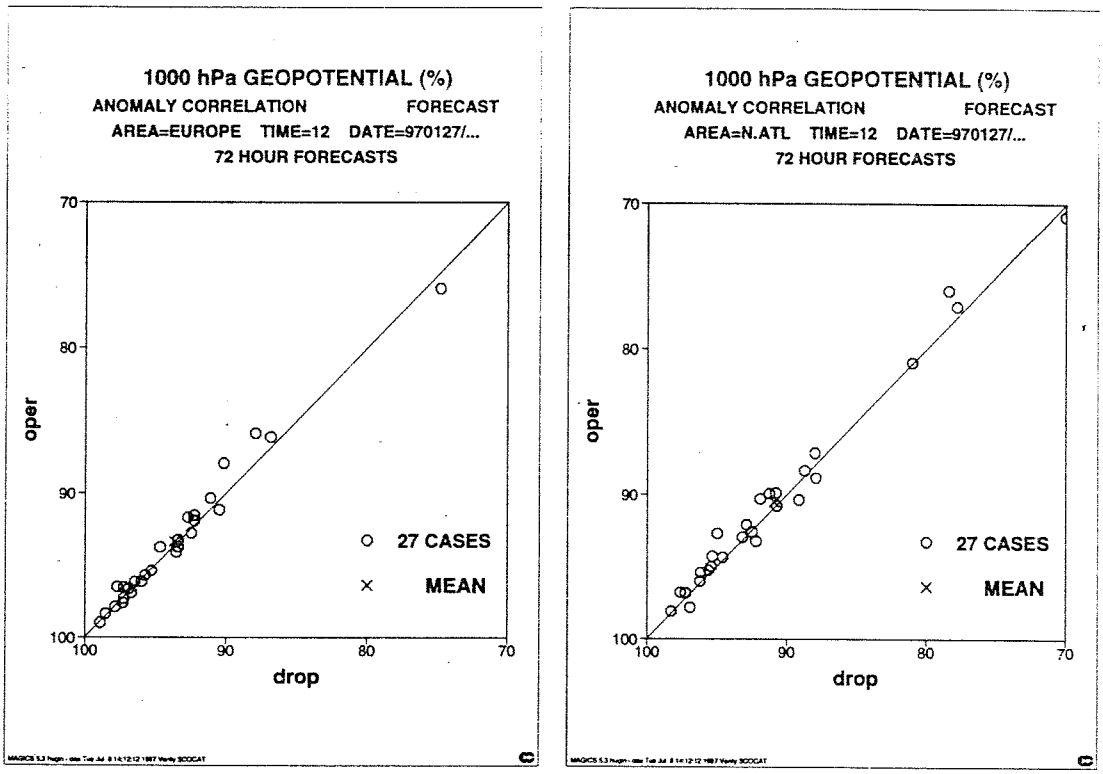

Figure 17. Scatter plots of day 3 1000 hPa geopotential forecast anomaly correlations over Europe and North Atlantic.

Most forecasts showed only small synoptic differences. One case for which there was a noticeable synoptic improvement is shown in Fig. 18. The dropsonde two-day 500 hPa forecast from 19970204 12 UTC shows an improved definition of the low southwest of Iceland (upper left, when you have turned the page) compared with operations (upper right). The verifying analysis is at he bottom right. Absolute forecast error differences at the bottom left. Negative isolines show where the dropsonde experiment has lower forecast errors. Also the through at 25° W is in a more advanced (easterly) position, in better agreement with the verification. Another interesting aspect is the cut off, or Genoa cyclone, north of Sicily, which is better defined in the experiment.

Figures 19a and b show difference of RMS 500 hPa two-day forecast errors for the first 13 days and all the 27 days. respectively. The experiment has lower RMS errors over most of the North Atlantic and Europe with particular improvements in two stripes over the North Atlantic and over central Europe. Intermingled areas of larger errors are also apparent, but at lower magnitude. Figure 19a shows a reduction of up to 7 m in RMS height error over the Atlantic west of the British Isles. For the whole period the mean improvement is reduced to areas of about 3 m. Later on in the forecast range the signals become more mixed and difficult to interpret.

A problem with this type of impact studies with localised observing systems is that the effects of the extra data are mixed with many very non-linear effects in the data assimilation system, which introduce quite large random noise in the forecast results. A more direct way of measuring the impact of the dropsondes is to perform single analyses and have an almost exclusively local analysis impact of the data. Another reason for doing single analyses was to include only

dropsondes which were in the area of sizeable amplitude of the ECMWF singular vectors. These observations could then be regarded as the targeted ones based on the singular vectors. (For a discussion of this, see Palmer et al., 1997.) This approach emerged as a result of discussions with A. Thorpe and A. Montani of Reading University, who have been following this experimentation. Five cases of such targeted dropsondes (one or sometimes two 6 hour periods analysed) were selected by A. Montani (pers. communication), see Table 2. They were then analysed or assimilated without the enhanced radiosonde network. Forecasts were run out to 3 days and compared with forecasts from the assimilation without the enhanced network and without dropsondes. Most of the cases had improved forecast scores over the North Atlantic and Europe at day 2 and 3 (see Fig. 20). Synoptically the improvements were mainly in terms of slightly better positioning of systems but in areas where the errors were already large. The most striking improvement is the forecast from 19970217 18 UTC for 19970219 12 UTC. With the dropsondes the deep low north-west of Scotland (Fig. 21) has been deepened to 961 hPa compared with 968 without dropsondes. The position is also closer to the analysis and the ECMWF operationally analysed depth is 961 hPa; the before mentioned dropsonde assimilation (aodj) 957 hPa and manual Deutscher Wetterdienst (DWD) analysis about 954 hPa (Europäisher Wetterbericht).

Experiment	Date and time
app3/zpp3	19970218 00 UTC
appp/zppp	19970217 18 UTC
apq3/zpq3	19970208 12-18 UTC
apqe/zpqe	19970204 12-18 UTC
apqz/zpqz	19970201 12-18 UTC

Table 2. Experiment names and analysis times/periods for the 5 targeted dropsonde analyses.

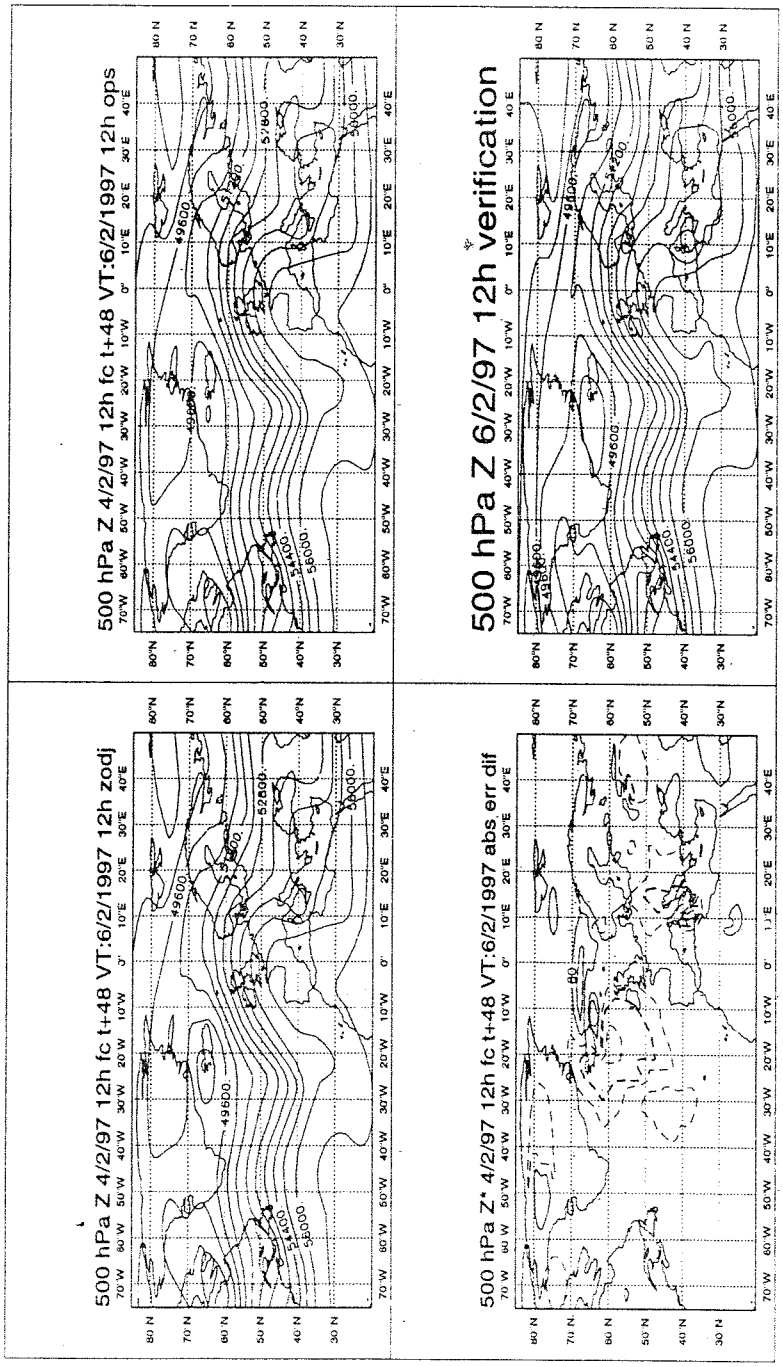

Figure 18. 500 hPa day geopotential forecast from dropsonde experiment (lower left), operations (upper left), verifying analysis and differences of absolute error between dropsonde forecasts and operations. In geopotential units (J/kg).

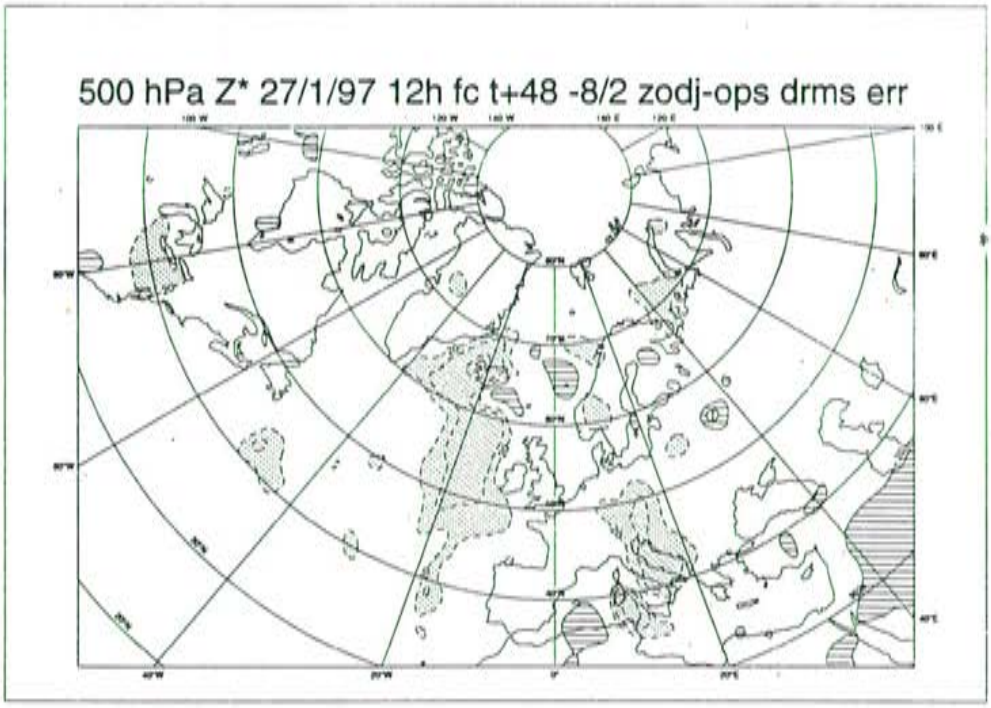

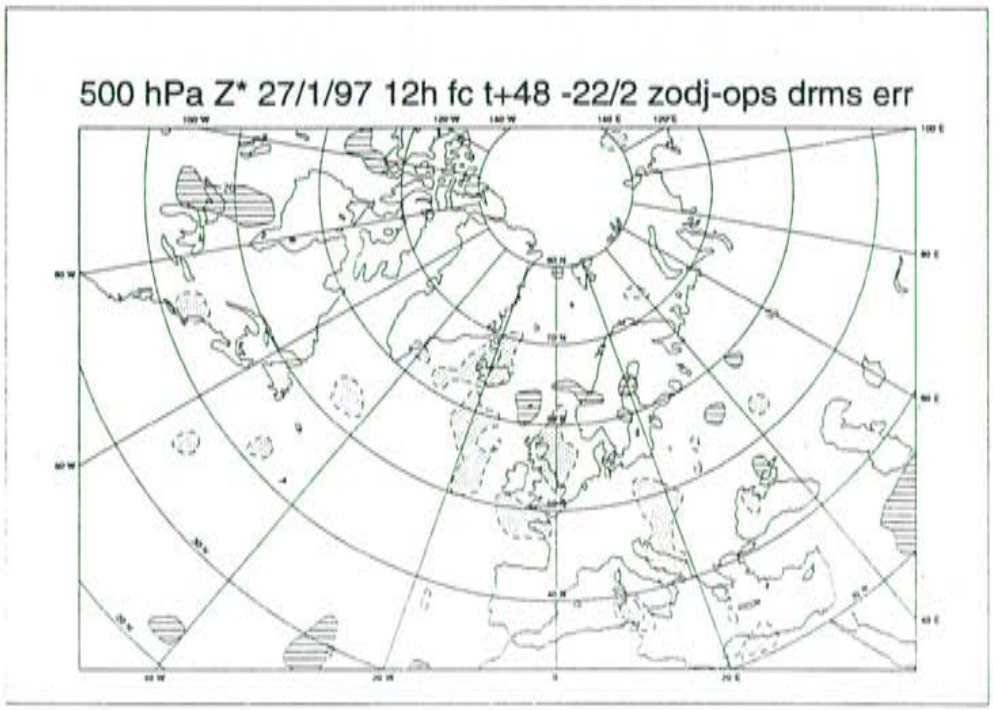

Figure 19. Difference between 500 2 day height forecast RMS errors with dropsondes and without. Isolines as in Fig. 15.

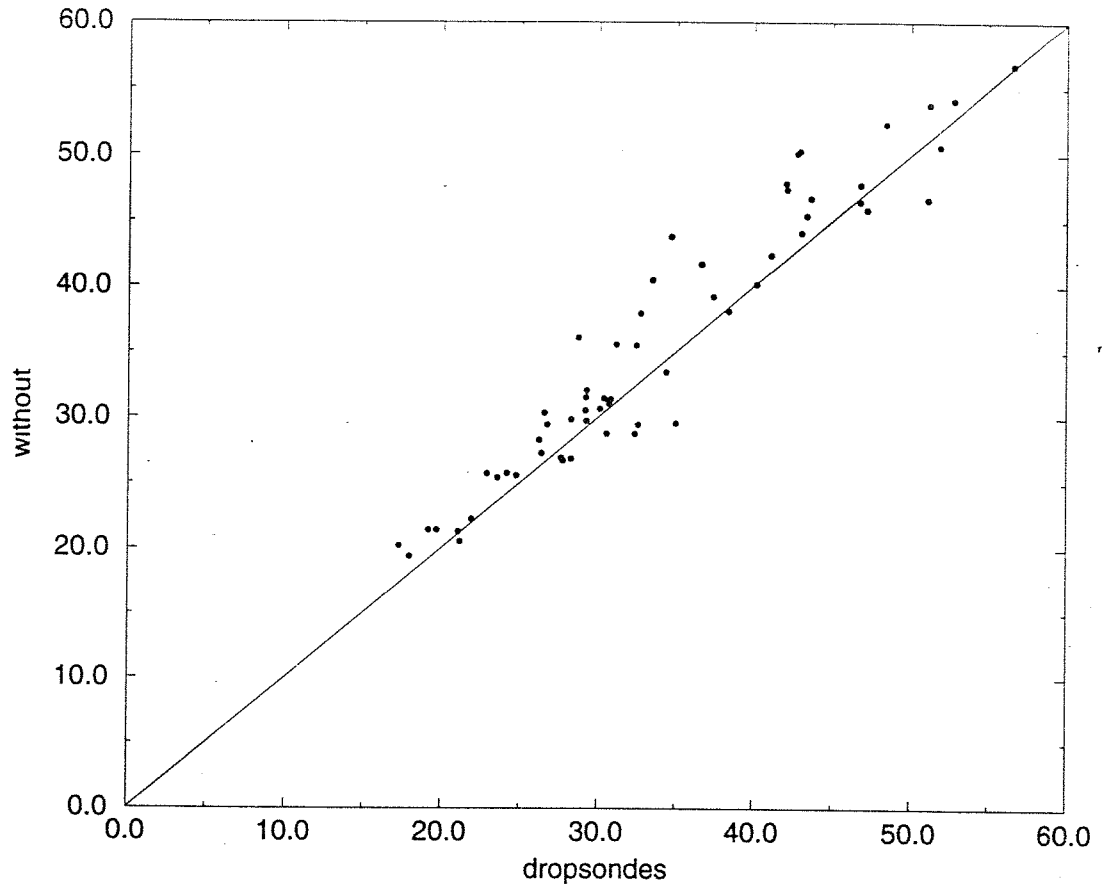

Figure 20. Scatter plot of 1000 and 500 hPa height RMS forecast errors at 48, 60 and 72 hours forecast range from targeted dropsonde analyses and control without dropsondes.

4. Conclusions

In general the results of the observing system experiments are quite encouraging since they show that the current operational ECMWF data assimilation system is able to gain benefits from both conventional and satellite based systems. Global observing system experiments show a very large impact from radiosondes and PILOTs in the Northern Hemisphere and the tropics. The aircraft data also have quite a large positive impact, particularly over the North Pacific and North America. The TOVS data have very large impact over the Southern Hemisphere and in the tropics. This observing system seems to have at least as large impact as SATOBs in the tropics. The SATOBs show also a small but significant positive impact in both hemispheres. In the Northern Hemisphere the major impact from the satellite based systems comes from the SATOBs.

The forecast impact of the enhanced FASTEX radiosonde network is at most marginally positive. Over Europe and the North Atlantic there is a slightly clearer positive impact from using dropsondes in addition to the FASTEX radiosondes. It is easier to demonstrate positive impact of the dropsondes in single (or two consecuetive) analyses for interesting cases when dropsondes are available in targeted areas. These analyses showed a significant improvement of the two- and three-day forecasts for the North Atlantic and Europe.

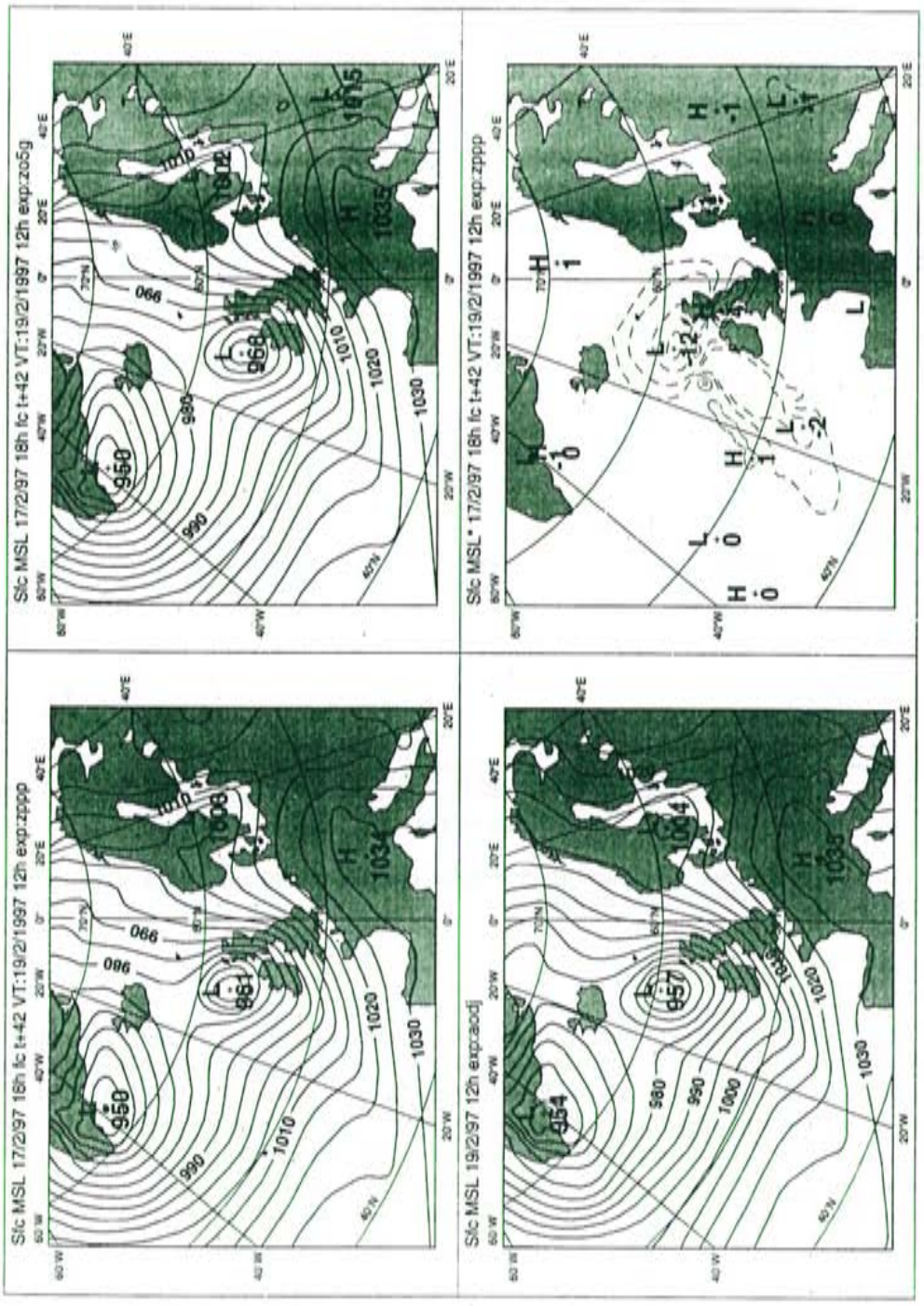

Figure 21. 42hour mean sea level pressure forecasts from 19970217 18 UTC from analyses using dropsondes (a, upper left), without dropsondes (b, right) and verifying analysis (c, lower left). Lower right panel (d) shows differences of absolute errors with isolines at +- 1,2,5,10, 15 and 20 hPa.

There is a small but measurable average positive impact in the early medium range forecasts from the FASTEX observing system enhancements. Only occasionally is it possible to find significant synoptic improvements. It should be pointed out that the enhancements of the observing systems were an area which is the most well observed of any of the ocean areas in the world. It is probably more cost effective to improve the observing network in other less well observed areas of the globe in order to get larger medium range forecast impacts.

A significant reduction of the radiosonde network in the Northern Hemisphere or the tropics would have a profound impact on forecast quality. At least with today's data assimilation systems the loss of radiosondes cannot be compensated by aircraft data (with current coverage and instruments) although they would become increasingly important. TOVS data still seem to show very small average benefits for the Northern Hemisphere forecasts, but again they might play a bigger role in a reduced radiosonde configuration.

References

Andersson, E., A. Hollingsworth, G. Kelly, P. Lönnberg, J. Pailleux and Z. Zang 1991: Global observing system experiments on operational statistical retrievals of satellite sounding data. Mon. Wea. Rev., Vol 119, 1851-1864.

Andersson, E., J. Haseler, P. Undén, P. Courtier, G. Kelly, D. Vasiljevic, C. Brankovic, C. Cardinali, C. Gaffard, A. Hollingsworth., C. Jakob, P. Janssen, E. Klinker, A. Lanzinger , M. Miller, F. Rabier, A. Simmons, B. Strauss, J-N. Thépaut and P. Viterbo 1996: The ECMWF implementation of three dimensional variational assimilation (3D–Var). Part III: Experimental results. Accepted to appear in Quart. J. Roy. Met. Soc.

Andersson E., J. Pailleux, J–N. Thépaut, J.R. Eyre, A.P. McNally, G. Kelly and P. Courtier 1994: Use of cloud–cleared radiances in three/four–dimensional variational data assimilation. Q.J. R. Meteorol. Soc., 120, 627–653.

Bouttier F., J. Derber and M. Fisher 1997: The 1997 revision of the J_b term in 3D/4D–Var. ECMWF Tech. Memo. No. 238.

Eyre, J.R., G. Kelly, A.P. McNally, E. Andersson and A. Persson, 1993: Assimilation of TOVS radiance information through one–dimensional variational analysis. Quart. J. Roy. Met. Soc., 119, 1427–1463.

Kelly, G. and J. Pailleux, 1988: Use of satellite vertical sounder data in the ECMWF analysis system, ECMWF Tech. Memo. No. 143.

Kelly, G., E. Andersson, A. Hollingsworth, P. Lönnberg, J. Pailleux and Z. Zang 1991: Quality control of operational physical retrievals of satellite sounding data. Mon. Wea. Rev., Vol. 119, 1866-1880.

Kelly, G., J. Pailleux, F. Rabier and J-N. Thepaut 1993: Observing System Experiments made with the ECMWF System. World Weather Watch Tech. Report.16. WMO/TD No. 594.

Lorenc, A.C. 1981: A global three–dimensional multivariate statistical interpolation scheme. Mon. Wea. Rev., 109, 701–721.

Palmer, T. N., R. Gelaro, J. Barkmeijer and R. Buizza 1997: Singular vectors, metrics and adaptive observations. To appear in J. Atmos. Sci.

Uppala, S., A. Hollingsworth, S. Tibaldi and P. Kållberg 1985: Results from two recent observing system experiments. ECMWF Seminar/Workshop on "Data assimilation systems and observing system experiments with particular emphasis on FGGE", Reading, 165-202.

Appendix 1

```
if (OBSTYP = temp) then
     if   (( 030100 <= TIME <= 090000 )
     or ( 150100 <= TIME <= 210000 )  )
and  STATID in ("03354", "04220", "04270", "04339", "04360",
          "06011", "07110", "07145", "07510", "04018",
          "03953", "08508", "08522", "08001", "03005",
          "03026", "03496", "03502", "03808", "03240",
          "03920", "71801", "71816", "71906", "71600",
          "78016", "72402", "72208", "74494", "FNOR",
          "FNOU", "FNPH", "FNRS", "OXVH2", "OXYH2",
          "V2EZ", "KCEJ", "FZVN", "EOGW", "TFTA",
          "V2LV", "V2LX", "DBBH", "V2GH", "EHOA")
then fail(CONSTANT); endif;
     if   (( 090100 <= TIME <= 150000 )
     or ( TIME >= 210100 or TIME <= 030000 ) )
and  STATID in ( "KCEJ", "FZVN", "EOGW", "TFTA")
     then fail(CONSTANT); endif;
```

ANNEX F

- ECMWF summary report for the ERS-2 Radar Altimeter commissioning phase.

ECMWF Wind and Wave Calibration - Method

Björn Hansen - European Centre for Medium Range Weather Forecasts.

The European Centre for Medium Range Weather Forecasts (ECMWF) contributed to the calibration of the wind and wave measurements of the ERS-2 radar altimeter by utilizing operational global wind and wave analyses as a transfer standard between ERS-1 and ERS-2 so as to provide relative calibration coefficients and error estimates, based on wind and wave measurements of the radar altimeter onboard ERS-1.

Preprocessing of the satellite data

The calibration work at ECMWF was based on the ESA URA fast delivery products which are disseminated over the global telecommunication system (GTS) within three hours of observation time. This means that for ERS-2 only those observations received at the Kiruna ground station could be used. This is on average 75% of the number of ERS-1 observations, which were also available in near real time from the ground stations at Maspalomas and Gatineau. All incoming data are thoroughly checked to identify and eliminate unrealistic data. The wind speed measurements were not checked and were accepted whenever the corresponding wave height was accepted. The quality control is similar to that used for SEASAT by Bauer et.al. (1992) and yields a URA data set extended by a flag as follows:

1) flag as unreliable all observations which:
   a) cannot be co-located with wave data provided by ECMWF,
   b) are below 0.1m significant wave height,
   c) are above 20.0m significant wave height.
2) flag as unreliable outliers within a sequence of continuous observations. A sequence is defined by 20 to 30 consecutive observations where the time difference between each observation is less than 3 seconds. Observations are classified as outliers if:

   $\left|H_{s_i} - \overline{H_s}\right| \geq 3 \times STD$ and $\left|H_{s_i} - \overline{H_s}\right| > 1m$.

   H_{s_1} is also classified as an outlier if $\left|H_{s_1} - H_{s_2}\right| > 2m$ and

   H_{s_n} is classified as an outlier if $\left|H_{s_{n-1}} - H_{s_n}\right| > 2m$,

   where H_{s_i} is the i-th significant wave height observation within a sequence with i =1 to n, $\overline{H_s}$ is the mean significant wave height of a sequence and STD is the standard deviation of the sequence.
3) flag as unreliable all remaining observations of the whole sequence if there are less than 20 observations left after step 2 (short sequence).
4) flag all the observations within a sequence as unreliable if the standard deviation within the sequence exceeds $0.1 \times \overline{H_s}$ with a lower limit of the threshold of 0.5m.

All remaining observations are flagged as reliable.

Consequently, the quality control yields a reduced data set which is used in the compar-

ison with model data. This data set contains the mean values of the time, location, significant wave height and of the wind speed for each accepted sequence. These will be referred to as super-observations.

Operational model fields used

The wind and wave background fields used in this study are produced by the ECMWF Integrated Forecasting System (IFS) (*ECMWF, 1994*) and by the third generation wave model WAM cycle 4 (*Komen et.al.,1994)* respectively. Wave and wind information are available on a global scale with a resolution of 1.5° * 1.5° (Figure 1). A typical setup for these models is to perform a 6 hour forecast from 1200UTC to 1800UTC followed by a data assimilation step to correct the forecast at 1800UTC (also called first guess) by using all meteorological information available at that time to produce the analysed fields. This procedure is repeated four times to cover one full day. The result serves firstly as a base for the ten day forecast performed every day and secondly, as the starting conditions for the next days assimilation cycle. Since the ERS-1 RA wave heights are assimilated into the wave model, the first guess wave fields have been used in this study as they are independent of the newest ERS-2 data (*Guillaume and Hansen, 1993*). However, in the wind speed comparison analysed winds are taken. ERS-1 RA data are not used in the assimilation step of the atmospheric model.

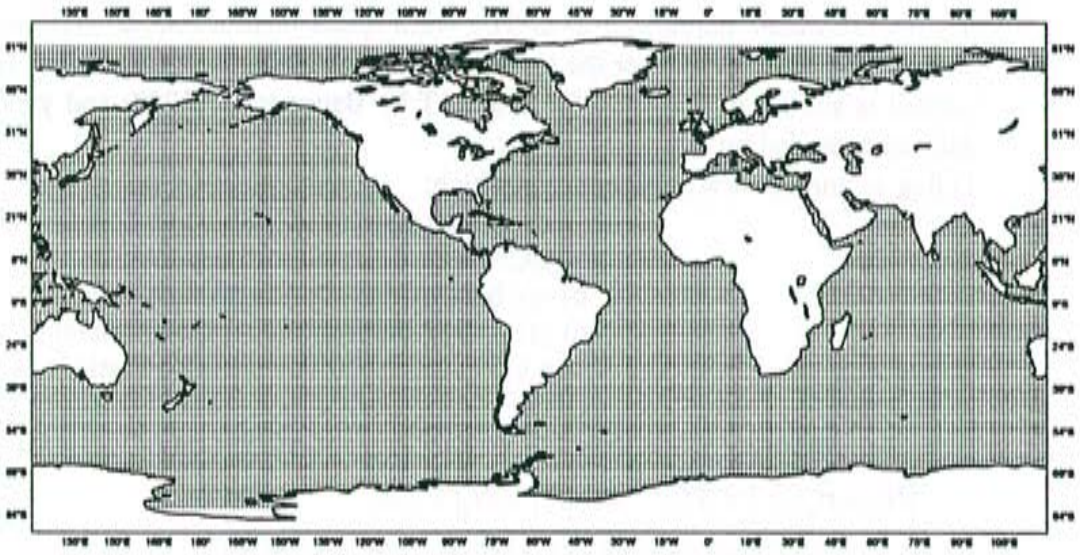

FIGURE 1. Distribution of sea points of the wave model (1.5° * 1.5° grid resolution)

Collocation

For the subsequent comparison of satellite data with model results the collocated model values had to be extracted from the global model data fields. This was achieved by bi-linear interpolation in space and by linear interpolation in time. Satellite data were used only if all four surrounding grid points of the wave model were sea points.

Evaluation of satellite and model data

The first step towards calibration and validation of the ERS-2 radar altimeter wind and wave data was to make simple statistical analyses of the incoming satellite data and the model data.

The data reception rate was monitored by plotting the number of all incoming observations, the number of all observations which were left after step 1a) of the quality control, the number of all observations which passed the quality control and finally the number of super-observations as a function of time with a bin width of 6 hours.

On a daily, weekly and monthly basis distributions were plotted for the backscatter coefficient with a bin width of 0.1 dB, for the wind speeds with a bin width of 0.1m/s and for wave heights with a bin width of 0.1m, normalized by the bin width, together with their mean value, the average deviation, the standard deviation, the variance, the skewness and the kurtosis.

Scatter diagrams of satellite data as a function of model data were plotted together with the mean values of both data sets, the bias defined as satellite mean value minus model mean value, the standard deviation of the differences, the scatter index, the correlation coefficient, the slope of the symmetric regression line, the regression coefficient and the regression constant of the least squares fit regression line. Additionally the standard error for the slope of the symmetric regression line, for the regression coefficient and the regression constant are also given. For the scatter diagrams the collocated data values are collected into bins of width 0.5m/s for winds and 0.25m for waves. The number of entries for each bin is plotted using an appropriate colour code. Additionally the mean of the satellite measurements as a function of model value and vice versa is given. Time series of main statistical values such as satellite mean, bias and standard deviation of the differences are plotted to provide an overview of the evolution of these parameters within the commissioning phase. Finally by eliminating the models in the regression functions the relation between ERS-2 and ERS-1 measurements is given.

References

Bauer, E. S. Hasselmann, K. Hasselmann and H. C. Graber, 1992: Validation and assimilation of Seasat altimeter wave heights using the WAM wave model. J. Geophys. Res. C97, 12671-12682.

ECMWF, 1994: User Guide to ECMWF Products, Meteorological Bulletin M3.2, edition 2.0

Guillaume, A. and B. Hansen, 1993: Operational use of the ERS-1 observations in ocean wave forecasting at ECMWF. 2nd ERS-1 Symposium, Hamburg, 11-14 October 1993, Proceedings

Hansen, B. and H. Günther, 1992: ERS-1 radar altimeter validation with the WAM model. Geophysical validation campaign, RENE, 1991. Workshop proceedings, ESA WPP-36

Komen, G. J., L. Cavaleri, M. Donelan, K. Hasselmann, S. Hasselmann and P. A. E. M. Janssen, 1994: Dynamics and Modelling of Ocean Waves, Cambridge University Press.

ECMWF Wind and Wave Calibration - Wind Speed Analysis

Björn Hansen - European Centre for Medium Range Weather Forecasts.

Within the cal/val period (29th April 1995 to 27th August 1995) ECMWF produced weekly reports for the ERS-2 radar altimeter and microwave radiometer commissioning working group. This report summarizes the results found within the cal/val period, provides final numbers based on data from September 1995 and gives an overview of the data quality between September 1995 and February 1996.

Data reception

On average 45776 ERS-2 and 65375 ERS-1 wind and wave observations passed the quality control per day at ECMWF at the end of the cal/val period. The larger number for ERS-1 is due to the fact that ESA decided to only distribute ERS-2 data from the Kiruna ground station. Figures 1 and 2 show the 6 hourly data reception rate for September 1995 for ERS-1 and ERS-2. After along track averaging the number of observations used in the comparison with the model results is reduced to around 1300 for ERS-1 and to 820 for ERS-2 (lower panel in figure 1 and figure 2).

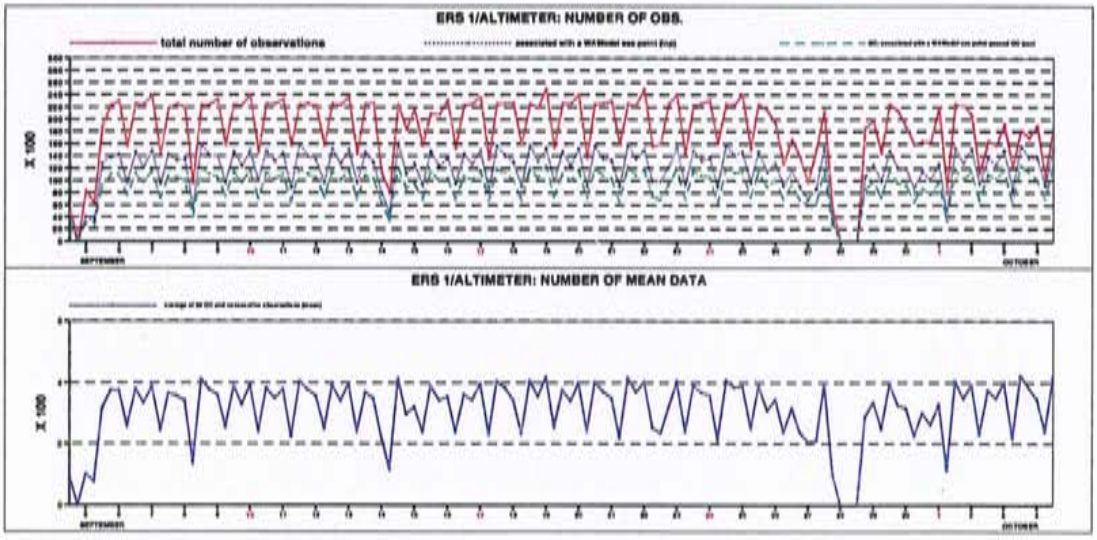

FIGURE 1. Data reception rate ERS-1 radar altimeter data for September 1995
Top panel: solid line: total number of observations
dotted line: observations associated with a sea point in the wave model
dashed line: passed the quality control.
Lower Panel: solid line: number of super-observations.

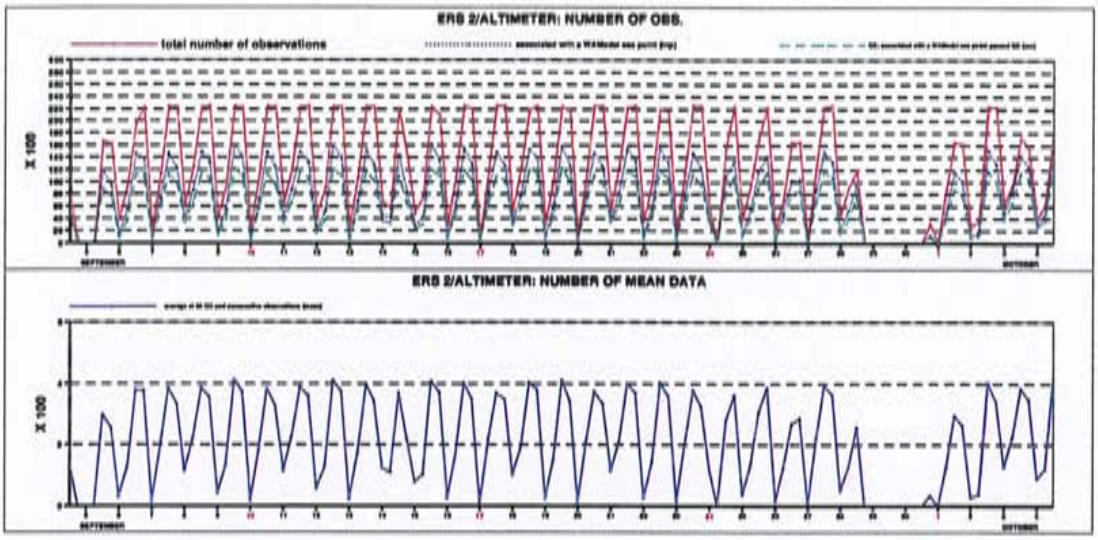

FIGURE 2. Data reception rate ERS-2 radar altimeter data for September 1995.
Top panel: solid line: total number of observations
dotted line: observations associated with a sea point in the wave model
dashed line: passed the quality control.
Lower Panel: solid line: number of super-observations.

Calibration

For May 1995, during the commissioning phase the wind speed measurements of the ERS-1 radar altimeter correlated to 86% with the model results and were biased low by 0.25m/s. The slope of the symmetric regression line was 0.98 (figure 3). On contrast, the ERS-2 radar altimeter winds correlated to only 79% with the model and were biased very low by 4.8 m/s. Additionally the slope of the symmetric regression line was only 0.4(figure 4).

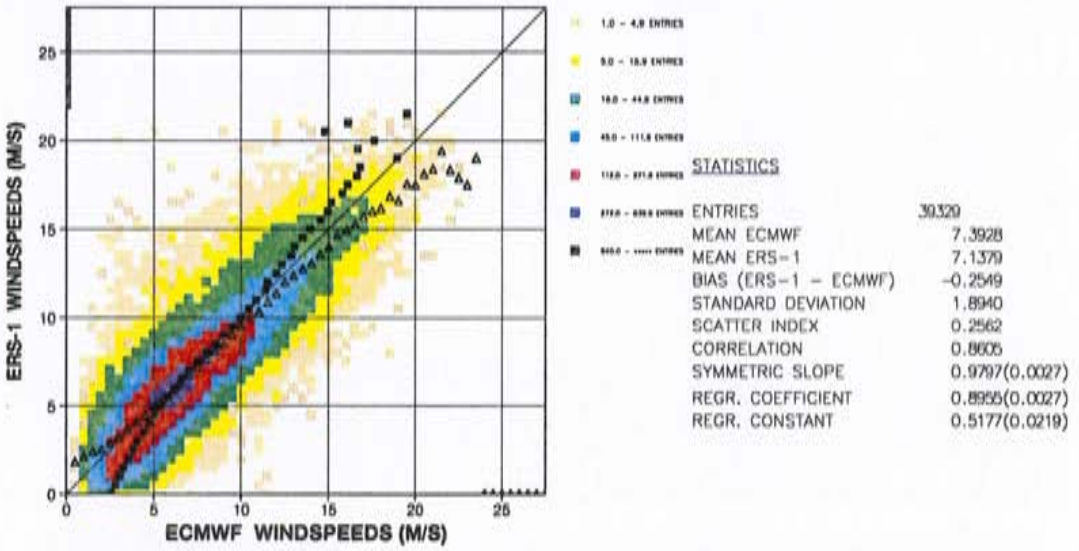

FIGURE 3. Comparison of ECMWF wind speed results with ERS-1 radar altimeter wind speed data for May 1995. The squares denote the mean values in the x-direction and the triangles in the y-direction The standard error is shown in brackets.

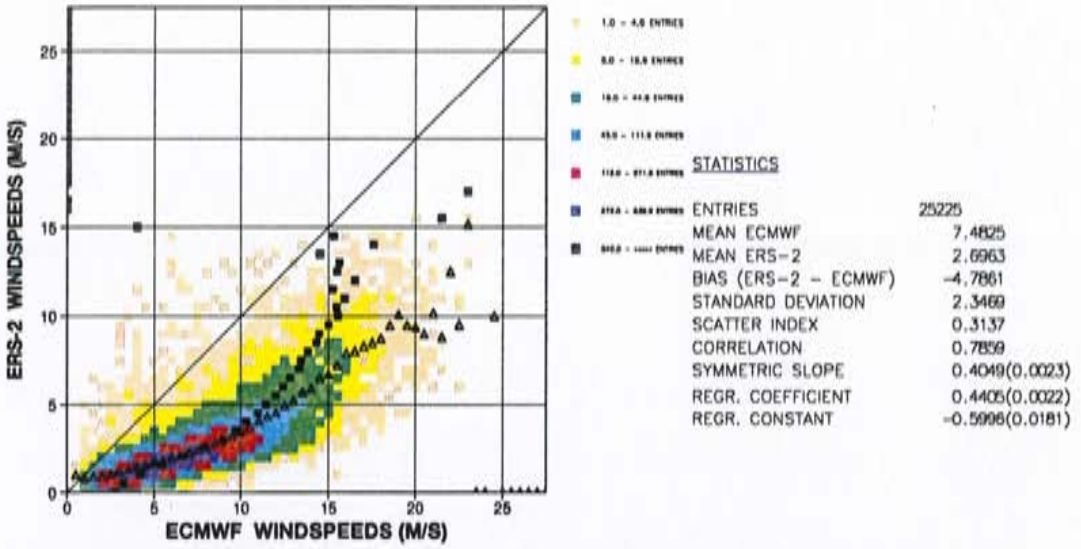

FIGURE 4. Comparison of ECMWF wind speed results with ERS-2 radar altimeter wind speed data for May 1995. The squares denote the mean values in the x-direction and the triangles in the y-direction. The standard error is shown in brackets.

To better understand the reason for the bad quality of the ERS-2 winds, histograms of the underlying backscatter signals (σ_0)were produced, and a shift by 2.06dB between the two instruments became apparent (figures 5 and 6).

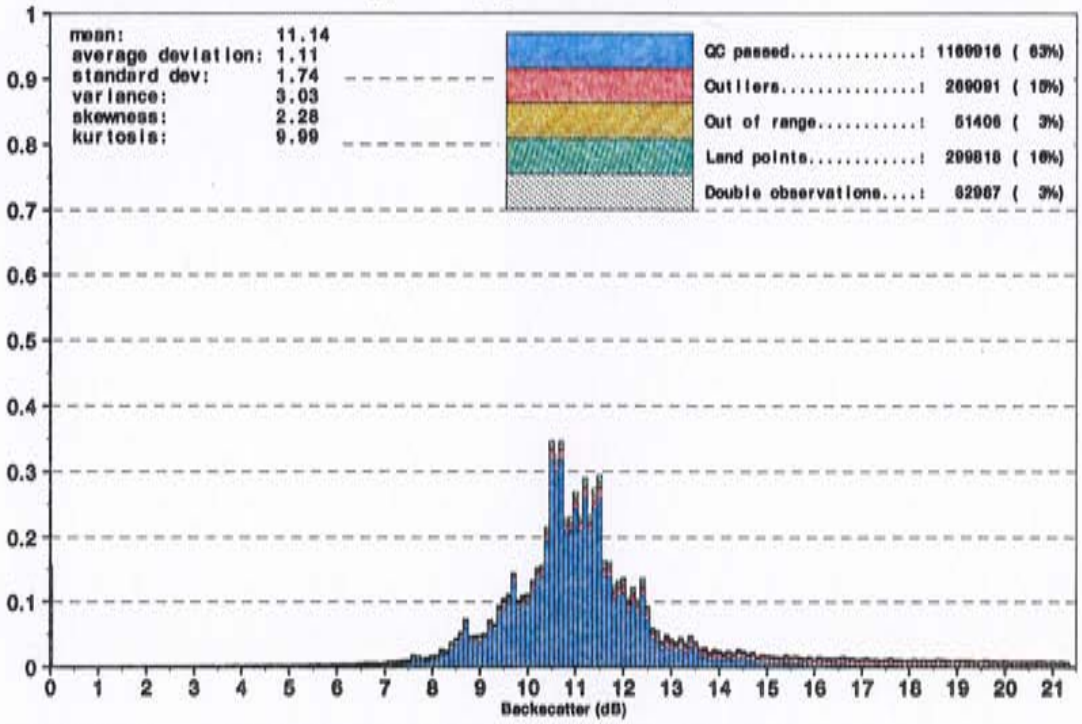

FIGURE 5. σ_0 - distribution of ERS-1 radar altimeter for May 1995.

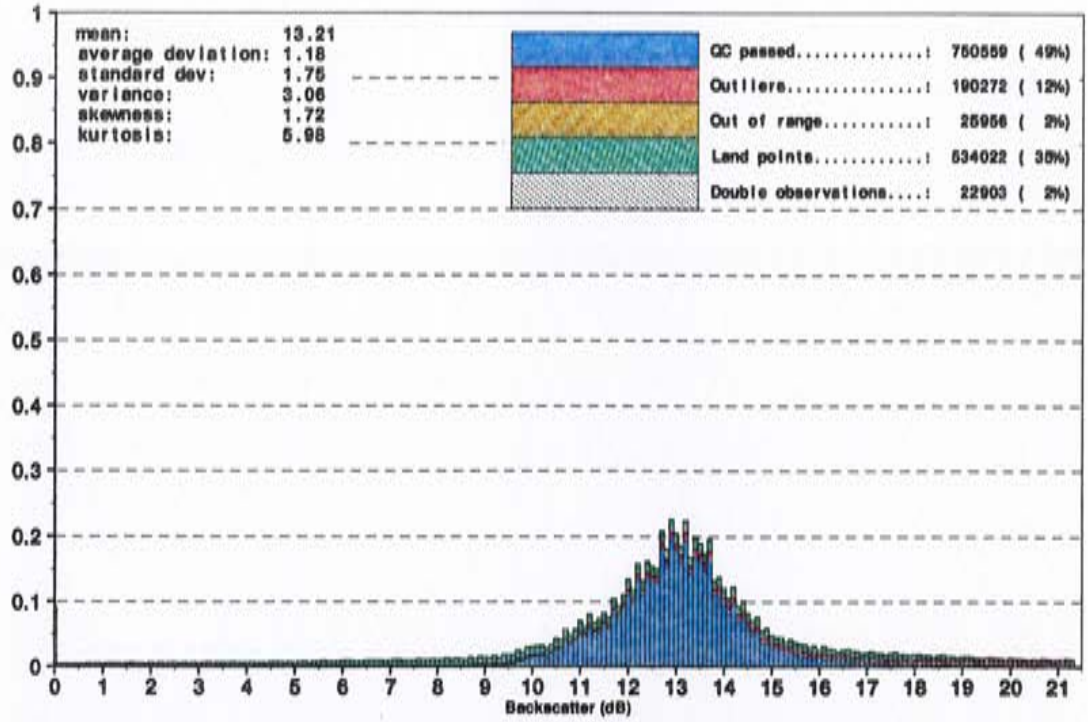

FIGURE 6. σ_0 - distribution of ERS-2 radar altimeter for May 1995.

Also the shape of the distribution function between the two instruments was different in the sense that the distribution of ERS-1 winds was double peaked whereas ERS-2 showed only one peak. On May 19th 1995, ESA updated the look up tables (LUT) at the ground stations to provide winds which should better agree with ERS-1 and the model. After this an even higher shift of about 2.45dB was found and on average the σ_0 were at about 13.6dB (figures 7 and 8). Consequently the resulting winds were biased even more negative reaching 5.25m/s (figures 9 and 10).

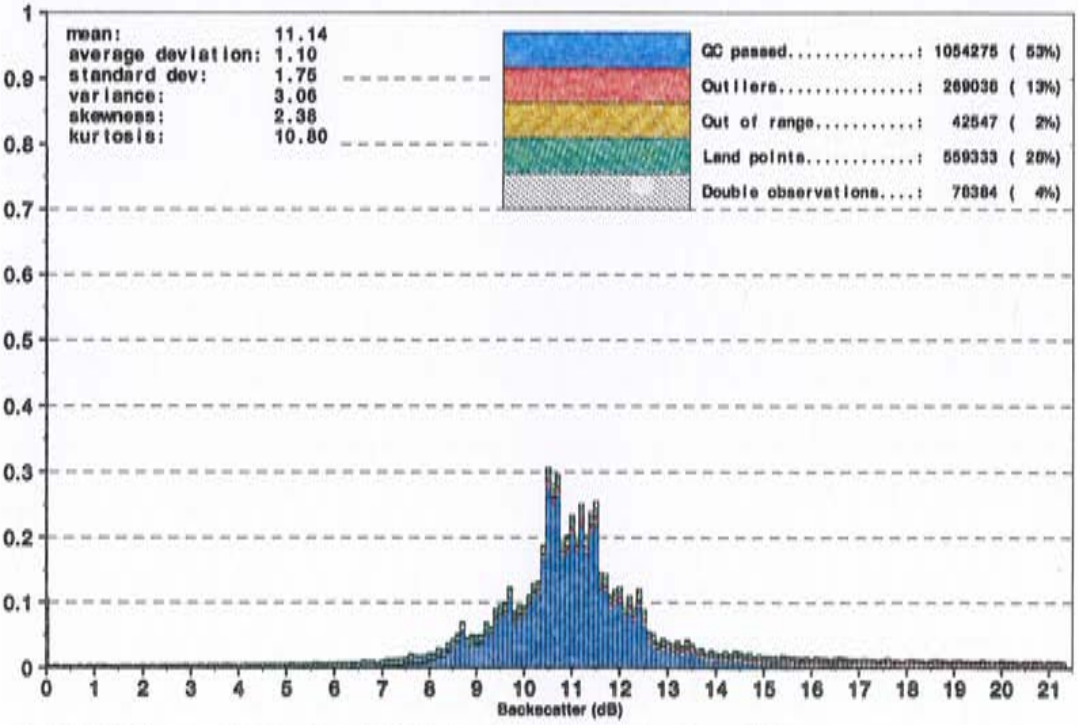

FIGURE 7. σ_0 - distribution of ERS-1 radar altimeter for June 1995.

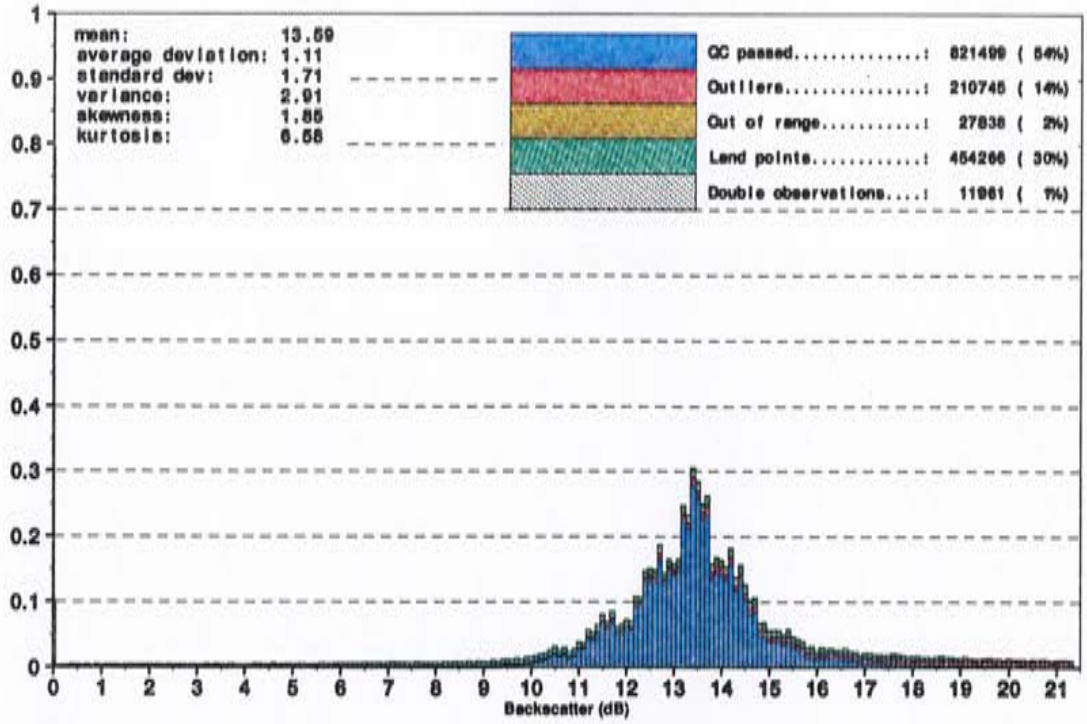

FIGURE 8. σ_0 - distribution of ERS-2 radar altimeter for June 1995.

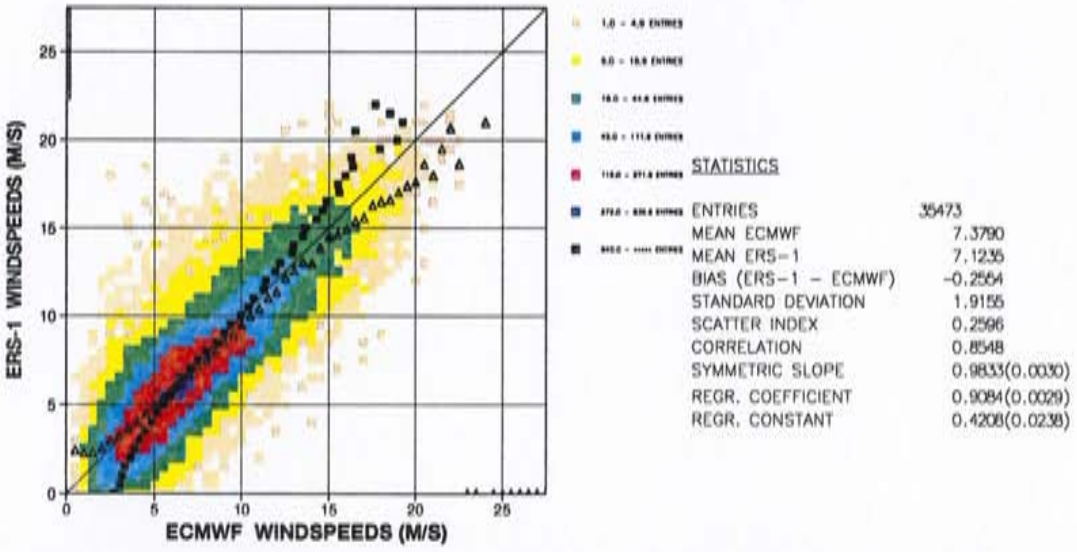

FIGURE 9. Comparison of ECMWF wind speed results with ERS-1 radar altimeter wind speed data for June 1995. The squares denote the mean values in the x-direction and the triangles in the y-direction The standard error is shown in brackets.

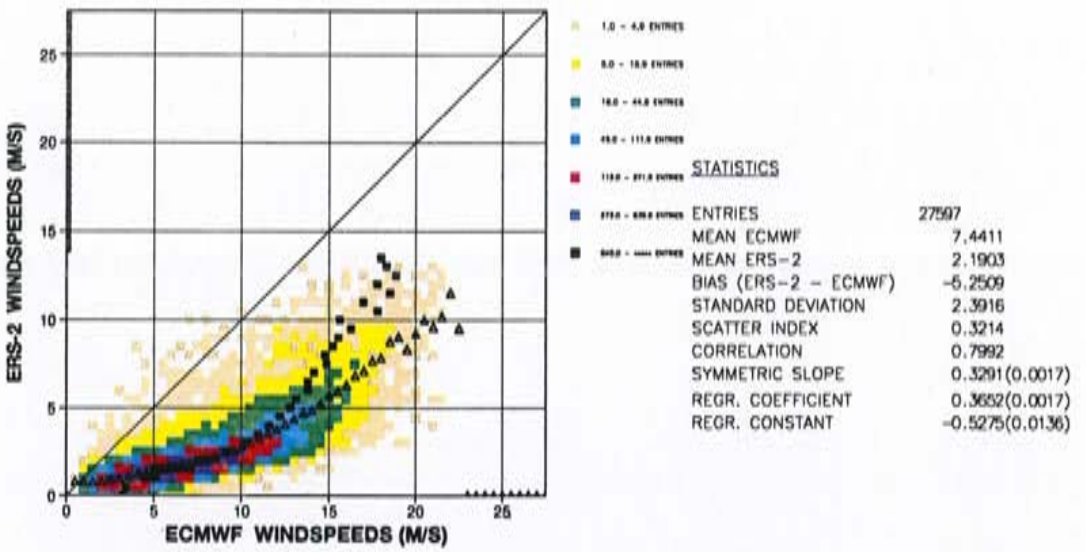

FIGURE 10. Comparison of ECMWF wind speed results with ERS-2 radar altimeter wind speed data for June 1995. The squares denote the mean values in the x-direction and the triangles in the y-direction. The standard error is shown in brackets.

The next change occurred on the 6th July 1995 when again new LUT were introduced. This removed the shift of 2dB σ_0 (figures 11 and 12) and resulted in a significant reduction of the ERS-2 bias from 5.3m/s to 0.75m/s. At the same time the slope of the symmetric regression changed from 0.33 to 0.92 (figures 13 and 14).

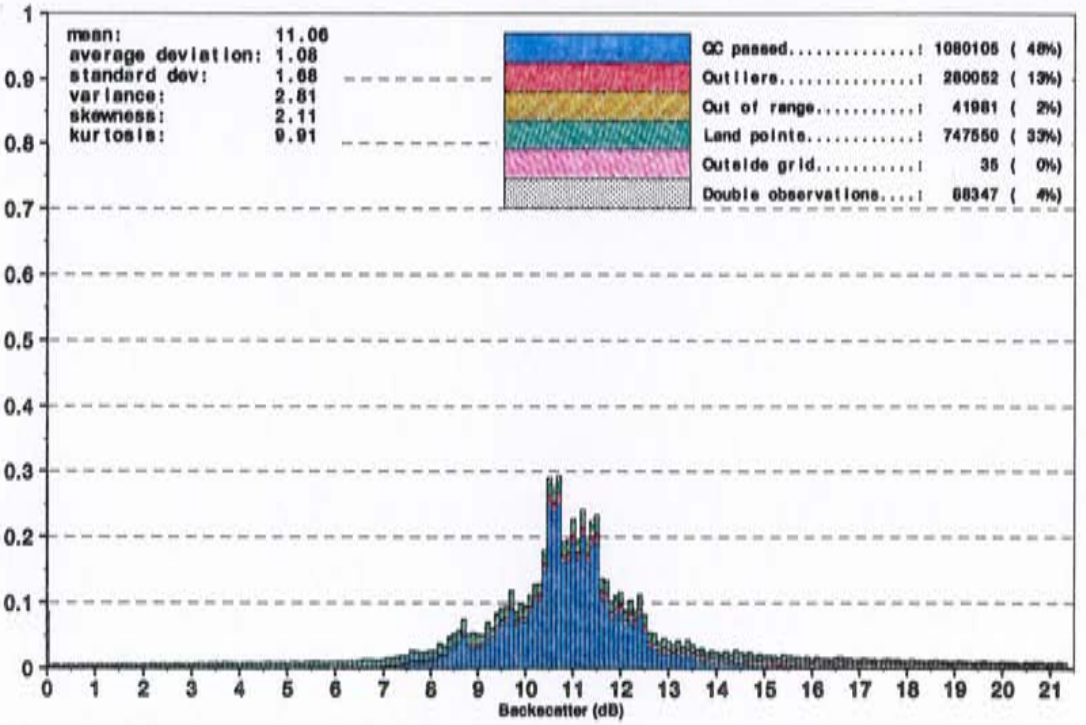

FIGURE 11. σ_0 - distribution of ERS-1 radar altimeter for September 1995

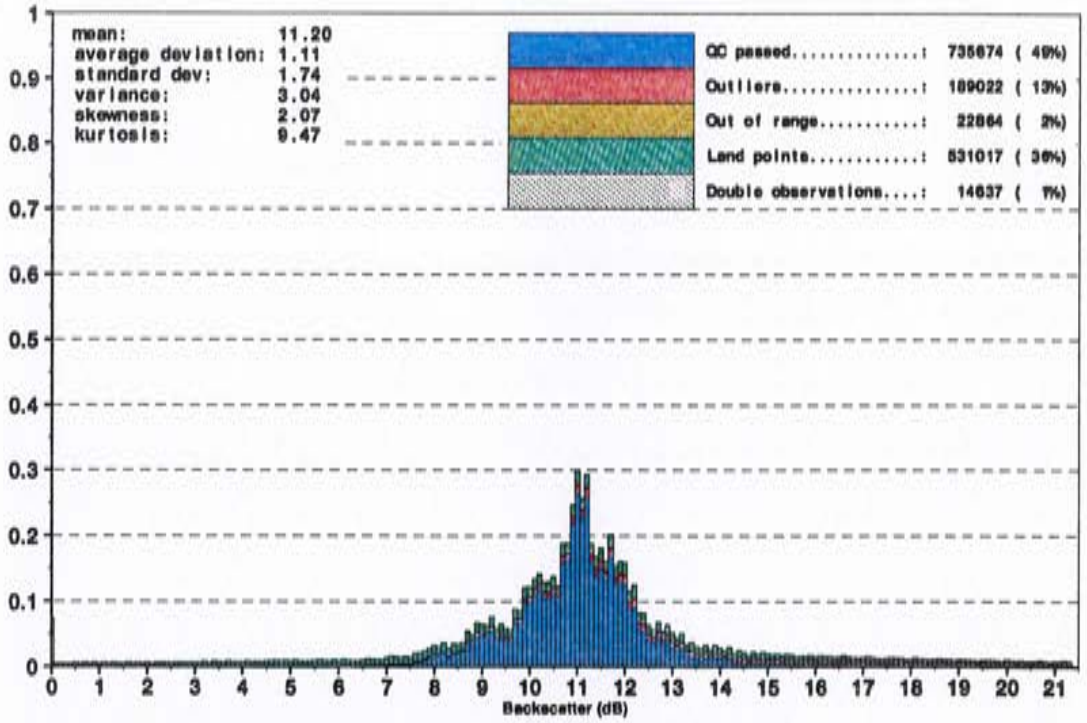

FIGURE 12. σ_0 - distribution of ERS-1 radar altimeter for September 1995

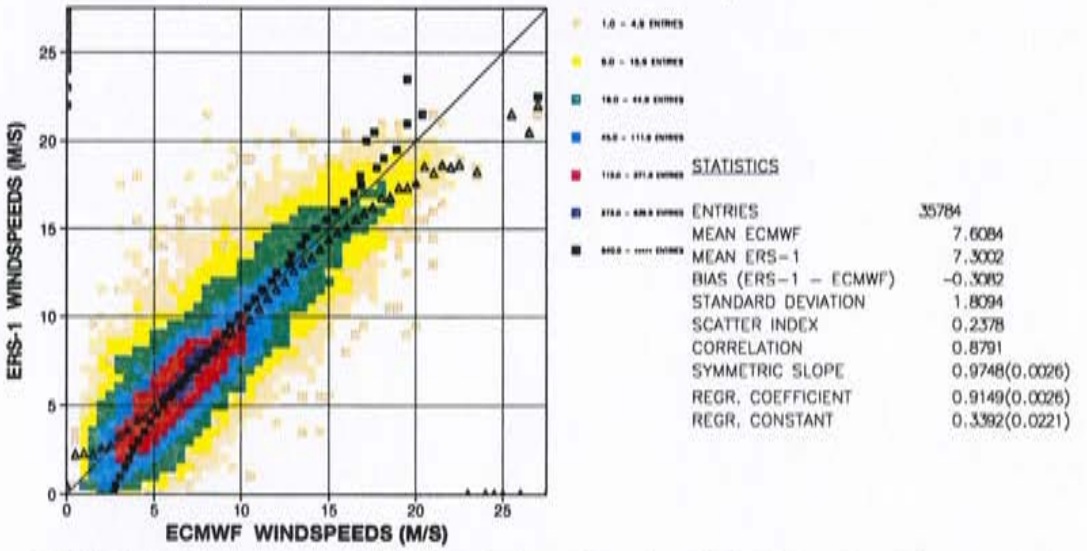

FIGURE 13. Comparison of ECMWF wind speed results with ERS-1 radar altimeter wind speed data for September 1995. The squares denote the mean values in the x-direction and the triangles in the y-direction. The standard error is shown in brackets

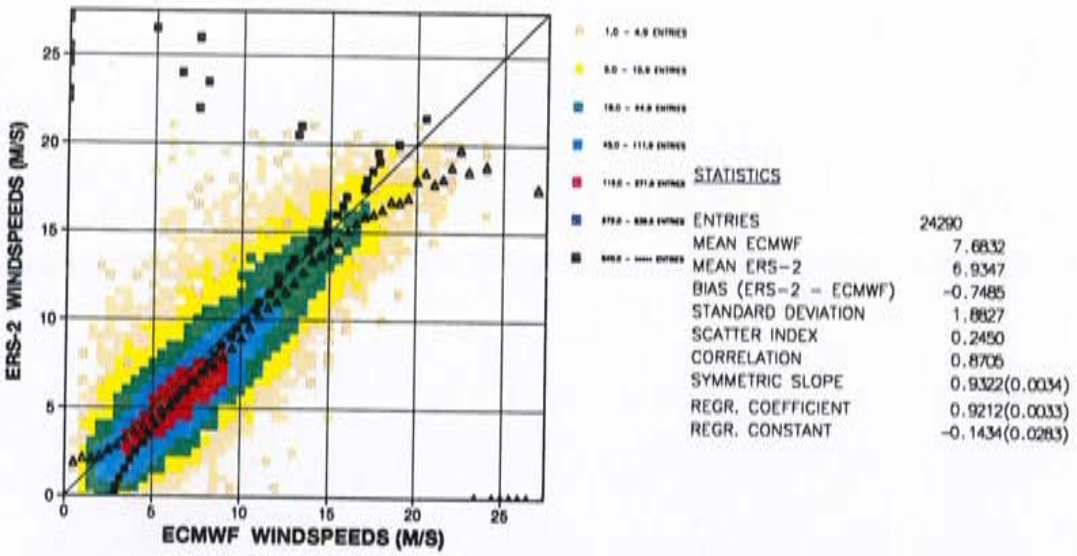

FIGURE 14. Comparison of ECMWF wind speed results with ERS-2 radar altimeter wind speed data for September 1995. The squares denote the mean values in the x-direction and the triangles in the y-direction. The standard error is shown in brackets

A summary of the regression analysis since this last change is given in table 1. Presented are the regression coefficient and the regression constant of the least squares regression line together with their standard errors. Taking now the model as the transfer standard one can eliminate the model term from the regression equations for ERS-1 and ERS-2. This gives the following relation between ERS-1 and ERS-2:

$$U_{10_{ers2}} = 0.993 \times U_{10_{ers1}} - 0.48$$

Additionally the regression coefficients for the symmetric regression line are given in table 2 and the following relation between ERS-1 and ERS-2 is found:

$$U_{10_{ers2}} = 0.956 \times U_{10_{ers1}}$$

The results from the linear regression assume that the atmospheric model is error free, which is unrealistic. The results from the symmetric regression allow for error in the satellite data and the atmospheric model, and so are more realistic.

Table 1: Least squares regression parameters $(\text{ERS-}(1/2) = b_1 \times \text{model} + b_0)$ **where** s_{b_1} **is the standard error of** b_1 **and** s_{b_0} **is the standard error of** b_0

U_{10}	$b_1\ (s_{b_1})$	$b_0\ (s_{b_0})$	n
ERS-1 = *f(model)*	0.915 (0.00265)	0.339 (0.0221)	35784
ERS-2 = *f(model)*	0.921 (0.00337)	-0.143 (0.0283)	24290
ERS-2 = *f*(ERS-1)	0.993	-0.48	

Table 2: Symmetric regression parameters

(ERS-(1/2) = $b_1 \times$ model) where s_{b_1} is the standard error of b_1

U_{10}	b_1 (s_{b_1})	n
ERS-1 = *f(model)*	0.975 (0.00265)	35784
ERS-2 = *f(model)*	0.932 (0.00337)	24290
ERS-2 = *f*(ERS-1)	0.993	

For ERS-1 and ERS-2, respectively, figures 15 and 16 give an overview of the changes, between May 1995 and January 1996, in the following statistical parameters: monthly mean model wind speed and the corresponding bias and the standard deviation of the satellite - model differences. It can be seen, that since the end of the 3rd cycle (28th August 1995) the statistics on the satellite - model differences have been stable.

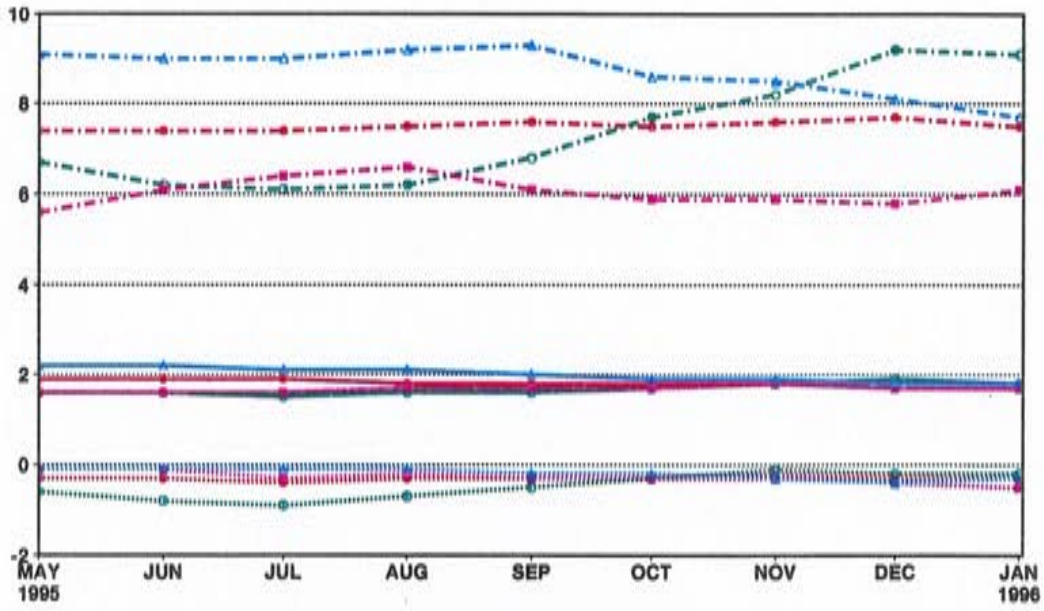

FIGURE 15. Development of ERS-1 radar altimeter wind speed measurements in the cal/val phase of ERS-2. Global and regional comparison with the ECMWF T213 Model. Bias is RA - model. Mean of the ECMWF T213 Model shown (units: m/s).

dash-dotted line: model mean, dashed line: bias (model minus ERS), solid line: standard deviation; regional decomposition: full circles: global, open circles: Northern Hemisphere Extratropics, full squares: Tropics, open triangles: Southern Hemisphere Extratropics.

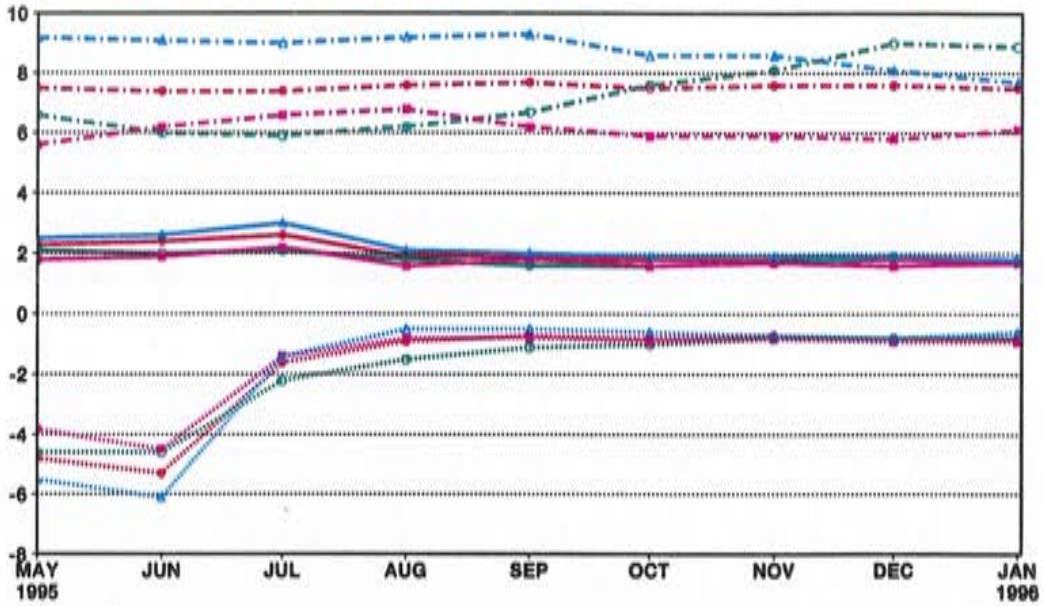

FIGURE 16. Development of ERS-2 radar altimeter wind speed measurements from May to December 1995. Global and regional comparison with the ECMWF T213 Model. Bias is RA - model. Mean of the ECMWF T213 Model shown (units: m/s).

dash-dotted line: model mean, dashed line: bias (model minus ERS), solid line: standard deviation; regional decomposition: full circles: global, open circles: Northern Hemisphere Extratropics, full squares: Tropics, open triangles: Southern Hemisphere Extratropics.

Conclusions on winds

- Initial look up tables produced unsatisfactory winds with biases as large as 4.8m/s relative to the ECMWF atmospheric model.
- The revision of the look up tables on 19 May 1996 produced winds which were even less satisfactory, with biases as large as 5.3m/s.
- The most recent revision of the look up tables, on 6 July 1995, has produced winds of much improved quality, but the quality is still not satisfactory, as the winds relative to the atmospheric model are too low by about 0.7m/s.
- Since the last change to the look up tables, on 6 July 1995, the statistics on the ERS-2 minus model wind differences have been quite stable.
- If we use the atmospheric model as a transfer standard, and calculate an implied relationship between ERS-1 and ERS-2 winds we find:

  $$U_{10_{ers2}} = 0.956 \times U_{10_{ers1}}.$$

- Further investigation of the bias with ERS-2 wind speeds is needed.

ECMWF Wind and Wave Calibration - Wave Height Analysis.

Björn Hansen - European Centre for Medium Range Weather Forecasts.

Data reception rate

The results on the data reception rate for ERS-2 waves are exactly the same as for winds, and have been discussed already within the wind speed section.

Calibration

The ERS-2 radar altimeter wave height observations were in good agreement with ERS-1 and with the wave model results from the time the first data became available early in May 1995. Since then ERS-2 waves have been biased high by 5 to 8 cm when compared with model results whereas ERS-1 waves have been biased low by 12 to 16 cm when compared with model results. The slope of the symmetric regression did not change noticeably within the period and was 0.95 for ERS-1 and 1.02 for ERS-2 (figures 1 and 2). On the other hand the minimum reported value of 0.63m for significant wave height of ERS-2 is 0.2m higher than that for ERS-1. Finally the saturation value is with 20.09m smaller for ERS-2 than for ERS-1 where we find 20.2m significant wave height as the saturation value (figures 3 and 4).
For September 1995 the results of the 2 parameter regression analysis is summarized in table 1. Presented are the regression coefficient and the regression constant of the least squares regression line together with their standard errors. Eliminating the model terms in the linear regression equations for ERS-1 and ERS-2, we find the following relation between the satellites:

$$H_{s_{ers2}} = 1.023 \times H_{s_{ers1}} + 0.1875$$

Additionally the regression coefficients for the symmetric regression line are given in table 2 and the following relation between ERS-1 and ERS-2 is found:

$$H_{s_{ers2}} = 1.085 \times H_{s_{ers1}}$$

As for the winds, the latter relationship is probably more reliable

TABLE 1. Least squares regression parameters $(\text{ERS-}(1/2) = b_1 \times \text{model} + b_0)$

where s_{b_1} **is the standard error of** b_1 **and** s_{b_0} **is the standard error of** b_0

H_s	b_1 (s_{b_1})	b_0 (s_{b_0})	n
ERS-1 = *f(model)*	0.928 (0.0016)	0.02 (0.0045)	35784
ERS-2 = *f(model)*	0.949 (0.002)	-0.208 (0.0058)	24290
ERS-2 = *f*(ERS-1)	1.023	0.1875	

TABLE 2. Symmetric regression parameters ($\text{ERS-(1/2)} = b_1 \times \text{model}$) **where** s_{b_1} **is the standard error of** b_1

H_s	b_1 (s_{b_1})	n
ERS-1 = *f(model)*	0.949 (0.00158)	35784
ERS-2 = *f(model)*	01.025 (0.0021)	24290
ERS-2 = *f*(ERS-1)	1.085	

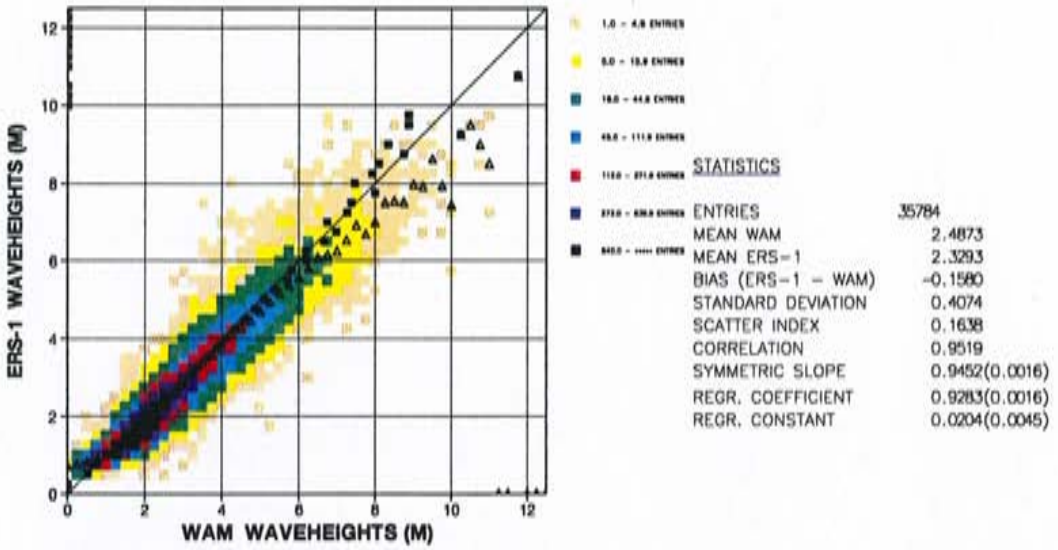

FIGURE 1. Comparison of ECMWF wave height results with ERS-1 radar altimeter wave height data for September 1995. The squares denote the mean values in the x-direction and the triangles in the y-direction.

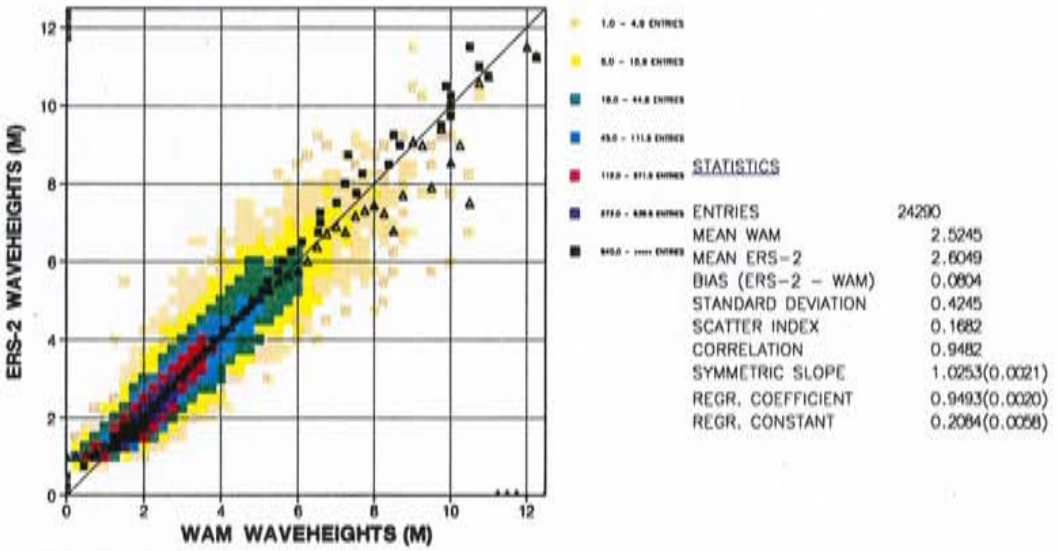

FIGURE 2. Comparison of ECMWF wave height results with ERS-2 radar altimeter wave height data for September 1995. The squares denote the mean values in the x-direction and the triangles in the y-direction.

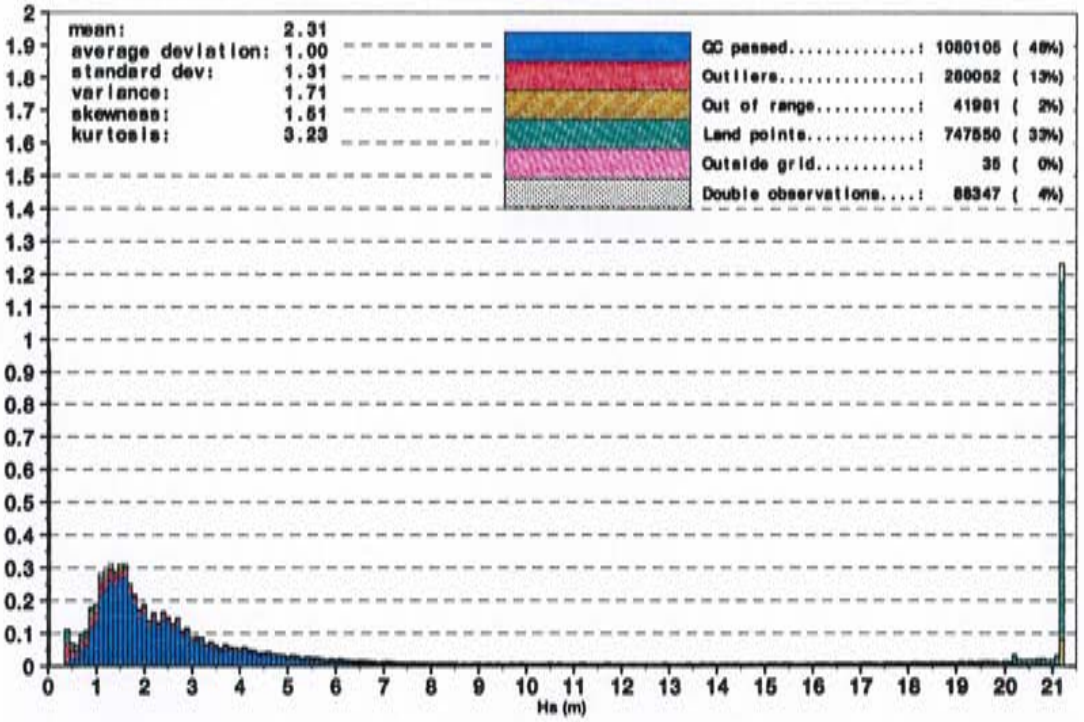

FIGURE 3. Distribution of wave height data from ERS-1 radar altimeter for September 1995 after quality control.

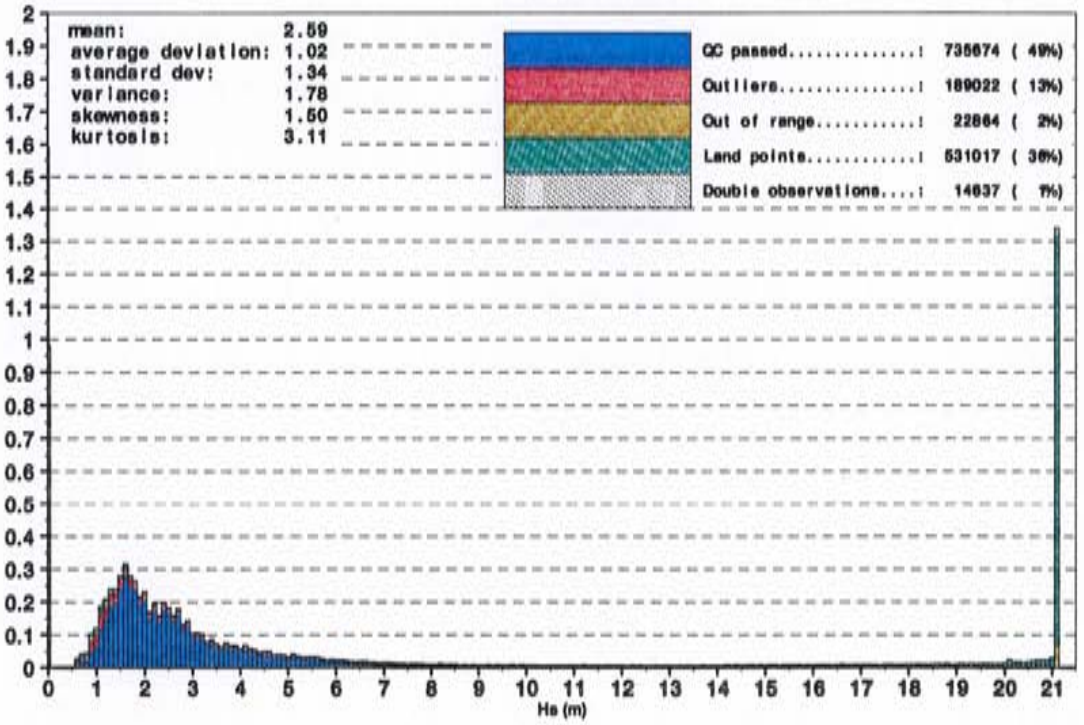

FIGURE 4. Distribution of wave height data from ERS-2 radar altimeter for September 1995 after quality control.

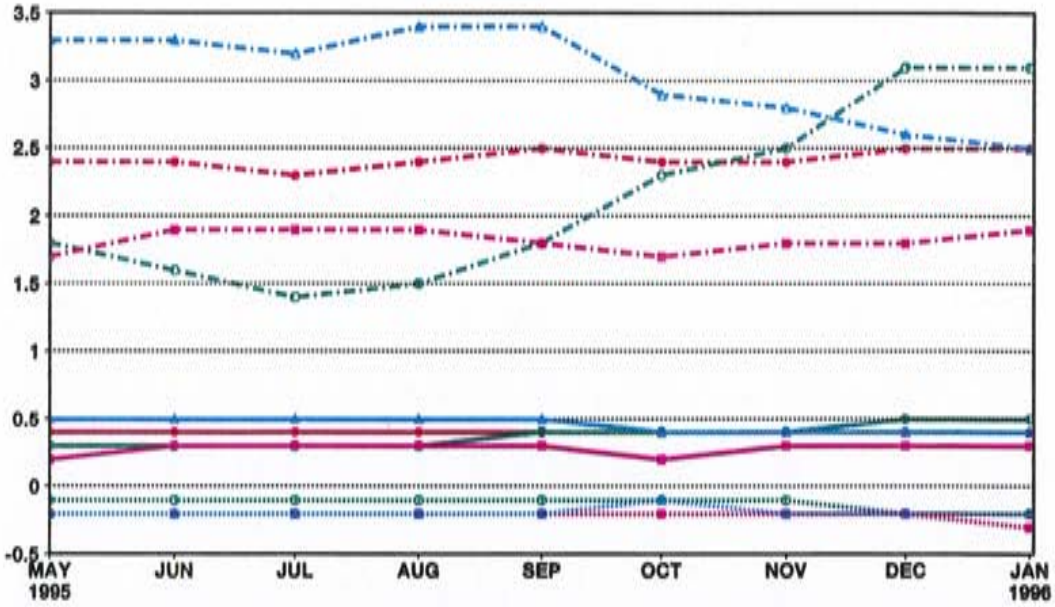

FIGURE 5. Development of ERS-1 radar altimeter wave height measurements in the cal/val phase of ERS-2. Global and regional comparison with the WAM Model. Bias is RA - model. Mean of the WAM Model shown (units: m).

dash-dotted line: model mean, dashed line: bias (model minus ERS), solid line: standard deviation; regional decomposition: full circles: global, open circles: Northern Hemisphere Extratropics, full squares: Tropics, open triangles: Southern Hemisphere Extratropics.

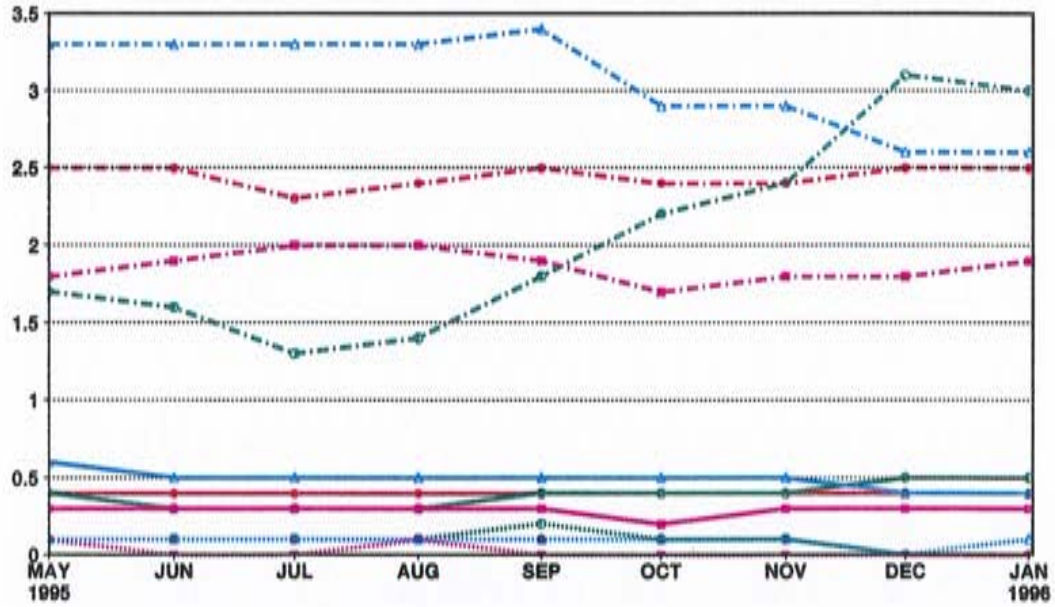

FIGURE 6. Development of ERS-2 radar altimeter wave height measurements in the cal/val phase of ERS-2. Global and regional comparison with the WAM Model. Bias is RA - model. Mean of the WAM Model shown (units: m).

dash-dotted line: model mean, dashed line: bias (model minus ERS), solid line: standard deviation; regional decomposition: full circles: global, open circles: Northern Hemisphere Extratropics, full squares: Tropics, open triangles: Southern Hemisphere Extratropics.

The evolution of the statistical parameters mean model wave height, bias and standard deviation of differences for ERS-1 and ERS-2 in time from May 1995 to January 1996 is shown in figures 5 and 6. Despite the seasonal variation of the mean model wave

height the differences between satellite and model have been stable throughout the entire period.

Conclusion on waves

- The quality of the ERS-2 wave height observations was reasonably good from the beginning of the cal/val period.
- The ERS-2 wave heights show a small positive bias of 7 to 9 cm when compared with the WAM model, whereas ERS-1 waves are biased low by up to 0.3 m.
- Most likely the ERS-2 waves are closer to the truth than the ERS-1 wave heights which are known to be too low.
- Using the wave model as a transfer standard we can calculate the following implied relationship between ERS-1 and ERS-2:

$$H_{sers2} = 1.085 \times H_{sers1}$$

- The difference between ERS-1 and ERS-2 in the highest reported waves (21.2 versus 20.1, respectively) is probably not important from a geophysical point of view, but may indicate problems in the processing software implemented at the ground stations.
- Finally ERS-2 shows an unacceptable cut-off at low waves. Especially for assimilation purposes in closed basins like the Mediterranean Sea or the Baltic Sea where low wave states are common ERS-2 will not provide sufficient information.

ANNEX G

- First results with ERS-2 Altimeter Assimilation.

MEMORANDUM
RESEARCH DEPARTMENT

From: J. Bidlot, B. Hansen and P. Janssen

Date: 1 April 1996

To: HR, R D Division/Section Heads, HO, HMD, HMOS

Copy: D

Ref.: R57.5.2/PJ/AD/42

Subject: **First results with ERS-2 Altimeter Assimilation**

---

1. Introduction

By means of test suite facilities developed by G. Konstantinidis, the WAM model was run for the period of December 1995 using ERS-2 Altimeter wave height data in the wave analysis. Results were compared with the operational wave suite results which were obtained using ERS-1 data in the assimilation. From this comparison, details of which are discussed below, it is concluded that ERS-2 data show a favourable impact on analysis and forecast. It is, therefore, suggested to introduce the assimilation of ERS-2 data in operations as quickly as possible and to switch off the assimilation of ERS-1 data.

2. Quality of ERS-2 data

During the past half year we have been involved in validating ERS-2 Altimeter wave heights and winds. Since ERS-1 and ERS-2 are not measuring waves and wind at the same location at the same time, the model wave heights were used as a go-between to establish a relation between ERS-1 and ERS-2 wave heights with the result that

$$H_{s,2} = 1.085\ H_{s,1}$$

where the index numbers refer to ERS-1 and ERS-2 respectively. Thus, ERS-2 gives about 8% higher wave height and since from collocations with buoy observations it is known that ERS-1 gives too low wave height, this change is in the right direction. Direct comparisons between modelled wave heights and the Altimeter data suggest that the scatter index for ERS-2 wave height is only 17% and nearly identical to the ERS-1 results (an example of scatter diagrams is given in Figure 1), hence assimilation of ERS-2 data seems to be promising.

3. December 95 analysis and forecast results

In order to study the impact of the assimilation of ERS-2 data, we ran the WAM model for the period of December 1995 and generated both analysis and 10-day forecasts for the globe. Assimilation of ERS-1 data was switched off. As control we used the corresponding results from the operational suite. Note that results obtained with the ERS-2 assimilation are denoted by experiment 14.

3.1 Quality of analysis and first guess

We verified the quality of the analysed fields by means of a comparison with buoy data. Scatter diagrams for test-suite and 0-suite are given in Figure 2 and Figure 3, respectively.

It is concluded from the comparison of the statistical parameters that the ERS-2 analysis agrees better with the buoy data than the ERS-1 analysis. For example, the wave height bias decreases by 12 cm (from -0.28 to -0.16 m), the rms error decreases from 0.56 to 0.52 m, while the symmetric slope for wave height increases from 0.91 to 0.94. Also, peak periods have increased slightly (by 0.3 s) in agreement with the small increase in wave height in the ERS-2 analysis.

The increase in mean wave height and period is confirmed by a plot of the difference in monthly mean analysed wave height and mean period as shown in Figure 4. Note that these difference fields are remarkably flat.

The verification of first-guess wave height against ERS-1 data (0-suite) and ERS-2 data (test suite 14) is shown in Figure 5. It confirms the small increase in wave height for the test suite once more. In addition, it suggests that the wave model forecasting system and ERS-2 data are better balanced because of a smaller wave height bias. It is remarked that since the introduction of the 1.5° version of the WAM model, the comparison of first-guess wave height against ERS-1 data has always given a higher model wave height, while also the extreme modelled wave heights were higher. With ERS-2 assimilation this seems to be less of a problem.

3.2 Quality of wave forecasts

The forecast performance (in absolute terms) has not been changed by the assimilation of ERS-2 data. This follows, for example, from the verification of the wave forecasts against buoy data. The bias in wave height as function of forecast day is shown in Figure 6 for both test-suite and 0-suite. Although the analysis error has been reduced in the test-suite from -0.30 to -0.18 m, from Day 3 onwards, the forecast error is very similar in the two suites. This remark also applies to the errors of different areas which are shown in Figure 6. (The main reason for this behaviour is that during a forecast the quality of the wave forecast is determined by the quality of the wind forecast.)

This also follows from the verification of the wave forecast against its own analysis. Verification scores for Northern and Southern Hemisphere are shown in Figures 7 and 8, respectively. Anomaly correlation and standard deviation have hardly changed. The only difference between test-suite and 0-suite is seen in the evolution of mean forecast error against forecast day. The test-suite shows reduced mean error. The reason for this is that the mean analysed wave height has increased by about 10-15 cm.

4. Conclusion

It is concluded that ERS-2 data assimilation has a favourable impact on the wave height analysis. Furthermore, because of the small increase in mean wave height by about 10-15 cm, analysis and forecast are better balanced.

It is, therefore, suggested to introduce the ERS-2 data assimilation in Operations as quickly as possible. The ERS-1 satellite will be switched off in the middle of May 1996 and by a timely change to ERS-2 data we are still able to check the wave analysis against ERS-1 data giving an extra check on the quality of the wave product.

TABLE 4. Symmetric regression parameters (ERS-(1/2) = $b_1 \times$ model)

where s_{b_1} is the standard error of b_1

H_s	b_1 (s_{b_1})	n
ERS-1 = *f(model)*	0.949 (0.00158)	35784
ERS-2 = *f(model)*	01.025 (0.0021)	24290
ERS-2 = *f*(ERS-1)	1.085	

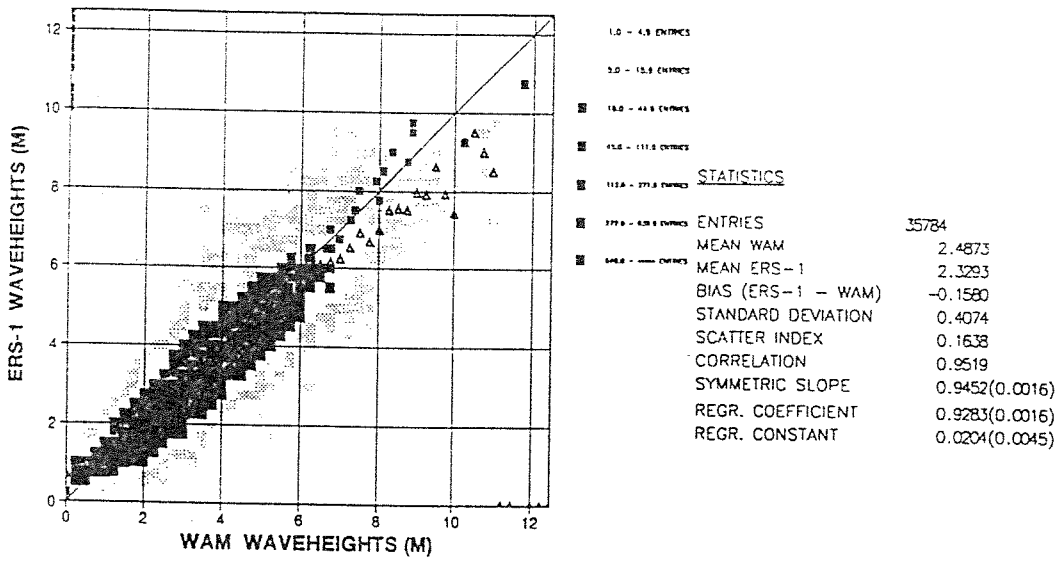

FIGURE 18. Comparison of ECMWF wave height results with ERS-1 radar altimeter wave height data for September 1995. The squares denote the mean values in the x-direction and the triangles in the y-direction.

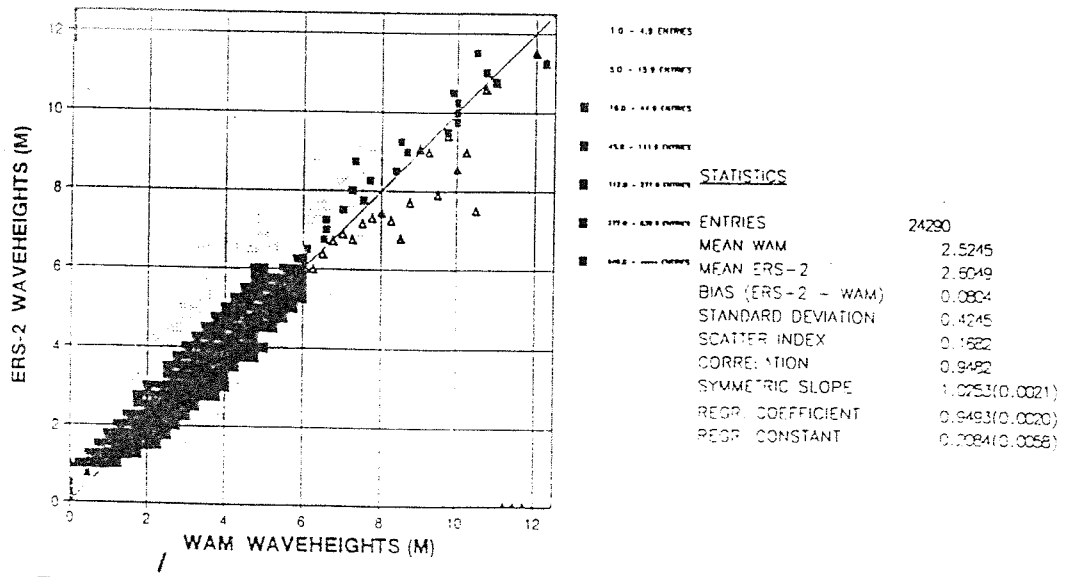

FIGURE 19. Comparison of ECMWF wave height results with ERS-2 radar altimeter wave height data for September 1995. The squares denote the mean values in the x-direction and the triangles in the y-direction.

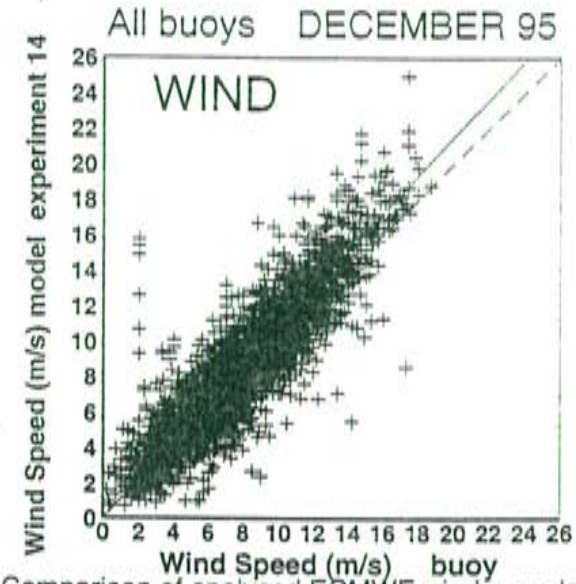

ENTRIES = 3161
MODEL MEAN = 8.615 STDEV = 3.639
BUOY MEAN = 8.069 STDEV = 3.249
LSQ FIT: SLOPE = 0.999 INTR = 0.554
RMSE = 1.733 BIAS = 0.546
CORR COEF = 0.892 SI = 0.204
SYMMETRIC SLOPE = 1.075

Comparison of analysed ECMWF wind speeds with averaged buoy data.

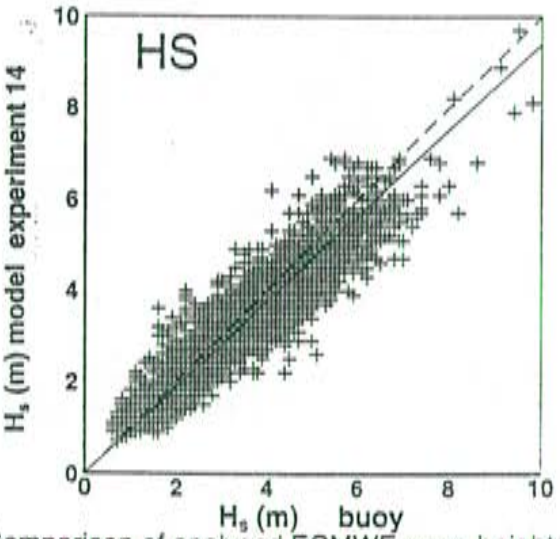

ENTRIES = 3311
MODEL MEAN = 3.010 STDEV = 1.228
BUOY MEAN = 3.166 STDEV = 1.400
LSQ FIT: SLOPE = 0.821 INTR = 0.411
RMSE = 0.524 BIAS = -0.156
CORR COEF = 0.936 SI = 0.158
SYMMETRIC SLOPE = 0.939

Comparison of analysed ECMWF wave heights with averaged buoy data.

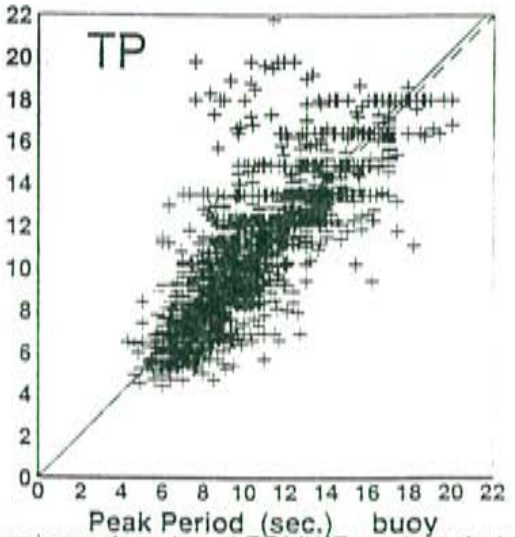

ENTRIES = 2293
MODEL MEAN = 10.655 STDEV = 3.123
BUOY MEAN = 10.485 STDEV = 2.979
LSQ FIT: SLOPE = 0.876 INTR = 1.470
RMSE = 1.763 BIAS = 0.170
CORR COEF = 0.836 SI = 0.167
SYMMETRIC SLOPE = 1.019

Comparison of analysed ECMWF peak periods with averaged buoy data.

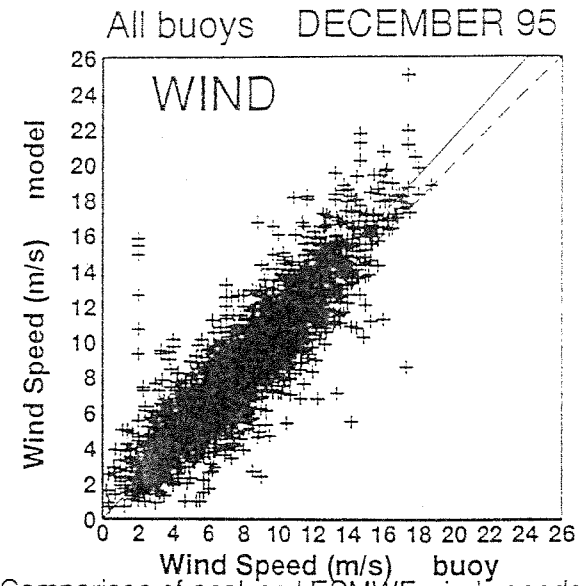

Comparison of analysed ECMWF wind speeds with averaged buoy data.

ENTRIES = 3161
MODEL MEAN = 8.615 STDEV = 3.639
BUOY MEAN = 8.069 STDEV = 3.249
LSQ FIT: SLOPE = 0.999 INTR = 0.554
RMSE = 1.733 BIAS = 0.546
CORR COEF = 0.892 SI = 0.204
SYMMETRIC SLOPE = 1.075

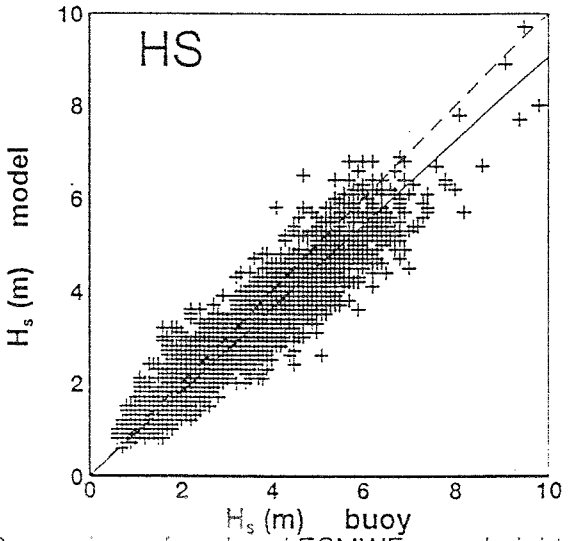

Comparison of analysed ECMWF wave heights with averaged buoy data.

ENTRIES = 3311
MODEL MEAN = 2.890 STDEV = 1.215
BUOY MEAN = 3.166 STDEV = 1.400
LSQ FIT: SLOPE = 0.815 INTR = 0.309
RMSE = 0.564 BIAS = -0.276
CORR COEF = 0.939 SI = 0.155
SYMMETRIC SLOPE = 0.906

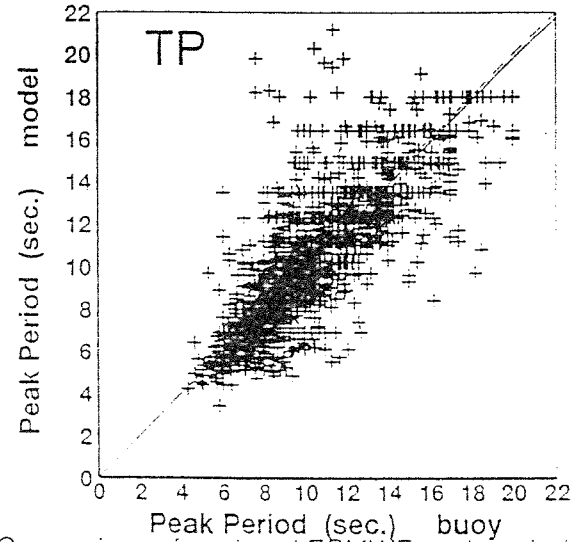

Comparison of analysed ECMWF peak periods with averaged buoy data.

ENTRIES = 2293
MODEL MEAN = 10.317 STDEV = 3.108
BUOY MEAN = 10.485 STDEV = 2.979
LSQ FIT: SLOPE = 0.875 INTR = 1.143
RMSE = 1.742 BIAS = -0.167
CORR COEF = 0.839 SI = 0.166
SYMMETRIC SLOPE = 0.989

Fig. 63

WAM / ERS-2 Comparison
Altimeter Waveheights
GLOBAL 1.5° DEC 1995
model field: fg, ERS-2 alt. assimilation: on

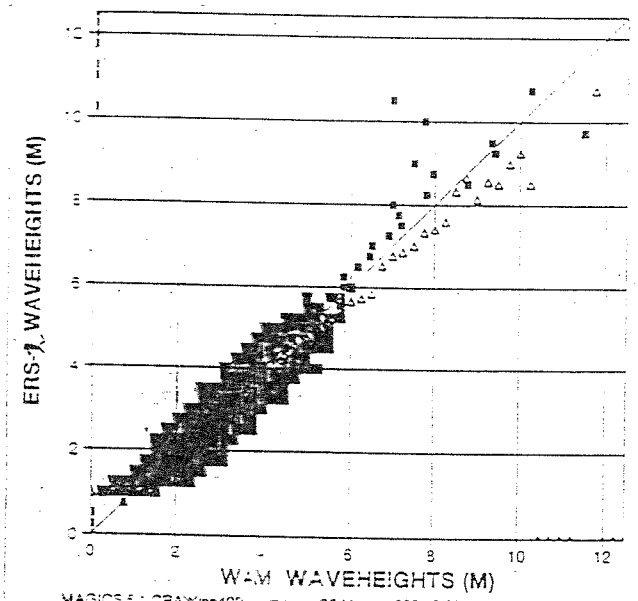

STATISTICS

ENTRIES	37765
MEAN WAM	2.60
MEAN ERS-2	2.51
BIAS (ERS-2 - WAM)	-0.10
STANDARD DEVIATION	0.47
SCATTER INDEX	0.18
CORRELATION	0.93
SYMMETRIC SLOPE	0.97

MAGICS 5.1: CRAY/sn4004 emos_2 26 March 1996 15:56:15 - Hansen,B.

WAM / ERS-1 Comparison
Altimeter Waveheights
GLOBAL 1.5° DEC 1995
(model field: fg, ERS-1 alt. assimilation: on)

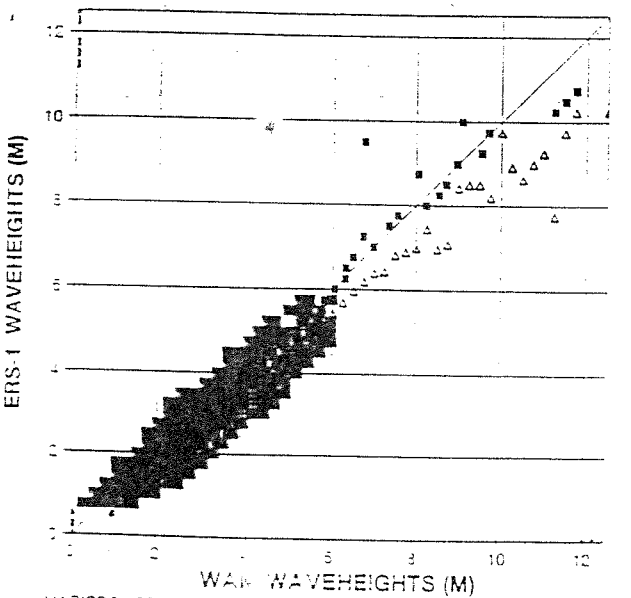

STATISTICS

ENTRIES	39892
MEAN WAM	2.50
MEAN ERS-1	2.39
BIAS (ERS-1 - WAM)	-0.11
STANDARD DEVIATION	0.45
SCATTER INDEX	0.18
CORRELATION	0.94
SYMMETRIC SLOPE	0.98

MAGICS 5.1: CRAY/sn4004 emos_1 3 January 1996 00:26:39 - Hansen,B.

FORECAST VERIFICATION
HEIGHT OF WAVES SURFACE LEVEL
MEAN ERROR FORECAST
AREA=N.HEM TIME=12 MEAN OVER 20 CASES
DATE = 951201 TO 951220
WAVE_G
E_WAV_14
Forecast Day

FORECAST VERIFICATION
HEIGHT OF WAVES SURFACE LEVEL
MEAN VERIFYING ANALYSIS
AREA=N.HEM TIME=12 MEAN OVER 20 CASES
DATE = 951201 TO 951220
WAVE_G
E_WAV_14
Forecast Day

FORECAST VERIFICATION
HEIGHT OF WAVES SURFACE LEVEL
ANOMALY CORRELATION FORECAST
AREA=N.HEM TIME=12 MEAN OVER 20 CASES
DATE = 951201 TO 951220
WAVE_G
E_WAV_14
Forecast Day

FORECAST VERIFICATION
HEIGHT OF WAVES SURFACE LEVEL
STANDARD DEVIATION OF ERROR FORECAST
AREA=N.HEM TIME=12 MEAN OVER 20 CASES
DATE = 951201 TO 951220
WAVE_G
E_WAV_14
Forecast Day

Fig 7

ANNEX H

- Test with proposed κ_1 and κ_2 values for the wave height retrieval algorithm in the fast delivery product generation.
- Comments on the κ_1 and κ_2 discussion within the CWG meting #10, ESRIN, Frascati.

Tests with the proposed κ_1 and κ_2 values.

Björn Hansen - European Centre for Medium Range Weather Forecasts.

This is a brief note summarizing the results of tests with the estimates of the κ_1 and κ_2 values as proposed by Challenor (1996) and by Francis and O'Leary (1995).

The period chosen for the following comparisons is December 1995. Table 1 presents the values for $\kappa 1$ and $\kappa 2$ valid for this period together with the proposed corrections.

Table 1: κ_1 and κ_2 values used for the tests.

	κ_1	κ_2
valid for December 1995 (URA FDP)	21856	0.07
SOC (JRD)	30778.7	0149
ESTEC/ECMWF	19596	0.0655

Based on relation (1) given in Francis and O'Leary (1995) we can theoretically estimate the correction applied to a given wave height using (2), where κ_{1new} and κ_{2new} are

$$H_s = \sqrt{\frac{\kappa_1}{s^2} - \kappa_2} \qquad (1)$$

the proposed κ_1 and κ_2 values tested and H_s is the wave height generated within the FDP using the applied κ_1 and κ_2 for the period in question.

$$H_{s_{new}} = 4 \cdot \sqrt{\kappa_{1_{new}} + \frac{\left(\frac{H_s}{4}\right)^2 + \kappa_2}{\kappa_1} - \kappa_{2_{new}}} \qquad (2)$$

Figure 1 shows the impact the proposed corrections will have on the generated wave heights. It can be seen that when applying Challenors's values there will be a considerable decrease for waves of the range below 2.2 m. For all waves above this level an increase by 17-20% will be the consequence. The correction proposed by Francis and O'Leary on the other hand will never cause an increase, but there will be a decrease for the low waves. This decrease however will be less pronounced as with the correction proposed by Challenor.
The proposed corrections were subsequently applied to the ERS-2 FDP wave heights for December 1995 and which were then compared with the wave model results as described in the methods section of the report of the commissioning phase of ERS-2. Figure 2 shows the results using the original FDP wave heights. As already known there is a good agreement between model and altimeter, but the low waves are not seen

by the altimeter. Figure 3 shows the corresponding picture after applying Challenor's κ_1 and κ_2 values and as expected the altimeter represents the low waves much better, but waves above 2.5 m are now overestimated and for the whole dataset we find a bias of about 0.32 m.
The corrections proposed by Francis and O'Leary on the other hand cause a negative bias of 0.13 m and there is no improvement of the low waves as can be seen in figure 4.

These results confirm what is already known from figure 1. and it is also in accordance with the findings of Queffeullou (1996), who performed a very similar study using TOPEX/POSEIDON wave observations to compare with corrected ERS-2 wave heights using Challenor's κ_1 and κ_2 values.

The correction of the low waves using Challenor's κ_1 and κ_2 values is surely desirable while a change of the higher waves in either direction is questionable if not undesirable as in the case of a decrease when applying Francis and O'Leary's κ_1 and κ_2 values. It has to be discussed whether the higher waves should be corrected in the way proposed by Challenor. One has to note that only 111 collocated wave height pairs were used by Challenor and only 4 of them exceeded 4m wave height for the buoy observations. So therefore it is doubtful whether the proposed κ_1 is applicable, taking into account, that also Queffeullou mentions uncertainty for the high waves.

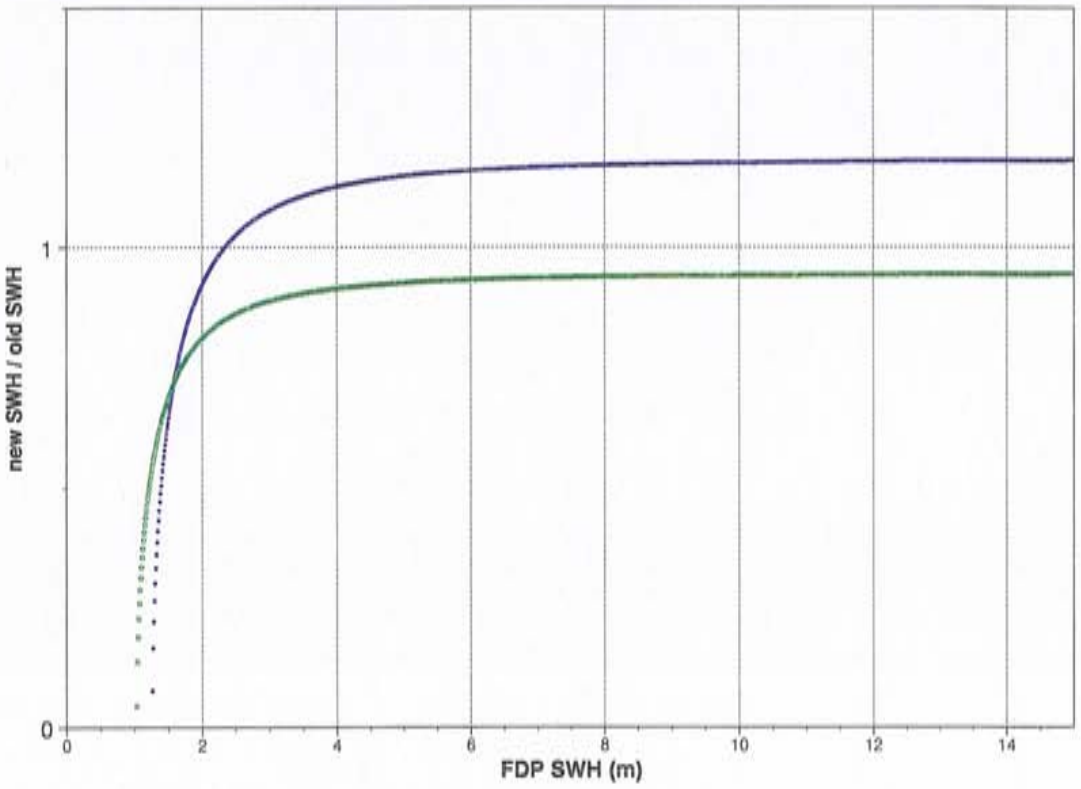

FIGURE 1. Ratio of new to old significant wave height.
green: using ESTEC/ECMWF proposals for κ_1 and κ_2.
blue: using SOC(JRD proposals for κ_1 and κ_2.

On the other hand we know that WAM might underestimate high waves due to the fact that ERS-1 wave height data are routinely used to correct the initial condition of the wave field, where ERS-1 is known to underestimate high waves. At this point no attempt was made to fit κ_1 and κ_2 values using model results directly.

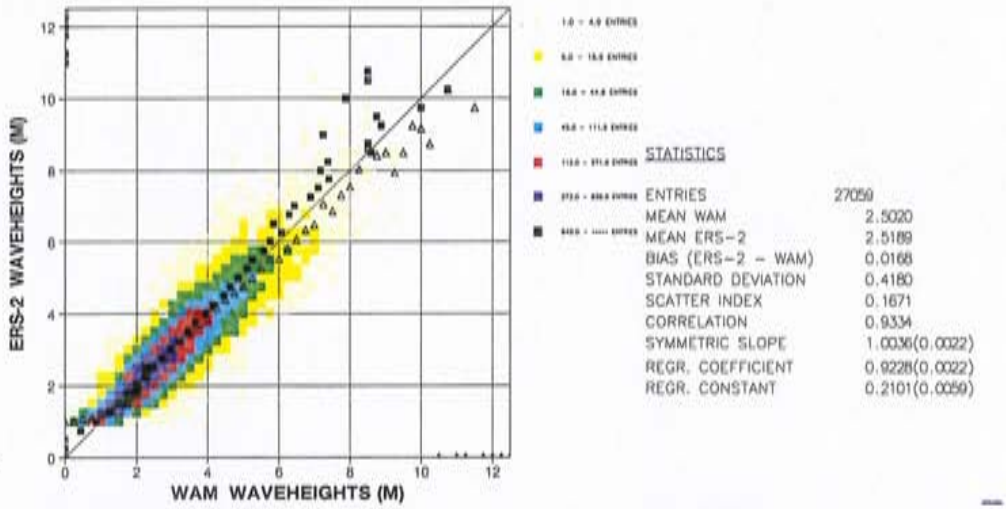

FIGURE 2. Comparison of ECMWF wave height results with ERS-2 radar altimeter wave height data for December 1995. No correction applied to the FDP data.

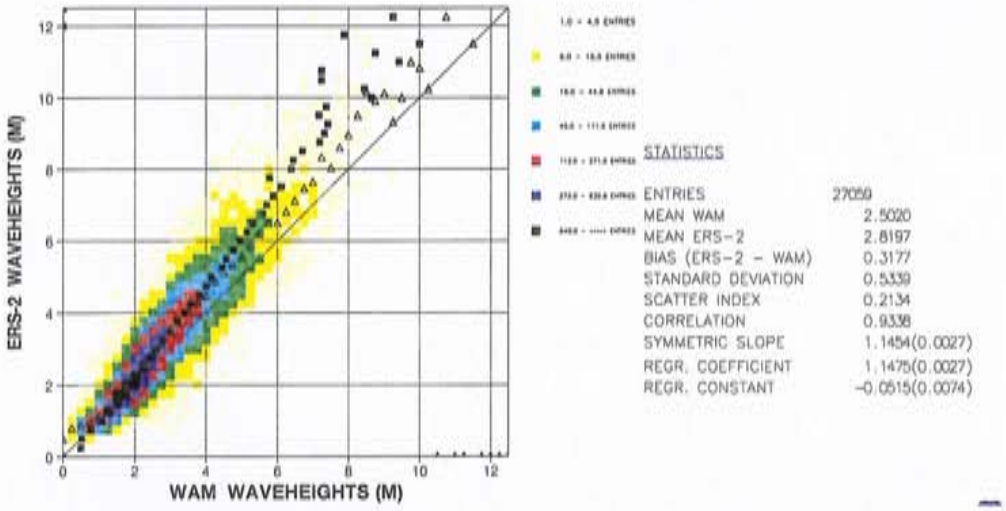

FIGURE 3. Comparison of ECMWF wave height results with ERS-2 radar altimeter wave height data for December 1995.
Correction proposed by Challenor applied.

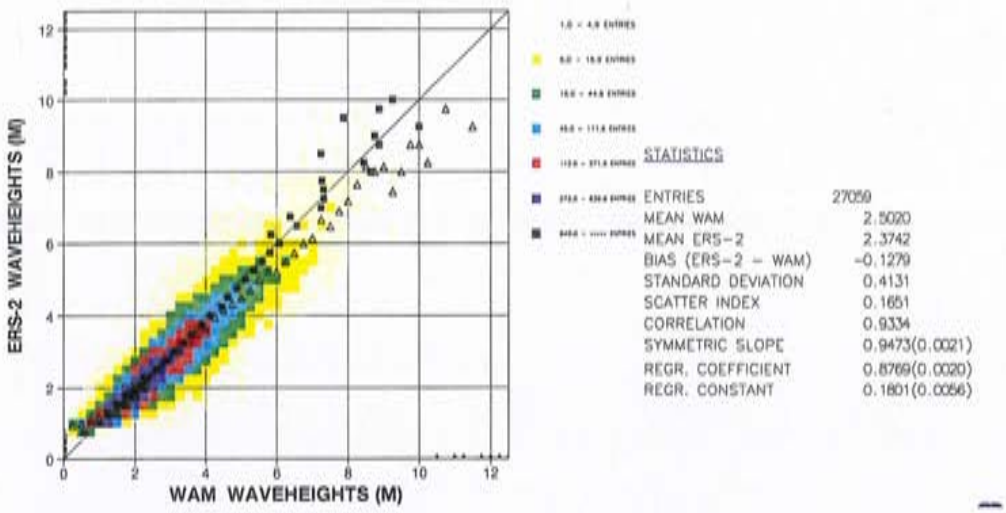

FIGURE 4. Comparison of ECMWF wave height results with ERS-2 radar altimeter wave height data for December 1995.
Correction proposed by Francis and O'Leary applied.

Comments on the K1 and K2 discussion within the commissioning working group meeting #10, Esrin, Frascati

Jean R. Bidlot, B. Hansen, Peter A. E. M. Janssen.
European Centre for Medium Range Weather Forecasts, Reading, England

This is to let you know that we are not at all satisfied with the recent proposals for changing the Altimeter wave height algorithm. The reasons for this are described below, and we will mainly discuss the fast delivery products, although similar remarks apply to the off-line products.

Challenor recently suggested new estimates of k1 and k2 based on a collocation of altimeter and buoy wave heights. The number of collocations was about 100-200 and the wave heights were typically of the order of 2 to 3 metres with a few heights around 4 metres. In this estimate of k1 and k2 it was assumed that the buoy data had no error. This assumption is, however, not true. These buoys have an instrument error of the order of 10%, and in addition one should also estimate errors caused by the fact that the collocation is not done at the same location and the same time. Nevertheless, assuming for the moment that this is not a problem (but, to be definite, we think it is) Challenor suggests new values of k1 and k2 which are considerably larger then the ones suggested by the standard theory of a Gaussian random sea surface. We think this is a serious problem, because, for example, it is well-known that swell (note that in practice two-thirds of the ocean surface has swell) is a very linear state, of which the probability distribution is Gaussian. It implies that in cases of swell the Challenor proposal would give a too high altimeter wave height by about 10% in the wave height range of 2 to 3 metres. This is not acceptable as it will affect wave heights in a large area of the globe. Incidentally, we recently performed one month of data assimilation experiments with ERS-2 altimeter data and when comparing the analysed wave heights with buoy data near Hawaii (note buoy data are not used in our analysis system; also swell conditions prevail near Hawaii) hardly no bias in analysed wave height was found. We also did an analysis run without assimilation of altimeter data. Comparing the verification scores of the two assimilation experiments revealed that the present ERS-2 altimeter algorithm makes in case of swell an error of about -5 cm, which is of course quite small.

Furthermore, when Challenor compares the new altimeter algorithm with buoy data including outliers it appears that above 2.5 metres wave height the new algorithm is overestimating (although the number of collocations is too small to make definite conclusions).

Finally, the Challenor proposal is based on a very limited wave height range, while in practice the wave height range extends to much higher waves. Note that high sea states are not necessarily strongly nonlinear (for example, it takes more than two days to get 10 m of wave height with a 20 m/s wind, so these states are fairly old and gentle). Therefore also in this case the probability distribution of the sea surface is fairly Gaus-

sian and the standard altimeter theory applies. It is only for young windseas, which are strongly nonlinear and which occur for short fetches or near the passage of a front, that considerable deviations from the Gaussian probability distribution occur and therefore corrections to the standard altimeter theory should be applied (Remark: for a wind speed of 20 m/s the strong nonlinear state occurs in the wave height range of two to 4 metres).

However, when the Challenor proposal is applied to cases where wave heights are of the order of 10 m a considerable increase in wave height is found of almost 2 metres. We have illustrated this in the Figs. 1 and 2 where for the month of December 1995 the current ESA ERS-2 algorithm and the Challenor proposal is compared with operational results from the WAM model first guess forced by ECMWF winds. Now it may be argued that the WAM model produces too low wave heights for the extreme cases, but this possibility may be excluded by inspecting Fig.3. In Fig.3 we compare analysed wave height with wave height observations from 25 selected buoys, evenly distributed over the Northern Hemisphere, for the period of December 1995 until March 1996. We have chosen such a long period in order to get a sufficient number of extreme states. Clearly the comparison with the buoy data shows that there is no need for a correction at 8 m by about 2 m. In fact a good agreement between model analysis and observations is found (rms=0.56,scatter index = 16%, the bias of -0.27 m is caused by the assimilation of ERS-1 altimeter data).

It should be pointed out that we have made sure that the selected buoys produce a (almost) continuous time series and that we have averaged the buoy data around the synoptic times within a time window of 6 hours in order to guarantee that we are comparing data which have similar spatial and temporal scales. Nevertheless, over a 4 month period over 12,000 collocations occur. A similar quality control is applied to the comparison of altimeter data with first-guess wave height.

To summarize, it is concluded that it is not a good idea to introduce the Challenor proposal for k1 and k2. First of all there are no scientific reasons why we should deviate so much from the standard altimeter algorithm. The seastate has most of the time a Gaussian probability distribution, and only for young seastates (which occur 10% of the time) deviations from the Gaussian state are to be expected. In order to incorporate effects of strong nonlinearity an extension of the standard altimeter algorithm is required. It therefore does not make sense to retune k1 and k2. Furthermore, comparison between on the one hand WAM model data with the Challenor algorithm and on the other hand buoy data and the WAM model data reveals that the Challenor algorithm gives serious problems for the extreme states. A similar remark applies to the discussion of the off-line products which suggests changes in the present ERS-2 algorithm of 15%.

It should therefore be clear that we are not at all happy with the proposed changes of the ERS-2 algorithm. In fact, we are quite content with the present algorithm and we have switched from ERS-1 to ERS-2 assimilation of wave height data as of Tuesday, april 30 1996.

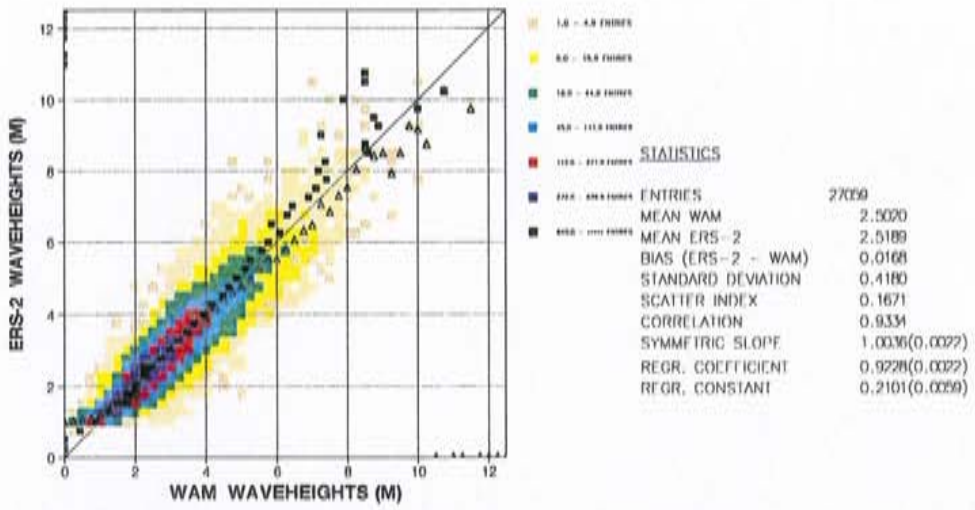

FIGURE 1. Comparison of ECMWF wave height results with ERS-2 radar altimeter wave height data for December 1995. No correction applied to the FDP data.

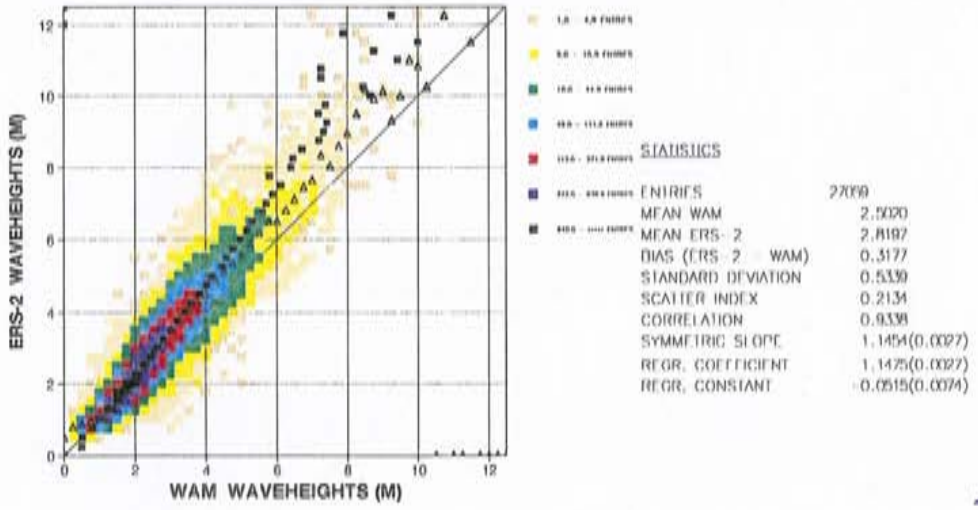

FIGURE 2. Comparison of ECMWF wave height results with ERS-2 radar altimeter wave height data for December 1995.
Correction proposed by Challenor applied.

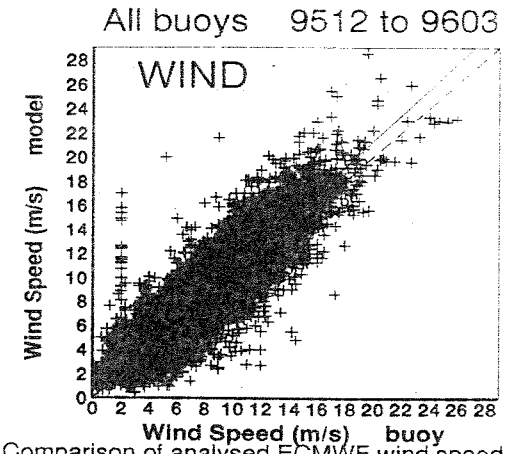

ENTRIES = 12293
MODEL MEAN = 8.653 STDEV = 3.749
BUOY MEAN = 8.189 STDEV = 3.396
LSQ FIT: SLOPE = 0.985 INTR = 0.583
RMSE = 1.753 BIAS = 0.464
CORR COEF = 0.893 SI = 0.206
SYMMETRIC SLOPE = 1.064

Comparison of analysed ECMWF wind speeds with averaged buoy data.

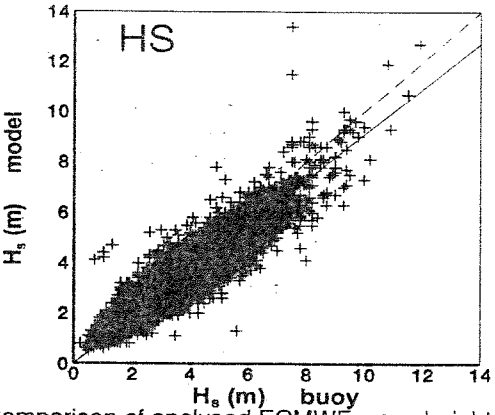

ENTRIES = 12634
MODEL MEAN = 2.818 STDEV = 1.256
BUOY MEAN = 3.087 STDEV = 1.413
LSQ FIT: SLOPE = 0.833 INTR = 0.245
RMSE = 0.564 BIAS = -0.270
CORR COEF = 0.938 SI = 0.161
SYMMETRIC SLOPE = 0.909

Comparison of analysed ECMWF wave heights with averaged buoy data.

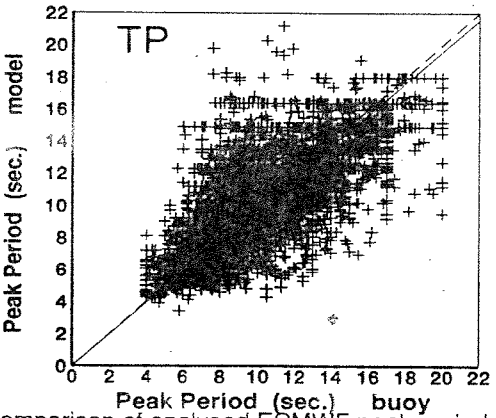

ENTRIES = 8957
MODEL MEAN = 10.131 STDEV = 2.738
BUOY MEAN = 10.304 STDEV = 2.931
LSQ FIT: SLOPE = 0.752 INTR = 2.381
RMSE = 1.788 BIAS = -0.174
CORR COEF = 0.805 SI = 0.173
SYMMETRIC SLOPE = 0.980

Comparison of analysed ECMWF peak periods with averaged buoy data.

FIGURE 3. Scatter diagram of buoy - model comparison for the period December 1995 to March 1996.

ANNEX I

- ECMWF Analysis of the QLRWD products.
- ECMWF Analysis of the second set of QLRWD products.
- ECMWF Analysis of corrected winds using URA FDP products

ECMWF Analysis of the QLRWD products

Björn Hansen - European Centre for Medium Range Weather Forecasts.

These are the results of the comparison of the wind speed data of the Quick-Look-Reprocessed-WinD products (QLRWD) with ECMWF's analysed surface wind speeds.

The QLRWD provided by Esrin covered one full cycle for the period 1. 12. 1995 0:00UT to 4.1.96 0:00UT. To compare with the previously performed analysis only the data of December 1995 have been considered (1,719,047 observations in total). The figures 1 and 2, showing the distributions of the backscatter coefficient (σ_0) and wind-speed, respectively, are provided for reference. Obvious already here is that many of the bins of the windspeed distribution are completely empty. This is not seen in the URA data. To further support this, figure 3 shows the retrieved windspeed as a function of the underlying backscatter coefficient for all windspeeds between 3.0 and 17.0 m/s from 1.12.1995 0UT to 1.12.1995 23:54 UT. At this point it is essential to understand why the QLRWD windspeed distribution shows these undesirable gaps. Unfortunately this has been discovered at the end of the analysis performed. Therefore all the material produced is presented now bearing in mind that the results might be wrong.

In order to apply all the processing steps of the existing quality control and collocating software the wind speed and σ_0 information of the QLRWD products had to be merged with the original URA FDP's. This left 1,016,831 observations for the subsequent steps. For many of the QLRWD data there was no corresponding observation in the URA products. But also for quite some URA observations no QLRWD observation was found. The produced new URA products were the analysed as described in the methods section of the draft cwg-report. Figures 4 to 7 show again the distribution of σ_0 and windspeed data after quality control. On average we now have 11.11dB instead of 11.25dB for σ_0 and in turn the mean windspeed has changed from 6.77m/s to 7.11m/s.

When comparing these reprocessed and quality controlled winds with model results we find that the bias has reduced from -0.82m/s to -0.42m/s while all other statistical parameters remained the same. Figures 8 and 9 show the corresponding scatter diagrams. The bias between QLRWD and Model is now in better agreement with what is found when comparing ERS-1 and model results (-0.31m/s, figure 10).

Until the open question regarding the empty bins in the windspeed distribution is resolved we are reluctant to draw firm conclusions at this point, but we don't expect that the statistics will change much once the binning problem is resolved. The preliminary conclusion is, that the QLRWD wind speeds agree better than the original URA FDP winds with the ECMWF model results and that the proposed change should be applied.

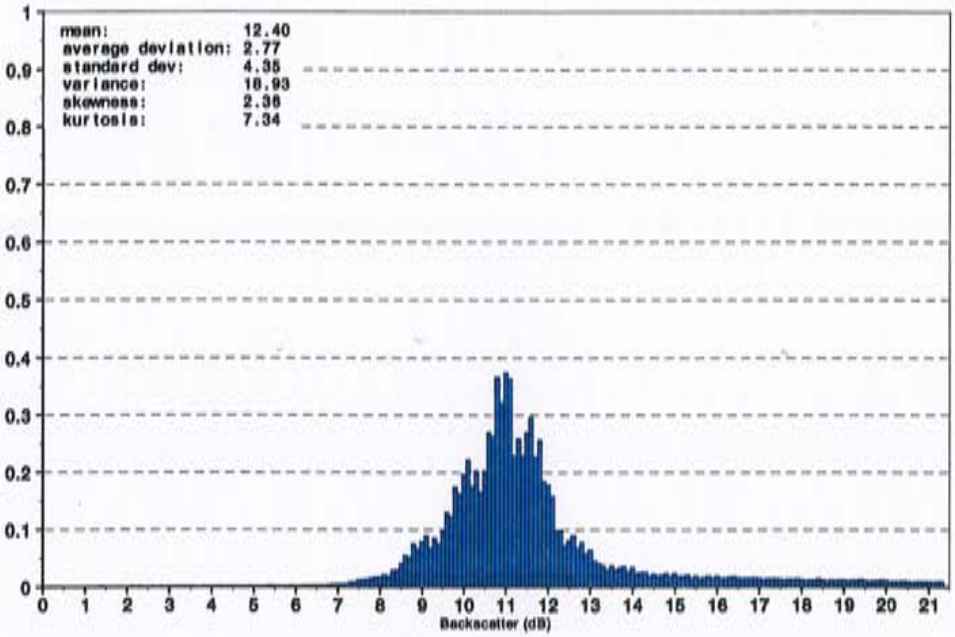

FIGURE 1. QLRWD: σ_0 - distribution of ERS-2 radar altimeter for December 1995.
1,719,047 observations without any quality control.

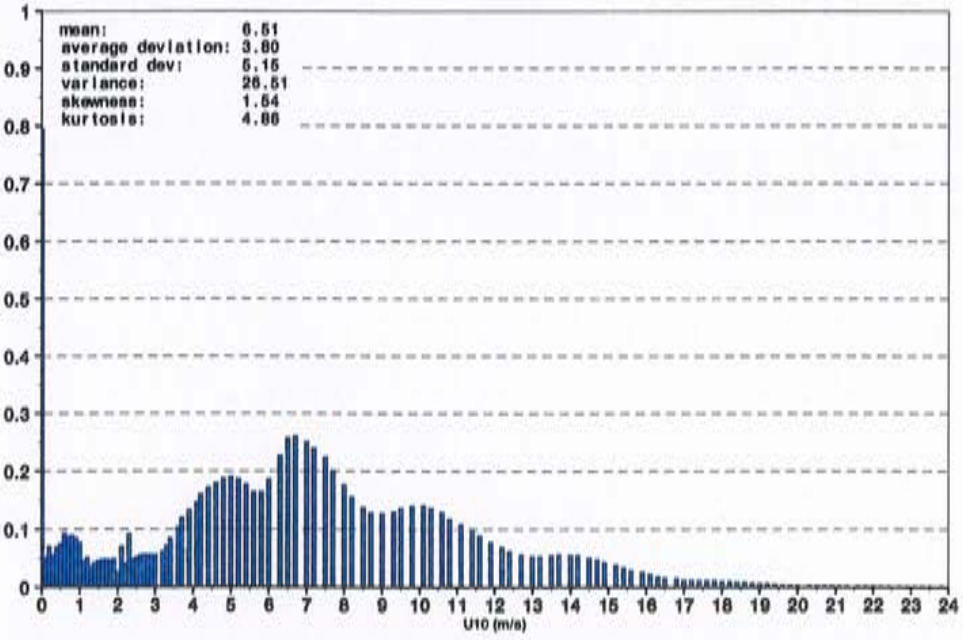

FIGURE 2. QLRWD: Windspeed - distribution of ERS-2 radar altimeter for December 1995.
1,719,047 observations without any quality control.

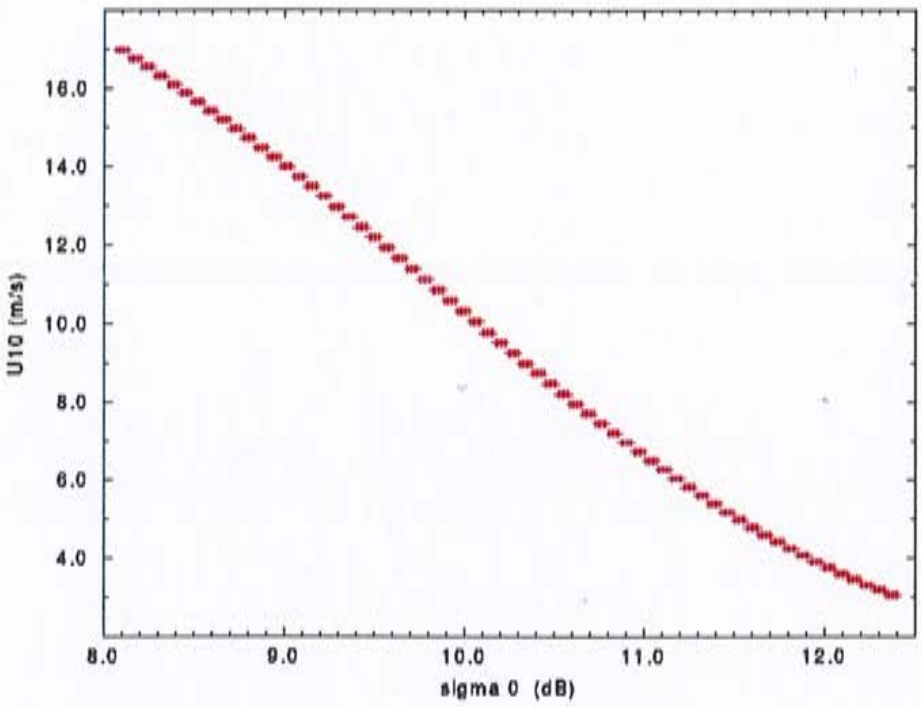

FIGURE 3. Quick Look Reprocessed ERS-2 Winds versus σ_0.
1.12.1995 0:00 to 23:55, windspeed range selected: 3.0 to 17.0 m/s.

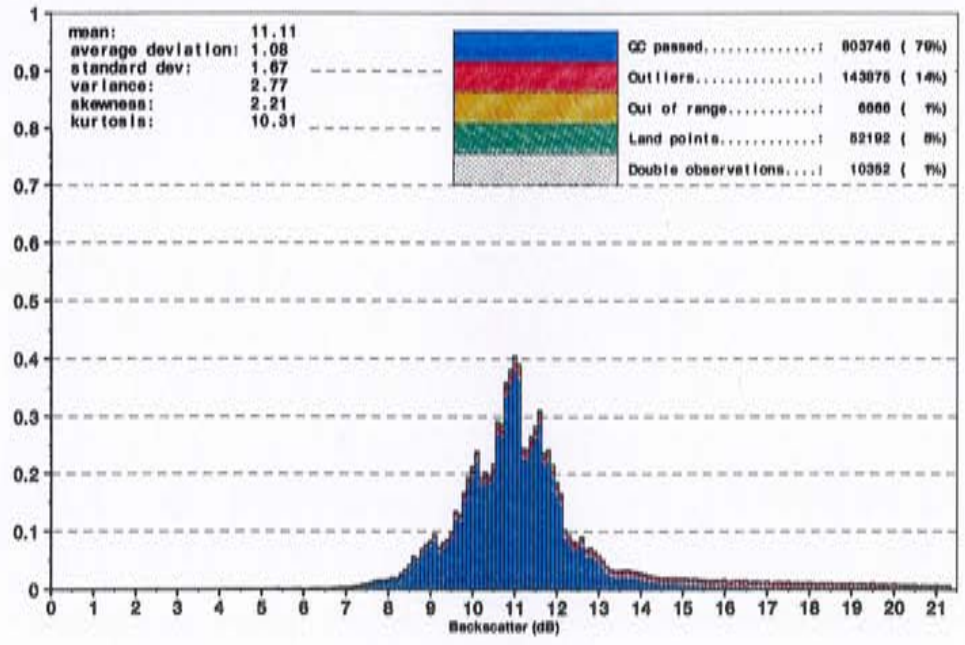

FIGURE 4. QLRWD: σ_0 - distribution of ERS-2 radar altimeter for December 1995.
1,016,831 observations after merge with URA FDP and quality control

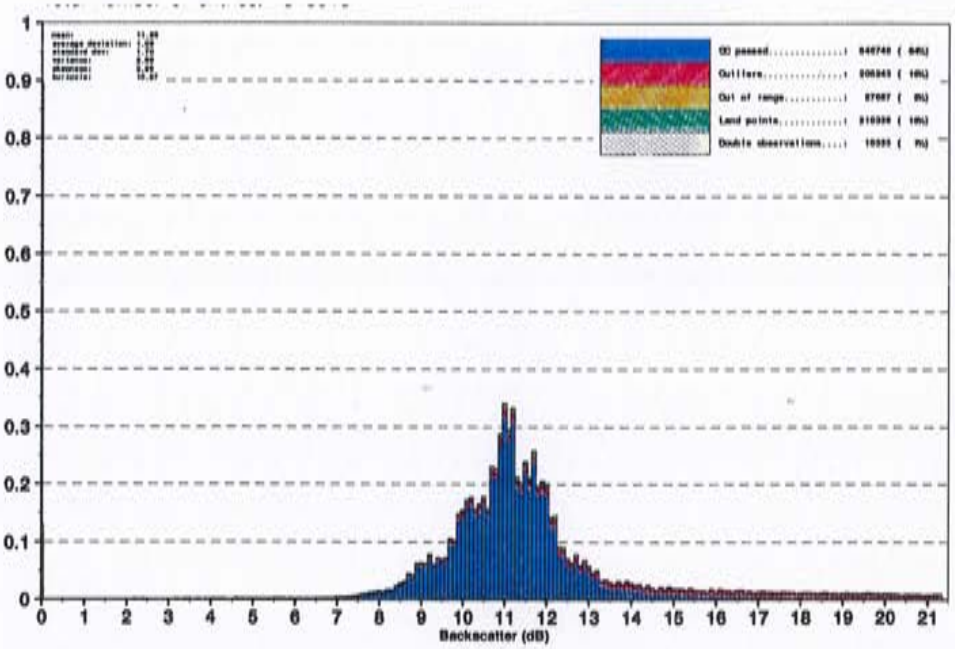

FIGURE 5. σ_0 - distribution of ERS-2 radar altimeter for December 1995.
Data from URA FDP's.

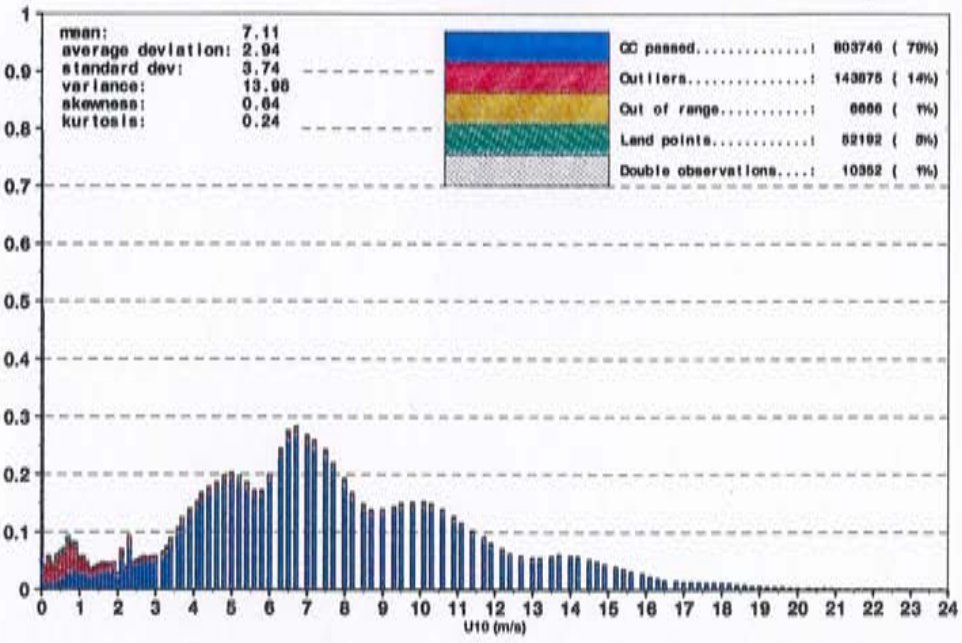

FIGURE 6. QLRWD: Windspeed distribution of ERS-2 radar altimeter for December 1995.

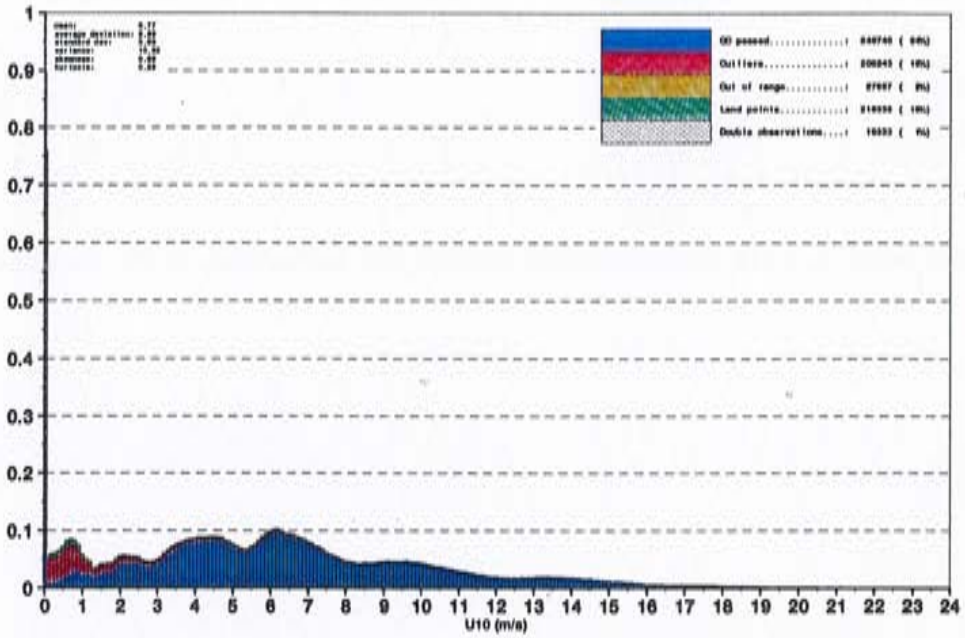

FIGURE 7. Windspeed - distribution of ERS-2 radar altimeter for December 1995.
Data from URA FDP's.

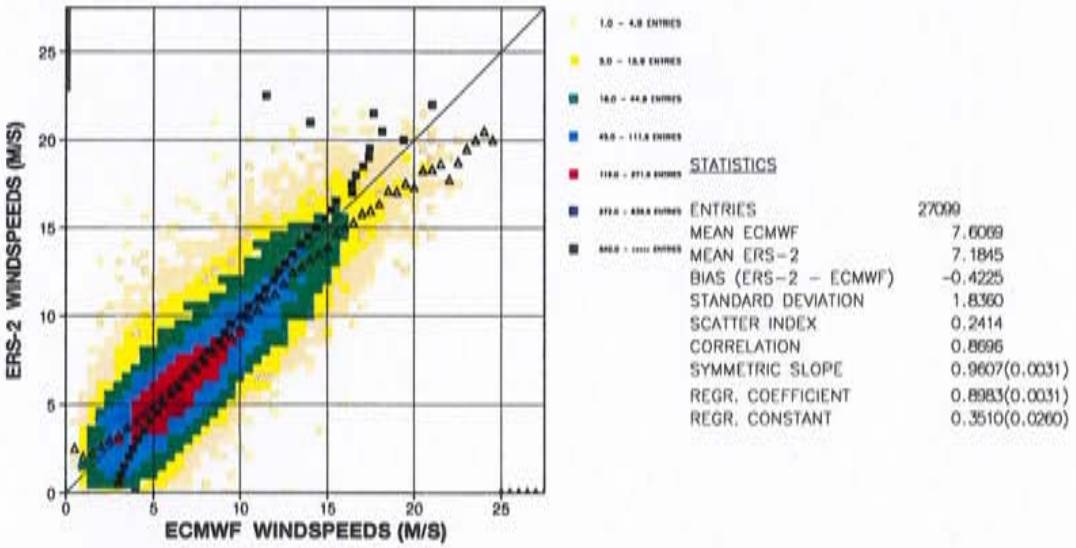

FIGURE 8. QLRWD: Comparison of ECMWF wind speed results with ERS-2 radar altimeter wind speed data for December 1995.
The squares denote the mean values in the x-direction and the triangles in the y-direction The standard error is shown in brackets.

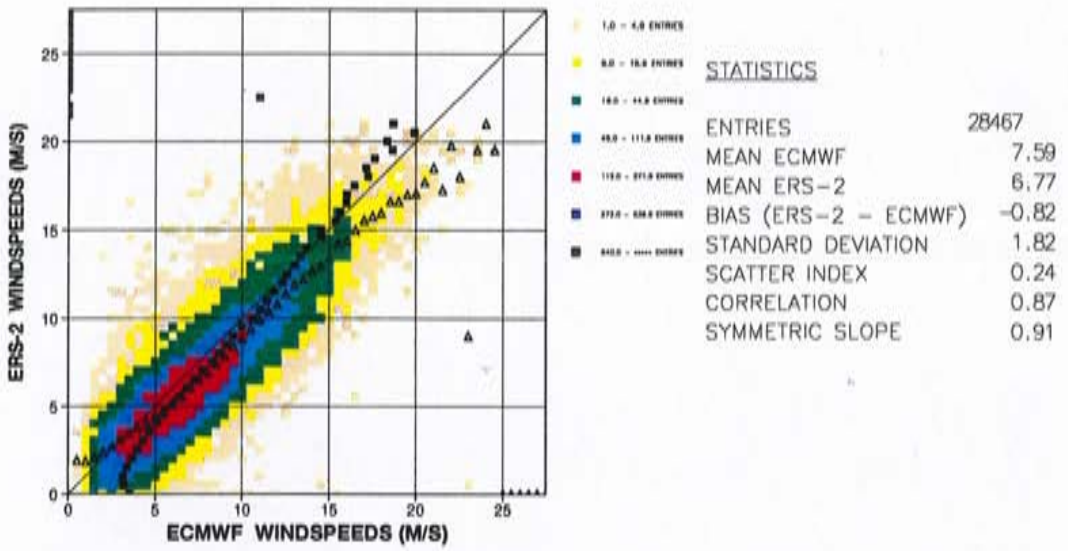

FIGURE 9. Comparison of ECMWF wind speed results with ERS-2 radar altimeter wind speed data for December 1995.

Data from URA FDP's.

The squares denote the mean values in the x-direction and the triangles in the y-direction The standard error is shown in brackets.

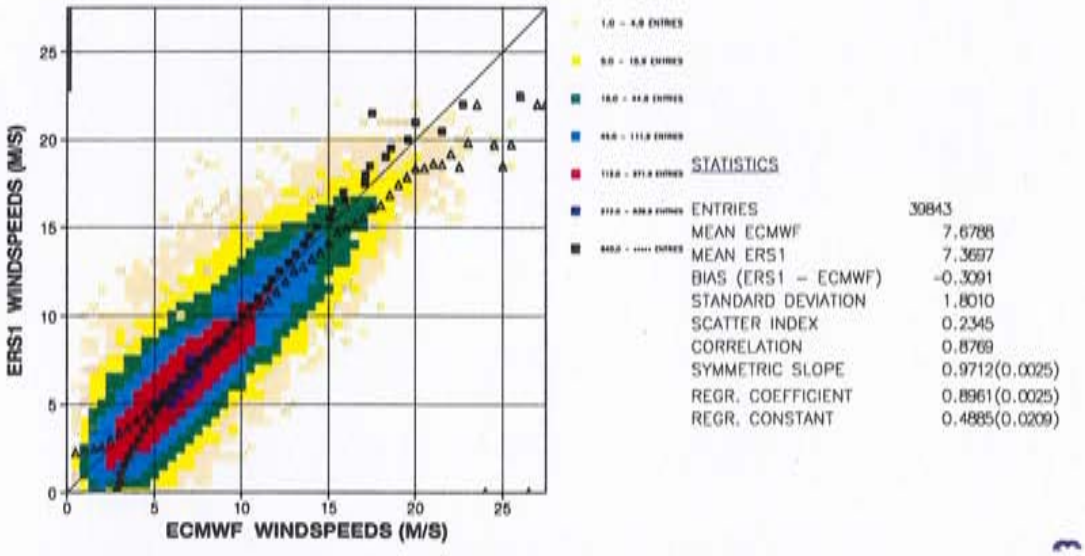

FIGURE 10. Comparison of ECMWF wind speed results with ERS-1 radar altimeter wind speed data for December 1995.

The squares denote the mean values in the x-direction and the triangles in the y-direction The standard error is shown in brackets.

ECMWF Analysis of the second set of QLRWD products

Björn Hansen - European Centre for Medium Range Weather Forecasts.

This report presents the results of the comparison of the wind speed data of the second set of Quick-Look-Reprocessed-WinD products (QLRWD) with ECMWF's analysed surface wind speeds. The first set was created with backscatter coefficients (σ_0) reduced by 0.12 and subsequently using a nearest neighbour - scheme to recalculate the 10m surface wind speeds (U_{10}). According to D. Cotton the applied correction was probably too small. Therefore a second set was created by ESRIN with σ_0 reduced by 0.16. Furthermore an interpolation scheme instead of the nearest neighbour scheme was used to recalculate U_{10} . The period and the amount of data are the same as for the first set.

With the new scheme there are no empty bins in the histograms any more but there are still some bins systematically shorter than their neighbours (figures 1 and 2). The reason for this is visible when plotting U_{10} as a function of σ_0 (figure 3, the data from the first set are also shown for reference). The picture found is not quite what one would expect. It still looks to a certain extend discrete and also some outliers can be found. The limited precision used for transferring the data from Esrin to ECMWF (0.01 m/s and 0.01 dB) cannot be used to explain this.

The method to compare the QLRWD data with model results is the same as described in the first report.

No significant changes in the overall statistics have been found. Figures 4 to 7 show again the distribution of σ_0 and windspeed data after quality control. On average we now have 11.07dB instead of 11.25dB for σ_0 and in turn the mean windspeed has changed from 6.77m/s to 7.30m/s.

When comparing these reprocessed and quality controlled winds with model results we find that the bias has reduced from -0.82m/s to -0.42m/s while all other statistical parameters remained the same. Figures 8 and 9 show the corresponding scatter diagrams. The bias between QLRWD and Model is still in better agreement with what is found when comparing ERS-1 and model results (-0.31m/s, figure 10).

Since there are no changes to the statistics our conclusion remains the same as before and it is recommended to apply the proposed correction to the σ_0 to produce winds of higher quality.

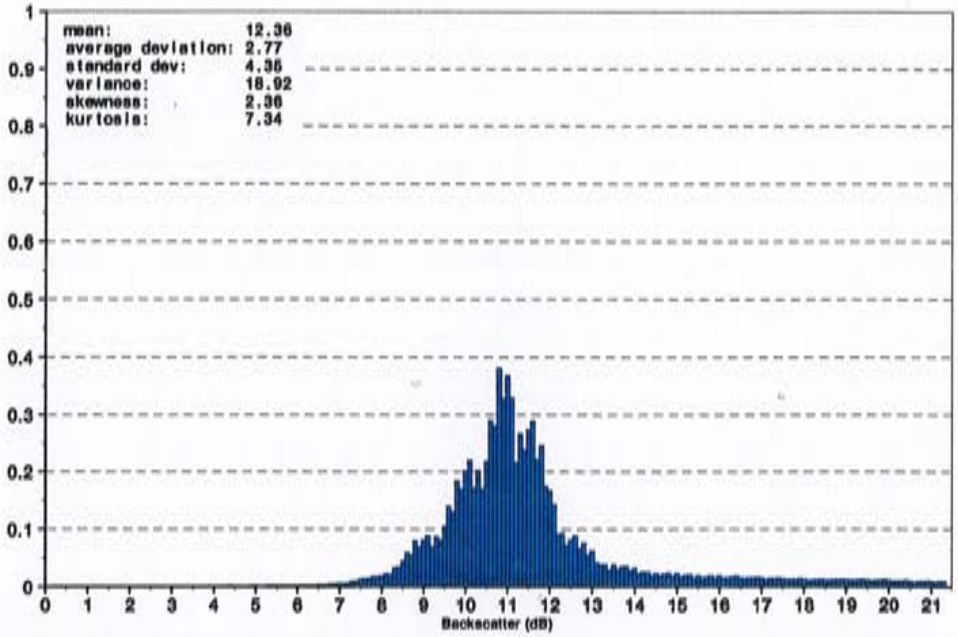

FIGURE 1. QLRWD: σ_0 - distribution of ERS-2 radar altimeter for December 1995.
1,719,047 observations without any quality control.

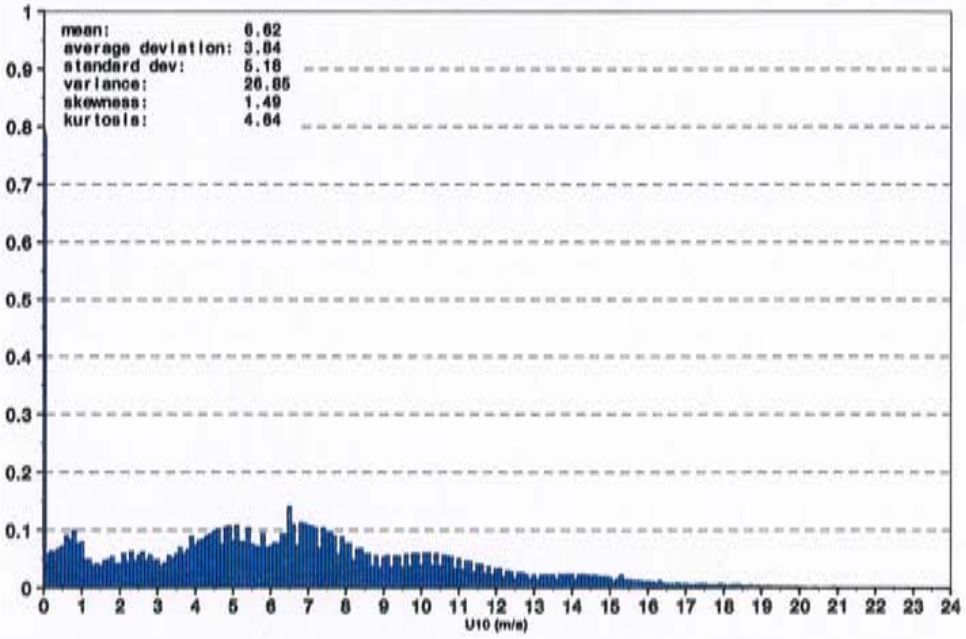

FIGURE 2. QLRWD: Windspeed - distribution of ERS-2 radar altimeter for December 1995.
1,719,047 observations without any quality control.

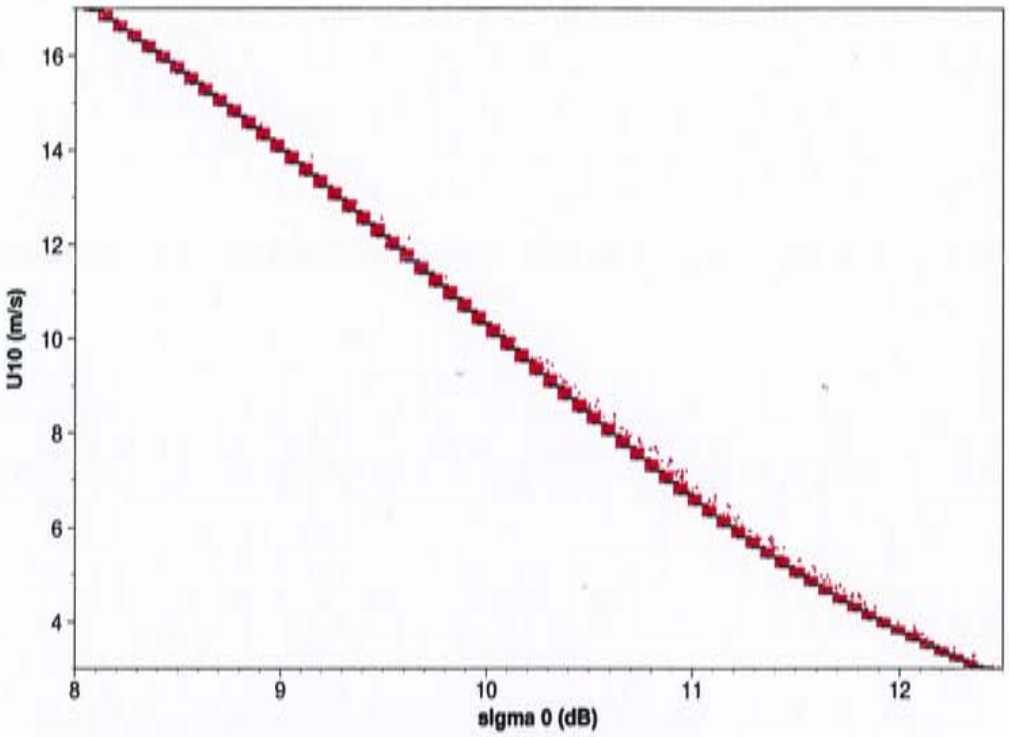

FIGURE 3. Quick Look Reprocessed ERS-2 Winds versus σ_0.
1.12.1995 0:00 to 23:55, windspeed range selected: 3.0 to 17.0 m/s.
red: second set of QLRWD, black: first set of QLRWD

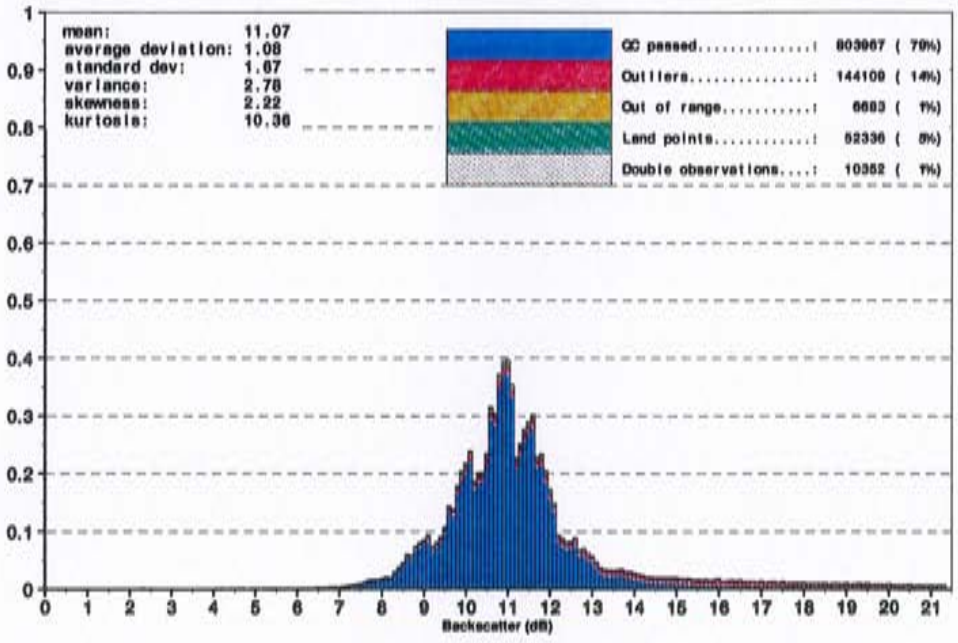

FIGURE 4. QLRWD: σ_0 - distribution of ERS-2 radar altimeter for December 1995.
1,016,831 observations after merge with URA FDP and quality control

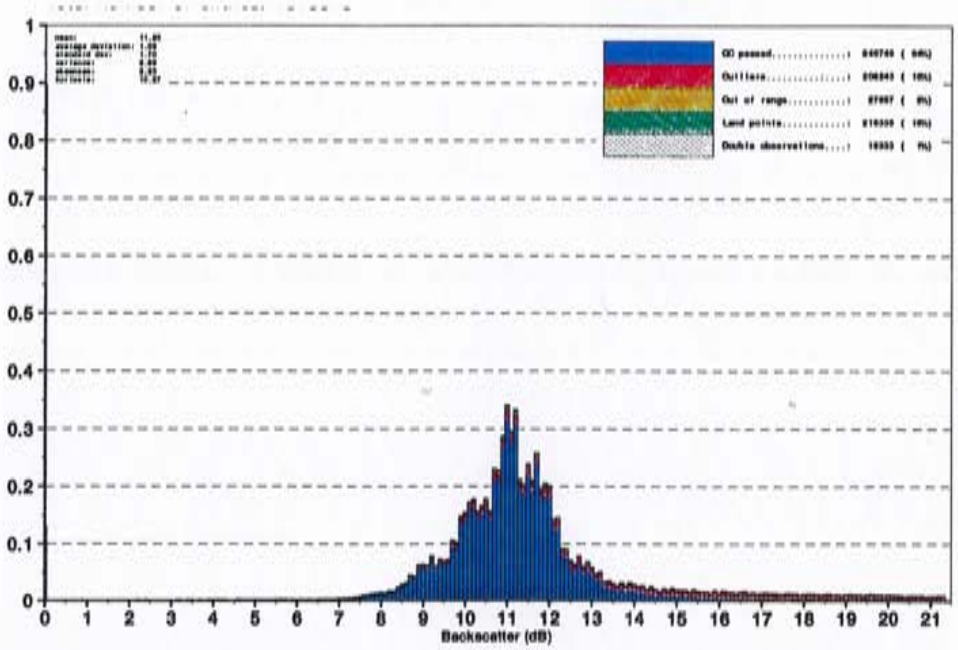

FIGURE 5. σ_0 - distribution of ERS-2 radar altimeter for December 1995.
Data from URA FDP's.

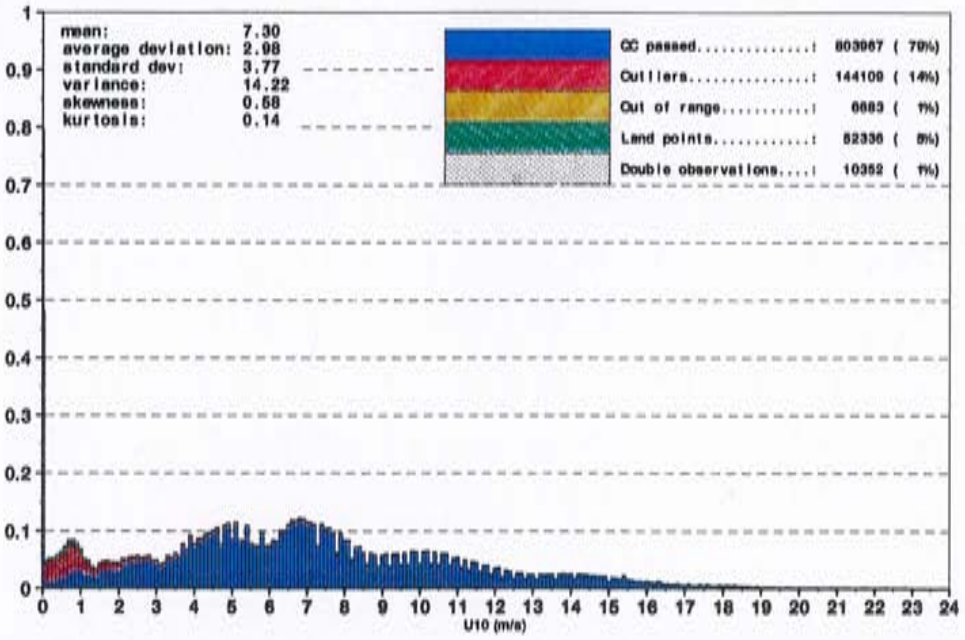

FIGURE 6. QLRWD: Windspeed distribution of ERS-2 radar altimeter for December 1995.

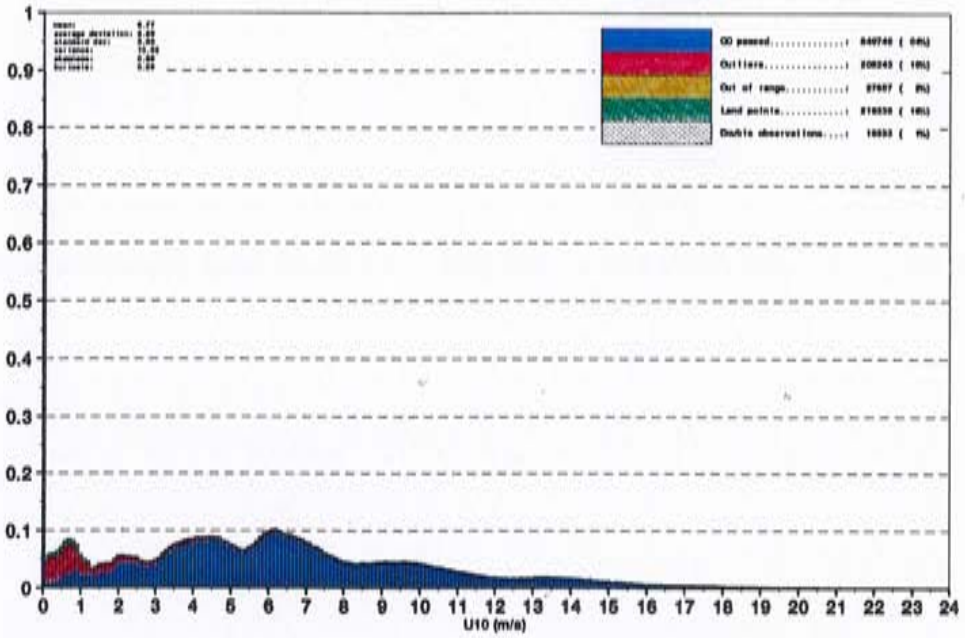

FIGURE 7. Windspeed - distribution of ERS-2 radar altimeter for December 1995.
Data from URA FDP's.

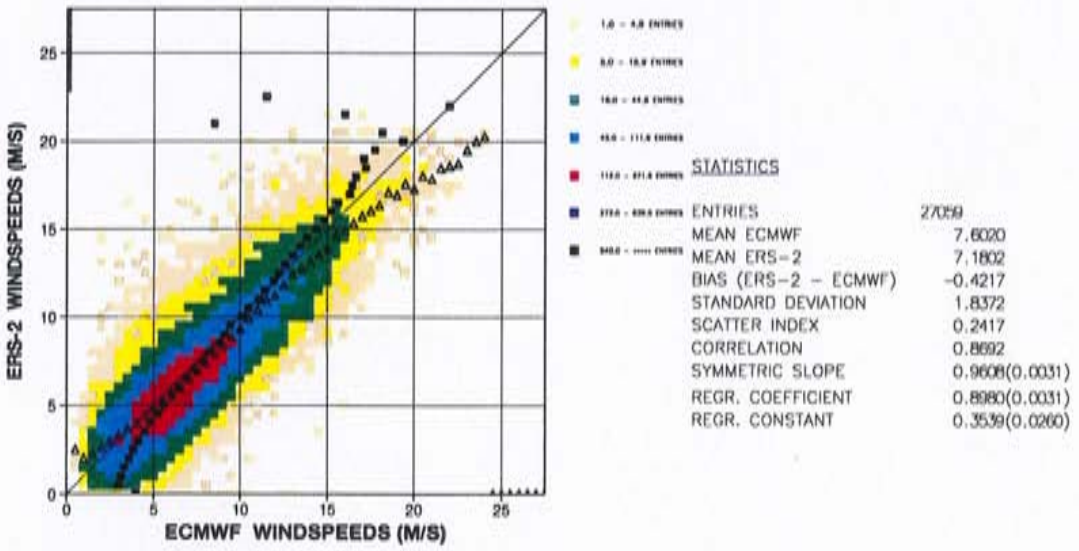

FIGURE 8. QLRWD: Comparison of ECMWF wind speed results with ERS-2 radar altimeter wind speed data for December 1995.
The squares denote the mean values in the x-direction and the triangles in the y-direction The standard error is shown in brackets.

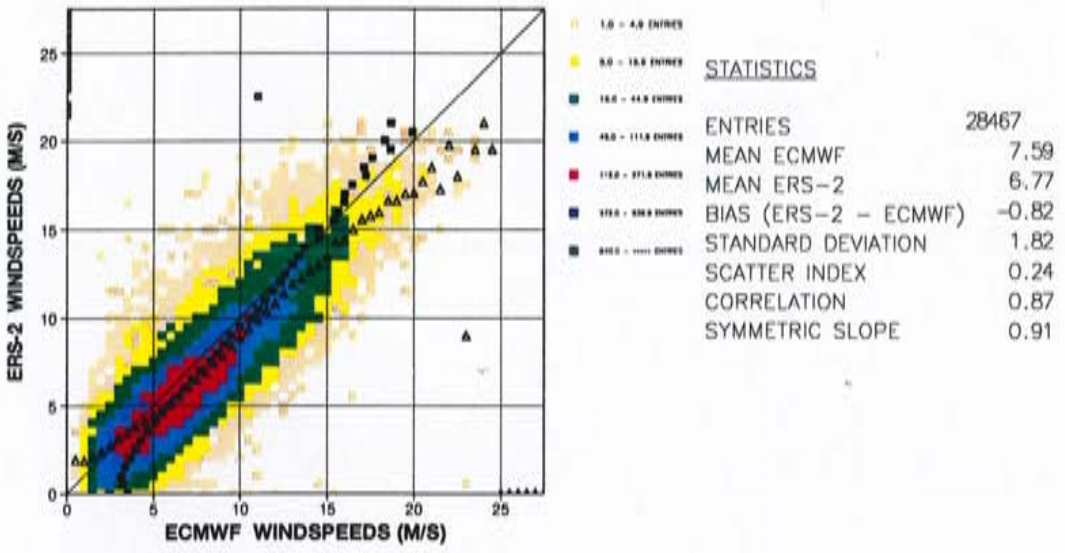

FIGURE 9. Comparison of ECMWF wind speed results with ERS-2 radar altimeter wind speed data for December 1995.

Data from URA FDP's.

The squares denote the mean values in the x-direction and the triangles in the y-direction The standard error is shown in brackets.

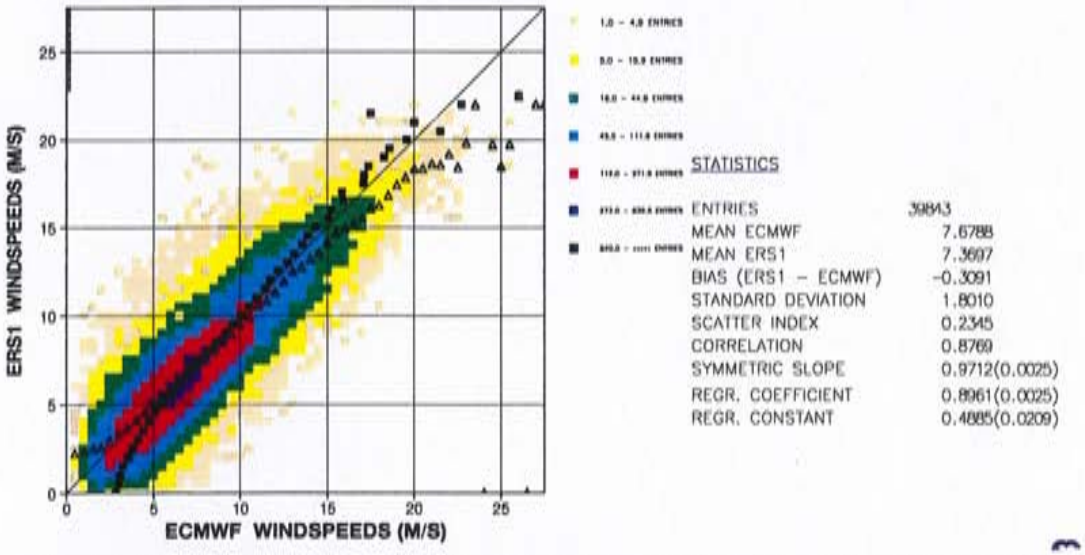

FIGURE 10. Comparison of ECMWF wind speed results with ERS-1 radar altimeter wind speed data for December 1995.

The squares denote the mean values in the x-direction and the triangles in the y-direction The standard error is shown in brackets.

ECMWF Analysis of corrected winds using URA FDP products.

Björn Hansen - European Centre for Medium Range Weather Forecasts.

In the following the impact of a bias correction of -0.16dB to the backscatter coefficient (σ_0) on the computed surface winds (U_{10}) within the fast delivery products from ERS-2 is presented.

The dataset used was the original ERS-2 fast delivery product URA for the period 1.12.1995 3:00UTC to 1.1.1996 3:00UTC. Before applying the standard quality control as described earlier a correction of -0.16dB was applied to σ_0 and the surface wind speeds supplied were replaced with interpolated wind speeds using a look-up table provided by ESRIN.

Earlier studies showed discontinuities and non-uniformities of U_{10} versus σ_0. These have disappeared (Fig.1). But when examining the distribution of the corrected and quality controlled wind speed data (Fig.2), there are still bins systematically smaller than others, which we also saw in the earlier studies, but here it is purely the result of the limited precision of the σ_0 data within the FDP, which is 1/100 dB.

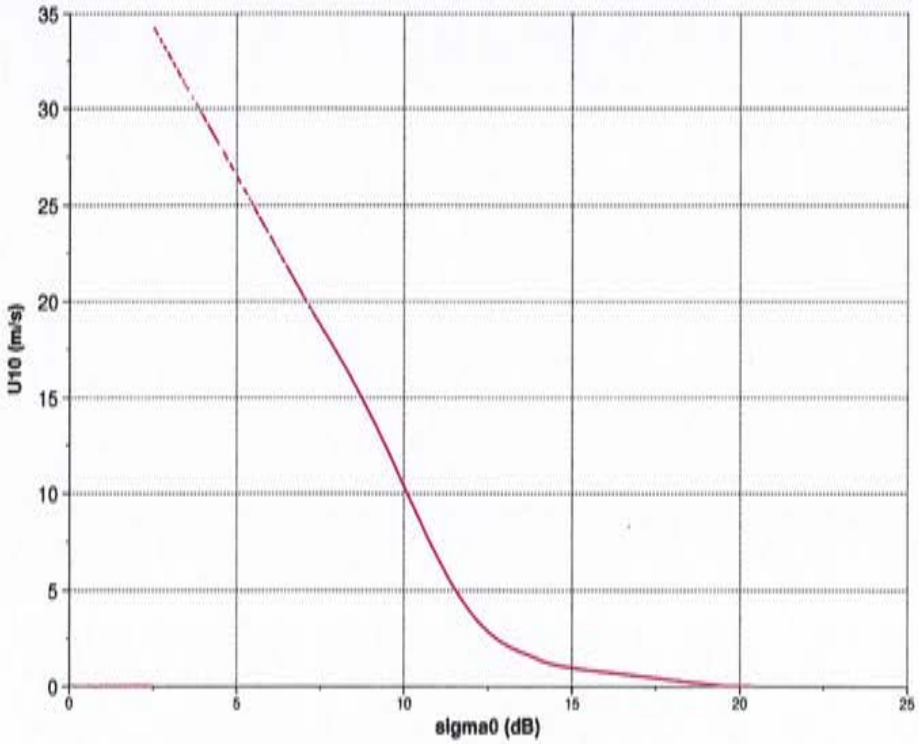

FIGURE 1. Reprocessed ERS-2 URA FDP Winds versus σ_0.
1.12.1995 15:00UTC to 21:00UTC, windspeed range selected: 0.0 to 35.0 m/s.

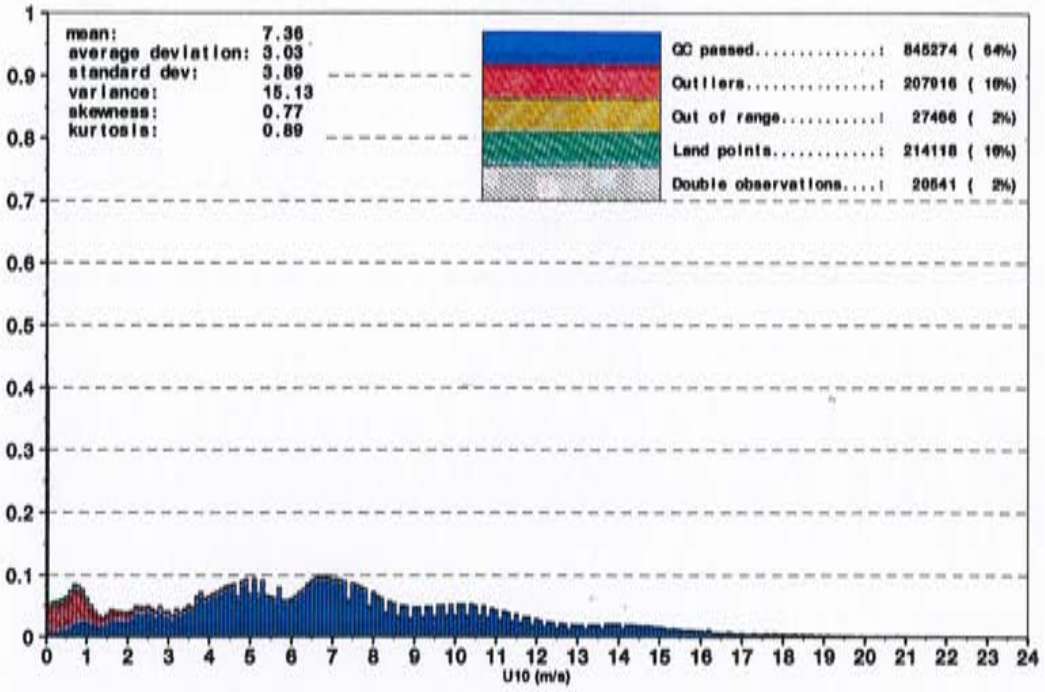

FIGURE 2. Reprocessed ERS-2 URA FDP Winds for December 1995.
Correction of -0.16dB applied to URA FDP σ_0 and winds updated using look-up table

The method to compare the reprocessed wind data with model results is the same as described in the first report.

The reprocessed winds are biased low by 0.26m/s witch reduces the bias of the uncorrected winds by 0.56m/s and the average wind speed is now 7.42m/s (Figs. 3 and 4). When we compare model results with ERS-1 wind speeds we find ERS-1 biased low by 0.31m/s.

From the least squares regression we now find that:

$$U_{10_{ers2}} = 0.998 \times U_{10_{ers1}} + 0.064$$

and from the symmetric regression:

$$U_{10_{ers2}} = 1.007 \times U_{10_{ers1}}$$

The results show that if a correction of -0.16dB is applied to ERS-2-σ_0 ESR-2 winds will match ERS-1 winds very well. It is therefore recommended to apply the proposed correction to σ_0 to produce winds of the same quality as ERS-1.

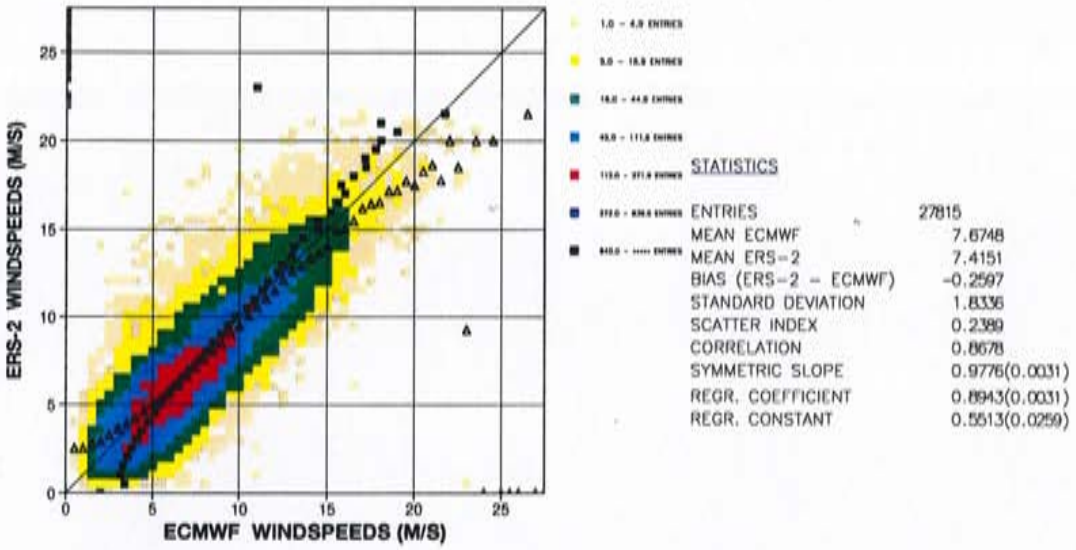

FIGURE 3. Comparison of ECMWF wind speed results with corrected ERS-2 radar altimeter wind speed data for December 1995.

Correction of -0.16dB applied to URA FDP σ_0 and winds updated using look-up table.
The squares denote the mean values in the x-direction and the triangles in the y-direction The standard error is shown in brackets.

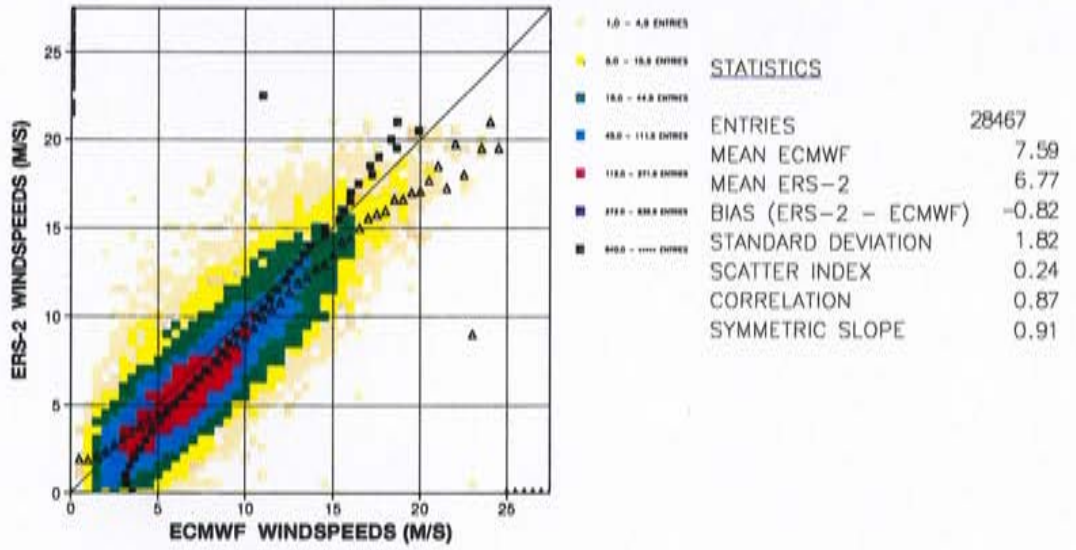

FIGURE 4. Comparison of ECMWF wind speed results with ERS-2 radar altimeter wind speed data for December 1995.

Data from URA FDP's.
The squares denote the mean values in the x-direction and the triangles in the y-direction The standard error is shown in brackets.

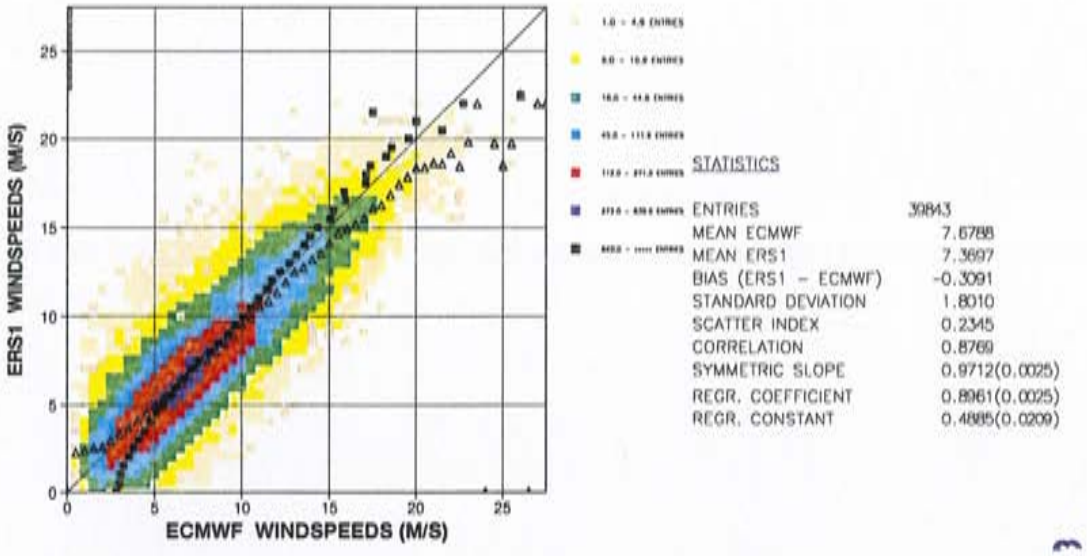

FIGURE 5. Comparison of ECMWF wind speed results with ERS-1 radar altimeter wind speed data for December 1995.

The squares denote the mean values in the x-direction and the triangles in the y-direction The standard error is shown in brackets.

ANNEX J

- Sea state dependence of alimeter wave height retrieval.

VALIDATION OF ERS SATELLITE WAVE PRODUCTS WITH THE WAM MODEL

P A E M Janssen, B Hansen and J Bidlot

European Centre for Medium-range Weather Forecasts,
Shinfield Park, Reading RG2 9AX, UK

Abstract

A brief summary of the ECMWF validation effort of the ERS satellite wave products is presented. Using the WAM spectra (Ref. 1) as first-guess SAR spectra from the AMI in wave mode have been inverted on a routine basis and the resulting significant wave height has been compared against modelled wave height. First comparisons suggested that the significant wave height from the SAR was too large especially for high waves. A modification to the SAR inversion algorithm (Ref. 2-3) resulted in a closer agreement between SAR and modelled wave height and has increased confidence in the usefulness of SAR image data in a real time data assimilation system. An extensive effort has been performed to validate the ERS Radar Altimeter wind and wave products. Regarding ERS-1 validation, after some debugging of the ground station software and a retuning of sigma0, comparisons of the Radar wind and wave product with ECMWF wind and wave fields suggested that the Radar Altimeter winds and waves were reliable. Although it was known that the Altimeter wave heights were too low by 10-15% ECMWF decided to assimilate this product in the WAM wave model from August 1993. The validation of the ERS-2 Altimeter wind and wave product was made easier because ERS-2 operated in tandem with ERS-1. Using the WAM model results as a reference standard it could be shown that ERS-2 wave heights were 8% higher than ERS-1 wave heights. Assimilation of ERS-2 wave heights into the ECMWF wave forecasting system therefore had a beneficial impact on the wave analysis as followed from comparisons of analysed wave height with buoy data. Finally, evidence is presented that the underestimation of wave height by the Altimeter occurs for steep wind waves and not necessarily for extreme wave height. This agrees with the theory of Altimeter wave height retrieval which is only valid for waves with a small steepness.

1. INTRODUCTION

The necessary calibration/validation of a satellite sensor requires large amounts of ground truth data which should cover the full range of possible events. In particular the number of reliable wave measurements is very limited and because of financial restrictions dedicated field experiments are only possible at a few sites. In contrast to that model data are cheap and provide global data sets for comparison. Therefore the combination of both in-situ observations and model data seems to be an optimal cal/val data set.

Before model data can be used for validation purposes, it must be shown that the performance of the WAM model(Ref. 1) is reliable. An extensive validation study of the quality of the analyses and forecasts of the ECMWF wave forecasting system (Ref. 4) shows the good quality of both ECMWF surface winds and ocean waves. In Section 2 we show additional verification scores which are relevant for the validation of the satellite wave products.

We next describe our validation efforts of the Synthetic Aperture Radar (SAR) wave spectra in Section 3. Using WAM spectra as first-guess, SAR spectra from the AMI in wave mode have been inverted by means of the Hasselmann & Hasselmann(Ref. 2) inversion algorithm. Comparison of the SAR wave height with modelled wave height revealed a considerable overestimation by the SAR but when Hasselmann et al (Ref. 3) improved the SAR retrieval algorithm the discrepancies disappeared.

In Section 4 an overview is given of the validation efforts of the Radar Altimeter wind and wave products. We start with briefly describing our contribution to the validation of the ERS-1 and ERS-2 Altimeter wind and wave products. We also discuss examples of the use of the Altimeter data. For example, Altimeter wave height data have been assimilated in our wave forecasting system since August 1993 and by comparison of the analysed wave height with buoy data we have observed a considerable improvement when we

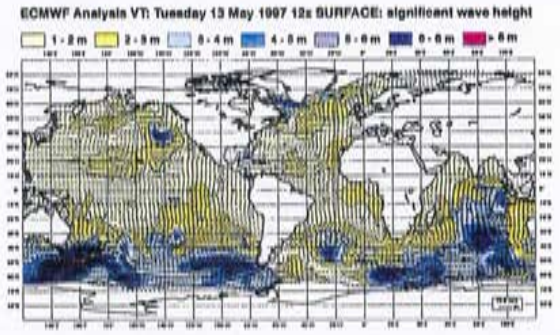

Fig.1: An example of a global significant wave height map. Mean wave directions are shown as well.

switched from ERS-1 to ERS-2 data. We do not use the Altimeter wind speeds in our data assimilation system and since they are independent we use these data for global validation of changes in the atmospheric forecasting system. The Altimeter wind speed data proved to be invaluable in showing that the ERS scatterometer data had a positive impact on the analysis of the weather over the southern Oceans.

The Altimeter wave height retrieval algorithm is based on first principles. Nevertheless, the joint probability distribution of surface elevation and slope is assumed to be given by the Gaussian distribution, an assumption which is only valid for small wave slope. For steep waves, which usually occur for young wind sea, one would therefore expect that the Altimeter wave height retrieval is less satisfactory, and in Section 5 we present

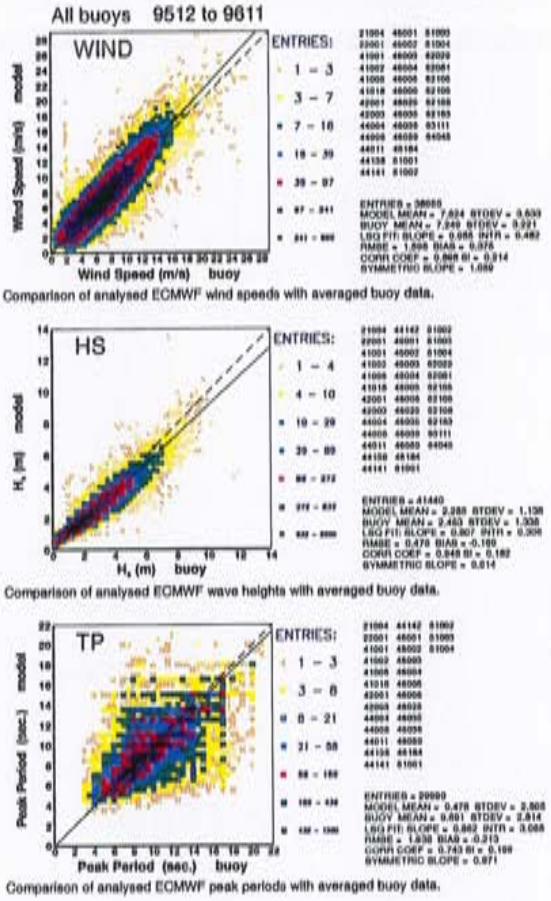

Comparison of analysed ECMWF wind speeds with averaged buoy data.

Comparison of analysed ECMWF wave heights with averaged buoy data.

Comparison of analysed ECMWF peak periods with averaged buoy data.

Fig.2: Comparison of analysed wind speed, wave height and peak period with averaged buoy data over the period of December 1995 until November 1996.

evidence for this based on a detailed comparison of modelled wave height and Altimeter wave height.

Finally, in Section 6 we present our conclusions.

2. THE ECMWF WAVE FORECASTING SYSTEM

Since July 1992 cycle 4 of the WAM model has been running operationally at ECMWF, It has been implemented on the globe with a current resolution of 55 km and on the Mediterranean and Baltic Sea with a resolution of 0.25 deg. Following a one day analysis, which uses analysed ECMWF wind fields and ERS Altimeter wave height data, a 10-day forecast is issued once a day.

Integrated parameters such as significant wave height, mean wave period and mean wave direction (for total sea, windsea and swell) are disseminated once a day to the ECMWF member states involved in the wave project. Furthermore, ECMWF archives all integrated parameters for the analysis and forecast every 6 hours, while also the 12Z analysed two-dimensional wave spectra are stored. In addition, monthly means have been archived since January 1995. An example of a wave height field that may be retrieved is presented in Fig.1

An extensive verification of the wave forecasting system has recently been carried out (Ref. 4) and shows the net improvement of the system over the years to an extent that we have an improved confidence in the model analysis and forecast results. Fig.2 shows scatter diagrams of the comparison between analysed wind speed, wave height and peak period against buoy observations over a one year period. In order to match with the spatial scales of the model, which had during this period a resolution of 1.5 deg, buoy observations have been averaged over a

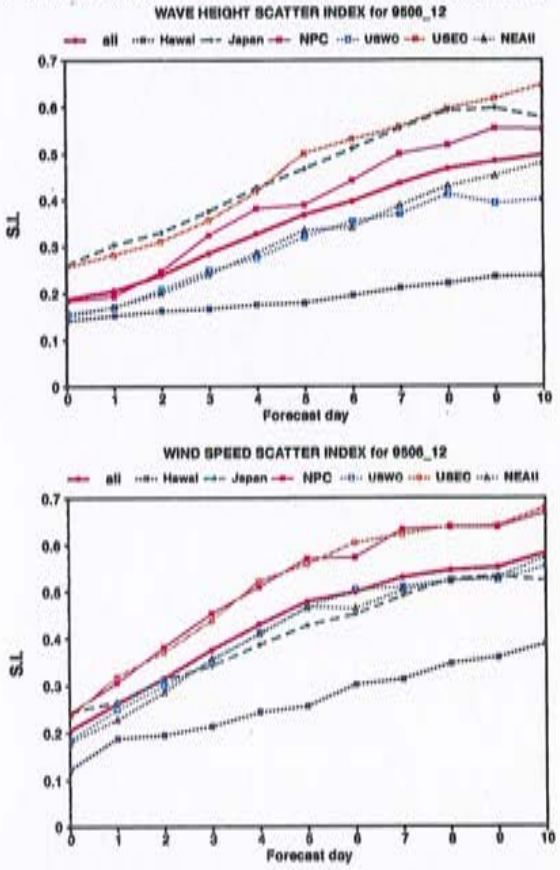

Fig.3: Verification of wave and wind forecast against buoy data for the period of June until December 1995.

6 hour period centred around the synoptic times, whilst we only selected buoys which reported observations fairly continuous enabling quality control of the observations. Regarding the wind speed comparison it is noted that analysed wind speed is too high by 6%. This apparent over prediction is caused by the fact that buoys report winds at a height of on average 5 m whilst the model

wind refers to the standard height of 10 m. This height difference may give rise to relative differences of about 10%. The analysed waveheight is too low by 9 % and the analysed peak frequency shows hardly no bias. As will be discussed in Section 4 an important reason for the too low analysed wave height is the under estimation of wave height by the Radar Altimeter.

In Fig. 3 we show the verification of wave and wind forecast against buoy data for a period of 6 months in 1995. The quantity we show is the so-called scatter index(S.I.) which is the ratio of standard deviation of the difference and the mean observed wave height. The line styles refer to different areas on the globe and clearly these areas have different characteristics of error growth. In swell dominated areas such as Hawaii there is hardly no error growth over the 10 day period whereas in areas where significant wind-wave growth occurs (e.g. North Pacific and the North-east Atlantic) the scatter index more than doubles over the forecast period. It is also of interest to note that during the first two days error growth for wave height is slower than for wind speed. The reason for this is that the sea state consists of a mixture of wind sea and swell and only the wind sea part is affected by the errors in wind forcing. Beyond day 2 errors in wind sea dominate and the wave height then shows similar error growth as the wind speed.

We conclude that the ECMWF wave forecasting system produces reliable results and therefore may be of use in validating satellite wave products.

3. VALIDATION OF SAR SPECTRA

Since 1991 observed two-dimensional wave spectra from SAR wave mode images have been produced on a routine basis at ECMWF. The inversion of the SAR image spectrum is based on the Hasselmann and Hasselmann (Ref. 2) relation for the mapping of the surface wave spectrum into the SAR image spectrum. This nonlinear mapping relation needs to be inverted and the inversion method minimises a cost function representing the error between the observed and computed SAR image spectrum. The inversion is not unique because of the 180 deg directional ambiguity inherent in the frozen image spectrum and the loss of information beyond the azimuthal cut-off of the SAR. To remove this indeterminacy an additional term is added to the cost function which penalises deviations from a first-guess wave spectrum. For an overview of this problem see Ref. 1.

The inversion at ECMWF is performed by using the WAM model wave spectrum at the location of the SAR image spectrum as a first-guess. Comparison of the significant wave height from the SAR spectrum with modelled wave heights from the WAM model suggested that SAR wave heights were much larger(Ref.5, see also Ref. 1). This is illustrated in Fig.4a where we show a scatter diagram of the comparison between SAR wave

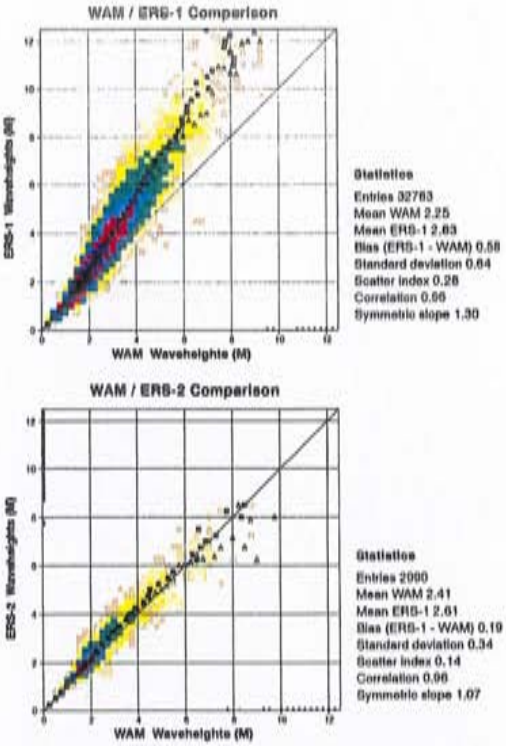

Fig.4: Comparison of SAR wave height and first-guess wave height before (top) and after (bottom) improving the SAR inversion scheme.

height and WAM wave height for the month of October 1995. Since the WAM model is in reasonable agreement with buoy observations (and also with the Altimeter wave heights) it was concluded that SAR wave heights were too high. Recent improvements in the SAR retrieval algorithm (Ref. 3) have resulted in a much closer agreement between SAR wave height and WAM wave height as is shown in Fig. 4b. This has led to increased confidence in the use of SAR image data in a real time data assimilation system. While the use of the original algorithm would have led to considerable inconsistencies with for example the Altimeter wave height the new algorithm has much improved in this respect.

The use of SAR data in wave data assimilation seems therefore promising, in particular because compared to Altimeter wave height data it contains much more relevant information regarding the sea state. At ECMWF work in this direction is in progress.

4. VALIDATION OF ERS RADAR ALTIMETER WIND AND WAVE PRODUCTS

As described by Hansen and Guenther (Ref. 6) the Altimeter wind and wave data first pass a quality control program that checks the internal data consistency. Next mean wave height and wind speed are obtained by averaging the Altimeter time series over a period that matches the spatial resolution of the WAM model. These averaged observations are called super observations, and the Radar altimeter products have been validated by comparing these super observations with wave and wind

model data.

4.1 ERS-1 wave and wind data validation

Regarding ERS-1 validation we follow Hansen and Guenther (Ref. 6) closely. During the ERS-1 cal/val the results of the Altimeter WAM comparisons were weekly reported to ESA and have been very effective in identifying errors and problems in the Altimeter software and retrieval algorithms. In August 1991 the global mean Altimeter wave height was about 1 m higher than computed by the model. The investigation of the detected bias led to the discovery of a small offset in the pre-launch instrument characterisation data. When the processing algorithm was updated at all the ground stations the performance of the Altimeter wave height was found to be satisfactory as follows from an almost zero wave height bias and a standard deviation of error of 0.5 m. The Altimeter wave height retrieval algorithm was based on standard Altimeter theory with the assumption of a Gaussian ocean surface.

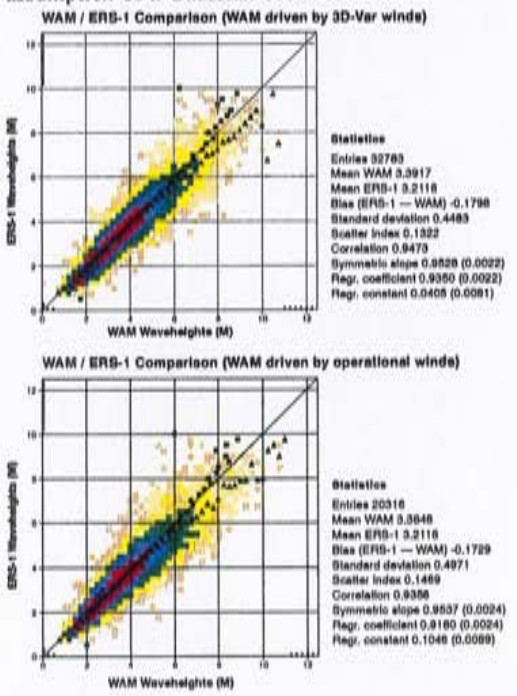

Fig.5: Scatter diagrams of ERS-1 Altimeter and WAM first-guess wave height for the Southern Hemisphere between 24.8.195 and 5.10.1995. Panel a) surface winds are analysed using Scatterometer winds, and Panel b) Scatterometer data are not used in the atmospheric analysis.

During the operational phase of ERS-1 another bug was discovered in the processing algorithm which led to unrealistically shaped wave height distributions. This bug was removed in the beginning of 1994 and resulted in a much improved shape of the histograms at low wave height. Furthermore, in the period 1991-1995 there have been considerable changes in the operational wave forecasting system at ECMWF. These changes affected the quality of the driving surface wind fields and therefore also the quality of the modelled wave height. Moreover, the resolution of the global wave model was increased from 3 to 1.5 deg in July 1994. An example of the impact of an operational change is given in Fig.5, where we show for the Southern Hemisphere scatter diagrams of the comparison between ERS-1 altimeter wave height data and first-guess modelled wave height for the case when scatterometer data are used in the atmospheric analysis or not. The positive impact of the use of scatterometer data is evident from the reduction of the standard deviation of error by 10% from 0.5 to .45m. All in all these operational changes have resulted in some gradual changes in the comparison statistics. By the end of the period that the ERS-1 altimeter was operational the wave heights were on a global scale too low by as much as 20 to 25 cm, while the standard deviation of error was only between 40 and 45 cm.

Regarding the Altimeter winds, engineering calibration and geophysical calibration could not be separated, as there is no access to independent data from man-made targets or stable known targets of opportunity. For the initial data calibration the system gain was used as determined by pre-launch instrument characterisation and for the initial geophysical calibration algorithms from previous altimeter missions were used (SeaSat and Geosat).

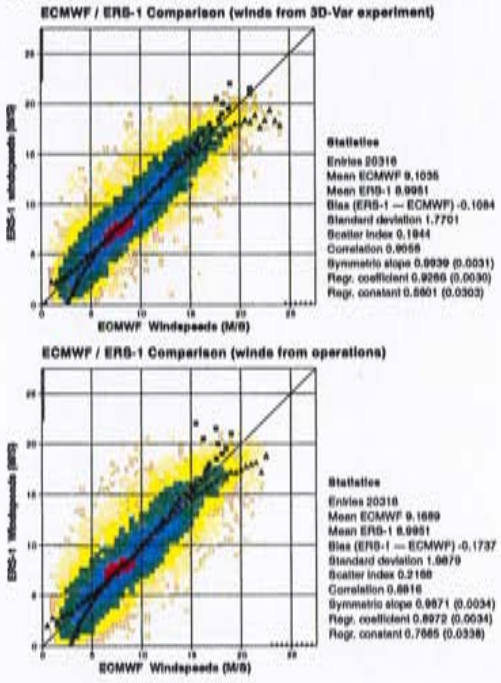

Fig.6: The same as Fig. 5 but now for ERS-1 Altimeter and analysed ECMWF winds.

First comparisons with ECMWF winds uncovered several problems in the initial algorithm. The problems were solved in a couple of weeks but differences of 20 % in wind speed remained. This difference corresponds to a small (0.8 dB) bias in antenna gain. After thorough

validation of the ECMWF reference data set it was shown that the observed antenna gain bias was well within the error budget for pre-launch characterisation. The data calibration was updated in early December 1991. The

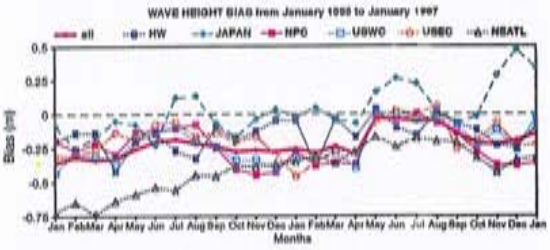

Fig.7: Mean difference between analysed wave height and buoy observation between January 1995 and January 1997

.ESA altimeter wind product algorithm has been quite good since then as shown in Fig. 6. This Figure shows

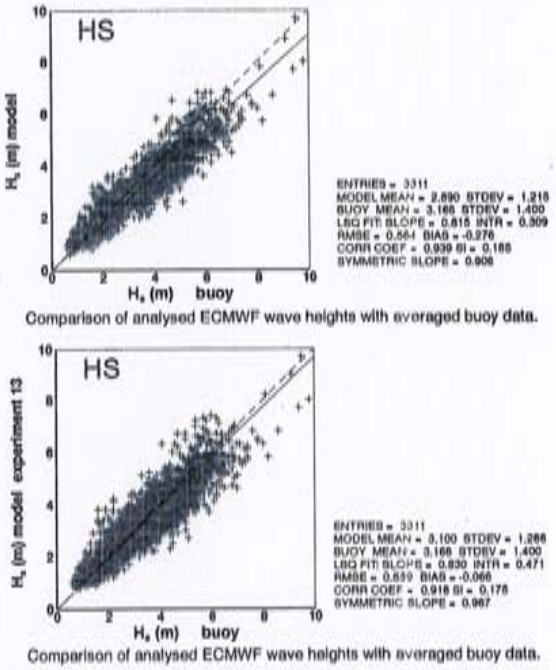

Fig 8: Impact of the assimilation of ERS-1 wave height data on analysed wave height. Panel a) comparison of analysed and buoy wave height with ERS-1 assimilation, and Panel b) the same as Panel a) but now with ERS-1 assimilation switched off. The period is December 1995.

scatter diagrams of the comparison of ERS-1 altimeter wind speed against ECMWF analysed wind speed for the same cases as in Fig.5. Apart from the good quality of the Altimeter wind speeds it is also evident from this Figure that inclusion of the scatterometer data has resulted in an improved wind speed analysis. Thus, there seems to a certain extent consistency between Altimeter and Scatterometer wind speeds.

Because of the promising validation results ECMWF introduced in August 1993 the assimilation of Altimeter wave heights into the wave forecasting system. Generally, this has led to an improved specification of the

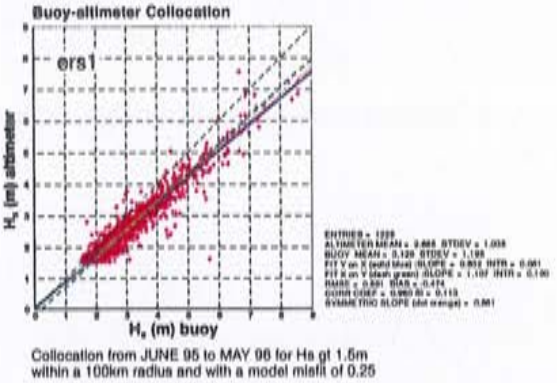

Fig.9: Verification of ERS-1 wave heights against buoys during the ERS-1/ERS-2 tandem mission.

wave analysis. This follows from work done by Bauer and Staabs (private communication) who compared ECMWF wave analyses with TOPEX/POSEIDON Altimeter wave height data and who found an improved correlation between the two after the ERS-1 wave height data assimilation was switched on. However, in the comparison with buoy data an underestimation of analysed wave height was found by about 25 cm. We have illustrated this in Fig. 7 where we have plotted analysed wave height bias as function of month over the two year period starting from January 1995. Note that ERS-1 data were used in the assimilation up to April 1996. In order to make sure that the assimilation of the Altimeter wave height data was the cause of the too low analysed wave height we redid analysis and forecasts with our wave forecasting system for the month of December 1995, however now without assimilation of ERS-1 wave heights. A comparison of analysed wave height with the buoy data, as done in Fig.8, then revealed that the ERS-1 data were the cause of the too low analysed wave height since without data assimilation the under estimation of wave height was only 3% whilst in the opposite case then underestimation was 9%. This picture was confirmed by a direct comparison of ERS-1 Altimeter and buoy wave height over a one year period, shown in Fig.9, which gives an underestimation of wave height by the ERS-1 Altimeter of about 15%. Similar findings have been reported, for example, by Carter et al(Ref. 7) for Geosat Altimeter data, by Queffelou and Lefevre(Ref. 8), by Mastenbroek et al(Ref. 9) for ERS-1 data in the North Sea and by Cotton et al (Ref. 10). The general consensus nowadays is that Altimeters perform satisfactorily but that there may be problems at extreme wave heights. We discuss this issue in more detail in the next Section.

4.2 ERS-2 wind and wave validation

The validation of the ERS-2 wind and wave products

followed a similar pattern as the one for ERS-1, although also some additional remarks should be made.

The validation of the ERS-2 wind speeds was however fairly straight-forward. The main problem was again to determine the antenna gain factor. However, since during the commissioning phase of ERS-2 the ERS-1 satellite was still operational one could compare histograms of Radar back scatter from the two satellites and from the mean difference between the two the antenna gain bias for ERS-2 could be determined. A comparison of the thus obtained Altimeter wind speeds and the analysed ECMWF winds was favourable and showed that the tuning procedure was sound.

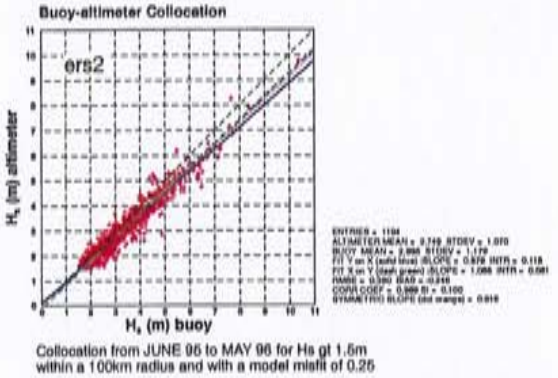

Fig.10: The same as Fig.9 but now for ERS-2 data.

The ERS-2 Altimeter wave heights showed from the first day onwards a remarkably good agreement with the first-guess modelled wave height, except at low wave height where ERS-2 had a higher cut-off value than ERS-1. This higher cut-off value is caused by the somewhat different instrumental specifications of the ERS-2 Altimeter. Because of the tandem mission it was possible to compare ERS-1 Altimeter wave height data with those of ERS-2 by using the WAM model data as a reference standard. As a result we found that ERS-2 Altimeter wave heights were 8% higher than the ones from ERS-1, and this change was, because of the already mentioned underestimation of wave height by ERS-1, regarded as favourable. Since both Altimeters use the same wave height retrieval algorithm the improved performance of the ERS-2 Altimeter must be related to a different specification of the Altimeter instrument or a different processing of the data. According to R. Francis (private communication, 1997) the latter is the case, because the on-board signal processor on ERS-2 uses a more accurate procedure to obtain the wave form, which results in a better estimation of wave height.

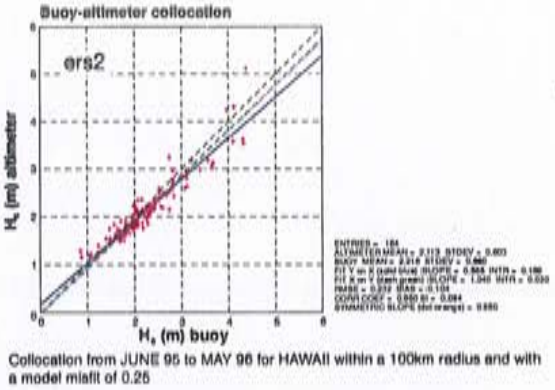

Fig.11: The same as Fig. 10 but now for the swell dominated area of Hawaii only.

The improved performance of the ERS-2 Altimeter wave height is illustrated in Fig.10 where we show for the period of the tandem mission a comparison with buoy data. Comparing this Figure with Fig.9 which shows the verification of the ERS-1 wave height data, reveals the much improved quality of the ERS-2 data since the underestimation is now only 9% and the relative error has decreased from 11 to 10%. However, when swell is dominant (for example, near Hawaii) the agreement is even better (see Fig. 11) since the underestimation is now only 5%.

The introduction of ERS-2 Altimeter wave height data in our wave forecasting system on April 30 1996 therefore had a positive impact as shown by a reduction in analysis

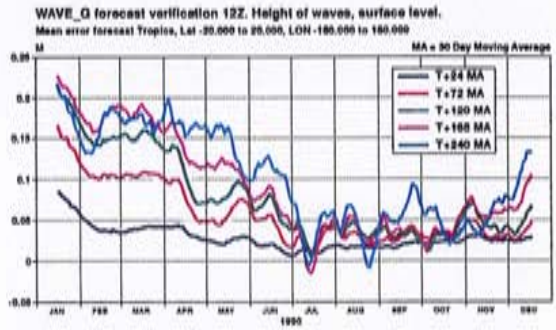

Fig.12: Forecast error in wave height in the Tropics for the year 1996.

error(see for this Fig.7) and as follows from a reduction of error growth during the forecast, shown in Fig. 12 for the Tropics. It is emphasized that the improved forecast performance is found in particular in the Northern Hemisphere summer and the Tropics because the sea state is dominated by swell. This is evident from Fig.7 which shows that in the winter of 1996-1997 an increase of analysed wave height bias is seen. All this suggests that the Altimeter wave height retrieval might be to some extent problematic for wind-generated seas.

5. SEA-STATE DEPENDENCE OF ALTIMETER WAVE HEIGHT RETRIEVAL

The standard theory of Altimeter wave height retrieval is, as already mentioned, based on the assumption that the joint probability distribution of surface elevation and slopes is Gaussian. The assumption of Gaussianity is however only valid for small steepness. Therefore, for steep waves, a state which usually occurs for young wind sea, one would therefore expect that the Altimeter wave height retrieval is less satisfactory.

The Altimeter-buoy comparison of the previous Section indeed suggests that the Altimeter wave height retrieval depends on the sea state. However, to be convincing more collocations are needed. Hence it was thought of interest to reinvestigate the comparison between Altimeter wave height data and the modelled wave height, and to stratify the collocations by means of the root mean square slope of the waves. Results of this study are summarised

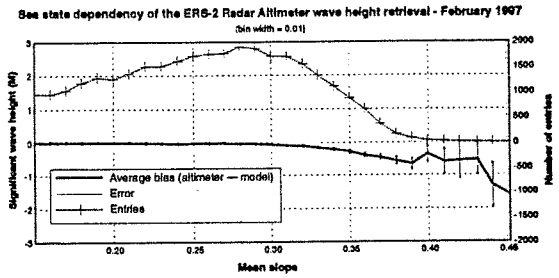

Fig.13: Mean difference between Altimeter and first-guess wave height as a function of root mean square slope for February 1997. The number of collocations is shown as well.

in Fig. 13 where we show the mean difference between Altimeter wave height and WAM wave height as function of the modelled mean slope. The error bars denote the uncertainty in the estimate of the bias while also the number of collocations as function of slope is given. In this context it is remarked that we have established a clear relation between the sea state being wind sea or swell and the value of the mean square slope. In practice, it turns out that wind seas have root mean square slopes above 0.3 while swells have slopes below 0.3. Fig.13 suggests that the Altimeter wave height is biased low for wind seas with large slope. This underestimation may be as much as 50 cm.

Therefore in contrast to the general consensus it is concluded that there may be problems with the Altimeter wave height retrieval for steep waves, which are not necessarily extreme waves. The young wind sea cases typically occur in the wave height range of 2-5 m. It is emphasized that this conclusion is based on the known limitations of the standard Altimeter theory, on collocations with buoy data and on collocations with the modelled wave height.

6. CONCLUSIONS

In this paper we have discussed in some detail the role wave model data can play in the validation and interpretation of Satellite wind wave data. The wave model results were of great help in detecting initial problems in the ERS-1 Altimeter wave height retrieval, in validating the ERS-2 Altimeter wave height product and in detecting a possible sea-state dependence of the retrieval procedure. Furthermore, WAM model spectra are needed as a first-guess for the inversion of the SAR image spectra, while the model data were also of help to detect problems in a first version of the SAR inversion algorithm. Similar remarks apply for the helpful role of ECMWF winds.

Our impression is that the ERS-2 Altimeter wave heights are of good quality, in particular for swell which dominates the sea state on a global scale. For steep wind waves the situation may be less satisfactory. Two ways out of this undesirable situation are suggested here. One could establish an empirical fit between the wave height bias of the Altimeter and the mean square slope and use the observed mean square slope, which also follows from the Altimeter waveform, to correct the Altimeter wave height. Alternatively, following Srokosz (Ref. 11) one could attempt to extend the Altimeter wave height retrieval algorithm by including deviations from the Gaussian state.

ACKNOWLEDGEMENTS

The help of Heinz Guenther and Anne Guillaume who were involved in the initial validation efforts is greatly appreciated. We acknowledge useful discussions with Evert Attema, Richard Francis, Anthony Hollingsworth and Remko Scharroo.

REFERENCES

(1) Komen G J, L Cavaleri, M Donelan, K Hasselmann, S Hasselmann and P A E M Janssen 1994, Dynamics and Modelling of Ocean Waves, Cambridge University Press, 532 pp.

(2) Hasselmann K, and S Hasselmann, 1991, On the nonlinear mapping of an ocean wave spectrum into a SAR image spectrum and its inversion, J Geophys Res, **C96**, 10, 713-10,729.

(3) Hasselmann S, C Bruening, K Hasselmann and P Heimbach, 1996, An improved algorithm for the retrieval of ocean wave spectra from SAR image spectra, J Geophys Res, **101**, C7, 16,615-16,629.

(4) Janssen P A E M, B Hansen and J Bidlot, 1997, Verification of the ECMWF Wave Forecasting System against Buoy and Altimeter Data, accepted by Weather and Forecasting.

(5) Hansen B, C Bruening and C Staabs, 1994, Global Comparison of significant wave heights derived from

ERS-1 SAR wave mode, ERS-1 altimeter and TOPEX altimeter data, in Space at the Service of our Environment, Proceedings of the Second ERS-1 Symposium, Hamburg, Germany, October 1993, Euro. Space Agency Spec. Publ.,
ESA SP-361,33-36.

(6) Hansen B and H Guenther, 1992, ERS-1 Radar Altimeter Validation with the WAM model, Proceedings of the ERS-1 Geophysical Validation workshop, Penhors, Bretagne, France, April 1992, European Space Agency, ESA wpp-36, pp.157-161.

(7) Carter D J T, P G Challenor and M A Srokosz, 1992, An Assesment of Geosat Wave Height and Wind Speed Measurements, J Geophys Res, **97**, C7, 11, 383-11, 392.

(8) Queffelou P and J M Lefevre, 1992, Validation of ERS-1 wave and wind fast delivery products, Proceedings of the ERS-1 Geophysical Validation workshop, Penhors, Bretagne, France, April 1992, European Space Agency, ESA wpp-36, pp. 163-168.

(9) Mastenbroek C, V K Makin, A C Voorrips and G J Komen, 1994, Validation of ERS-1 Altimeter Wave Height Measurements and Assimilation in a North Sea Wave Model, The Global Atmosphere and Ocean System, **2**, 143-161.

(10) Cotton P D, P G Challenor and D J T Carter, 1997, An Assessment of the accuracy and reliability of Geosat, ERS-1, ERS-2, TOPEX and Poseidon measurements of Significant Wave Height and Surface Wind Speed, Proceedings of the CEOS Wind and Wave Validation Workshop, ESTEC, Noordwijk, The Netherlands.

(11) Srokosz M A, 1986, On the joint distribution of surface elevation and slope for a non-linear random sea, with application to radar altimetry, J Geophys Res, **91**, 995-1006 .

ANNEX K

- Timeseries of the monthly statistics scatter index and bias

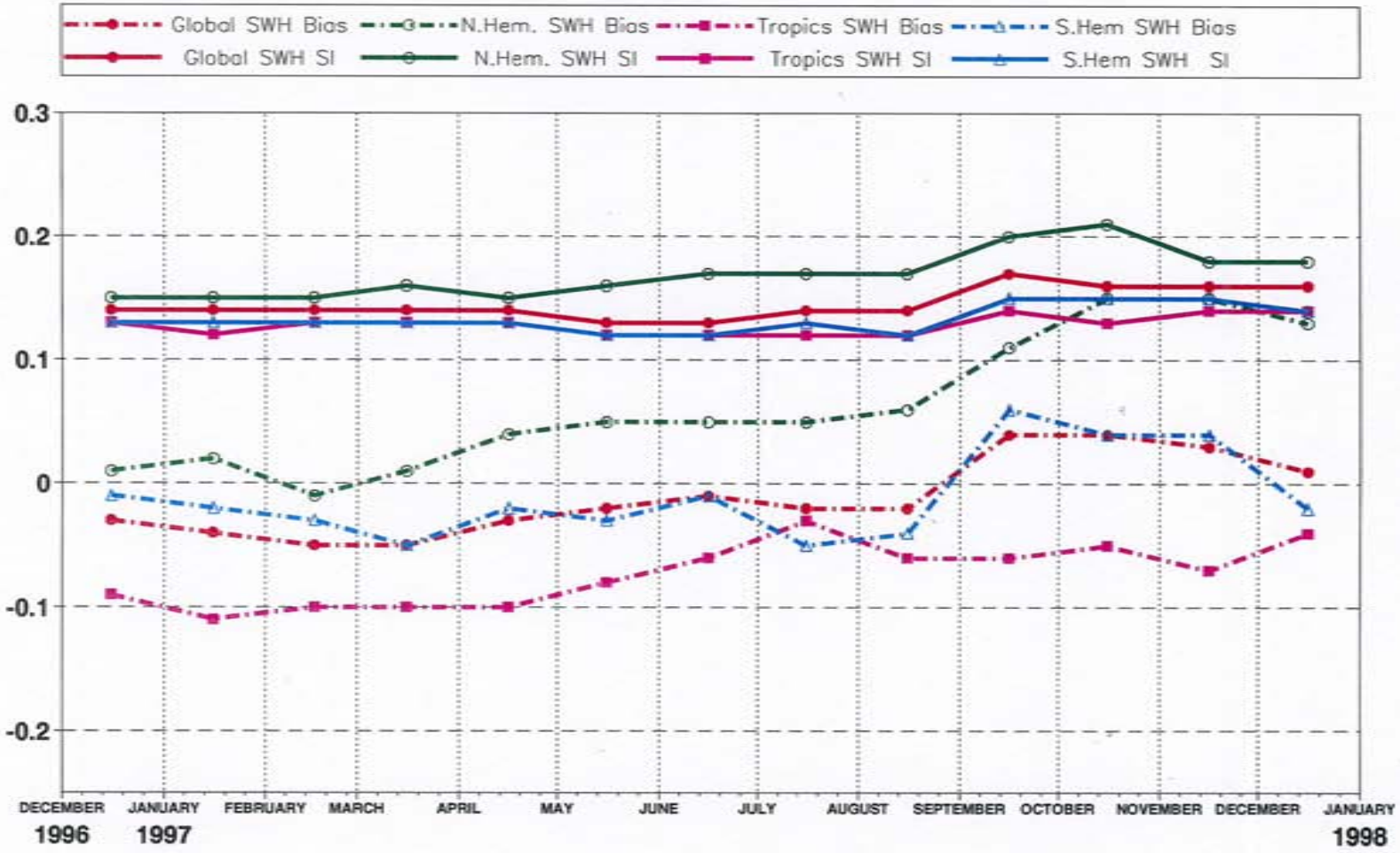

Figure 1: ERS–2 Altimeter wave heights: Timeseries of bias (ERS–2 – model) and scatter index (SI)

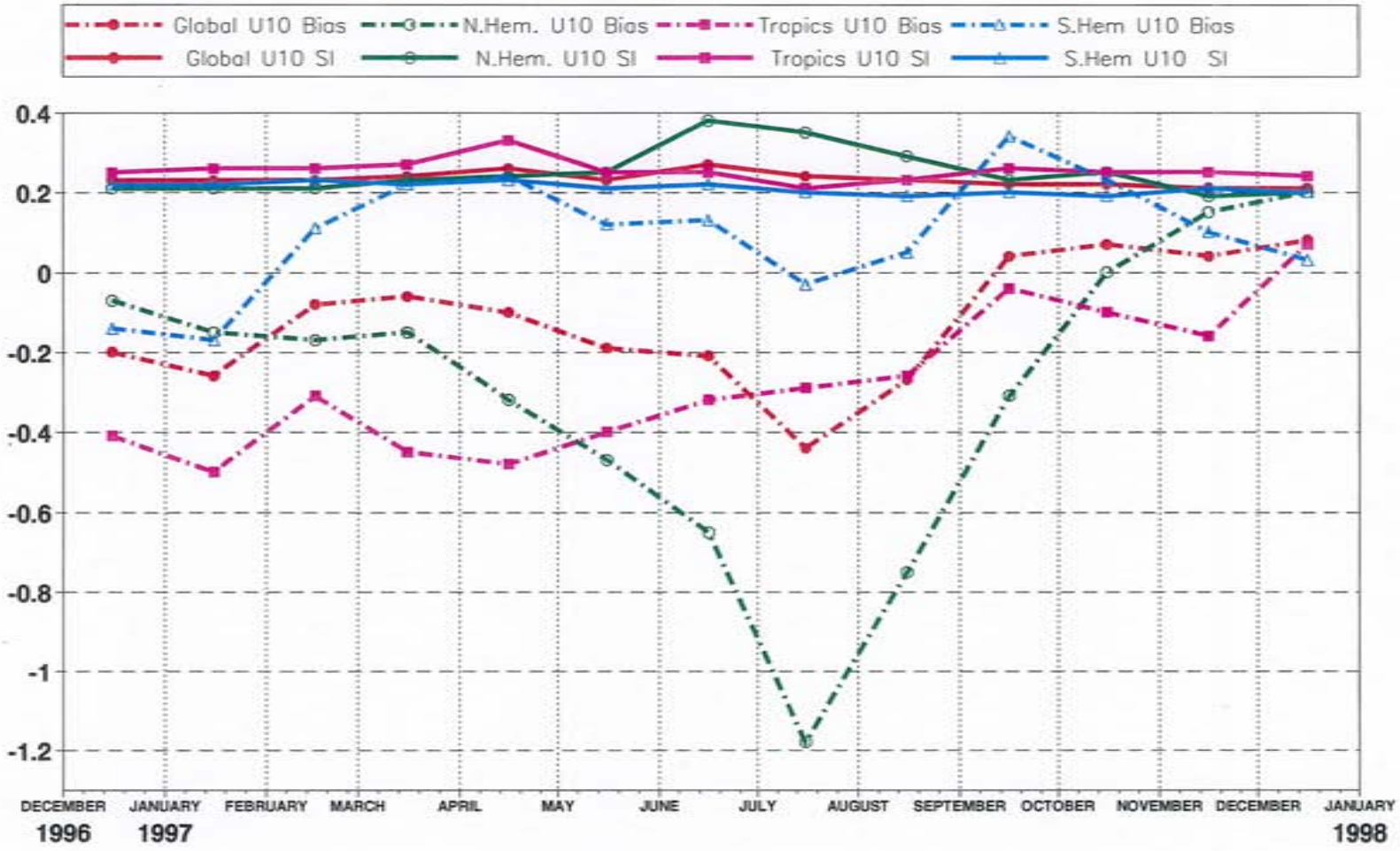

Figure 2: ERS–2 Altimeter wind speeds: Timeseries of bias (ERS–2 – model) and scatter index (SI)

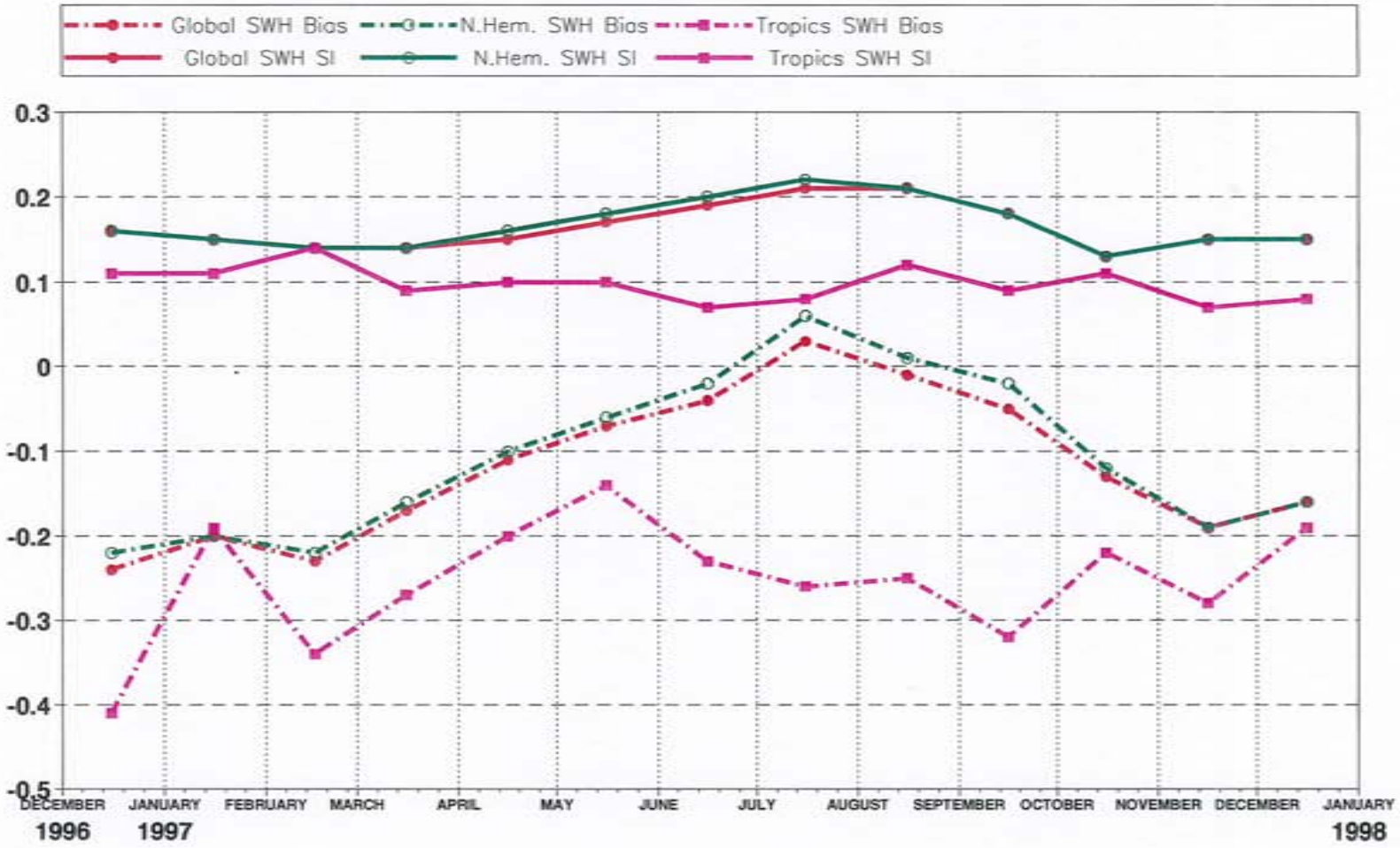

Figure 3: ERS–2 Altimeter wave heights: Timeseries of bias (ERS–2 – buoy) and scatter index (SI)

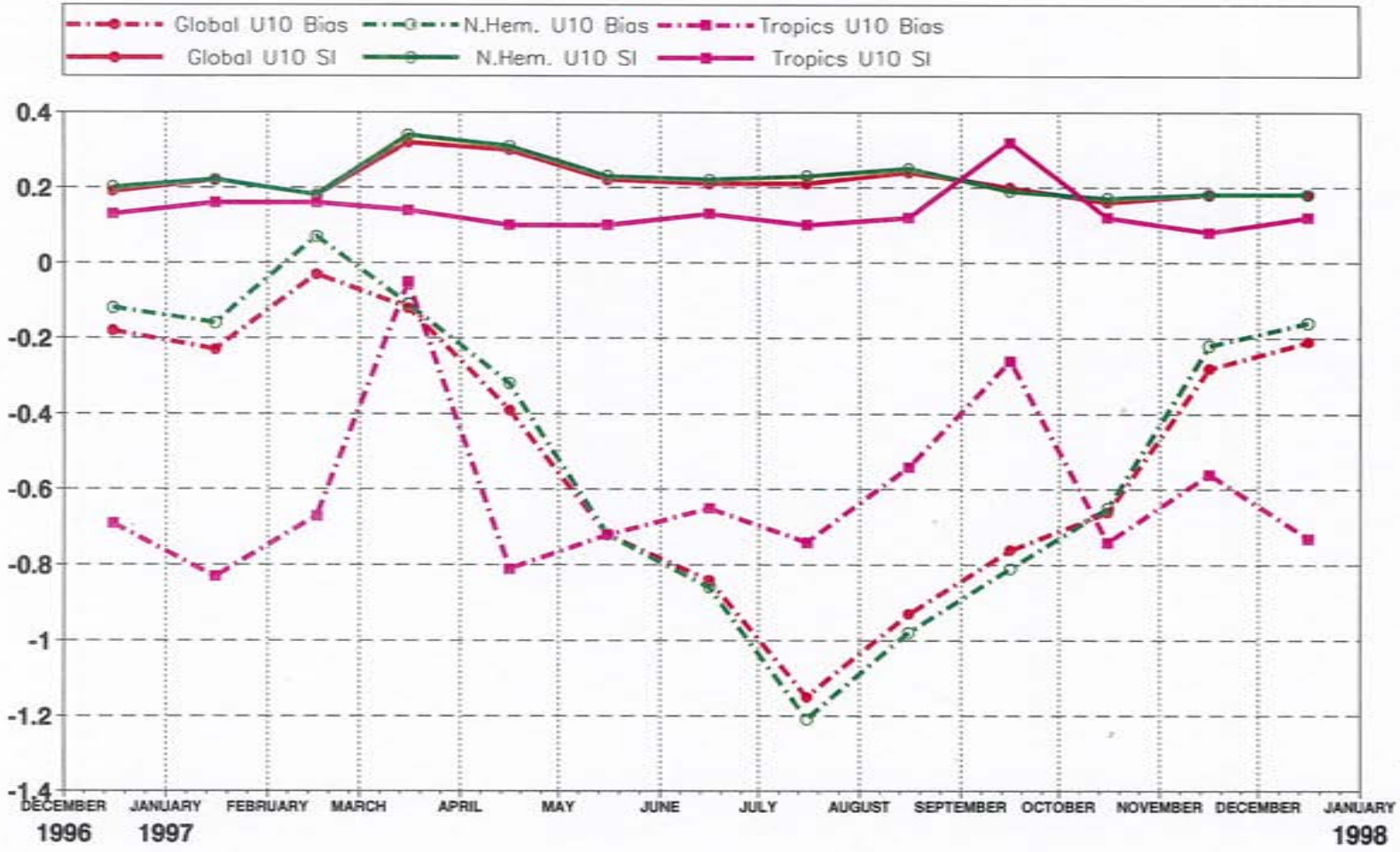

Figure 4: ERS–2 Altimeter wind speeds: Timeseries of bias (ERS–2 – buoy) and scatter index (SI)

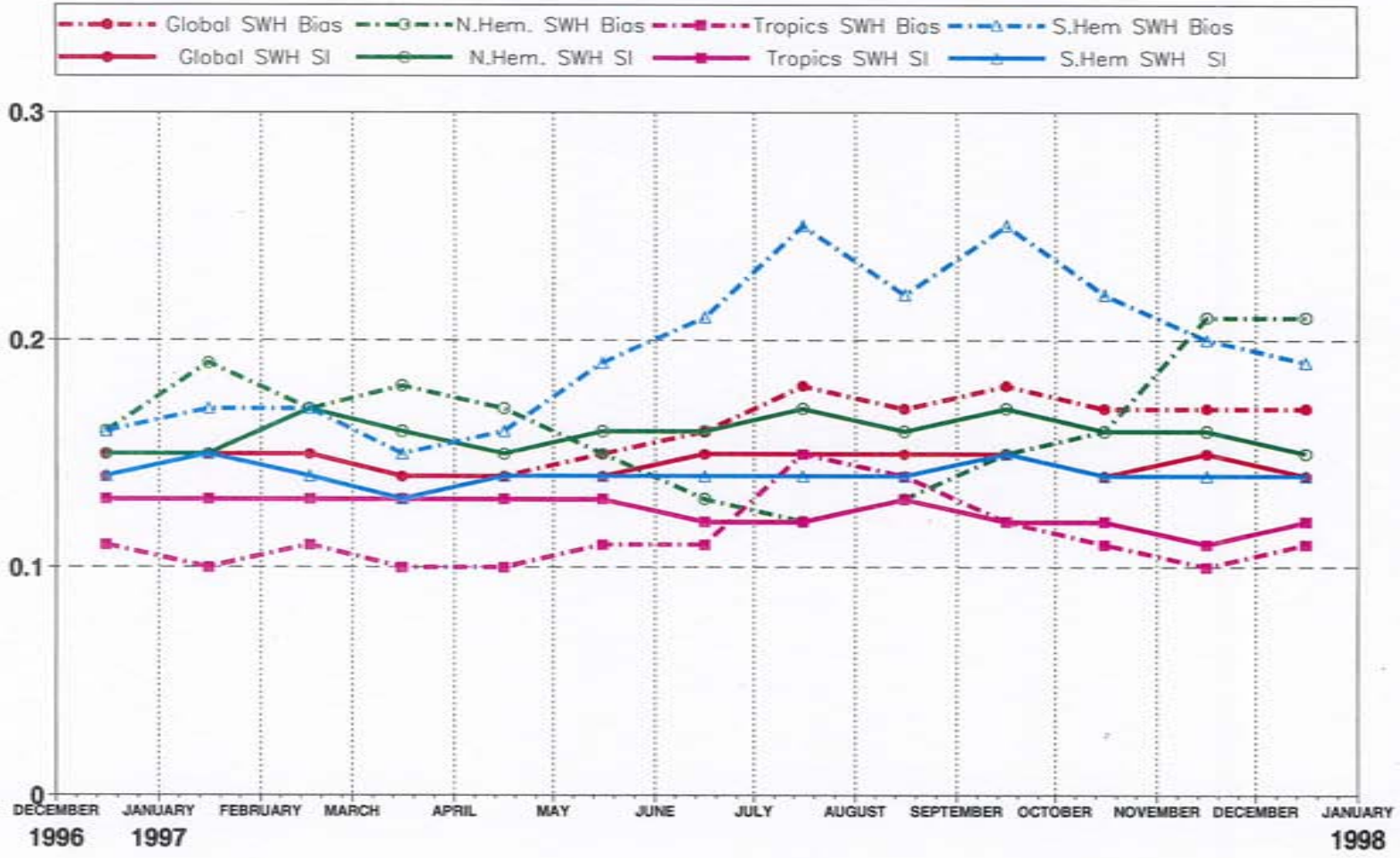

Figure 5: ERS–2 SAR wave heights: Timeseries of bias (ERS–2 – model) and scatter index (SI)